Department of Pharmacology

UCL School of Pharmacy, Brunswick Sq, London

Modulation of LRRK2 mediated signaling in immune cells

Sultan Almudimeegh

Thesis submitted for the degree of Doctor of Philosophy University College London

2021

Supervisors:

Prof. Kirsten Harvey

Department of Pharmacology

UCL School of Pharmacy, Brunswick Sq, London

Prof. Ahad Rahim

Department of Pharmacology

UCL School of Pharmacy, Brunswick Sq, London

Declaration

I, Sultan Almudimeegh, confirm that the work presented in this thesis is my own, describing the research completed between May 2016 and March 2021 under Professor Kirsten Harvey and Professor Ahad Rahim's supervision. Where information has been derived from other sources of collaboration, I confirm that this has been indicated in the thesis. I wrote all text, and those parts which have appeared in publications have been indicated by citation.

Acknowledgement

First and foremost, I would like to thank Allah (GOD). Without his gifts and strength, I wouldn't be able to get this far in life.

I want to thank Professor Kirsten Harvey for her continuous support, guidance, and patience. My journey was not a smooth one, yet Kirsten has been accommodating and understanding. I would also like to thank Professor Ahad Rahim and Dr Michael Hughes for providing the lentivirus constructs and help with the transduction. Furthermore, I would like to thank professor Towers for his insight regarding immune cell transduction. My gratitude continues with officemates including Emma, Giulia, Michael, Maha, Joanna, Sammie, Ed, Ghada, Jonny, Kim, Yusheng, Timpson, Anthony, Alex, Simone, Fatma, Ike, George, and Clinton, who made the journey smooth and enjoyable.

A special thanks to my brothers: Ibrahim, Bander and Mohammed, and my friend Nasser whom their support was vital in continuing my studies. I would also express my gratitude to my employer King Saud University for sponsoring me. I am looking forward to returning to Riyadh and contribute to the thriving community of teaching and research.

I want to express My deepest appreciation for my daughters Alanood and Tarfah. Alanood asked endless times to play and stay with her asking me, "What is more important, your work or your daughter". I will admit that doing a PhD while parenting is not a wise idea. I also would like to thank the Richard Desmond Children's Eye Centre. They have provided excellent care for my daughters during our stay in London. Tarfah had to do two surgeries into each eye totalling in four surgeries during her first

year in life. I can tell she is a fighter as she could smile despite the pain 24 hours after the surgery. My appreciation also extends to National health services (NHS) for the extreme efforts made by them despite the financial constraint during the pandemic COVID-19. It was not an ordinary time by any means, and many lives have been lost, unfortunately.

A warranted and special thank you for Nada, my beautiful wife. She is a great mother and soul companion, and her devotion to my daughters is appreciated. Her continuous support and patient was vital in finishing my PhD. The journey wasn't easy, and without her, it would be ne'er impossible to reach the finish line Thank you, Nada.

Finally, I would like to express my gratitude to my parents. Despite being one of the most intelligent people I have ever known, my mum was denied education, and she didn't even complete secondary school. I named my daughter after her, and I promise I will do everything in my abilities to make my daughter's education and career as smooth as possible. My gratitude also continues to my father, a great supporter and advocate.

Abstract

Mutations in *LRRK2* are considered the most common cause of familial and sporadic Parkinson's disease (PD), a neurodegenerative movement disorder. PD is characterised pathologically by the death of dopaminergic neurons and symptomatically by tremor, bradykinesia and impaired coordination. *LRRK2* variants is also linked to an increased risk of Crohn's inflammatory bowel disease and increased susceptibility to leprosy. All those diseases share a common immune dysfunction theme. The exact physiological function of LRRK2 remains largely elusive. However, multiple reports suggest that LRRK2 is involved in Wnt and NFAT signalling. Those pathways are known to mediate a variety of physiological functions, including immune system regulation and synaptic functions.

In this study, I investigate the role of LRRK2 in mediating the inflammatory responses in macrophages and T cells and associated changes in Wnt signalling components. Challenging the *LRRK2* WT and *LRRK2* KO RAW 264 macrophages with Lipopolysaccharides (LPS) resulted in changes in the release of Nitric oxide (NO) and expression of several cytokines, including tumour necrosis factor-alpha (TNFα), cyclooxygenase-2 (COX-2) and others. Furthermore, the phagocytic activity of the *LRRK2* KO cells appears to be substantially lower compared to *LRRK2* WT cells. I observed changes in Wnt signalling activity in response to LPS across the different genotypes. Interestingly, the expression of the LRRK2 kinase substrate RAB10 and its phosphorylated form, decreased significantly in response to LPS in *LRRK2* KO cells compared to WT, providing a possible mechanistic explanation for the decrease in cytokines and NO release. Wnt-related changes were confirmed *ex-vivo* in bone-

marrow-derived macrophage (BMDM) and T cells across WT, KO and G2019S genotypes. In conclusion, this study substantiates a role for LRRK2, in mediating inflammatory responses in immune cells and highlights the significance of Wnt signalling and Rab10 in this LRRK2 immune function.

Impact statement

The work presented here re-emphasises LRRK2 inflammatory role in immune cells and highlights the significance of Wnt signalling in mediating the inflammatory response. Furthermore, it suggests that both Wintless protein and Rab10, a LRRK2 substrate, play an important role in LRRK2 mediated inflammatory response. Understanding molecular mechanism by which LRRK2 executes its inflammatory role could be crucial for unveiling the pathomechanisms in diseases associated with LRRK2 including PD, CD, leprosy and cancer.

Table of Contents

List of Figures

List of Tables

Abbreviations

Abbreviation	Name
AD	Alzheimer disease
AD	Autosomal dominant
AR	Autosomal recessive
ALP	Autophagy-lysosome pathway
ANK	ANKyrin repeats
AP1	Activator protein 1
APC	Antigen presenting cells
ARM	ARMadillo repeats
Atg	Autophagy-related genes
ATP	Adenosine triphosphate
AIDS	Acquired immunodeficiency syndrome
ATP13A2	ATPase 13A2
BDC	β-catenin destruction
BMDMs	Bone-marrow-derived macrophages
BCA	bicinchoninic acid
BBB	Blood-brain barrier
CamKII	Calcium/calmodulin-dependent kinase II
CD	Crohn's disease
CHCHD2	Coiled-coil-helix-coiled-coil-helix domain containing 2
CK1α	Casein kinase1α
CMA	Chaperone mediated autophagy
CN	Calcineurin
COR	C-terminal of ROC
COX-2	Cyclooxygenase 2
CREB	C-AMP response element-binding protein
CsA	Cyclosporine A
CSF	Cerebrospinal fluid
CAS9	CRISPR associated protein 9
CRISPR	Clustered regularly interspaced short palindromic repeats
DEPC	Diethylpyrocarbonate
cDNA	Complementary Deoxyribonucleic Acid
DKK1	Dickkopf-related protein 1
Dvl	Disheveled
DMEM	Dulbecco's Modified Eagle Medium
DJ-1	parkinsonism associated deglycase
DMSO	Dimethyl sulfoxide
EAU	Experimental autoimmune uveitis
EGFR	Epidermal growth factor receptor
EIF4G1	Eukaryotic translation initiation factor4 gamma 1
ELISA	Enzyme-linked immunosorbent assay
FACS	Fluorescence-activated cell sorting
FBXO7	F-box protein 7
FZD	Fizzled receptor
FBS	Fetal bovine serum
GBA	Glucocerebrosidase
GDP	Guanine diphosphate
GIGYF2	GRB10 interacting GYF protein 2
GSK3β	Glycogen synthase kinase 3
GTP	Guanosine triphosphate

Abbreviation	Name
GWAS	Genome wide association studies
HBSS	Hank's Balanced Salt Solution
Hsp40	DnaJ heat shock protein family
HTRA2	HtrA serine peptidase 2
HRP	Horseradish peroxidase
HIV	Human immunodeficiency viruses
IBD	Inflammatory bowel disease
IFN-γ	Interferon gamma
IFITM3	interferon-induced transmembrane protein 3
IL	Interleukin
iPSC	induced pluripotent stem cell
IVIS	*in-vivo* imaging system
JAK	Janus kinase
JNK	C-Jun terminal kinase
ISG	interferon-stimulated genes
KI	Knock-in
KO	Knock-out
LAMP2	Lysosome-associated membrane protein 2
LC3	Cytosolic protein microtubule-associated protein 1 light chain 3
LiCl	Lithium Chloride
LPS	Lipopolysaccharides
LRP	Low-density lipoprotein receptor-related protein
LB	Lysogeny broth
LRR	Leucine Rich Repeats
LRRK2	Leucine-rich repeat kinase 2
LIMP2	lysosomal integral membrane protein type 2
LIMK1	LIM domain kinase 1
M. leprae	Mycobacterium lepromatosis
MAPKKK	Mitogen-activated protein kinase kinase kinase
MHC	Major histocompatibility complexes
MKK4	MAPK kinase 4
MPP	1-methyl-4-phenyl-4-propionoxypiperidine
MPTP	N- methyl-4-phenyl-1,2,5,6-tetrahydropyridine
MTT	3 -(4,5-dimethythiazol-2-yl)-2,5-diphenyl tetrazolium bromide
MOI	Multiplicity of infection
MCP-1	Monocyte Chemoattractant Protein-1
mTOR	Mammalian target of rapamycin
MCSF	Macrophages colony stimulating factor
NO	Nitric oxide
NO_2^-	nitrite
NP-40	Nonyl-phenoxypolyethoxylethanol-40
NFAT	Nuclear factor of activated T-cells
NFκ B	Nuclear factor kappa-light-chain-enhancer of activated B cells
NED	N-1-napthylethylenediamine dihydrochloride
P62	p62/sequestosome-1
PAK	p21-activated kinase
Parkin	PRKN
PBMC	Peripheral blood mononuclear cells
PD	Parkinson’s disease
PDE4	Phosphodiesterase 4
PINK1	PTEN induced putative kinase 1

Abbreviation	Name
PKA	Protein kinase A
PKC	Protein kinase C
PLA2G6	Phospholipase A2 group VI
PBS	Phosphate buffer saline
PARPi	Poly (ADP-ribose) polymerase inhibitors
PMA/IO	Phorbol myristate acetate/ Ionomycin
qPCR	Quantitative polymerase chain reaction
RPMI	Roswell Park Memorial Institute
RIC3	Acetylcholine receptor chaperone
ROC	Ras of complex proteins
RPM	rounds per minute
ROCO	ROC and COR domains
ROR1/2	Receptor tyrosine kinase–like orphan receptor-1 and -2
ROS	Reactive oxygen species
RT	reverse transcriptase
SNc	Substantia nigra pars compacta
SFRP	Secreted frizzled-related protein
SNP	Single nucleotide polymorphism
SYNJ1	Synaptojanin 1
siRNA	Short interfering RNA
SDS-PAGE	Sodium dodecyl sulphate–polyacrylamide gel electrophoresis
STAT	Signal transducers and activators of transcription
T1R	Type-1 reactions
TB	Tuberculosis
TCF/LEF	T-cell transcription factor/lymphoid enhancement factor
TLR	Toll-like receptor
TMEM230	Transmembrane protein 230
TNF-α	Tumor necrosis factor alpha
TBST	Tris-buffered saline-Tween 20
UCHL1	Ubiquitin C-terminal hydrolase L1
VPS13C	Vacuolar protein sorting 13 homolog C
VPS35	Vacuolar protein sorting-associated protein 35
WD40	Tryptophan- aspartate repeats
WHO	World health organization
Wnt/PCP	Wnt / planar cell polarity
WT	Wild type
WISP1	WNT1-inducible signalling pathway protein 1
WLS	Wntless
Wnt	Wingless/Int
α-Syn	α-Synuclein

Chapter 1 General Introduction

1.1 Parkinson's disease

1.1.1 History and epidemiology

Historically, some of Parkinson's disease (PD) symptoms had been depicted in many early sources. For example, a King was mentioned to have sialorrhea in an Egyptian papyrus. An Ayurveda medicine treatise has described a disease that progresses with tremor, drooling and lack of movement in 10th century BC. In modern history, James Parkinson described the manifestation of PD symptoms in an essay entitled "An Essay on the Shaking Palsy". The term "Parkinson's disease" was later proposed by William Sanders and then advocated by Jean-Martin Charcot (Goetz 2011, Cuenca et al. 2019).

In the 1950s-60s, a consequential work by Arvid Carlsson and others led to the characterization of the neurotransmitter dopamine and the finding that it is present at a high level in the basal ganglia. Later, Oleh Hornykiewicz highlighted that PD is due to the loss of dopamine in the brain. In due course, he contributed to the development of L-dopa, a dopamine precursor, which is still considered the standard treatment of PD today(Cuenca, 2019). L-dopa can temporarily restore the symptoms caused by the dopamine deficiency in the brain (Goetz 2011).

After Alzheimer's disease, PD is considered the most common neurodegenerative disease, affecting 1% of the population in the sixth decade of life and its incidence increases with age(Xiromerisiou, 2010). Moreover, 4% of PD patients are diagnosed with PD before the age of 50. Today, an estimated 10 million people have PD, and the number is projected to double by 2030 (Tanner 2013).

1.1.2 Clinical manifestation:

Patients with PD often suffer from disturbances in motor function, cognition, behaviour and autonomic nervous system function (Alkhuja 2013). Classical motor features of PD include tremors, rigidity, bradykinesia and postural instability. Hyposmia, a decreased ability to smell, is common among PD patients, and some data indicate that this might be an early indicator of PD. Cognition deficits are common features; about 50% of PD patients eventually will develop dementia. Behaviour changes such as depression, apathy and anxiety are also common(Poewe et al. 2017). Additionally, some PD patients experience autonomic nervous system disturbances, including constipation, sexual dysfunction, increased urinary frequency, and sweating. In advanced stages, difficulty swallowing and respiratory impairment are frequent, and aspiration pneumonia is the most common cause of death in PD patients (Alkhuja 2013).

1.1.3 Pathology:

PD has distinct pathological features, which distinguish it from other neurodegenerative diseases. A severe dopaminergic neuron loss is observed in the substantia nigra pars compacta(SNc) in the basal ganglia that gives rise to the motor impairment seen in PD (Gasser 2009).

This results in a deficiency in the neurotransmitter dopamine in the striatum. Typically, PD patients need supplementation of that loss by administrating L-dopa, a dopamine precursor that can cross the blood-brain barrier(BBB). The SNc has a distinctive dark colour due to the presence of neuromelanin, and in PD, the colour subsides and lightens as the dopaminergic neurons progressively degenerate (**Figure 1-1**). L-dopa can alleviate the motor impairment seen in PD patients. However, its efficacy subsides

with time. Additionally, L-dopa long term use is associated with atrocious side effects such as dyskinesia. In addition, protein aggregates of α-synuclein(α-Syn) and ubiquitin that form cytoplasmic inclusions, known as Lewy bodies, are also present in the brain of patients with PD and thought to contribute to non-motor symptoms (Exner et al. 2012).

Figure 1-1 ***Degeneration of SNc dopaminergic neurons in PD****. Figure adapted from (Dickson and Weller 2011).*

1.1.4 Aetiology of PD:

The primary risk factor for PD is age. Although PD symptoms were recognized two centuries ago, the exact molecular mechanisms that lead to the disease's progression are still unknown. While family inheritance and genetics play a pivotal role in the development of familial forms of PD, 90 % of PD cases are sporadic, implying a complex interplay between environmental and genetic factors contributing to the progression of the disease. Epidemiological studies have suggested a correlation between exposure to certain environmental toxicants and the risk of developing PD (Chin-Chan, Navarro-Yepes and Quintanilla-Vega 2015).

1.1.4.1 Environmental factors

Several epidemiological studies and clinical report cases have substantiated the involvement of environmental risk factors for PD. In a tragic story, Langston et al. documented Parkinsonism's symptoms in four drug addict patients that developed after injecting themselves with 1-methyl-4-phenyl-4-propionoxypiperidine (MPPP-Heroin analogue). The symptoms reported in those four patients were similar to another patient mentioned in another report. In both cases, the intention was to consume MPPP. However, it was revealed that MPPP was contaminated with N-methyl-4-phenyl-1,2,5,6-tetrahydropyridine(MPTP) due to imperfect synthesis, which was responsible for the toxicities reported in those two cases(Langston et al. 1983).Today, MPTP is a well-established neurotoxin used in animal models to produce symptoms mimicking PD. Its toxicity mechanism involves the conversion to MPP^+ by monoamine oxidase after crossing the blood-brain barrier and appears to be selectively uptaken by the dopaminergic neurons and causes them to degenerate(Przedborski et al. 2000). While the cascade of events leading to cell death is not certain, it seems to be mediated by inhibiting the complex 1 enzyme in the inner mitochondrial membrane, dysregulating oxidative phosphorylation processes leading to oxidative stress, ultimately disturbing cellular function resulting in cell death.

Another environmental factor linked to developing PD in epidemiological studies is the chronic exposure to certain pesticides, insecticides and herbicides. In a case-control study, Gorell and others documented a significant association between the use of insecticide and herbicides and the development of PD among farmers living in rural areas(Gorell et al. 1998). This finding was supported in several subsequent studies (Chin-Chan et al. 2015). Rotenone, a natural pesticide found in the roots of Lonchocarpus and Derris species, is a common pesticide that has been documented

to have similar effects on the mitochondrial complex I to MPTP(Heinz et al. 2017). Subsequent studies on rats injected with rotenone revealed selective neurodegeneration in the dopaminergic neurons in the SNc. In addition, those rats displayed behavioural features of PD commonly observed in humans, including motor deficits and abnormal posture(Alam and Schmidt 2002). Both rotenone and MPTP were used extensively in the literature to produce PD models in animals and cultured cells.

Other environmental factors that are thought to contribute to PD development have also been reported involving exposure to heavy metals and trace elements, including iron, zinc, magnesium, and selenium. However, epidemiolocal studies are not in line with the experimental evidence from animals and culture cells, and thus the topic is considered controversial, and further testing is needed(Ball et al. 2019).

1.1.4.2 Genetic Factors:

Traditionally, PD has been thought to be an idiopathic disease in which environmental toxins and age are considered risk factors. However, in the late 1990s, several genetic analysis studies in families with a history of PD have revealed several disease-causing mutations that segregate with certain families(Bandres-Ciga et al. 2020). In 1997, the first gene to be associated with familial PD was identified to be *SNCA* which encodes for the protein α-Syn (Polymeropoulos et al. 1997). In the following years, another set of genes were additionally found to be associated with familial PD, including leucine rich repeat kinase 2 (*LRRK2*), vacuolar protein sorting-associated protein 35 (*VPS35*), parkin (*PRKN*), glucocerebrosidase (*GBA*) and parkinsonism associated deglycase (*DJ-1)*(Bandres-Ciga et al. 2020). Today, family history is approximately responsible

for 15%, whereas mendelian PD represents around 5 % of all PD cases(Deng, Wang and Jankovic 2018).

In addition to genes associated with familial PD, genome-wide association studies (GWAS), which are studies designed to establish an association between genetic regions in the chromosomes and traits, including diseases, have revealed several associations between multiple loci and the risk of developing PD(Manolio 2010). The first GWAS that was conducted to establish the association recruited 5074 PD patient cases and 8551 case controls of European ancestry. It revealed a significant correlation between developing PD and genetic variation in *SNCA* and *MAPT* locus(Simon-Sanchez et al. 2009). Several GWAS have followed with a more substantial increase in participants, and more associated loci have been documented. Recently, the largest GWAS to date recruited 37,700 cases, and 1.4 million controls have revealed 90 independent risk signals that are associated with sporadic PD(Nalls et al. 2019). Individual loci that are associated with PD have been designated with the name "PARK", and the number following the designation indicates the order in which they were discovered. To date, there are more than 19 loci that have been confirmed to correlate with PD. Table 1 summarizes gene locus and disease-causing genes of PD along with the mode of inheritance.

Locus	Gene	Mode of inheritance
Park 1,4	*SNCA*	Autosomal dominant (AD)
Park 2	parkin RBR E3 ubiquitin protein ligase	Autosomal recessive (AR)
Park 5	ubiquitin C-terminal hydrolase L1 (*UCHL1*)	AD
Park 6	PTEN induced putative kinase 1 (*PINK1*)	AR
Park 7	*DJ-1*	AR
Park 8	*LRRK2*	AD
Park 9	ATPase 13A2 (*ATP13A2*)	AR
Park11	GRB10 interacting GYF protein 2 (*GIGYF2*)	AD
Park 13	HtrA serine peptidase 2 (*HTRA2*)	AD
Park14	phospholipase A2 group VI (*PLA2G6*)	AR
Park15	F-box protein 7 (*FBXO7*)	AR
Park17	VPS35, retromer complex component	AD
Park18	eukaryotic translation initiation factor 4 gamma 1(*EIF4G1*).	AD
Park19	DnaJ heat shock protein family (Hsp40) member C6(*DNAJC6*)	AR
Park20	synaptojanin 1 (*SYNJ1*)	AR
Park21	transmembrane protein 2 (*TMEM230*)	AD
Park22	coiled-coil-helix-coiled-coil-helix domain containing 2 (*CHCHD2*)	AD
Park23	1. VPS13C 2. RIC3 acetylcholine receptor chaperone (RIC3).	AD and AR.

Table 1-1 ***Gene locus and disease-causing genes of PD,*** *adapted with modification from(Deng et al. 2018).*

1.2 LRRK2

1.2.1 Overview

The first study indicating the significance for the later identified LRRK2 protein was a study conducted by Funayama et al. in 2002 on a large Japanese family with a Mendelian form of PD(Funayama et al. 2002). A linkage analysis revealed a PD locus within chromosome 12, which was named PARK8. In the subsequent two years, Paisán-Ruíz et al. and Zimprich et al. were working independently and have identified mutations at the PARK8 locus that segregate with two different families with familial PD (Zimprich et al. 2004, Paisan-Ruiz et al. 2004). Several subsequent studies have identified additional mutations in *LRRK2* segregating with familial PD. Furthermore, the clinical presentations and post-mortem analysis of individuals with familial PD having *LRRK2* mutation exhibit similarity with sporadic PD in terms of the symptoms and the pathological features of the disease, which highlight the significance of elucidating the physiological and pathological functions of LRRK2(Gandhi, Chen and Wilson-Delfosse 2009).

Later on, several GWAS have substantiated the importance of *LRRK2* in relation to idiopathic PD as they confirmed that the loci containing the *LRRK2* gene is a risk for developing sporadic PD(Bandres-Ciga et al. 2020). Consequently, *LRRK2* is involved in both familial and sporadic PD and studying the pathological mechanism by which *LRRK2* contributes to the development of PD could be of tremendous value in shedding some light on the pathogenesis of PD.

Currently, mutations in *LRRK2* are considered the most common cause of familial PD, representing 5% of familial PD and 1-2 % of idiopathic PD cases. Today, seven causative *LRRK2* mutations (I2020T, Y1699C, R1441C, R1441G, R1441H, G2019S

and N1437H) have been linked to PD in addition to several risk variants (G2385R and R1628P) of *LRRK2* that increase the risk of individuals to sporadic PD(Taylor and Alessi 2020).

Interestingly, PD is not the only disease associated with LRRK2. Crohn's disease (CD), Tuberculosis (TB) and Leprosy have also been reported to associate with *LRRK2* variants through GWAS(Wang et al. 2015a, Liu et al. 2011).

1.2.2 Structure and biochemistry

The identification of the PARK8 locus is associated with hereditary PD in 2002 initiated a series of studies that culminated in 2004 when *LRRK2* was first cloned by Paisan-Ruız and others(Paisan-Ruiz et al. 2004). The LRRK2 protein comprises 2527 amino acids with a molecular weight of around 286 kDa and is thought to exist as a dimer(Greggio et al. 2008). It belongs to the ROCO superfamily of proteins, which are generally characterised by several conserved domains, including the ROC (Ras of complex protein) domain, which possesses GTPase activity, and the COR (C-terminal of ROC) domain. In addition, LRRK2 domain architecture includes the presence of ARM (ARMadillo repeats), ANK (ANKyrin repeats), LRR (Leucine-Rich Repeats) and WD40 (tryptophan-aspartate repeats), which are thought to be mainly involved in maintaining protein-protein interactions. LRRK2 proteins also include a serine/threonine kinase domain(Lewis 2009). Those characteristics contribute to the complexity of LRRK2 biological functions and how it contributes to the pathomechanism of PD, CD, Leprosy and perhaps other disorders. An overall schematic of the LRRK2 domain structure is depicted in **(Figure 1-2).**

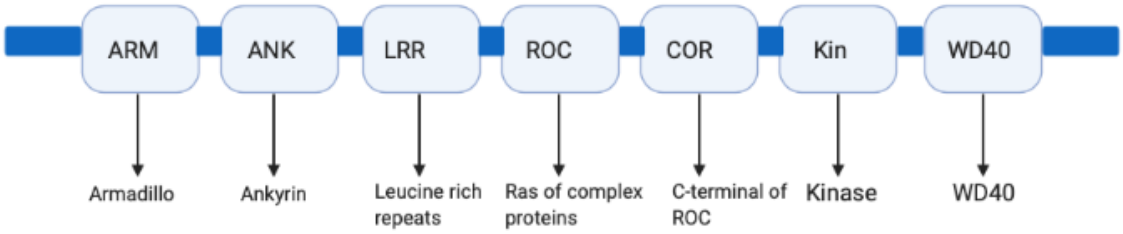

Figure 1-2 ***Schematic representation of LRRK2 structure generated by Biorender®***

1.2.2.1 LRRK2 kinase domain

The LRRK2 kinase domain has received the most attention within the LRRK2 structure by far for several apparent reasons. First, the most common mutation in *LRRK2* resides within the kinase domain's activation loop, whereby a glycine is substituted for serine at amino acid 2019 (G2019S). The G2019S mutation (and the I2020T) were reported to increase the activation capacity of the enzyme to phosphorylate its targets (discussed later)(West et al. 2005).

Second, the initial *in-vitro* and *in-vivo* studies have documented a gain of function in the kinase activity. It was hypothesized that perhaps the overactivity of the kinase enzyme could be the driving toxicity in PD. Moreover, Greggio and others documented in an *in-vitro* model that having an overactive kinase domain increased neural cells' tendency to form inclusion bodies and accelerate cell death. Interestingly, manipulating the kinase activity by having a mutant that abolished its activity resulted in lower toxicity(Greggio et al. 2006, Lee et al. 2010).

Third, developing small molecules that target the kinase domain is relatively approachable and potentially easy to design and optimize from a drug discovery

perspective. Consequently, LRRK2 seemed a "druggable" target. Several pharmaceutical companies and academic labs have developed different LRRK2 kinase inhibitors that presented promising data in preclinical studies, and a handful of them went into early phases of clinical trials(Williamson et al. 2017, West 2017).

The kinase domain of LRRK2 is a serine-threonine kinase that belongs to the mitogen-activated protein kinase kinase kinase (MAPKKK) family. The LRRK2 kinase domain phosphorylates proteins by transferring phosphate groups from adenosine triphosphate (ATP) to target proteins, changing their activation status and their cellular function. Kinases play an essential and consequential role in signal transduction pathways(Gandhi et al. 2009). In the case of LRRK2, the kinase domain is not only found to phosphorylate different heterologous substrates but also involved in phosphorylating the serine residues in the LRRK2 ROCO domain(Sheng et al. 2012).

The physiological substrates for the kinase domain of LRRK2 have been a subject for debate for more than a decade since the reporting of *LRRK2* as a causative gene for PD in 2004. Earlier reports mainly were employing co-immunoprecipitation assays or yeast two-hybrid screenings in mostly non-physiological context with several potential substrates identified, including endophilinA, p53, akt1, snapin, SQSTM1, auxillin and others(Soukup et al. 2016, Seol, Nam and Son 2019, Yun et al. 2013, Ohta et al. 2011). The LRRK2 kinase domain has also been reported to phosphorylate itself at Roc domain. Despite the plethora of earlier studies trying to identify LRRK2 substrates, the scientific community was sceptical since most of the studies were done in *in-vitro* settings and were not corroborated independently(Seol et al. 2019, Taylor and Alessi 2020).

However, the developments of specific LRRK2 kinase inhibitors and specific antibodies for the phosphorylated forms of potential substrates, and facilities for validation of endogenous substrates, along with advances in systemic proteomic analysis has culminated in the discovery of Rab GTPases as validated LRRK2 kinase substrates(Seol et al. 2019). Steger et al. used an elegant phosphoproteomical approach and identified T73 of Rab10 and S935 of LRRK2 site, as LRRK2 kinase substrates. Further examination revealed that the phosphorylation site in Rab10 (T73) is a conserved site among Rab proteins, and it was predicted that LRRK2 could have additional Rab proteins as substrates. Indeed, systematic tests of Rab GTPases have revealed Rab3A/B/C/D, Rab8A/B, Rab10, Rab12, Rab35, and Rab43 as *in-vivo* substrates and Rab5B/C and Rab29 as potential substrates(Steger et al. 2017, Steger et al. 2016).

1.2.2.2 LRRK2 GTPase domain

The LRRK2 GTPase domain is classified under the small G-protein superfamily of Ras-like GTPases (ROC). Generally, GTPases are enzymes that bind and hydrolyses guanosine triphosphate (GTP) to guanosine diphosphate (GDP) and act as molecular switches. They control a wide variety of biological processes. The LRRK2 GTPase enzymatic core is located within the ROCO domain, and they are similar to Ras proteins. Ras is a small GTPase protein that belongs to the G protein superfamily. G proteins, including Ras, act typically as signal transduction mediators activating and deactivating certain biological processes(Lewis 2009).

While the focus within the LRRK2 structure mainly was on the kinase domain, several observations highlighted the importance of the GTPase domain in relation to LRRK2: all *LRRK2* mutations segregating with familial PD except for G2019S and I2020T, are

in the GTPase domain (Y1699C, R1441C, R1441G, R1441H, and N1437H). Those mutations result in either a decrease in the GTPase activity or an increase in the affinity of LRRK2 to GTP or both, resulting in LRRK2 being present in the confirmation state where it is bound to GTP(Nixon-Abell et al. 2016). This is thought to be the “active or on“confirmation since the autophosphorylation at Ser1292 and substrate phosphorylation of Rab is enhanced three to four-fold(Purlyte et al. 2018).

Interestingly, there is a complex interplay between the kinase and GTPase functions. Mutations in these individual domains have been reported to have a consequential effect on the activity of the other. For instance, Genta ito and others manipulated LRRK2 genetically by introducing a mutation (T1348N) that prevents LRRK2 from binding to GTP. As a result, the kinase activity was abolished, implying perhaps a complex regulatory role for the GTPase in LRRK2 in mediating the kinase activity(Ito et al. 2007).

1.2.3 LRRK2 biological functions:

While it has been over a decade and a half since the identification and cloning of *LRRK2*, the exact physiological functions still remain elusive. Perhaps the complex multidomain structure of LRRK2 or dual enzymatic activity are playing a role in the this conundrum. Experts in the LRRK2 field puzzle over the identification of the substrate for the kinase enzyme, which in itself has been a daunting journey until recently. It has been long thought knowing the substrates will help to elucidate some of the mechanisms by which LRRK2 executes its physiological function.

LRRK2 is ubiquitously expressed throughout the body, with high expression levels in the lungs and kidneys. It is also expressed in immune cells (neutrophils, monocytes,

lymphocytes (T cells and B cells), the intestine and the brain, including the dopaminergic neurons(Berwick et al. 2019).

Several experiments that followed LRRK2 localisation within the cell have revealed a close association with organelle membranes and vesicular structures, indicating that LRRK2 is involved in autophagy and endocytosis.

1.2.3.1 Autophagy

Autophagy is a well-conserved sophisticated catabolic physiological process by which cells are able to remove cellular waste, including damaged, misfolded aggregated proteins and dysfunctional and damaged organelles(Albanese, Novello and Morari 2019). Extended life span has been suggested to be associated with consistent induction of autophagy(Pyo et al. 2013). By contrast, several neurodegenerative diseases, including PD and AD, are attributed to a common theme, which is misfolded proteins and a tendency of impaired autophagy(Albanese et al. 2019). Thus, extensive examinations of autophagy processes have been undertaken within the research community. It is broadly classified based on the mode of entry into three categories: microautophagy, chaperone-mediated autophagy(CMA) and macroautophagy(Dikic and Elazar 2018).

Microautphagy is whereby direct engulfment of substrates into the lysosomes happens without any mediator, and it is the least characterized and understood. CMA involves cargo sequestration of proteins with a specific sequence called KFERQ-like motif recognized by heat-shock HSC70 cytosolic protein forming a chaperone complex. After that, the complex translocates the tagged protein to the lysosomal lumen after binding to the lysosomal membrane receptor, lysosome-associated membrane protein 2 (LAMP2).

Macroautophagy(called autophagy thereafter), the most studied pathway, is a multi-step process regulated by the autophagy-related genes (Atg), which are involved in the formation of phagophore and autophagosomes. Autophagy is usually initiated by deactivating or inhibiting the mammalian target of rapamycin (mTOR), resulting in transcription of Atg and activation of the Ulk1 complex, which together with Atg products form phagophores. Phagophores engulf cellular waste and form autophagosomes. An essential step in the formation of autophagosomes is converting the cytosolic protein microtubule-associated protein 1 light chain 3 (LC3) 1 to LC3-II, which is commonly used as a marker for autophagy. The last step is the fusion with lysosomes. Lysosomal hydrolase activity and acidic environment degrade the content of autophagosomes(Albanese et al. 2019, Manzoni and Lewis 2017). An overview of the autophagy process is illustrated in **(Figure 1-3).**

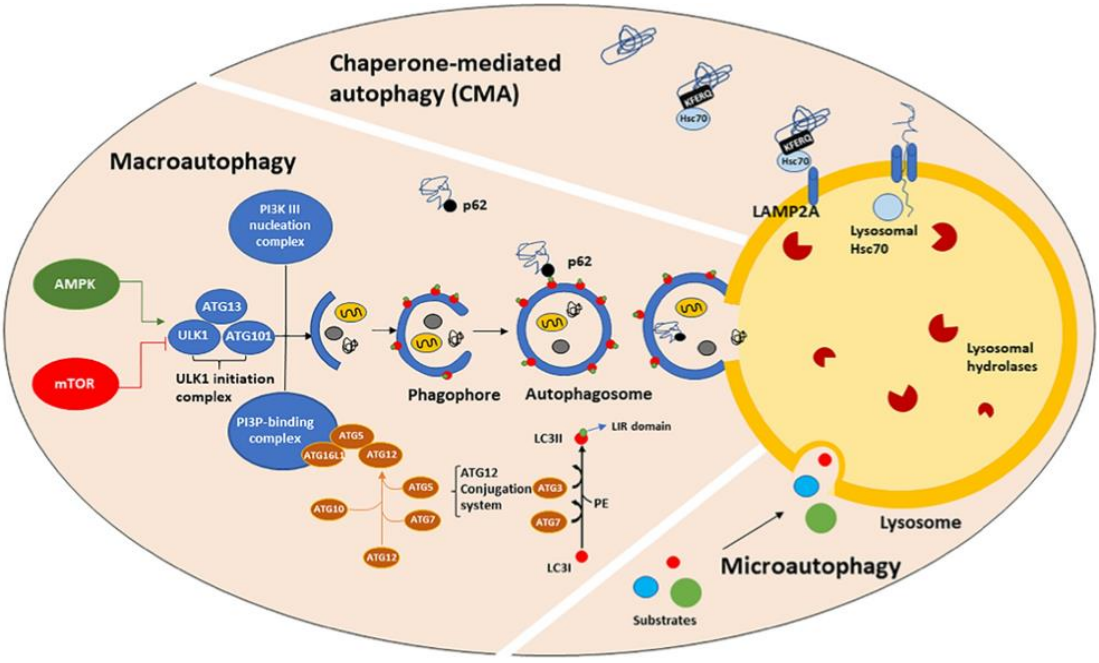

Figure 1-3 ***illustration of the three types of autophagy.*** *Figure adapted from (Albanese et al. 2019)*

The evidence that indicates a role of LRRK2 in the autophagic catabolic processes in both macroautophagy and CMA is overwhelming. One of the first studies that shed some light on the involvement of LRRK2 in macroautophagy was an *in-vitro* study in differentiated SH-SY5Y neuroblastoma cells. Transfection of mutant *LRRK2* G2019S constructs resulted in shortening of neurite processes associated with an increase of autophagic markers (LC3). Both of those observations were not reported in SH-SY5Y cells transfected with either wild type LRRK2 or control constructs. Remarkably, cells transfected with the kinase-dead mutant (*K1906M*) construct showed similar effects to the WT or the control group(Plowey et al. 2008).

Orenstein and colleagues showed that LRRK2 is a substrate for CMA. The pathogenic G2019S mutant tended to compromise and inhibit CMA in cultured cells, animal models, and induced pluripotent stem cell (iPSC)-derived dopaminergic neurons from patients with a familial *LRRK2* G2019S form of PD. Interestingly, likely as a consequence of compromised CMA, cells tended to compensate by upregulating LAMP-2A, an observation consistent with levels in the brains of patients with familial forms of PD(Orenstein et al. 2013).

One of the main misfolded proteins associated with familial and sporadic PD, α-Syn, is a substrate for CMA. An attractive mechanistic converging hypothesis is that mutant *LRRK2* could be causing malfunction of CMA processes causing α-Syn to accumulate and causing toxicity. This was supported by at least 2 independent studies(Orenstein et al. 2013, Ho et al. 2020). The involvement of LRRK2 in autophagy was also corroborated by the notion that LRRK2 kinase inhibition either by manipulating it genetically or pharmacologically resulted in alteration of this process(Henry et al. 2015).

1.2.3.2 Endocytosis, lysosomes and vesicular trafficking

Endocytosis is a fundamental physiological process whereby cells are able to move certain substances across different cellular membranes, including plasma membrane and organelle membranes, up to the lysosomes. It is an exceptionally tightly regulated process requiring a plethora of signalling components. Cells utilise endocytosis to transfer nutrients, regulate plasma membrane homoeostasis, and respond to extracellular cues(Kaksonen and Roux 2018)

Recently, there has been a consensus among the LRRK2 community about the physiological substrates for LRRK2, which turned out to be members of Rab GTPases(Steger et al. 2016, Taylor and Alessi 2020). The main functions of the Rab proteins are in the regulation and coordination of vesicular trafficking, including vesicle formations and movement along microtubules, membrane fusion and regulation of synaptic vesicle trafficking(Wandinger-Ness and Zerial 2014, Berwick et al. 2019).

Several studies substantiate the role of LRRK2 in vesicular trafficking. Shin et al. demonstrated several cues about the association of Rab5b and LRRK2. First, by using yeast two-hybrid assay, the authors showed that LRRK2 interacted physically with Rab5b. Second, LRRK2 was found to be co-localised with Rab5b in synaptic vesicles. Third, manipulating LRRK2 expression genetically either by overexpression or downregulation resulted in disruption of synaptic vesicular endocytosis in primary rat hippocampal neurons(Shin et al. 2008, Yun et al. 2015).

Another elegant report linking LRRK2 to Rab GTPases and endocytosis is a study conducted by Eguchi et al. showing LRRK2 co-localising with LAMP1, a lysosomal marker. The cells were challenged with chloroquine in a lysosomal stress cellular model. Chloroquine is an antimalaria agent, and it is used in laboratory settings to

induce stress in lysosomes. Stressed lysosomes were suggested to be one of the features of PD. Rab7L1(Rab29) was found to recruit LRRK2 to the lysosomal compartment, and downregulating Rab7L1 resulted in a reduction of LRRK2 expression. After that, LRRK2 phosphorylates its target substrates, Rab8 and Rab10 and recruit them to the lysosomes. The recruitment appears to be a kinase-dependent manner as pharmacological inhibition of LRRK2 kinase activity or using mutants phosphorylation sites in Rab8 and Rab10 prevented them from being recruited the lysosomes(Eguchi et al. 2018).

LRRK2 was also associated with late-stage endocytosis. It has been found that wild type LRRK2, and especially the pathogenic G2019S mutation, impaired the degradation of epidermal growth factor receptor (EGFR), and the deficit could be avoided with kinase inhibitors or expression of Rab8a(Gomez-Suaga et al. 2014). The association between LRRK2 and Rab8a has been corroborated in another study by Rivero-Rios et al showing that pathogenic G2019S mutation caused malfunctions in endolysosomal membrane trafficking that was rescued by expression of active Rab8a. Moreover, Rab8a knock-down mimicked the effect of the G2019S mutation on endolysosomal membrane trafficking as measured by a decrease in the epidermal growth factor (EGF) surface binding and EGFR degradation(Rivero-Rios et al. 2019). Taken together, those studies provided substantial evidence of the involvement of LRRK2 in the different stages of endocytosis and vesicular trafficking.

1.2.3.3 LRRK2 and cell signalling

Since LRRK2 is a large complex protein with 6 domains, four being mainly involved in protein-protein interaction (ARM, ANK, LRR and WD40) and two additional domains with enzymatic core activities, it is not surprising that it is involved in a wide range of

cellular signalling transduction pathways. Furthermore, LRRK2 possesses scaffolding characteristics manifesting in its protein-interacting domains(Price et al. 2018). For instance, proteins containing ANK repeats and WD40 domain are typically involved in cell to cell signalling and are involved in aiding in protein interactions and recognitions. The signalling pathways associated with LRRK2 are predicted and hypothesized based on LRRK2 interaction with particular signalling components. Elucidating and characterizing those pathways in health and disease might provide tremendous value in understanding how LRRK2 is involved in the pathogenesis of PD, CD and leprosy(Price et al. 2018). LRRK2 has been associated with multiple pathways, including but not limited to: Wnt, mitogen-activated protein kinase (MAPK), Rac/ p21-activated kinase (PAK), Akt, and protein kinase A (PKA) pathways, which mediate a wide variety of cellular biological functions, including neuronal development and haemostasis, synaptic transmission, immune response, autophagy and endocytosis(Harvey and Outeiro 2019, Price et al. 2018).

One example of the signalling pathways associated with LRRK2 is the PAK6-LRRK2 pathway. PAK6 is a member of the group of serine/ threonine kinases involved in the remodelling of the actin cytoskeleton and synaptic formations. LRRK2 was found to physically interact through its ROC domain and colocalize with PAK6. LRRK2 was also found to mediate the physiological action of PAK6, evidenced by a decreased neurite length when *LRRK2* is knocked-out *in-vivo*. Furthermore, LRRK2 was suggested to be part of a scaffolding complex involved in activating PAK6, and its downstream effector, LIM domain kinase 1(LIMK1), as *LRRK2* knockout mice displayed a decrease in the activation of PAK6 and LIMK1. Remarkably, post-mortem tissues from human brains from idiopathic PD and people with the *LRRK2* G2019S

mutation showed an increase in the phosphorylation of PAK6, suggesting a functional relationship between LRRK2 and PAK6(Civiero et al. 2015).

The MAPK kinase 4 (MKK4) - c-Jun terminal kinase (JNK) pathway, which is critical for neuronal function, has also been associated with LRRK2. In an *in-vivo* and *in-vitro* model of PD. Overexpression of *LRRK2* G2019S mutation resulted in an increase in the phosphorylation of the MKK4 and its downstream effectors (JNK and c-Jun) along with upregulation in the mRNA levels of its target genes *Bim and FasL*. Interestingly and in contrast to most studies in the field, the *LRRK2* G2019S transgenic model in this study displayed degeneration of the dopaminergic neurons in the SNc(Chen et al. 2012).

The glycogen synthase kinase 3 (GSK3β), a serine/ threonine kinase involved in wide variety of cell signalling pathways, has been associated with LRRK2 in several reports in different systems. Kawakami documented that LRRK2 interacted physically with GSK3β by co-immunoprecipitation and performed an *in-vitro* pull-down assay with recombinant proteins confirming the association, which seems to increase GSK3β kinase activity in a manner that is not dependent on the kinase activity of LRRK2. Furthermore, The SH-SY5Y cells overexpressing *LRRK2* G2019S have been shown to increase GSK3β mediated tau phosphorylation(Kawakami et al. 2014). The association between LRRK2 and GSK3β was also confirmed in another set of studies and will be discussed more in the Wnt signalling section(Lin et al. 2010a, Berwick and Harvey 2012b).

The transcription factor, nuclear factor kappa-light-chain-enhancer of activated B cells (NFκB), signalling has also been associated with LRRK2 in number of studies. NFκB is ubiquitously expressed in all cells, and it is thought to regulate about 500 genes. It

has a well-established role in innate and humoral immunity but has other cellular functions, as well(Wang, Nag and Zhang 2015b). In lipopolysaccharides (LPS) treated primary microglia culture, LRRK2 knock-down or kinase inhibition resulted in a decrease of proinflammatory cytokines associated with a reduction in NFκB signalling, which was probably due to LRRK2 being a negative regulator of protein kinase A (PKA)(Russo et al. 2015). The effects of LRRK2 knock-down on NFκB were further corroborated in BV2 cells and brain lysate of mice. In another study, Kim and others reported similar results in which the authors showed a decrease in NFκB transcriptional activity measured by luciferase assays in LRRK2 knock-down microglia(Kim et al. 2012). In both studies mentioned above, LRRK2 knock-down seems to suppress NFκ B transcriptional activity indicating LRRK2 could be a positive modulator of NFκB. In a subsequent study, Russo and others hypothesized that LRRK2 affect the NFκB signalling by perturbing the PKA activity. They suggested that inhibiting the kinase activity of LRRK2 lead to inhibition of phosphodiesterase 4 (PDE4), which in turn causes accumulation of c-AMP resulting in activating PKA. As a result, PKA phosphorylates the inhibitory subunit of the NFκB p50 subunit and causes its accumulation in the nucleolus resulting in the repression of NFκB target genes(Russo et al. 2018).

1.2.3.4 LRRK2 in the Immune system

LRRK2 is expressed in several immune cells and has been linked to biological and pathological functions germane to immune cells, such as regulating inflammation and cytokine release, phagocytosis and autophagy. Moreover, LRRK2 expression in cells was shown to increase after exposure to pro-inflammatory signals such as LPS. Furthermore, *LRRK2* genetic polymorphism have been linked through GWAS to CD, Leprosy and TB, in all of which immune cells and inflammation play a vital part.

Therefore, LRRK2 seems to mediate essential inflammatory and immune processes(Lee, James and Cowley 2017).

Indeed, several studies have been published pointing to a substantial role for LRRK2 in immune responses. For instance, LRRK2 expression in immune cells obtained from peripheral blood mononuclear cells (PBMC) from PD patients was increased compared to healthy matched control (Atashrazm et al. 2019, Cook et al. 2017). In addition, stimulation of bone-marrow-derived macrophages (BMDMs) and microglia with LPS resulted in an increase of LRRK2 expression(Hakimi et al. 2011, Moehle et al. 2012). A similar observation was recorded for B cells, T cells and monocytes when they were treated with interferon-gamma (IFN-γ)(Gardet et al. 2010, Thevenet et al. 2011). Interestingly, the increase in LRRK2 expression in response to inflammation is augmented by PD linked mutations. For instance, primary microglial cells obtained from adult mice with *LRRK2* R1441G mutation and challenged with LPS exhibited an increase in protein levels of LRRK2 compared with wild type(Gillardon, Schmid and Draheim 2012).

LRRK2 expression changes in immune cells could have biological implications. For instance, Dzamko and others documented that serum from asymptomatic *LRRK2* G2019S mutation carriers exhibited more peripheral inflammation compared to neurologically normal controls, and the inflammation was in line with idiopathic PD. interleukin (IL)-1β, Tumor necrosis factor-alpha (TNF-α), IL-6, IL-10, IL-12, and monocyte chemoattractant protein-1 (MCP-1) cytokines were elevated. Interestingly, cerebrospinal fluid (CSF) samples didn't significantly differ across the different groups(Dzamko, Rowe and Halliday 2016). The difference in cytokines release was corroborated in other *in-vivo* and *in-vitro* studies. Primary microglia isolated from mice bearing the PD associated mutation *LRRK2* R1441G displayed increased pro-

inflammatory cytokines IL-1β, TNF-α and IL-6 and decreased anti-inflammatory cytokine IL-10 release in response to LPS treatment compared to WT control(Gillardon et al. 2012). By contrast, *LRRK2* KO or inhibition of the kinase activity resulted in lower IL-1β and cyclooxygenase 2 (COX-2) cytokine release in primary microglia and BV-2 immortalized microglia cells(Russo et al. 2015). In addition, lymphocytes from spleen cultures from *LRRK2* KO mice secreted less IFN-γ and IL-17 in experimental autoimmune uveitis (EAU) relative to the WT control(Wandu et al. 2015).

Cytokine release perturbation is not the only associated consequence as a result of *LRRK2* mutation or LRRK2 kinase inhibition in immune cells. Many biological and pathological processes are affected. Phagocytosis, which is the ability of cells with myeloid lineage to engulf foreign particles, including pathogens, has been reported to be compromised. For instance, Hartlova and colleagues documented that genetic deletion or kinase inhibition of LRRK2 in BMDM and human iPSC-derived macrophages had a better control of Mtb replication and targeted them more efficiently into phagolysosomes(Hartlova et al. 2018). In addition, augmentation of phagocytic activity has been reported as a result of *LRRK2* G2019S mutation in macrophages obtained from the serum of PD patients and was confirmed in primary microglia culture from mice. Interestingly, *LRRK2* KO and LRRK2 kinase inhibition had the opposite effect (Kim et al. 2018). However, primary microglia culture obtained from *LRRK2* KO mice and challenged with *Mycobacterium tuberculosis* showed enhanced phagosome maturation and mycobacterial control. Moreover, this observation was confirmed *in-vivo,* where *LRRK2* KO exhibited enhanced innate immunity(Hartlova et al. 2018). The contradicting data could indicate LRRK2 has pleiotropic effects that could be immune cell or bacteria specific(Wallings and Tansey 2019).

1.2.4 LRRK2 pathological role

1.2.4.1 Overview

Despite the discovery and cloning of *LRRK2* more than a decade and a half ago, the exact molecular mechanisms that drive mutant LRRK2 toxicity remain elusive. While *in-vitro* and *in-vivo* studies have provided a tremendous wealth of information, those models don't recapitulate the exact pathomechanism of LRRK2 accurately.

1.2.4.2 LRRK2 in PD Pathology

A major challenge and conundrum in the PD community is that transgenic rodents expressing different mutant *LRRK2* forms do not recapitulate PD's motor symptoms and pathological hallmarks. Those animals, however, showed a consistent phenotype in lungs and kidneys related to aberrant autophagy(Rui et al. 2018). They also showed a decrease in dopaminergic transmission, indicating that perhaps the short life span of rodents (2-3 years) is simply not long enough to mimic the motor and pathological hallmarks of PD. Nevertheless, understanding how LRRK2 mediates the neurodegeneration in PD is of paramount importance since patients with familial forms of PD with *LRRK2* mutations display similar clinical and pathological hallmarks to idiopathic PD patients implying common pathogenesis between the sporadic and familial forms of the disease (Gasser 2009).

The quest to find a defined role for LRRK2 in PD pathogenesis is a daunting task that started more than a decade ago. The complexity is driven by LRRK2's multidomain structure and dual enzymatic activities. In addition, LRRK2 has been found to interact with a number of proteins implicated in PD physically or genetically, placing LRRK2 as a consequential protein in PD. Nevertheless, several studies have implicated pathogenic *LRRK2* mutations in aberrant synaptic transmission, adult neurogenesis

and alteration in signal transduction pathways (Esteves, Swerdlow and Cardoso 2014). However, there is an increasing evidence that LRRK2 mutant toxicity might be mediated by dysfunction in autophagy, endocytosis and the lysosomal system.

1.2.4.2.1 LRRK2 and the Autophagy-lysosomal pathway (ALP)

The evidence suggesting that malfunction of the ALP is a contributing factor in the pathogenesis of PD is overwhelming. Post-mortem studies on the human PD brain have shown aberrant expression of LC3-II, LAMP1 and LAMP2A and some members of the heat-shock protein family (such as hsc70 and hsp35), all of which are components of the ALP system(Chu et al. 2009, Alvarez-Erviti et al. 2010). Moreover, many genes associated with the ALP system are associated with PD. Examples include *VPS35*, *ATP6V0A1*, *ATP13A2*, *GBA* and lysosomal integral membrane protein type 2 (*LIMP2).* Importantly, *LRRK2* mutations have been documented to interfere within the ALP at different stages, impacting different cellular processes and hence been suggested to play a vital role.

LRRK2 has been documented to interact and colocalize with components of the ALP system. For example, Rab5, a Rab GTPase involved in the late stage of endocytosis, is indeed reported to interact with LRRK2 physically and functionally with PD associated mutants having a detrimental effect on synaptic functions (mentioned earlier in section 1.2.3.1). p62/sequestosome-1(P62), a protein critical in the formation of autophagosomes, is another component of the ALP system that has been reported to interact with LRRK2(Park et al. 2016). Additionally, the *LRRK2* G2019S mutation was shown to have a detrimental impact on neuritic processes, causing them to shorten and retract. Those anomalies were associated with aberrant changes in a couple of autophagy markers, including an increased in the autophagic vacuole in SH-

SY5Y neuroblastoma cells. Furthermore, silencing LC3B or Atg7 genes abolished the effects of the *LRRK2* G2019S effects on the neuritic processes and the increased autophagic vacuole suggesting that *LRRK2* pathogenic mutation is mediated via malfunction in the autophagic processes(Plowey et al. 2008).

The *in-vitro* observation was further corroborated *in-vivo* in several reports. The *LRRK2* G2019S KI mouse model has been reported to have elevated levels the autophagy marker LC3-II compared to WT mice(Yue et al. 2015). Fibroblasts isolated from PD patients with G2019S mutations exhibited an enhancement in the autophagic activity as measured by an increase in the accumulation of LC3-II, Beclin-1 and a decrease in the degradation of the p62 protein. Also, fibroblast expressing the *G2019S* mutation exhibited a higher degree of cell death when the autophagy processes were altered either by the autophagy inhibitor bafilomycin a1 or by starvation(Bravo-San Pedro et al. 2013).

It is well established that one of the PD pathological hallmarks, Lewy bodies, is made mainly of protein aggregate of α-Syn, which is implicated in a wide variety of pathological links to PD, and one of them is the ALP system. Interestingly, connections between α-Syn, LRRK2 and the ALP system have been reported in several studies. Expressing either *LRRK2-WT* or *LRRK2*-G2019S in *C.elegans* results in a decline in the autophagic function that is exacerbated when the *G2010S* mutant is co-expressed with α-Syn (Saha et al. 2015). A more physiologically relevant study was done on primary cortical neurons obtained from *G2019S* KI mice showing an increase in the accumulation of insoluble α-Syn aggregate that is associated with change in lysosomal microenvironments compared to WT control. By using live-cell Lysotracker dye, which enables the track of acidic organelles within the cells, primary cultures expressing *G2019S* mutation showed an increase in lysosomal number but a

decrease in their size that is associated with an increase in the lysosomal protein LAMP-2.

Furthermore, enzyme-linked immunosorbent assay (ELISA) analysis of α-Syn protein in the conditioned media from the G2019S primary culture exhibited an increase in the release of α-Syn compared to WT. The detrimental impact of the G2019S mutation on lysosomes phenotype and α-Syn degradation was ameliorated in the presence of the GSK2578215A, a specific LRRK2 kinase inhibitor(Schapansky et al. 2018). There are a plethora of studies documenting the impact of pathogenic mutation of *LRRK2* on α-Syn, suggesting a partial explanation of how pathogenic *LRRK2* mutations contributes to the pathogenesis of PD(Lamonaca and Volta 2020).

1.2.4.3 LRRK2 in Leprosy

Leprosy is a long-lasting infectious disease that is caused by the bacterium *Mycobacterium lepromatosis*. It is characterized by the presence of the skin lesions and deformities, and long-term complications can lead to neuronal damage in the extremities, skin, respiratory tract and eyes. While tremendous efforts have been made to eradicate the disease in the last century by the World health organization (WHO) and others, 210,758 new cases were reported in 2015. The past outbreak had ever lasting socio-economic ramifications that are still present today.

Interestingly, *LRRK2* has been nominated in several GWAS studies to be associated with leprosy. In Han Chinese population, single nucleotide polymorphism (SNP) in *LRRK2* gene variant rs1873613A/G has been associated with leprosy that was confirmed in a subsequent study. Furthermore, Type-1 reactions (T1R), which is a long-term complication of uncontrolled leprosy leading to everlasting nerve injury, has been associated with variants in *LRRK2*. Those. studies provide accumulating

evidence of the involvement of *LRRK2* in leprosy. However, there is still a scarcity of data regarding the ways *LRRK2* contributes to leprosy's pathomechanism (Berwick et al. 2019, Wang et al. 2015a).

Remarkably, *LRRK2* R1628P variant, which has been reported to be a risk factor for PD, appears to be protective against T1R, thereby acting as an antagonistic pleiotropic gene in 2 different diseases. Moreover, *LRRK2* R1628P variant appeared to abrogate the apoptosis induced by the bacterium *bacillus Calmette–Guérin* in RAW 264 macrophages, perhaps explaining the protective role *LRRK2* R1628P variant has in patients with leprosy(Fava et al. 2019).

1.2.4.4 LRRK2 in CD

CD, a type of inflammatory bowel disease (IBD), is a chronic inflammation that can affect some parts of the gastrointestinal tract. The complex interplay between genetic and environmental factors contribute to the disease. However, the exact cause is unknown.

In 2008, a meta-analysis of three GWAS had revealed an association between *LRRK2* and the pathogenesis of CD, and though the correlation was week , it was confirmed in several subsequent studies(Torres et al. 2017, Hui et al. 2018). Interestingly, Ken and colleagues have shown that *LRRK2* N551K and R1398H variants are protective against CD while the N2018D variant is a risk factor. The functional impacts of those genetic polymorphism were further investigated *in-vitro* in HEK cells and have revealed several observations. First, the *LRRK2* N2018D variant increases the kinase activity in a similar manner to the *LRRK2* G2019S mutation. Second, combination of *N551K* + *R1398H* and *R1398H* variants resulted in an increased GTPase activity. Third, acetylation of α-tubulin was impaired in the *LRRK2* N2018D variant. Fourth,

autophagic markers including SQSTM1/p62 and lysosomal PH were compromised in *LRRK2* N2018D variant. Most, if not all, those observations have been reported in the context of PD, and given the fact *LRRK2* is associated with PD, a common inflammatory component might be shared between CD and PD(Hui et al. 2018).

1.2.4.5 LRRK2 in Cancer

LRRK2 biological and pathological functions is not linked to PD and inflammatory disorders but also been suggested to be associated with cancer but the topic used to controversial(Allegra et al. 2014, Agalliu et al. 2015, Saunders-Pullman et al. 2010). PD traditionally has been associated with a lower risk of developing cancer(Bajaj, Driver and Schernhammer 2010). However, a couple of epidemiological studies in the first half of the last decade have suggested patients carrying *LRRK2* G2019S and R1441G mutation had an increased risk of developing cancer(Ruiz-Martinez et al. 2014). Moreover, *LRRK2* role within context of cancer is growing rapidly as more studies examining and sequencing tumour biopsies revealed several *LRRK2* variants as candidate associated gene(Parrilla Castellar et al. 2020, Jin et al. 2021, Cheung et al. 2021). Furthermore, a recent study reported an increased sensitivity and responsiveness of ovarian cancer cells to cytotoxic effects of Poly (ADP-ribose) polymerase inhibitors (PARPi) when LRRK2 kinase inhibitor is combined with PARPi. Additionally, examining biopsies from patient with ovarian cancer revealed that elevated LRRK2 expression is associated with poor prognosis and worse clinical presentation(Chen et al. 2021). Taken together, LRRK2 involvement in cancer is evident and it is expected that future studies will provide more insights into LRRK2 pathological rule in tumours.

1.3 Wnt signalling

1.3.1 Overview

Wingless/Int (Wnt) signalling pathways are conserved signal transduction pathways that consist of proteins that transfer the signal from outside the cell to mediate intracellular signalling executing a variety of cellular functions. Wnt signalling has been documented to be involved in embryonic development, neurogenesis, cell fate specification, migration, synaptogenesis, and mediating some immune-related biological functions(Zhang et al. 2011). Three signalling pathways have been characterised based on signalling components: the canonical Wnt pathway, the noncanonical Wnt / planar cell polarity (Wnt/PCP) pathway, and the noncanonical Wnt/calcium (Wnt/Ca^{2+}) pathway. Other noncanonical pathways are still emerging and being discovered and characterise. For instance, receptor tyrosine kinase-like orphan receptor-1 and -2 (ROR1/2) involved in cancer developments is a relevantly recently characterised noncanonical Wnt pathway (Wang 2009, Yu et al. 2016). Those pathways are activated upon binding of Wnt protein, which acts as a ligand to the fizzled receptor (FZD) on the plasma membrane. Wnt ligand-receptor interaction results in a conformational change which results in the initiation of intracellular signalling by activating the cytoplasmic scaffolding protein Disheveled (Dvl). Wnt proteins are highly conserved glycoproteins encoded by 19 genes and are approximately 40 kDa in size(Mukherjee and Balaji 2019). Schematic overview of Wnt signalling pathways are illustrated in the following (**Figure 1-4**).

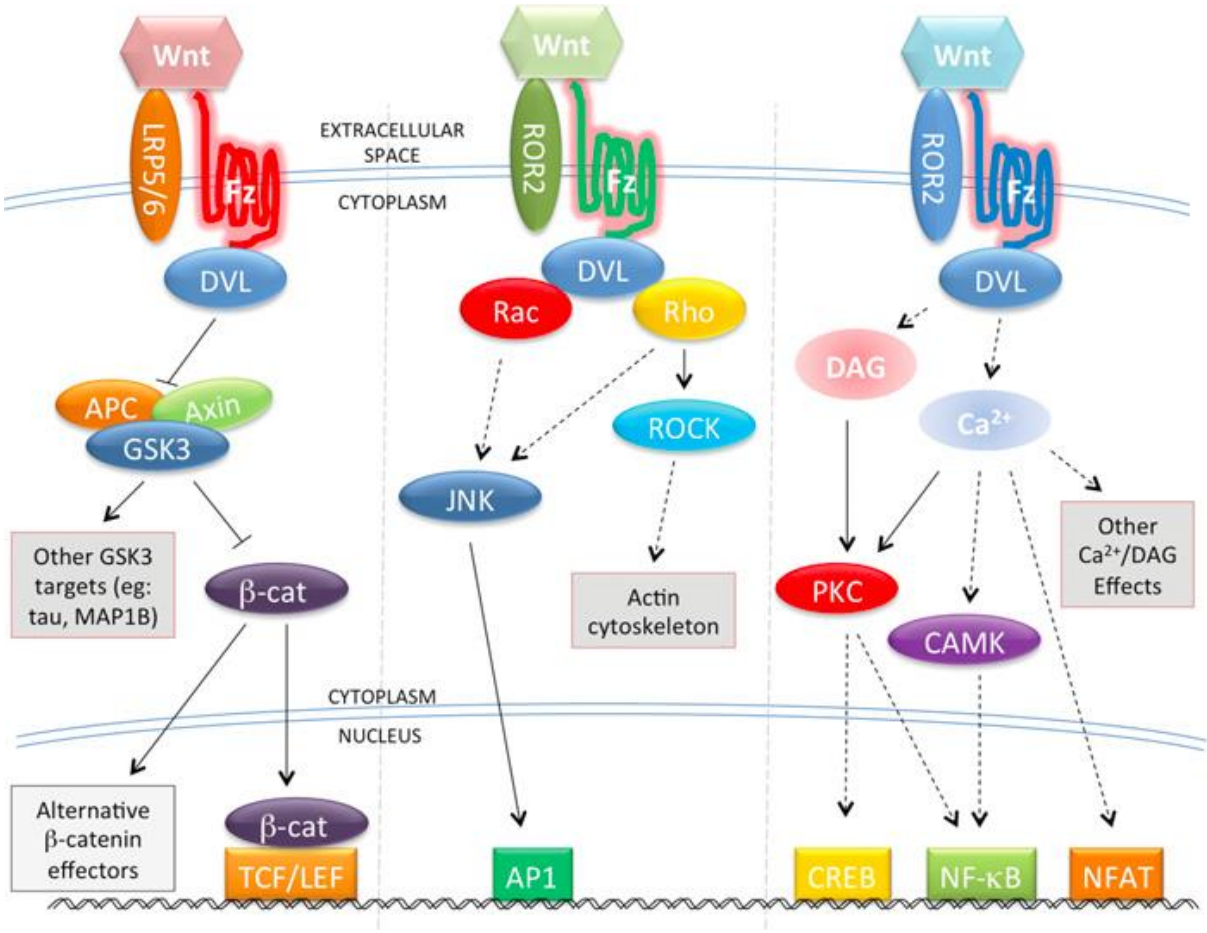

Figure 1-4 ***Schematic representation of Wnt signalling pathways:.*** *Figure adapted from (Berwick and Harvey 2012a)*

1.3.2 Canonical Wnt signalling

Canonical Wnt signalling, also called Wnt β-catenin signalling, is the best characterized of the Wnt signalling pathways. The molecular events that are involved in this pathway are depicted in **(Figure 1-4)**. In the absence of a stimulus (Wnt protein), β-catenin is continuously ubiquitinated and undergoes proteasomal degradation as a result of β-catenin being continuedly phosphorylated by GSK3β and Casein kinase1α(CK1α). GSK3β is part of a cytosolic complex known as the β-catenin destruction complex, which also contains the scaffold protein axin, the tumour suppressor protein adenomatous polyposis coli (APC), and CK1α. This complex

prevents the accumulation of β-catenin in the cytosol and subsequent translocation to the nucleus(MacDonald, Tamai and He 2009).

In the activated state, Wnt protein binds to FZD receptors and low-density lipoprotein receptor-related protein (LRP) 5/6 co-receptors. This results in the recruitment of DVL proteins and the β-catenin destruction (BDC) complex to the plasma membrane. Following this membrane localization, β-catenin accumulates in the cytosol and translocates to the nucleus. Here, β-catenin acts as a coactivator interacting with T-cell transcription factor/lymphoid enhancement factor (TCF/LEF) to initiate target gene transcription(MacDonald et al. 2009). More details outlining canonical Wnt signalling involvement in PD are given in section 1.3.5.3.

1.3.3 Planar cell polarity

The Wnt/PCP pathway name is derived from the initial studies on Drosophila, where mutations in the Wnt/PCP pathway components change the epithelial structures' orientation (Nubler-Jung 1987). It is β-catenin independent and uses the GTPases RhoA, Rac1 and others to transmit the signal from the extracellular components to tissue-specific downstream effectors, most notably, the JNK, which in turn result in the activation of activator protein 1 (AP1)-dependent transcription. In addition to the Wnt/PCP pathway's established role in cell polarity and movement and cytoskeletal rearrangements, its malfunctions have been linked extensively to tissue metastasis, angiogenesis, and cancer developments(Wang 2009). Another example of Wnt signalling components interacting with PD related proteins is LRRK2, which I will discuss later.

1.3.4 Wnt/Ca^{2+} pathway

The Wnt/Ca^{2+} pathway is the most well studied noncanonical Wnt pathway. Similar to the PCP pathway, it is an β-catenin independent but uses different signalling components and downstream effectors compared to the PCP pathway. The Wnt/Ca^{2+} pathway relies on releasing Ca^{2+} from intracellular stores through activation of various G proteins. The increase in the intracellular Ca^{2+} results in the activation of Ca^{2+} sensitive enzymes, namely the protein kinase C (PKC), calcineurin (CN), and calcium/calmodulin-dependent kinase II (CamKII). Those enzymes are involved in diverse cellular processes and activation of different transcription factors, including the nuclear factor of activated T-cells (NFAT), cAMP response element-binding protein(CREB) and the NF-κB (Jordan et al. 1988).

NFAT is a series of activity-dependent transcription factors containing at least four members: NFATc1, NFATc2, NFATc3, and NFATc4. They have been characterized first in the immune system, where they have a prominent role in mediating inflammatory responses (see immune section1.3.5), but they also mediate other processes in other systems (Vihma et al. 2016). NFAT has to be dephosphorylated by phosphatases to translocate from the cytoplasm to the nucleus and act as a transcription factor either alone or in association with other transcription factors to regulate the expression of target genes, which in turn mediate a wide variety of cellular processes that tend to be either cell, tissue or time specific. NFAT has been reported in the nervous system to regulate neurobiological development, synaptic plasticity, memory formation, nociception, and others(Quadrato et al. 2012, Cai, Chen and Pan 2013).

Interestingly, CN/NFAT signalling pathway has been reported to mediate the toxic effects of α-Syn. In HEK embryonic kidney cells and primary midbrain dopaminergic neuronal cultures overexpressing PD-related A53T mutant α-Syn, CN was shown to be overactivated as it exhibits an increase in the phosphatase activity. Moreover, there was an increase in the translocation of NFAT3c from the cytoplasm to the nucleus compared to WT- α-Syn groups. Remarkably, utilizing cyclosporine A (CsA) , an inhibitor of CN and a medication commonly used as immunosuppressant, result in the reduction of the toxicity induced by overexpression of A53T mutant α-Syn *in-vitro* and *ex-vivo,* suggesting that the CN/NFAT signalling pathway could be a contributing factor in mediating the harmful effects of α-Syn in PD(Luo et al. 2014).

1.3.5 Wnt signalling role in Immunology

Historically, research of Wnt signalling in the immune system was initially reported by immunologists to mediate the developments of T cells in the thymus. It was found that the presence of Wnt β-catenin signalling, specifically the Tcf1 and Lef1 response elements, is a requirement for the development of T cells in the thymus(Staal and Clevers 2003). Today, Wnt signalling pathways are recognized to play a substantial and pivotal role in the immune system. Their role starts in the development, regeneration and activation of immune cells, and it's even reported to mediate the inflammatory response during infection(Mukherjee and Balaji 2019, Gatica-Andrades et al. 2017). Dysregulation of the Wnt signalling has been linked to haematological malignancies, and Wnt signalling has been discussed in the context of cancer immunotherapy(Haseeb et al. 2019, El-Sahli et al. 2019). An illustration of Wnt signalling's roles in the immune cells is depicted in **(Figures 1-5).**

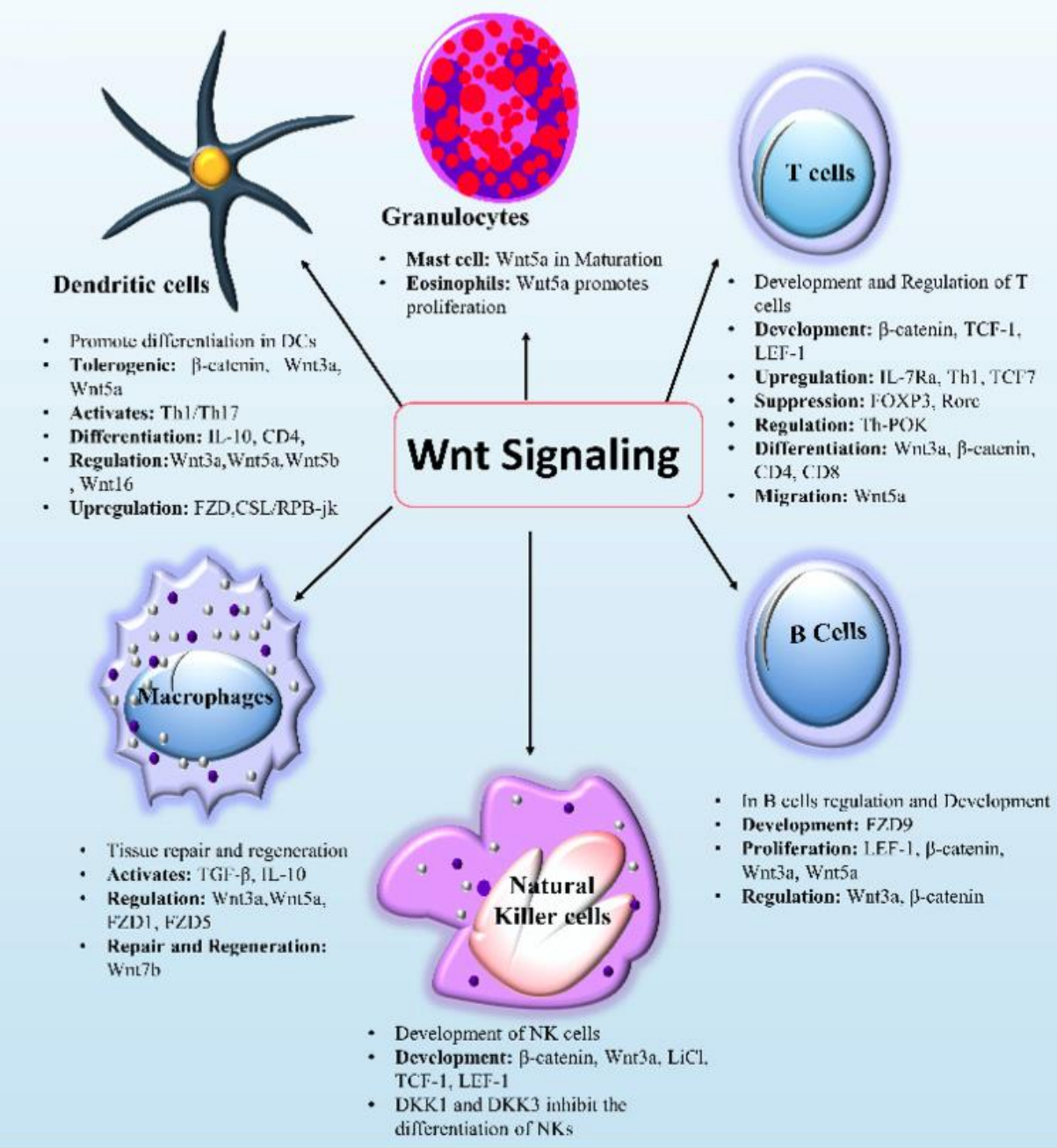

Figure 1-5 ***:Immune cell regelation and involvement of Wnt signalling****. Figure adapted from (Haseeb et al. 2019)*

1.3.5.1 Wnt signalling in Macrophages

Macrophages are cells that can engulf harmful substances, including microbial pathogen or part of them, cancer cells, cellular debris, in a process known as phagocytosis. They are mainly involved in the innate immune system but also plays a role in the adaptive immune system as they can act as antigen-presenting cells (APC)

to the T cells(Wynn, Chawla and Pollard 2013). In addition to the involvements of the immune responses, macrophages also have a significant role in tissue repair and haemostasis and inflammation. Macrophages have a unique set of biophysical and biochemical characteristics that make them malleable and adaptable according to the tissue microenvironment(Vannella and Wynn 2017).

Wnt signalling pathways are not just involved in mediating the immune response of macrophages but also contribute to the inflammatory processes and tissue remuddling and regeneration. Wnt5a, a Wnt protein that activates the noncanonical Wnt signalling pathways, has been associated with macrophages in several studies. In primary human macrophages challenged with LPS and different strains of mycobacteria, including *tuberculosis* and *avium*, Wnt5a mRNA expression was revealed to be upregulated 5 to 10 folds using gene screen based on the microarray. In addition, NF-κB and DVL-3 expressions were also increased. Interestingly the increase in the Wnt5a expression was not observed in Lymphocyte activated by either phorbol ester/calcium ionophore or antiCD3/CD28, suggesting the specificity to macrophage and myeloid lineage cells. Toll-like receptor 2 (TLR-2) and NF-κB appear to mediate the increase in Wnt5a expression.

Moreover, FZD5, a Wnt3a receptor, mRNA appears to be upregulated, and it was critical for the release of IFN-γ from lymphoid cells(Blumenthal et al. 2006). Wnt5a was also found to upregulated in patients with sepsis, psoriasis and rheumatoid arthritis(Pereira et al. 2008, Schaale et al. 2011).Wnt5a is not the only Wnt component associated with the immune response to infection as GSK3β has also been reported to play a critical part. In murine peritoneal macrophages challenged with *Francisella tularensis*, a bacterium that causes rabbit fever(tularemia), inhibition of GSK3β with Lithium chloride (LiCl) was associated with a reduction of the cytokines IL-6, IL-12p40

and TNF-α and increase in the IL-10, anti-inflammatory cytokines. The change in cytokines profile was associated with activation of NF-κB and CREB. Those observations were further confirmed *in-vivo* in mice challenged with *Francisella tularensis* and treated with lithium has an increase in the survival rate compared to the infection only group(Zhang, Katz and Michalek 2009). Those studies suggested Wnt5a and GSK3β play a vital part in mediating the host response to an infection in the macrophage cells.

Wnt signalling also contributes to the macrophages' tissue healing and regeneration properties, releasing matrix metalloproteinases and cytokines involved in the angiogenesis process(Weinberger and Schulz 2015). In an induced myocardial infarction (MI) model in mice, macrophages from the infarcted heart display distinct transcriptional profile in relates to Wnt signalling compared to control non-infarcted heart. An increase in the mRNA expression of WNT1-inducible signalling pathway protein 1 (WISP1), secreted frizzled-related protein 2 (SFRP2), Wnt5a and Wnt11 and a decrease in SFRP4 and WNT4 were observed in infarct-related macrophages. Remarkably, somatic deletion of the Wntless (WLS) gene, which is vital for Wnt ligand secretion, resulted in a significant favourable event post- myocardial infarction. Those events include releasing angiogenic factors that help cardiac vascularity, cardiac contractility improvements, and increased anti-inflammatory cytokines, including IL-2 and IL-6, suggesting that perturbing Wnt signalling in macrophages could improve cardiac function and repair(Palevski et al. 2017). Other studies documented the association between other Wnt signalling components and tissue repair and regeneration, such as Wnt7b and DKK2 in kidney regeneration after injury(Lin et al. 2010b), activation of Wnt signalling promote mucosal repair and regeneration in murine IBD model(Cosin-Roger et al. 2016).

In summary, the involvement of Wnt signalling in macrophages biological functions is evident, and it contributes to mediating inflammatory and immune response as well as tissue healing and regenerative processes.

1.3.5.2 Wnt signalling in T lymphocytes

T cells are part of the adaptive immune responses mediating cell-mediated immunity. They originate in the bone marrow and develop in the thymus gland. T cells recognise parts of the antigen presented by the APC, which are generally present on the major histocompatibility complexes (MHC). They can be classified broadly into T helper cells, so-called $CD4^+$ or T cytotoxic cells, called $CD8^+$ (Yang, Jeremiah Bell and Bhandoola 2010).

There is an extensive study linking Wnt β-catenin signalling to the T cells. Development and differentiation of thymocyte to T cells in the thymus is dependents on the presence of Tcf1 and Lef1 response elements (Staal, Luis and Tiemessen 2008). The involvements are on multiple levels, from early development to late-stage maturation of T cells and lineage commitment of both CD4+ and CD+8(Verbeek et al. 1995). Dickkopf-related protein 1 (DKK1), a Wnt β-catenin signalling antagonist, was shown to negatively affect the differentiation of T cells(Weerkamp et al. 2006). Furthermore, using the FZD decoy receptor in an *ex-vivo* model of thymic culture showing consistent disturbance in the thymopoiesis process. Wnt β-catenin signalling role in T cells is not limited to T cells development. For instance, $CD8^+$ cells differentiation and self-renewal properties appear to mediate in part by Wnt β-catenin signalling. The aforementioned studies highlight the significance of Wnt β-catenin signalling in T cells development and differentiation(Lin et al. 2016, Staal et al. 2001).

1.3.5.3 Wnt signalling in PD

Wnt signalling pathways have been documented to be involved in neural development and neurogenesis throughout life(van Amerongen and Nusse 2009). Furthermore, manipulation Wnt signalling genetically has resulted in behavioural and cognitive defects in mice(Liu et al. 2014). Additionally, several Wnt signalling genes have been linked to PD, Alzheimer's disease and other neurological and psychiatric diseases, which suggests that deregulation of Wnt signalling might be critical to the pathophysiology of those disorders(Berwick and Harvey 2012a).

A significant number of genes encoding for Wnt signalling components are involved in developing midbrain dopaminergic neurons, which are severely degenerated in PD. Interestingly, Cantuti-Castelvetri et al. did a gene expression analysis of SNc of post-mortem PD patients and found that β-catenin is downregulated compared to control samples(Cantuti-Castelvetri et al. 2007). This observation was also confirmed in an MPTP mouse model of PD in which L'Episcopo and others reported an acute downregulation of both FZD receptors and β-catenin in mice after exposure to MPTP(L'Episcopo et al. 2014). Several proteins that have been linked to PD, including LRRK2, Parkin, VPS35, Nurr1 and GSK3β have been documented to regulate or interact with Wnt signalling components(Berwick and Harvey 2012a). For instance, Rawal et al. reported that parkin co-localizes and interacts with β-catenin and overexpression of parkin resulted in a decreased level of β-catenin in MN9D and COS7 cells. Also, in adult Parkin null mice, β-catenin levels were significantly higher than WT controls(Rawal et al. 2009). Therefore, parkin is suggested to be involved in the regulation and clearance of β-catenin. Another example of Wnt signalling components interacting with PD linked proteins is LRRK2, which I will discuss in detail below.

1.3.6 Relationship between Wnt signalling and LRRK2

There is a growing body of evidence connecting LRRK2 to Wnt signalling. Sancho et al. documented the interaction between DVL and LRRK2 through the Roc-COR domain by utilizing a LexA yeast two-hybrid (YTH) system(Sancho, Law and Harvey 2009). Then, a series of immunoprecipitation experiments in mice revealed that LRRK2 interacts with β-catenin, GSK3β and Axin1 in addition to DVL, suggesting that LRRK2 may be a component of the BDC. Furthermore, stimulation of canonical Wnt signalling with wnt3a results in recruitment of LRRK2 to cellular membranes and association with LRP6 aiding in the formation of Wnt signalosomes. This would result in the stabilization of β-catenin and translocating to the nucleus inducing target gene transcription. Overall, these results suggest a function of LRRK2 as a scaffold protein in the core of canonical Wnt signalling(Nixon-Abell et al. 2016).

Interestingly, pathogenic *LRRK2* mutants including R1441G, R1441C, Y1699C and G2019S and the PD risk variant G2385R have shown to impact the strength of interaction of LRRK2 with GSK3β, LRP6 and DVL. Furthermore, those mutations decreased the canonical Wnt signalling activity as measured by luciferase-based reporter assays that measure luminescence produced as a readout of β-catenin induced transcriptional activation(Berwick and Harvey 2012b). Remarkably, the protective *LRRK2* variant, R1398H, increased canonical Wnt signalling, and it is associated with increased axonal outgrowth in primary cortical neurons, opposite to the effect of pathogenic mutations and *LRRK2* wild type overexpression(Nixon-Abell et al. 2016). Given the fact that decreased Wnt signalling was reported in neurodegenerative diseases in general and PD in particular, aiming to increase Wnt signalling might be an attractive drug discovery approach.

The action of LRRK2 on canonical Wnt signalling as β-catenin repressor is supported by the notion that LRRK2 knockout *in-vivo* and *in-vitro* results in the accumulation of β-catenin in the cytoplasm and increase in canonical Wnt signalling. Additionally, overexpression of LRRK2 causes an activation of canonical Wnt signalling, suggesting that LRRK2 is involved in suppressing β-catenin in the BDC(Berwick et al. 2017).

1.4 Hypothesis

Mutations in *LRRK2* have been first linked to PD. However, recently, GWAS studies established several *LRRK2* variants as risk factors for CD and increased susceptibility to leprosy, all of which have an immunological component (Fava et al. 2016, Wang et al. 2015a). Additionally, post-mortem PD brains revealed microglial activation and infiltration of leukocytes. Thus, studying the role of LRRK2 in immune responses could be of tremendous value. In addition, as Wnt signalling has been linked to PD, LRRK2 function and immune physiological and pathological function, I hypothesised that *LRRK2* genetic manipulation will impact the immune response that is associated with changes in Wnt signalling.

1.4.1 Aims and objectives

The main aim of the thesis is investigating LRRK2 inflammatory role and associated changes on Wnt signalling in macrophages and T cells.

The overall objectives of this thesis are:

1) Determine the inflammatory response differences between *LRRK2* genotypes using a battery of immune assays including the release and expression of cytokines, phagocytosis and ROS production.

2) Determine the associated changes in Wnt and NFAT signalling activity and modulator expression.
3) Explore possible mechanistic insights explaining differences between *LRRK2* genotypes in response to inflammatory challenges, including investigating a possible involvement of the well-established physiological LRRK2 substrate Rab10.

Chapter 2 Materials and Methods

2.1 Cell culture maintenance

SH-SY5Y neuroblastoma and RAW 264 macrophage cells were supplied in cryogenic tubes from American Type Culture Collection (ATCC) and were stored at -150˚ Celsius(C) until use. Handling the cells was always carried out under sterile conditions in a biological safety cabinet supplied with laminar airflow. Upon use, the cells were thawed for 2 minutes in a 37˚C water-bath followed by centrifugation at 1500 rounds per minute (RPM) for 5 minutes to remove the Dimethyl sulfoxide (DMSO). The supernatant was discarded, and the pellet was suspended in 1 ml of Dulbecco's Modified Eagle Medium (DMEM), which contains 10% fetal bovine serum (FBS), 2 mM L-glutamine, and 1% penicillin/streptomycin, henceforth referred to as DMEM. Then, the vial content was transferred to a T-75 flask containing 15 ml pre-warmed and equilibrated DMEM. The flask is then transferred to the MCO-18AC Panasonic CO2 incubator, where the temperature is set to 37˚C and the Carbon dioxide (CO2) level is set at 5%.

The cells were left in the incubator for 2-3 days until the cells were ~ 80-90% confluent. Passaging of the cells or sub-culturing them involved aspirating of the old DMEM and then washing the cells with sufficient volume of Hank's Balanced Salt Solution (HBSS) followed by a trypsinization step (adding 1-3 ml of trypsin) for 3-5 minutes until the cells were no longer attached to the flask. 10 ml DMEM was added to the flask followed by centrifugation at 1500 RPM for 5 minutes. The supernatant was discarded, and the pellet was suspended in 9 ml DMEM, and the cells were counted with a hemocytometer. Generally, cells were seeded at sufficient density to allow them to grow to 70 to 80% confluence in 2 to 3 days.

2.2 Luciferase assays

Luciferase is a general term for a group of enzymes present naturally in mammalian and murine organisms that produce light. They are present in a variety of organisms, including fireflies, copepods, jellyfish, and the sea pansy. They are thought to serve multiple purposes, including defence, mating, camouflage and feeding. Luciferase assay systems are widely popular reporter tools used in molecular biology and biochemistry. They can be used to track changes in gene expression and transcriptional activity. They have the capacity to catalyse the oxidation of the photon emitting from the substrate (e.g. luciferin to oxyluciferin), which results in the phenomena of bioluminescence(England, Ehlerding and Cai 2016). The assay principle is that the reporter gene expression (luciferase) is under the control of a promotor of natively expressed proteins of interest (TCF/LEF or NFAT in this thesis). Thus, the reporter gene expression and the bioluminescence are directly proportional to the expression of the protein of interest.

2.2.1 SH-SY5Y cells stably expressing the TCF/LEF-Luciferase reporter

The SH-SY5Y cells stably expressing the TCF/LEF-Luciferase reporter (SH-SY5Y-Luc) were generated previously by Dr Berwick(Granno et al. 2019). Briefly, M50 Super 8x TOPflash construct was digested using NotI-BamHI restriction enzymes liberating the TCF/LEF-responsive promoter and luciferase reporter, which were cloned into the mammalian construct pcDNA3(with the CMV promotor removed). The pcDNA3 has an antibiotics selection marker which is Geneticin(G418). SH-SY5Y cells were stably transfected with pcDNA3 containing TCF/LEF-responsive promoter and luciferase reporter, and the responsiveness to LiCl was confirmed. The cells were cultured in DMEM in addition to G418 (800 µg/ml).

2.2.2 Detecting luciferase activity in Live SH-SY5Y-Luc

To detect luciferase activity in living cells, cells were seeded into 6 or 24 well plates and allowed 24 hours to attach, followed by the indicated treatments in the results section. 70 or 200 µL (50 µg/mL) of the luciferase substrate D-luciferin (556877, Systems Biosciences) was added directly to 6 or 24 wells, respectively. After 20 minutes, the luminescent signal produced by living cells was measured using an *in-vivo* imaging system (IVIS) instrument (Perkin-Elmer®).

2.2.3 Detecting luciferase activity in Lysed SH-SY5Y-Luc

After cell lysis, the Dual-Luciferase Reporter Assay kit (E1960, Promega) was used following the manufacture instruction to detect luciferase activity in cell lysate. Briefly, I seeded the cells into 24 well plates at 70,000 density and allowed the cells to attach for 24 hours. After treating the cells with the indicated treatments in the results section, the growth media was discarded. The cells were washed with phosphate buffer saline (PBS) followed by the addition of 50 µL passive lysis buffer and a gentle rocking/shaking for 10 minutes. Finally, 10 µL of lysed cells were added to the pre-aliquoted 50 µL D-luciferin assay substrate, and the luminescent signal was measured by a Turner Instruments 20/20 luminometer.

2.2.4 Detecting the secreted form of luciferase

The SH-SY5Y cells and immune cells utilized in this thesis, including Raw 264 macrophages and T lymphocytes, were transduced with lentiviruses encoding the secreted form of the luciferase enzyme under the control of either TCF/LEF or NFAT response elements . The expressed luciferase is called Nanoluc®(Nluc), which is derived from deep-sea shrimp Oplophorus gracilirostris after several clever biomedical engineering tweaks optimizing the stability, bioluminescence, size and development

of a specific substrate (Furimazine) that gives bioluminescence 150-times brighter than traditional luciferases substrate. The result is an enzyme that is much more stable and easier to incorporate in viral and nonviral vectors due to its smaller size(England et al. 2016).

To detect the luciferase activity of secNluc, the Nano-Glo® Luciferase Assay System (N1110, Promega) has been used following the manufacture recommendation. Briefly, the 96 well plate containing cells of interest was gently shaken, and 10 µL of culture media was aliquoted into an opaque 96 well plate containing 80 µL of deionized water. Then, 10 µL of Nano-Glo Luciferase Assay Reagent containing the substrate furimazine was added. The plate was incubated in the dark for 3 minutes then transferred to the Glomax plate reader or IVIS to measure the bioluminescence.

2.3 Cell transfection

DNA transfection throughout this thesis was utilized using FuGENE HD Transfection reagent (E2311, Promega) according to manufacture recommendation. Cells were seeded into 6 well plate and were allowed to attach overnight. 3 ug of DNA was dissolved in 150 ul of OptiMEM(31985062, ThermoFisher) followed by adding 9 ul of FuGENE HD and incubated at room temperature for 15 min. The mixture was added directly into cells and incubated further 48-72 hours prior to downstream application.

For the siRNA experiments for knocking down the WLS protein, DharmaFECT-1® (T-2001-01,horison) was used according to manufacture protocol. RAW 264 macrophages were seeded in 6 well plate and allowed to be attached. 10 ul of 5 uM of the short interfering RNA (siRNA) was added to 190 ul serum-free media and incubated for 5 minutes. In a separate tube, 10 ul of the transfection reagent was added to 190 ul of serum-free media. The content of the siRNA tube was added to the

transfection reagent mix and incubated further for 20 minutes, after which the content was added directly to cells and incubated for 72 hours prior to further assays.

2.4 Quantitative polymerase chain reaction (qPCR)

qPCR, also called real-time PCR, is a powerful molecular biological tool based on PCR. In traditional PCR, a particular sequence within DNA or cDNA is copied thousands to millions of times exponentially utilising specific oligonucleotides (primers), heat-stable DNA polymerase, and a thermal cycling instrument. Quantification and detection of the desired PCR product occurs at the end employing gel electrophoresis, image analysis and comparison to known standards. In qPCR, the detection and quantification of the products of interest (amplicon) occur in real-time with the assistance of fluorescent reporters and a thermal cycler equipped with a fluorescent detector and energy excitement source. After each cycle, the fluorescent intensity is directly proportional to the amount of DNA, and the data collected can be analysed and used to quantify the starting material with great precision. qPCR has many applications in basic research, diagnostic settings and forensic science(Taylor et al. 2010).

qPCR was used for the quantification of gene expression. The main steps involved in the process are RNA extraction from the sample, followed by cDNA generation and plate setup for qPCR.

2.4.1 RNA purification

The first step in measuring the gene expression by qPCR is RNA purification, which was accomplished using the RNeasy Mini Kit (74104, Qiagen). The cells in 6 well plates were washed with PBS and then lysed directly by adding 600 µL of RLT buffer (lysis buffer) and then transferred to microcentrifuge tubes. The lysates were

homogenized by passing them through a blunt 20-gauge needle attached to an RNase-free syringe 3-5 times. 600 µL of 70% ethanol was added to the cell lysate and then transferred to a RNeasy spin column attached to a 2 ml collection tube and centrifuged for 15s at 13500 RPM, and the flow-through was discarded. 700 µL of RW1(washing buffer) was added to the RNeasy spin column and centrifuged again at the same speed for the same amount of time. 500 µL Buffer RPE was added to the RNeasy spin column and centrifuged for 15s, followed by adding another 500 µL Buffer RPE and centrifuged for 2 minutes to dry out the ethanol. Finally, the column was placed on a 1.5 ml collection tube and the RNA was eluted with RNase-free water, and the RNA concentration was determined using a Nanodrop (ThermoFisher). The RNA was either immediately used for downstream application or stored at -80 C°.

2.4.2 cDNA generation

mRNAs are not considered stable, and they are prone to spontaneous degradation by the RNAases, and they have to be converted to complementary DNA(cDNA) by the naturally occurring viral enzyme reverse transcriptase(RT). To this end, the SuperScript® III First-Strand Synthesis System for RT-PCR kit(1808005, ThermoFisher) was used according to manufacture recommendation. The RNA mixture was prepared by diluting the required concentrations of RNA(500 ng for RAW 264, 100 ng for BMDM and 30 ng for T cells) obtained in 0 in diethylpyrocarbonate (DEPC)-treated water, and then 1 µL of random hexamers (50 ng/ µL), 1 µL of dNTP(10 mM) were added to the tube and completed to 10 µL of DEPC-treated water. The tube was heated at 65°C for 5 min and then placed on ice for 1 minute. On a separate tube, cDNA synthesis mix was prepared by adding the following in the indicated order: 2 µL of RT (10x) buffer, 4 µL of 25 mM $MgCl_2$, 2 µL of 0.1M DDT, 1 µL of RNaseOUT (40 U/µL) and 1 µL SuperScript® III RT (200 U/ µL). The cDNA mix

was added to the RNA mixture and then was incubated for 25 min at 25°C followed by heating to 50°C for 50 min. The reaction is halted by heating to 85°C for 5 min followed by placing the tube on ice. 1 µL of RNase H was added and further incubated for 20 min at 37°C. The cDNA generation at this stage is considered complete and stored at -20°C until use.

2.4.3 qPCR plate setup and run

Each cDNA preparation from the RAW 264 and BMDM was diluted at 1:10 in ddH2O prior to being used in the qPCR reaction. cDNA from the Tcells was diluted 1:4. Each qPCR reaction contained 1.5 µL(10µM) forward primer, 1.5 µL(10µM) reverse primer, 5µl of nuclease-free water, 10 µL of iTaq™ Universal SYBR Green Supermix (1725120,Biored) and 2 µL cDNA was added at the end. The assay was done in triplicate in a microamp fast 96-well reaction plate (4346907, Thermofisher) and was loaded in the StepOnePlus® Real-Time PCR System(Thermofisher). β-actin and GADPH were used as reference genes for quantification purposes. The qPCR was set to run under default conditions according to manufacture recommendations which are depicted in (**Figure 2-1)**. The primers were designed by lab members (Dr.Andrea Wetzel, Timpson and Anthony) by using guidelines in the qPCR handbook by life technologies. The primers used in this thesis are shown in table Table 2-1.

Name	Sequence
β-actin	FWD: GCC AAC CGT GAA AAG ATG AC REV: GGC GTG AGG GAG AGC ATA G
COX-2	FWD: GGG CAG GAA GTC TTT GGT CT REV: TGA AGT GGT AAC CGC TCA G
NFAT1C	FWD: CGG GAA GAA GAT GGT GCT REV: CTG GTT GCG GAA AGG TGG TA
β-catenin	FWD: CAT TGG TGC CCA GGG AGA REV: GAT CA GGC AGC CCA TCA ACT
NFκB	FWD: GGG CAT TCT TTC AGA AGC FWD: TGG GTA GTT CGG TTC CAC AC
Axin-2	FWD: GCC GAC CTC AAG TGC AAA CT REV: GCC GGA ACC TAC GTG ATA A
GADPH	FWD: GCC CAG AAC ATC ATC CCT REV: GTC CTC AGT GTA GCC CAA GA
TNF- α	FWD ATG AGC ACA GAA AGC AGT REV AGT AGA CAG GTG GT
IFN- γ	FWD TCA GCA GCGACT CCT TTT CC REV TTC TTC AGC AAC AGC AAG GC
IL-2	FWD TTG TGC TCC TTG TCA ACA GC REV CTG GGG AGT AGG TTC CT
IL-4	FWD TCT GCS GCT CCA TGA GAA CA REV AAC GAG G1C ACA GGA GAA GG
DKK	FWD TCT ACC ACA TGG ACG AGG AG REV GGC AAC TTG GCA TTG TCA TC
WNT3A	FWD TTT GGA GGA ATG GTC TCT CG REV GAC CCC ACC AAG TAG GAA CC
WNT5A	FWD GTG CCA TGT CTT CCA AGT TC REV: TGC CTG TCT TCG CAC CTT

Table 2-1 Primers used in the qPCR experiments

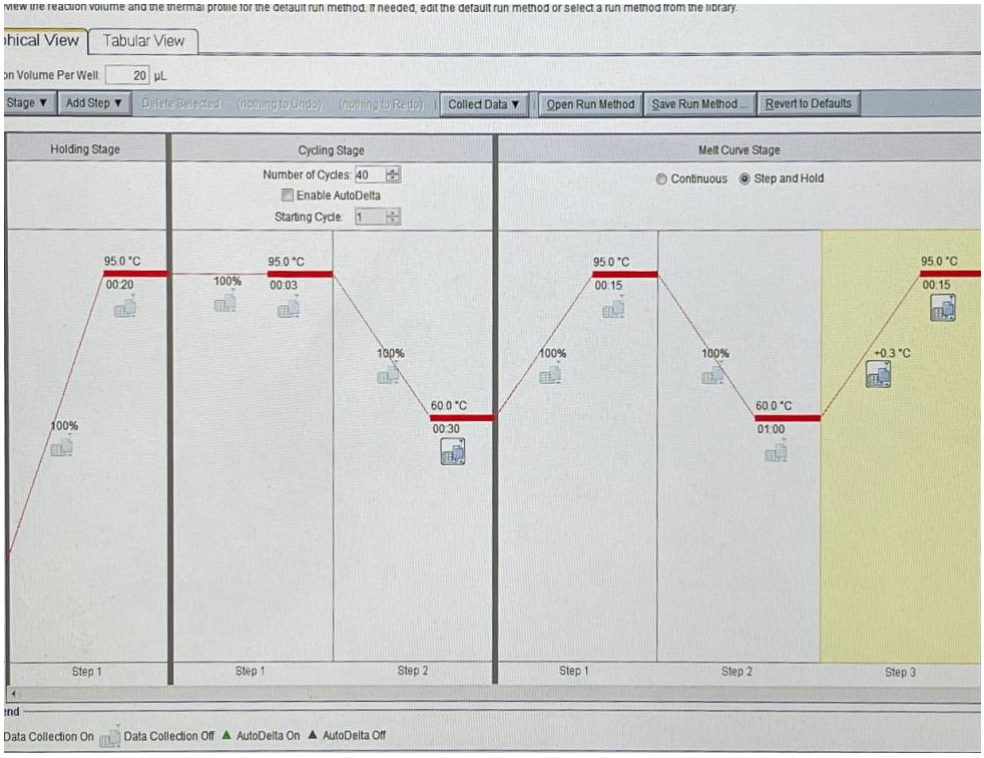

Figure 2-1 screenshot from the QPCR software depicting the QPCR running condition

2.5 Cell lysis, Protein separation and western blot

Throughout this thesis, protein separation was accomplished by using sodium dodecyl sulphate–polyacrylamide gel electrophoresis (SDS-PAGE), where protein (after being denatured) was run in a gel and separated based on their molecular weight. Prior to separation, the concentration of proteins in the samples were always quantified with Pierce™ bicinchoninic acid (BCA) Protein Assay Kit (23225, ThermoFisher) to ensure equal loading across different treatments. After the separation, Western blotting technique was employed. The stages in western blotting include transfer to the membrane, nonspecific blocking, primary antibody incubation, secondary antibody incubation and detection and imaging the blots.

2.5.1 Cell lysis and BCA assay

The cell lysis buffer used consists of 150 mM NaCl, 50 mM Tris pH 7.5, 5mM EDTA and 0.25% nonyl-phenoxypolyethoxylethanol-40 (NP-40). Prior to using the lysis buffer, a protease inhibitor tablet (11836170001, Roche) was added to a 20 ml lysis buffer to prevent internal protein degradation due to the proteolytic activity of the proteases. In addition, Halt phosphatase inhibitor (78420, Therofisher) was used (1:1000) to preserve the phosphorylation state of proteins. 1 ml of cell lysis buffer was used for 100 mm dishes and 300 ul for 6 well plate.

Cells were seeded in either a 100 mm dish or 6 well-plate and were 80-90 % confluent at the time of collection and lysis. For attached cells, the media was removed, and the cells were washed twice with ice-cold PBS. 1 ml or 300 µL of lysis buffer was added to the plates, and they were gently swirled before cells were collected with the aid of a cell scraper to pre-chilled microcentrifuge tubes. For suspended cells, the media containing cells was removed and collected in 15 ml falcon. The remaining cells were scraped in PBS and added to the same 15 ml falcon tube used for collecting suspending cells. The cells were centrifuged for 5 min at 1500 RPM. The supernatant was discarded, and the pellet was washed with PBS followed by the addition of 1 ml of cell lysis buffer and the lysates were collected in pre-chilled microcentrifuge tubes. The cell lysates were incubated in ice for 5 min followed by centrifugation for 10 min at 4°C to remove any cell debris and particles, and the cell lysates were frozen at -20°C until use.

2.5.2 SDS-PAGE and electrophoresis

Prior to loading the samples into the SDS-PAGE gels, proteins need to be denatured and unfold to be accessible for antibodies. To this end, two commercially available

reagents, NuPAGE® LDS Sample Buffer and NuPAGE® Sample Reducing Agent(NP0007&NP0004, Thermofisher), containing lithium dodecyl sulfate (LDS) and dithiothreitol (DTT), were used. From each sample, a volume containing 10-30 µg of protein was pipetted into pre-chilled tubes containing 7.5 µL LDS Sample Buffer(4x) and 3 µL DTT and completed to 30 ul with water. Thereafter, samples were heated for 10 min at 95 °C in an Eppendorf ThermoMixer®, followed by resting at RT for 5-10 min to cool. The samples then were loaded (30 µL for each lane) into pre-made gels, Bolt™ 4 to 12%, Bis-Tris (NW04125BOX, Thermofisher), which were fitted in an electrophoresis chamber (Mini Gel Tank, Thermofisher) filled with NuPAGE® MOPS SDS Running Buffer (50 mM MOPS, 50 mM Tris Base, 0.1% SDS, 1 mM EDTA, pH 7.7). A molecular weight ladder was used for identifying specific protein bands (5 µL, Amersham™ ECL™ Rainbow, Merk). The gel was run at 100 volts for 1.5-2 hours.

2.5.3 Transfer

After electrophoresis, proteins need to be transferred to a suitable membrane for subsequent immunoblotting and development. This can be accomplished by placing the gel in an electric field and passing electric current from the gel to the membrane. The gels were removed from the pre-casting plastic vehicle and put into a Trans-Blot® SD Semi-Dry Electrophoretic Transfer Cell (Biorad) containing a transfer stack and a 0.45 µm pore Immobilon polyvinylidene fluoride (PVDF) membrane above them. After the gel is placed, another transfer stack was placed, forming what is commonly named a semi-dry transfer sandwich **(Figure 2-2).** The transfer stacks were soaked in a transfer buffer prior to placing them in the sandwich, and the PVDF membrane was soaked in methanol to activate it and help protein binding. The semi-dry transfer ran at 25V for 15 min.

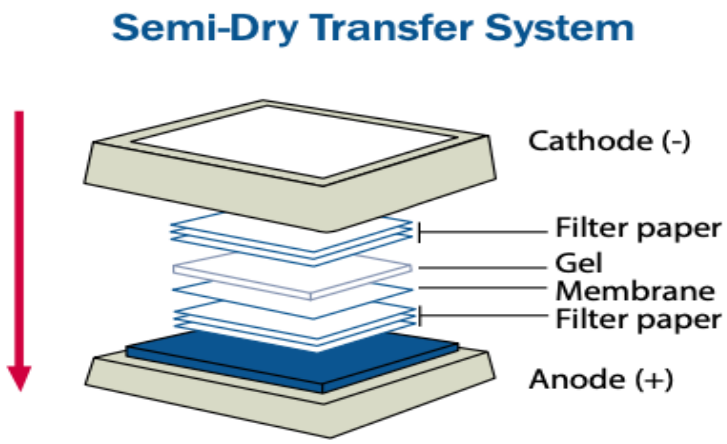

Figure 2-2 Illustration of semi-dry transfer setup

2.5.4 Blocking and primary antibody incubation

The blocking stage is essential to prevent non-specific binding in the subsequent steps. The membranes were placed in a container containing 10 ml of 5% skimmed milk dissolved in Tris-buffered saline-Tween 20 (TBST - 50 mM Tris-HCl, pH 7.4, 150 mM NaCl, 0.1% Tween 20) for 1 hr at room temperature or overnight at 4°C. Following the blocking periods, membranes were washed three times with TBST, with each wash lasting 5-10 min.

The primary and secondary antibodies were dissolved in 5% skimmed milk in TBST according to the manufacture recommended concentration listed in table 3-2. After the membranes were washed, the primary antibodies were added and incubated for 1 hr at room temperature or overnight at 4°C. Another extensive washing with TBST is performed three times. After that, the secondary antibodies were added, and the membranes were incubated for 1 hr at room temperature, followed by extensive washing.

2.5.5 Membrane development and imaging

The secondary antibodies employed for western blot in this thesis are conjugated to horseradish peroxidase (HRP) enzyme, which can catalyse the oxidation of substrates (luminol) to produce prolonged chemiluminescence that can be visualised using a chemiluminescence imager. Each membrane was subject to the 200-500 µL of either SuperSignal® West Femto or Pico (34094& 34579, ThermoFisher). Then, the membranes were incubated in the dark for 1min and placed into a GeneGnome® XRQ Chemiluminescence imager. The exposure time was adjusted based on the resulting antibody signal partially related to antibody specificity and antigen abundance.

Antibody	Company	Catalogue No	Diluting used
Anti- β-actin	SIGMA	A1978	1:2000
Anti-LRP6	Cell signalling	2560S	1:1000
Anti-pLRP6	Cell signalling	2568S	1:1000
Anti-NFAT	Cell signalling	4389S	1:2000
Anti-NKκB	Cell signalling	ab16502	1:2000
Anti-COX-2	Cell signalling	12282	1:1000
Anti-β- catenin	Merck Millipore	05-665	1:1000
Anti-$p\beta$catenin	Cell signalling	4176S	1:1000
Anti-LRRK2	Abcam	MJF-2	1:2000
Anti-pLRRK2	Abcam	ab172382	1:2000
Anti-WLS	Abcam	ab82897	1:1000
Anti-TLR4	Abcam	ab13556	1:500
Anti-AXIN-2	Abcam	ab109307	1:1000
Anti-RAB10	Abcam	ab237703	1:1000
Anti-pRAB10	Abcam	ab230261	1:1000

Table 2-2 Antibodies used in western blot

2.6 The Griess assay

Nitric oxide (NO), a free radical and ROS, is an important signalling molecule with many physiological and pathological functions. In macrophages, NO plays an essential role in host defence and is released upon activation to kill tumour cells and pathogens (Kvam and Moan 1990). While it is technically challenging to measure NO concentration directly as it is extremely unstable, measuring its metabolite nitrite (NO_2^-) has been a reliable measure of NO and been used extensively in the literature. To

this end, I used a commercially available kit (G2930, Promega), the Griess Reagent System. The assay principle is based on converting sulfanilamide and N-1-napthylethylenediamine dihydrochloride (NED) to an Azo compound **(Figure 2-3)** that has a distinctive purple colour that can be quantified spectrophotometrically, and the darker the colour, the higher the concentration of NO_2^-.

Prior to conducting the Griess assay, 25 µL of culture media from different treatments were aliquoted, and a BCA assay was carried out to ensure samples had equal protein concentration. The Griess assay was carried out according to manufacture specifications. After the cells were treated for 24 hr with LPS, 50 µL of culture media was aliquoted in a 96 well plate followed by an addition 50 µL sulfanilamide solution and incubated in the dark for 10 min. 50 µL of NED Solution was added and incubated 10 min further protected from light. The absorbance was taken at 550 nm with a Glomax® plate reader. For each experiment, a dilution series of known concentrations for the Nitrite dissolved in culture media were added and subjected to the same treatment as the samples and were used to generate a standard curve to help calculate the concentration of Nitrite in the experimental samples.

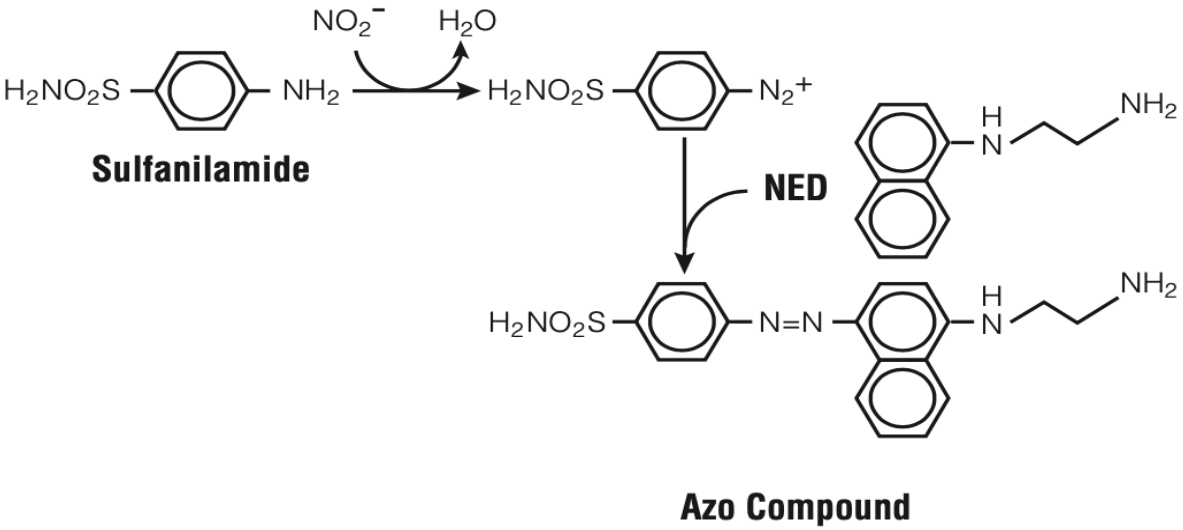

Figure 2-3 Principal reaction of Griess Assay. *Figure adapted from Promega handbook*

2.7 Cytokine's detection

For chemokines and cytokines detection, I have used the Mouse Cytokine Array Panel A kit(ARY006, R&D system). The assay provides nitrocellulose membranes where capture antibodies are spotted in duplicate, and associated blocking and washing buffers are included. The sample (culture media in this thesis, see 4.2.8.1.1) is mixed with a cocktail of biotinylated detection antibodies and applied directly into the membranes. Streptavidin-HRP and chemiluminescent detection reagents are used to develop the membranes, and the intensity of the light (chemiluminescent) produced by each spot is proportional to the amount of the cytokines/chemokines present in the sample. A schematic diagram of the membranes is depicted in **(Figure 2-3),** and the spot coordinates corresponding to the particular cytokines/chemokines are shown in Table 2-3.

The assay was carried out according to the manufacture recommendation with slight modifications. Prior, a BCA assay was conducted, ensuring an equal concentration of protein. Assay buffer 6(blocking buffer) was incubated with the nitrocellulose

membranes in the 4-Well Multi-dish for 1 hr at room temperature. 1 ml of samples were mixed with 1 ml assay buffer 5 followed by the addition of 15 µL of cytokine array detection antibody cocktail and incubated for 1 hr at room temperature. Assay buffer 6 was removed from the multi-well, and the sample/antibodies cocktail were added and incubated overnight at 4°C on the rocking platform shaker. The membranes then were washed extensively three times with wash buffer followed by the addition of 2 ml of streptavidin-HRP diluted by assay buffer 6 and incubated for 30 min at room temperature. Thereafter, the membranes were washed three times and then the membranes were placed on the GeneGnome® XRQ Chemiluminescence imager platform and aligned vertically. SuperSignal® West Femto (1ml) was added to the membranes, and a series of images were taken at different exposure times, and 1 min was found to be the optimal exposure time.

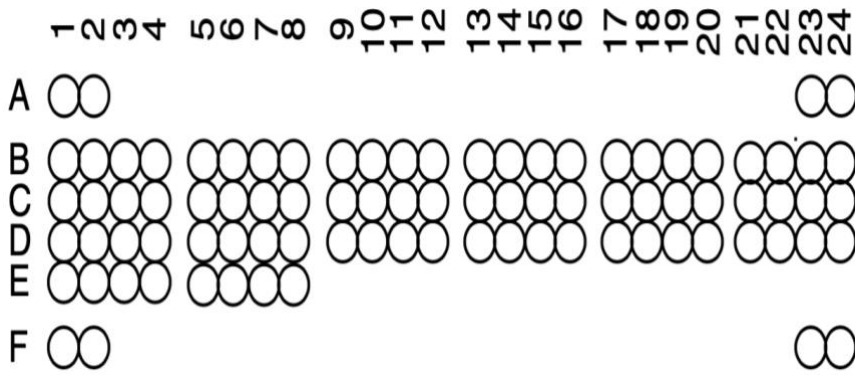

Figure 2-4 ***Schematic diagram of the nitrocellulose membranes showing capture antibodies***

Coordinate	Target	Coordinate	Target
A1, A2	Reference Spot	C17, C18	IL-16
A23, A24	Reference Spot	C19, C20	IL-17
B1, B2	BLC	C21, C22	IL-23
B3, B4	C5/C5a	C23, C24	IL-27
B5, B6	G-CSF	D1, D2	IP-10
B7, B8	GM-CSF	D3, D4	I-TAC
B9, B10	I-309	D5, D6	KC
B11, B12	Eotaxin	D7, D8	M-CSF
B13, B14	sICAM-1	D9, D10	JE
B15, B16	IFN-γ	D11, D12	MCP-5
B17, B18	IL-1α	D13, D14	MIG
B19, B20	IL-1β	D15, D16	MIP-1α
B21, B22	IL-1ra	D17, D18	MIP-1β
B23, B24	IL-2	D19, D20	MIP-2
C1, C2	IL-3	D21, D22	RANTES
C3, C4	IL-4	D23, D24	SDF-1
C5, C6	IL-5	E1, E2	TARC
C7, C8	IL-6	E3, E4	TIMP-1
C9, C10	IL-7	E5, E6	TNF-α
C11, C12	IL-10	E7, E8	TREM-1
C13, C14	IL-13	F1, F2	Reference Spot
C15, C16	IL-12 p70	F23, F24	PBS (Negative Control)

Table 2-3 Mouse Cytokine Array coordinates

2.8 Animal husbandry and general information

All mice of the C57BL/6J background were housed and bred at University College London (UCL), animal biological service unit at the School of Pharmacy. Handling of animals was in compliance with the UCL Ethics Committee and approved by the home office as detailed in the relevant project license 80/2486 (Kirsten Harvey). *LRRK2* KO and *LRRK2* G2019S were bought from the Jackson Laboratories (Yue et al. 2015, Lin et al. 2009). Regular genotyping of mouse tissue was performed in our lab by DNA extraction followed by PCR and agarose gel electrophoresis to confirm the genotype of animals.

2.9 Isolation of the splenocytes

Splenocytes were collected from male mice aged 8 to 12 weeks. Mice were euthanised by placing them in chambers connected to a CO2 gas tank which supplied an increasing dose of the gas, ensuring a painless death and then followed by cervical dislocation. The mice were then placed on a dissection board sprayed with 70% ethanol. All surgical instruments were autoclaved and submerged in 70% ethanol prior to using them to extract the spleen. After the animal was euthanised and placed on its back, the fur was sprayed with a slash of alcohol, followed by removing a small amount of fur and cutting a small incision into the left side of the abdominal cavity. The spleen was removed and trimmed of excesses fat and placed immediately into a 10 cm dish containing ice-cold PBS supplemented with a 5% FBS.

The spleen was then cut into small pieces (about 1mm in size), and a 4 ml spleen disassociation medium (07915, stemcell technologies) was added. This medium contains proteases and collagenases enzymes to help digest the connective tissue. After that, the spleen fragments were homogenised, mixed and incubated for 30 min

at room temperature and gently shaken on a rocking platform. EDTA was added to a final concentration of 10 mM and incubated for 5 min further. A smooth suspension was obtained by passing the spleen fragments through a 16-gauge blunt-end needle attached to a 3-ml syringe several times. The suspension was then poured into a 50 ml falcon tube attached to a cell strainer (100 µm), and 10 ml of Roswell Park Memorial Institute (RPMI) medium was additionally used to wash any remaining cells in the tube. Finally, the suspension was centrifuged at 300 x g for 10 minutes, and the supernatant was discarded. The pellet was suspended in a freezing medium (90% FBS and 10% DMSO), and the cells were placed in liquid nitrogen until further use.

2.10 T cells purification and characterisation

The T cells were isolated from splenocytes using a commercially available kit, the Pan T cell Isolation kit II (130-095-130, Miltenyl biotech). The principle of the isolation process is based on labelling unwanted cells with a cocktail of biotin-conjugated antibodies that recognise antigens not expressed on the T cells (CD11b, CD11c, CD19, CD45R (B220), CD49b (DX5), CD105, Anti-MHC-class II, and Ter-119) and then subjecting them with anti-biotin MicroBeads®, enabling indirect magnetic labelling. The cell suspension is then passed through a column based on a magnetic field where all unwanted cells are retained in the column, and the flow-through fraction represents the enriched untouched T cells.

The process was carried out following the manufacture recommendation. Briefly, splenocytes were defrosted, and 5 ml of RPMI media was added, followed by cells being counted by haemocytometer. Typically, between 70-90 million cells per spleen are present, and the volumes of buffers and reagents were adjusted according to the number of cells present in the sample. Splenocytes were then centrifuged at 300 g for

5 min, and the supernatant was discarded. The pellet was suspended in 40 µL of MACS® buffer (0.5% bovine serum albumin, 2mM EDTA in PBS,) per 10^7 cells followed by the addition of 10 µL/10^7 cells of biotin-Antibody Cocktail and incubated in the refrigerator for 5 min. 30 µL/10^7 cells of MACS® buffer followed by 20 µL/10^7 cells of anti-Biotin MicroBeads and the cells were incubated for 10 min in the fridge. The LS column was placed in the magnetic field within the MACS® separator and washed with 3 ml of MACS® buffer prior to applying the cell suspension**(Figure 2-5**). The flow-through fraction was collected and counted, representing the enriched untouched T cells. The LS column was then removed from the magnetic field, and the retained cells were eluted with 3 ml MACS® buffer representing the negative fraction or the non- T cells. All cells were culture in RPMI medium supplied with 10% FBS and 1% P/S for subsequent application.

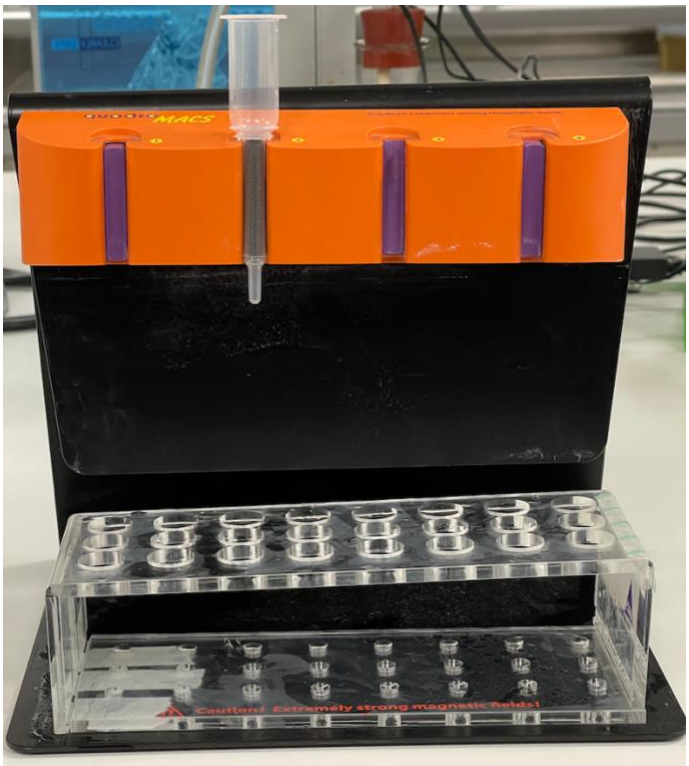

Figure 2-5 MACS® separator showing the LS column placed in the magnetic field

For T cell characterisation and determination of the purity, antibodies conjugated to fluorophore against CD+3, specific for T cells and CD+45, a non-specific marker of hematopoietic origin cells including B cells, T cells and dendritic cells were used to stain the cells and flow cytometry was used to determine the percentage of cells having CD+3 only, CD+3+CD+45, CD+45 only and non-stained cells.

The process of staining was carried out following the manufacture recommendation. After the separation and purification steps mentioned above, the cells were centrifuged and counted, and 10^6 cells were suspended in 45 µL of MACS® buffer followed by the addition of 5 µL of antibody and incubated for 10 min in the refrigerator. 1 ml of MACS® buffer was added, and the cells were centrifuged, and the pellet was suspended in 4% paraformaldehyde (PFA) dissolved PBS and analysed by flow cytometry. The handling and the data-plots generated**(Figure 6-1)** were performed by Robert G Pineda.

2.10.1 T cells activation

T cells were activated using the Dynabeads® Mouse T-Activator CD3/CD28 (11456D, ThermoFisher). The kit simulates the T cells' *in-vivo* activation, which involves binding of the T cells to CD3/CD28 on the antigen-presenting cells (APC). The process is depicted in**(Figure 2-6).**

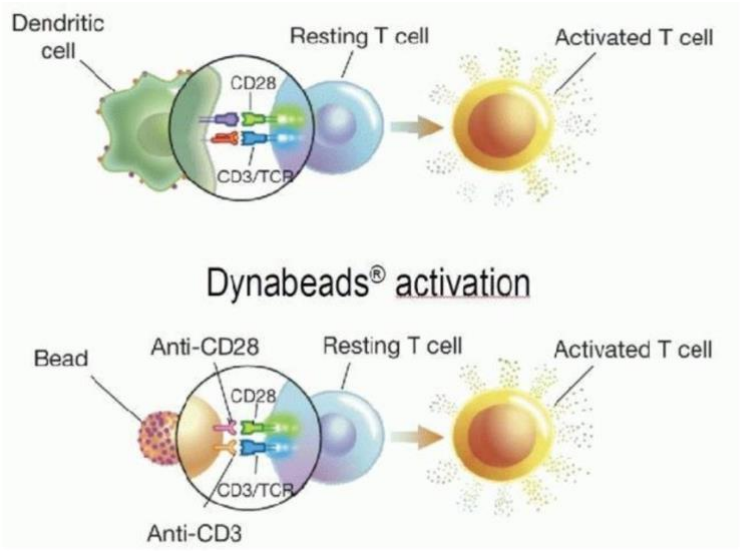

Figure 2-6 T cells activation using the Dynabeads®

The assay was carried out according to manufacture instructions, and the Dynabeads were used at a 1:1 ratio to cells. Prior to activating the cells, the Dynabeads were washed by placing them in the DynaMag for 1 min, and 1 ml of PBS with 1% FBS was added. The supernatant was discarded, and the washed magnetic beads were suspended in T cell culture media to be used directly on T cells separated as mentioned in section 2.8. The cells were stimulated for three days.

2.11 Generating *LRRK2* CRISPR Knock-out construct

For generating a construct that will knock-out the *LRRK2* gene in mammalian cells, I utilized a clustered regularly interspaced short palindromic repeats (CRISPR) - CRISPR associated protein 9 (CAS9) system. CRISPR-CAS9 is a genome engineering tool derived from the adaptive immune system of the bacterium *Streptococcus pyogenes*, which is used to cut the bacteriophage genome. CRISPR-CAS9 consists of an endonuclease CAS9 and guide RNA(gRNA) that will guide the endonuclease to cut at a specified location within the genome to induce a double-strand break (DSB). This site of the genome is complementary to the gRNA sequence

and located upstream (5') of a protospacer Adjacent Motif (PAM)**(Figure 2-7**). Once CAS9 mediates the DSB, the target locus can undergo DNA damage repair by non-homologous end joining (NHEJ), which will relegate the DNA resulting in insertion/deletion (indel) mutations. Indel mutations within a coding exon lead to frameshift mutations and premature stop codons resulting in gene knock-outs. Thus, the CRISPR/Cas9 system can be implemented in mammalian cells by co-expressing the bacterial Cas9 nuclease along with a guide RNA

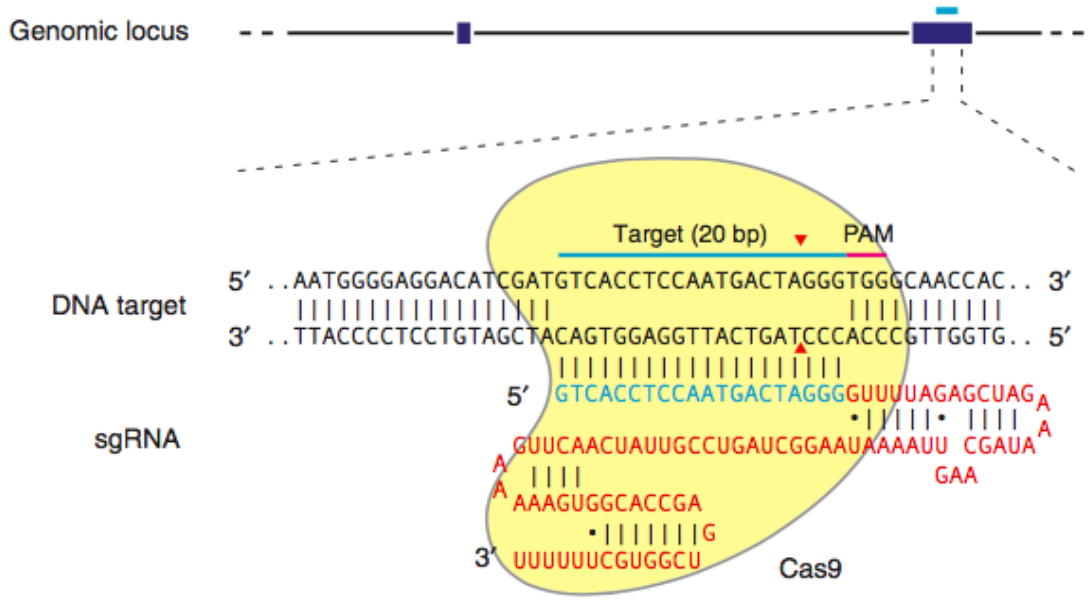

Figure 2-7 Schematic diagram illustrating the CRISPR-CAS9 enzyme

The process of making the plasmid encoding CAS9 attached to a gRNA specific for a certain gene involves the following steps: Designing the gRNAs, digesting the vector and cloning the gRNAs, followed by DNA amplification and sequence validation.

2.11.1 Designing gRNA

There are several considerations when designing a gRNA, which will determine the specificity of CAS9 nuclease to cut at the target location within the genome. The gRNA has to contain 20 nucleotides that must be preceded by a 5'-NGG (PAM), whereas N

can be A(Adenine), C(cytosine), G(Guanine), and T(Thymine). Also, another consideration is to decrease off-target effects. There are computational CRISPR design tools that are available and able to generate the primer sequences required for sgRNA constructs and provide a numerical value of each sgRNA generated. The better the value, the better are the chances that the sgRNA will guide the CAS9 to the desired location with minimum predicted off-targets. I used the benchling® design tool for its simple interface, and its analysis is similar to other designer's tools.

Using benching, I have chosen three sgRNAs from 3 different exons through the *LRRK2* gene that are summarized in the following table:

Guide	Primers	on/off target score	Location
GAGTCCAAGACGATCAACAG**AGG**	FWD CACCGAGTCCAAGACGATCAACAG REV aaacCTGTTGATCGTCTTGGACTC	50/89	Exon 2 (402,255,96).
TGTGCCAACGAGAATCACAG**GGG**	FWD CACCGTGTGCCAACGAGAATCACAG REV aaacCTGTGATTCTCGTTGGCACAC	85/66.	EXON31 (40310453).
GTGTTCACGTACTCCGAGCG**CGG**	FWD CACCGTGTTCACGTACTCCGAGCG REV aaacCGCTCGGAGTACGTGAACAC	70/97	EXON1 (402,252,78).

Table 2-4 gRNAs used in cloning in PX459

2.11.2 Cloning gRNAs into the vector PX459

Prior to cloning the gRNAs into the CRISPR construct, the primers had to be annealed, and the vector had to be digested and linearized. The annealing process involves adding 1µl of 100µM forward primer, 1µl 100µM reversed primer, 5 µl 10X annealing buffer(100 mM Tris, pH 7.5–8, 500 mM NaCl, 20mM MgCl2 and 10mM EDTA and 43

µl ddH_2O and putting them into a PCR tube placed into the thermocycler and the following conditions were applied: Heating for 5 minutes at 95°C and then decreasing the temperature by 5 degrees every 5 minutes until it reached 25°C. The PCR tubes were stored at -20°C until use.

The vector used is pSpCas9(BB)-2A-Puro (PX459) (62988, Addgene), which encodes CAS9 protein and contains a cloning site for sgRNA in addition to encoding a puromycine resistance protein(Puromycin N-acetyltransferase) for selection purposes. At first, I digested and linearized the PX459 using the FastDigest Bbsi (FD1014, ThermoFisher) restriction enzyme, which recognizes the GAAGAC site and cuts, allowing the sgRNA primers to be inserted and be ligated into the vector (Figure 2-8). The digestion was carried out at 37°C for 1 hour using 10 units of Bbsi (1 unit is defined as the amount of enzyme required to digest 1 µg of plasmid in 60 minutes), 1µg PX459, 5 µl CutSmart® buffer and completed with 50 µl sterile water.

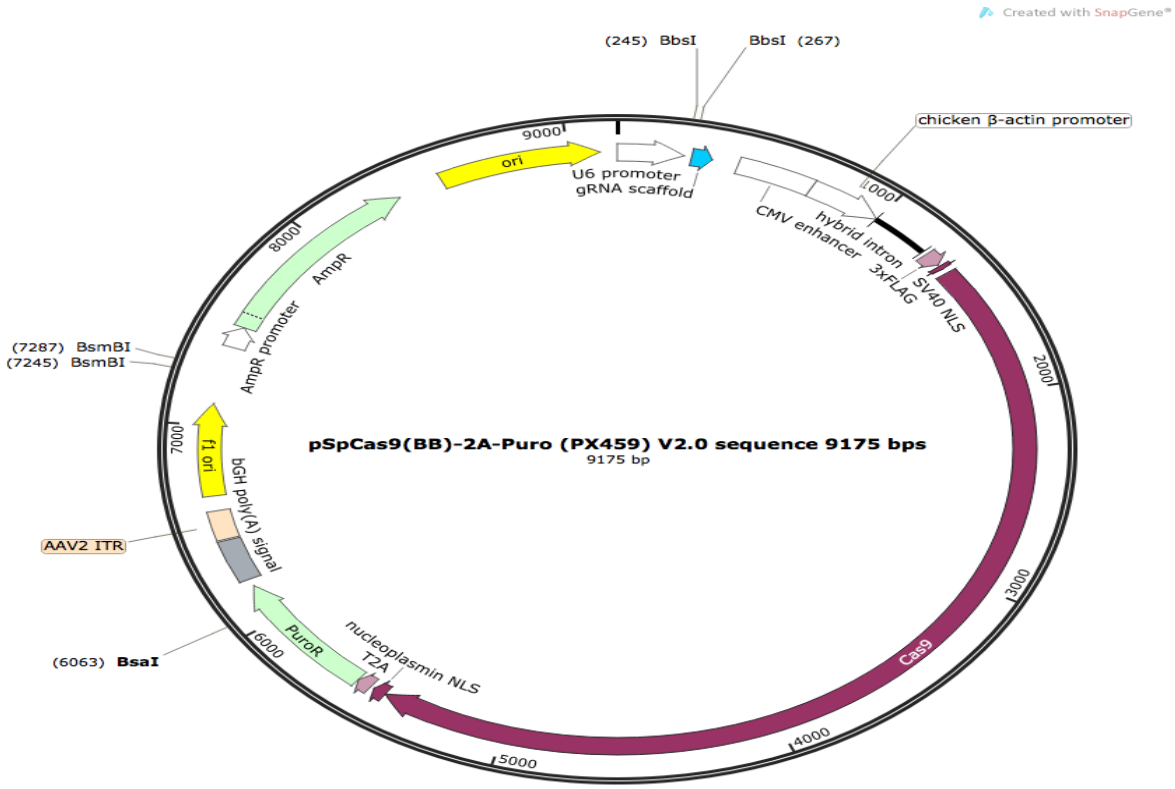

Figure 2-8 pSpCas9(BB)-2A-Puro (PX459) map

The 3 annealed sgRNA primers were each ligated with the linearized PX459 in 3 different tubes using the following amounts and conditions: 1 µl of linearized PX459, 3 µl of the annealed sgRNA and 1µl T4 DNA Ligase buffer(M0202S,biolab) and all were incubated at room temperature for 60 minutes, and cloning process is considered complete at this stage. The steps that follow, are for amplification and verification processes.

2.12 DNA Amplification and purification

The constructs used throughout this thesis were transformed into Escherichia coli (E. coli), followed by growing the bacterial cultures to amplify the plasmids. The purification steps are accomplished by either maxiprep or miniprep (QIAprep®) as required.

2.12.1Transformation

Plasmids in pure form can be introduced into the bacterial cells (transformation) to be amplified. For this purpose, I used commercially available competent cells (One Shot™ TOP10 Chemically Competent E.coli) to transform the plasmids into the bacteria. The transformation was carried out following the manufacture instruction. Briefly, 50 µl of competent cells were thawed on ice. Next, 1 µg from each plasmid or ligation reaction were added directly into the vials of competent cells, mixed by tapping gently and incubated on ice for 30 minutes. After that, the cells were heat-shocked for 45 seconds and incubated back on ice for 2 minutes, followed by the addition of 250 µL of pre-warmed lysogeny broth (LB) medium to each vial. Then, the vials were put on the heat-block and shaken at 300 RPM at 37°C for 1 hour. Finally, the content of each vial was spread on individual L.B. agar plates with the appropriate antibiotic (Ampicillin) and put into the incubator overnight. Colonies were selected for miniprep or maxiprep.

2.12.2Miniprep

Miniprep kits were used on ligation reactions generated in section 3.10.2. After the bacterial cells were transformed with the candidate plasmid, they needed to be extracted and purified in addition to being sequenced to verify successful cloning. A miniprep kit (QIAGEN) is ideal for extracting an appropriate amount of DNA for sequencing. The extraction process was done following the manufacture instructions. Briefly, a single bacterial colony was inoculated in a 5 ml LB medium culture containing the appropriate selective antibiotic and incubated overnight with vigorous shaking at 225 RPM at 37°C. The cells were centrifuged at 14000 rpm for 10 minutes at 4°C, and the supernatant was discarded. The pellet was then resuspended in 250 µl buffer P1

(50 mM Tris-HCL, 10mM EDTA, 100µg/ml RNaseA) followed by cell lysis by adding 250 µl Buffer P2 (200mM NaOH, 1% SDS). Then tubes were inverted gently 4-6 times and incubated for 5 minutes with 350 µl buffer N3 (4.2M Gu-Hcl, 0.9M potassium acetate) was added to the tubes to neutralise the lysis buffer. The tubes were then centrifuged at 13000 RPM for 10 min, followed by applying the supernatant to QIAprep spin columns, which will bind the plasmid DNA. The columns were then centrifuged for 30 seconds, and the flow-through was discarded, followed by a washing step by adding 0.75 ml Buffer PE. Finally, the QIAprep spin columns were put on a 1.5 ml collection tube and the DNAs were eluted with 50 µl Buffer EB (10 mM Tris·Cl, pH 8.5) and left standing for 1 minute. The concentrations of the plasmids were determined using a NanoDrop 2000 spectrophotometer (Thermo Scientific).

2.12.3 Sequence validation

After the plasmids have been purified, they were sent to the DNA sequencing service at the University of Dundee to check if the sgRNAs have been successfully cloned into the vectors. The plasmids were sent at a 25-30 ng/ul concentration as specified by the sequencing company. The primer used for sequencing recognises the human U6 promoter 5'(GACTATCATATGCTTACCGT)(Ran et al. 2013).

2.12.4 Maxiprep

While miniprep kits allow purifying plasmid DNA from bacteria on a small scale, HiSpeed Plasmid Maxi Kit®, commonly known as maxiprep (QIAGEN), allows for the purification of DNA on a larger scale of up to 500 µg compared with 20 µg using miniprep. The process of purification was carried out following the manufacture instruction. A single bacterial colony was picked from freshly streaked LB plates (see 2.12.1) and inoculated in 5 ml LB medium with selective antibiotic for approximately

8 h at 37°C with vigorous shaking (approx. 300 RPM). Then the starter culture was diluted 1/100 with LB and left at 37°C with vigorous shaking overnight. Then the bacterial cells were harvested by centrifugation 6000 x g for 15 min at 4°C followed by resuspension in 10 ml of buffer P1. A lysis buffer (P2) was added (10 ml), and the tube was inverted 4-6 times and incubated for 5 minutes. 10 ml P3 buffer was added, and the liquid was transferred quickly to QIAfilter Cartridge® and allowed to sit at room temperature for 10 min, and 2 layers were formed. Meanwhile, HiSpeed Tip® (The DNA binding resins) was equilibrated with QBT buffer (750 mM NaCl, 50 mM MOPS pH 7.0, 15% isopropanol, 0.15% Triton X-100) to optimise DNA binding capability. The lysates in the QIAfilter Cartridge® were filtered into HiSpeed Tip® followed by adding a 60 ml washing buffer QC (1.0M NaCl, 50 mM MOPS pH 7.0, 15% isopropanol).

The DNA was eluted with 15 ml of Buffer QF (1.25M NaCl, 50 mM Tris-HCl pH 8.5, 15% isopropanol) and placed into a 50 ml falcon tube. 10 ml of isopropanol was added to precipitate DNA and left for 5 min at room temperature. A 30 ml syringe was attached to a QIAprecipitator® module to serve as a final DNA purification step. The isopropanol/DNA mixture was applied and filtered through QIAprecipitator® and followed by a drying step by passing 2ml 70% alcohol through the QIAprecipitator®. An additional drying step was then employed by passing and forcing air through QIAprecipitator® until it is completely dried. Finally, The DNA was eluted by passing 1 ml TE (Tris-EDTA). The concentration of the DNA was counted using nanodrop and stored at -20°C until use.

2.13 Lentivirus production, titration and transduction

Lentiviruses are considered RNA viruses belonging to the *Retroviridae* family. They are responsible for several diseases, most notably, acquired immunodeficiency

syndrome (AIDS) caused by human immunodeficiency viruses (HIV). Lentiviruses evolved to deliver their RNA into an infected host. They infect the host cells and hijack the host cell machinery transcribing the RNA using RT and integrase enzyme, which facilitate the integration of the viral genome into host cell DNA, often killing the host cells in the process. Scientists took advantage of the lentiviruses ability to deliver their genetic materials. Today, lentiviruses are widely used in research either in the gene therapy or to deliver genetic materials to different mammalian and non-mammalian cells. Lentiviruses are pathogenic, and some form of manipulation of the virus sequence had to be undertaken: the virulent parts of the virus and the unnecessary portions in the sequence were removed and replaced with an expression cassette for gene delivery. Today, most current lentiviruses are based on HIV, which has been biomedically engineered and modified to be safer and optimize for gene delivery.

In some parts of my thesis, lentiviruses were used to measure the transcriptional activity of either TCF/LEF or NFAT. They were prepared using a 2nd generation lentiviral vector packaging system. Briefly, the packaging contains three main parts (plasmid or constructs): First, envelope plasmid(pMDG2), which encodes the pseudotyped vesicularstomatitis virus G-protein (VSV-G) envelope. Second, the Packaging plasmid(pCMVdR8.74) which encodes Gag, Pol, Rev, and Tat genes, which are necessary proteins for virus production. Third, the transfer plasmid encoding insert of interest, in this case, either pLNT Wnt NLuc2 (for LEF/TCF) or pLNT NFAT NLuc (for NFAT).

The plasmids were amplified (see 0) , and then 40 µg of either pLNT NFAT or pLNT Wnt NLuc2, 10 µg pMDG2, 30 µg pCMVdR8.74 were mixed with 10 ml of Opti-Modified Eagle's medium (Opti-MEM, Gibco) containing transfection agent PEI (branched Mw ~25,000, Sigma-Aldrich, 1mM) and allowed to incubate at room

temperature for 20 min. The complex was added to 10 CM dish containing confluent HEK-293T cells, which were washed with Opti-MEM medium prior to the addition and incubated for 4 hours in the cell culture incubator. Then, the complex media was removed and replaced with standard media and further incubated for 72 hours. The supernatant was collected and centrifuged 3000 g for 10 min, followed by filtrations through a 0.22μm filter (Millipore) for cell debris elimination. Finally, the pass-through filtered containing the virus was further centrifuged for 18 hours 3,500 x g, 4°C and the virus pellet was suspended in Opti-MEM and stored at -80°C until use.

The titter of the virus was assayed by utilizing a commercially available kit, the ZeptoMetrix p24® antigen enzyme-linked immunosorbent assay (ELISA), which provides a known concentration of the p24 antigen to compared to the p24 present in the sample, or in this case, the supernatant Opti-MEM containing the virus. The assay principle is based on supplying wells precoated with monoclonal antibodies conjugated to biotin specific for the p24 gag gene product of the pCMVdR8.74. The samples containing the p24 antigen in the virus samples are captured and then treated with Streptavidin-Peroxidase substrate, and the colour develops. The optical density is proportional to the amount of antigen present, which can be measured spectrometrically and compared to known standards of the p24 antigen to generate a standard curve. Dr Michael Hughes did all lentiviruses production and titre measuring.

The lentivirus titre used throughout the thesis are summarized in Table 2-5.

Lentivirus	Titre	Uses
pLNT Wnt NLuc2	1.3 x 10^9 vp/ml	TCF/LEF transcriptional activity
pLNT NFAT NLuc	5.6 x 10^8 vp/ml	NFAT transcriptional activity
VSV.G.CMV.eGFP.WPRE	2.8 x 10^9 vp/ml	Transduction efficiency studies
pLNT SFFV VLuc	8.3 x 10^8 vp/ml	Loading control

Table 2-5 Lentiviruses used in this study. Vp:Viral particles.

2.14 Bone Marrow derived macrophages

2.14.1Isolation and differentiation

BMDM were isolated and differentiated following the protocol published previously with minor modification(Davis 2013, Trouplin et al. 2013). BMDM were collected from mice aged 12 to 16 weeks. Mice were euthanised as previously mentioned in 2.9. After removing the muscles, connective tissue and fat, the femurs and tibias bones were removed and placed in 100 mm containing 10 ml PBS and 1% FBS. They were crushed using a mortar and pestle, and the supernatant was passed through a 16-gauge blunt-end needle attached to a 3-ml syringe several times, after which it was transferred to 50 ml Falcon tubes attached to a cell strainer. The cells were centrifuged at 1500 RPM for 5 minutes at four °C, and then the pellet was suspended in freezing media containing 90% FBS and 10% DMSO and stored at liquid nitrogen container.

For differentiation of BMDM, the cells were thawed in the 37 °C water-bath and then transferred to a 15 ml Falcon tube containing DMEM media and centrifuged 1500 RPM for 5 minutes. The pellet was suspended in 1 ml DMEM, and the cells were counted and resuspended at 1*10^^{7} cells/ml seeded into an appropriate plate. DMEM supplemented with 20% FBS , 1% penicillin/streptavidin, 1% amino acids and 1%

Glomax and 20 ng/ml macrophages colony-stimulating factor(MCSF). The BMDM were differentiated for 7-9 days.

2.15 Immunocytochemistry and fluorescent microscopy

The plates and coverslips used in immunocytochemistry (ICC) were pre-coated with 100 ng/ml poly-D-lysin for 2 hours and washed with sterile water three times, and left to dry in the hood overnight before cell seeding.

BMDM, RAW 264 or T cells were fixed with 100% Ice-cold methanol at 4 °C for 10 minutes, followed by three washes with PBS. Permeabilisation to allow antibodies to pass through the cell membranes was achieved by incubating the cells with 0.1% Triton-X dissolved in PBS. The blocking step was performed by incubating the cells with 5% goat serum dissolved in PBS for 30 minutes. Appropriate primary antibodies were added and incubated overnight at 4°C with gentle shaking. Three prolonged washing steps were performed (5 min) followed by DAPI staining for 15 minutes. Additional prolonged washes were performed, followed by mounting the coverslip with Prolong Gold mounting media (Life Technologies). The slides were left to dry for at least 4 hours. The slides were imaged using the EVOS XL Core Imaging System.

2.16 Phagocytosis

Phagocytotic activity in RAW 264 macrophages and BMDM was determined utilizing a commercially kit, Vybrant® Phagocytosis Assay Kit (V6694,Thermofisher). The assay tests the ability of the cell to phagocyte a fluorescently labelled dead E.coli (K-12 strain). The fluorescence intensity is proportional to the Phagocytotic function, and it can monitor in either a fluorescence microscope set to GFP filter (470/525 nm) or microplate reader or both.

The assay was carried out according to the manufacture instruction with minor modification. Briefly, After the cells have been treated with either LPS or control vehicle for 24 hours, the media was removed, and 300 ul of fluorescent BioParticle suspension(0.1mg/ml) was added to the cells and incubated for 2 hours. The BioParticle were discarded, and 100 ul of trypan blue was added, followed by extensive washing with PBS. The fluorescence intensity was measured in the SpectraMax® M Series, and the fluorescence imaging was utilized using EVOS XL Core Imaging System.

2.17 Cathepsin D Activity

The lysosomal enzyme Cathepsin D activity was measured utilizing a commercially available kit, Cathepsin D Activity Assay Kit (ab65302, Abcam). The assay principle is based on the proteolytic activity of the enzyme toward a synthetic substrate that has been fluorescently labelled with 7-Methoxycoumarin-4-acetic acid (MCA). Once the substrate is cleaved, it will emit fluorescence that can be measured using a fluorescence plate reader at Ex/Em = 328/460 nm.

The assay was carried out according to the manufacture instruction. The cells were harvest from the plate by adding trypsin followed by centrifugation. The cells were washed with ice-cold PBS followed by the addition of 200 µL of chilled CD® Cell Lysis buffer and incubated on ice for 10 minutes. Then, the cells were centrifuged at 4°C at 14000 RPM for 5 minutes to remove any insoluble cell debris. 50 ul of each cell lysate samples were transferred to 96 well plate containing 50 ul Reaction buffer®, and 2 ul of the substrate was added. The plate was incubated for two hours at 37°C followed by measuring the fluorescence in SpectraMax® M Series microplate reader.

2.18 The MTT assay

The cell viability was utilized using the MTT assay. It is based on the reduction of yellow 3-(4,5-dimethythiazol-2-yl)-2,5-diphenyl tetrazolium bromide (MTT) by metabolically active cells to a purple-coloured formazan product, which can be quantified spectrophotometrically(van Meerloo, Kaspers and Cloos 2011). The absorbance of the formazan is proportional to the number of living cells. The assay was used to determine the minimum concentration of the puromycin that can kill 90% of cells or more in chapter 3.

The cells were seeded into 24 well plate and allowed to attach overnight. A range of concentration of puromycin were added, and the cells were incubated for 7 days. The media was removed, and the MTT was added (0.5 mg/ml) to the cells and incubated for 4 hours. Minimum sufficient volume of DMSO was added to dissolve the formed crystals, and the absorbance was measured in the plate reader at 550 nm.

Chapter 3 Modulating canonical Wnt signalling in SH-SY5Y cells

3.1 Introduction

The interplay between LRRK2 and Wnt signalling has been suggested to contribute to PD pathogenesis. Initially, LRRK2 was shown to interact physically with components of canonical Wnt signalling, including DVL proteins, GSK3β, and LRP6, with the strength of the interaction altered by *LRRK2* pathogenic mutations(Lin et al. 2010a, Sancho et al. 2009). Furthermore, overexpressing *LRRK2* augments canonical Wnt signalling, whereas pathogenic mutations have the opposite effect(Berwick and Harvey 2012b). Interestingly, the protective *LRRK2* R1398H variant has been shown to increase canonical Wnt signalling compared to wild type *LRRK2* and pathogenic mutation. The increase in canonical Wnt signalling was associated with increased axonal length in primary cortical neuronal cultures(Nixon-Abell et al. 2016). Finally, some LRRK2 kinase inhibitors have displayed differential effects on canonical Wnt signalling, warranting additional studies elucidating the precise effect(Berwick et al. 2017). Taken together, the aforementioned studies substantiate a functional role for LRRK2 in mediating canonical Wnt signalling.

LRRK2 is emerging as a promising therapeutic target. Several studies have provided experimental evidence that *LRRK2* PD mutations might increase kinase and/or GTPase activity, possibly contributing to PD pathogenesis. This has prompted academia and the pharmaceutical industry to develop small molecules that target primarily the LRRK2 kinase domain, but some target the GTPase domain. In primary rat cortical neuronal cultures, the kinase activity of LRRK2 PD mutants was shown to mediate the pathogenic effects and led to the formation of inclusion bodies(Greggio et al. 2006). Furthermore, Anastasia and others documented that the *LRRK2* G2019S,

R1441C and Y1699C mutations in primary astrocyte resulted in enlarged and malfunctioning lysosomes compared with WT control. However, those defects were rescued when cells were treated with PF-06447475, a potent and selective LRRK2 kinase inhibitor or when transfected with a plasmid encoding kinase-dead mutant form of LRRK2(Henry et al. 2015).

Those studies and others led to the development of several LRRK2 inhibitors that are potent, selective and can cross the BBB. However, some challenges need to be addressed and elucidated before the progression into the clinical phase. First, the precise function of LRRK2 is still controversial, and there is no consensus about its physiological role or even its cellular substrate until recently, whereas accumulating evidence indicates Rab GTPases seems candid substrate (Taymans and Greggio 2016, Taylor and Alessi 2020). Second, several pre-clinical models have shown unusual phenotypes in the kidney and lungs due to treatments with LRRK2 kinase inhibitors. For instance, three specific LRRK2 kinase inhibitors with different pharmacophore group (GNE-7915, GNE-0877 and Mli-2) were found to induce irregular build-up of lamellar bodies (secretary organelles) in type II pneumocytes in cynomolgus monkeys and mice(Fell et al. 2015, Fuji et al. 2015). This was consistent with previous reports observing this anomaly in lung phenotypes. Two candidate LRRK2 inhibitors (DNL201 or DNL151) are currently in phase 1 clinical trial for safety and dose evaluation.

SH-SY5Y neuroblastoma cells have been extensively used in PD models as they express some dopaminergic markers including tyrosine hydroxylase (Kovalevich and Langford 2013, Xicoy, Wieringa and Martens 2017). However, SH-SY5Y also has catecholaminergic characteristics as they expresse dopamine-β-hydroxylase which enable them to synthesise both dopamine and noradrenaline. SH-SY5Y

neuroblastoma cells stably expressing the TCF/LEF-Luciferase reporter were used in this chapter to measure the perturbation in canonical Wnt signalling(Granno et al. 2019).

Chapter objectives:

1) Elaborate on the functional relationship between LRRK2 kinase activity and canonical Wnt signaling utilizing SH-SY5Y neuroblastoma cells stably expressing the TCF/LEF-Luciferase reporter.
2) Generate *LRRK2* KO SH-SY5Y neuroblastoma cells using CRISPR gene editing tool.

3.2 Results

3.2.1 LICL mediated canonical Wnt signal activation

Here, I reproduced the activation of canonical Wnt signalling with previously well-known activators. First, LiCl which increases β-catenin translocation to the nucleus by inhibiting GSK3β, allowing β-catenin to dissociate from BDC. LiCl has been shown to activate canonical Wnt signalling in SH-SY5Y neuroblastoma cells and HEK 293 (Berwick et al. 2017). Consistent with previous reports, 40 mM LiCl treatment results in a significant increase in bioluminescence which infer an increase in β-catenin mediated transcriptional activity. The bioluminescence was quantified in living cells as well as cell lysates. In living cells, the increase was more than 5.5-fold compared to cells treated with NaCl, while the increase measured in cell lysates was approximately 4-fold **(Figure 4-1,2).** As the concentration of LiCl used was the same in both experimental setups, the difference could be attributed to differences in instrument sensitivity or perhaps the loss of the luciferase enzyme during the lysing process.

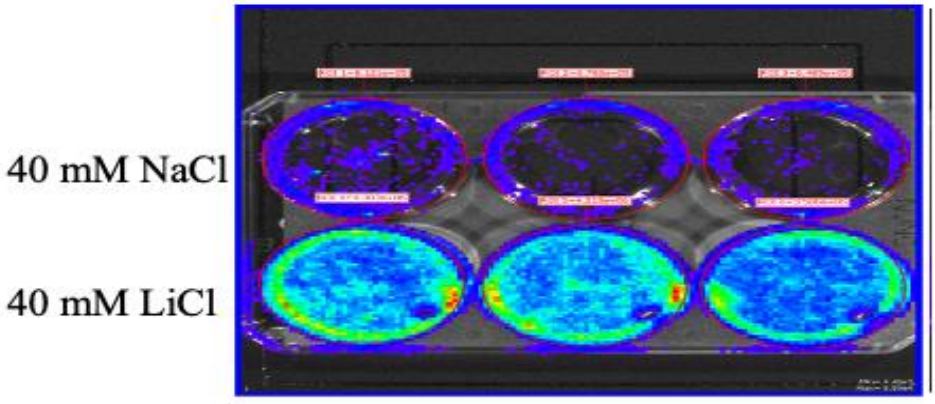

Figure 3-1: ***Activation of canonical Wnt signalling by LiCl 40 mM:*** *TCF/LEF-Luciferase reporter activity was measured 5 hours after exposure to 40 mM LiCl in SH-SY5Y cells. A representative image taken with the IVIS instrument showing increased bioluminescence as a result of LiCl treatment (bottom row) normalized to the control group (NaCl 40 mM, top row).*

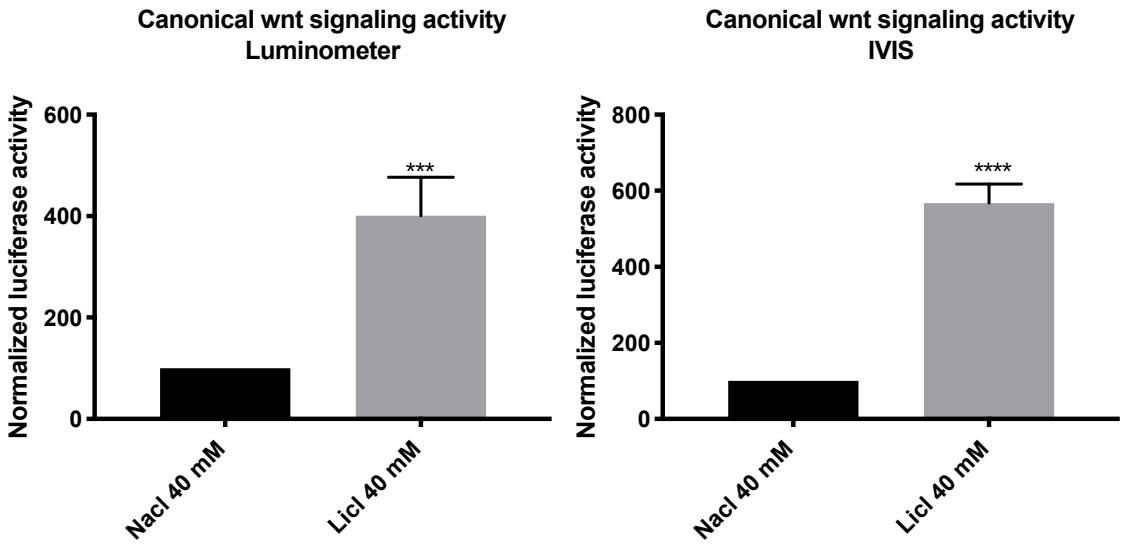

Figure 3-2: ***Activation of canonical Wnt signalling by LiCl 40 mM:*** *TCF/LEF-Luciferase reporter activity was measured 5 hours after exposure to 40 mM LiCl in SH-SY5Y cells. Quantification of the bioluminescence as a result of LiCl treatment compared to NaCl using IVIS (n=4) (Left). Quantification of the bioluminescence as a result of LiCl treatment compared to NaCl using the luminometer(n=3)(Right). Statistical significance was determined by student's t-test. ***p < 0.001, ****p < 0.0001.*

3.2.2 Wnt3a mediated canonical Wnt signal activation

The other well-known activator of Wnt signalling is Wnt3a, which is an essential member of the Wnt protein family. Wnt3a activates canonical Wnt signalling by binding to FZ and LPR/6 receptor dimers. Similar to LiCl, Wnt3a has been documented to increase canonical Wnt signalling *in vivo* and *in vitro* (He et al. 2015). Herein, wnt3a (100 ng/ml) activated canonical Wnt signalling **(Figure 3-3).** Compared to LiCl, Wnt3a treatment resulted in an approximately 10-fold increase as compared to 5.5-fold in living cells. In lysed cells, Wnt3a treatment resulted in a 12.5-fold increase compared to 4-fold.

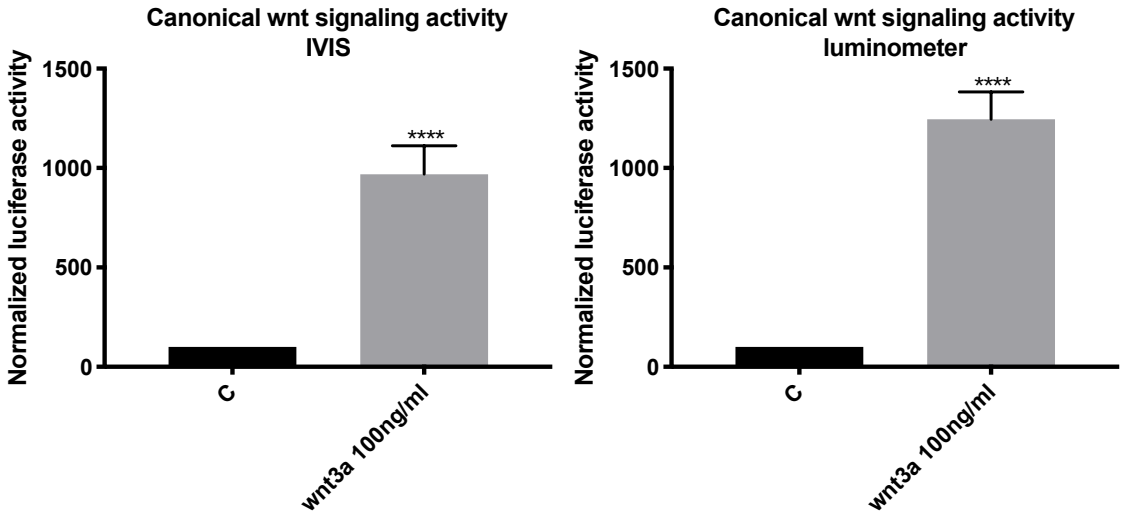

Figure 3-3: ***Activation of canonical Wnt signalling wnt3a (100ng/ml):*** *TCF/LEF-Luciferase reporter activity was measured 5 hours after exposure to Wnt3a (100 ng/ml) in SH-SY5Y cells. Quantification of the bioluminescence as a result of Wnt3a treatment compared to PBS using IVIS (n=4)(Right). Quantification of the bioluminescence as a result of Wnt3a treatment compared to PBS using the luminometer (n=3)(Left). Statistical significance was determined by student t-test. ****p < 0.0001.*

3.2.3 ETC-1922159

ETC-1922159 (hereafter called ETC-159) is a small molecule that targets the enzyme porcupine and inhibits its activity. The porcupine enzyme is an endoplasmic reticulum resident membrane-bound O-acyltransferase that is responsible for post-translation modification of Wnt proteins. It catalyzes the palmitoylation (The addition of fatty acids such as palmitic acid) of Wnt protein resulting in their secretion and activation of cellular Wnt signalling responses. Palmitoylation is an essential step allowing Wnt proteins to bind to their receptors and execute their function (Madan et al. 2016)**(Fig 4-4).** ETC-159 is a potent porcupine enzyme inhibitor with a very low IC_{50}. It decreases β-catenin dependent transcriptional activation in a dose-dependent manner. ETC-159 showed promising results in several cancer models, including a human colorectal

cancer xenograft model. It is currently in phase 1 clinical trials to be tested for safety and tolerability (Madan et al. 2016).

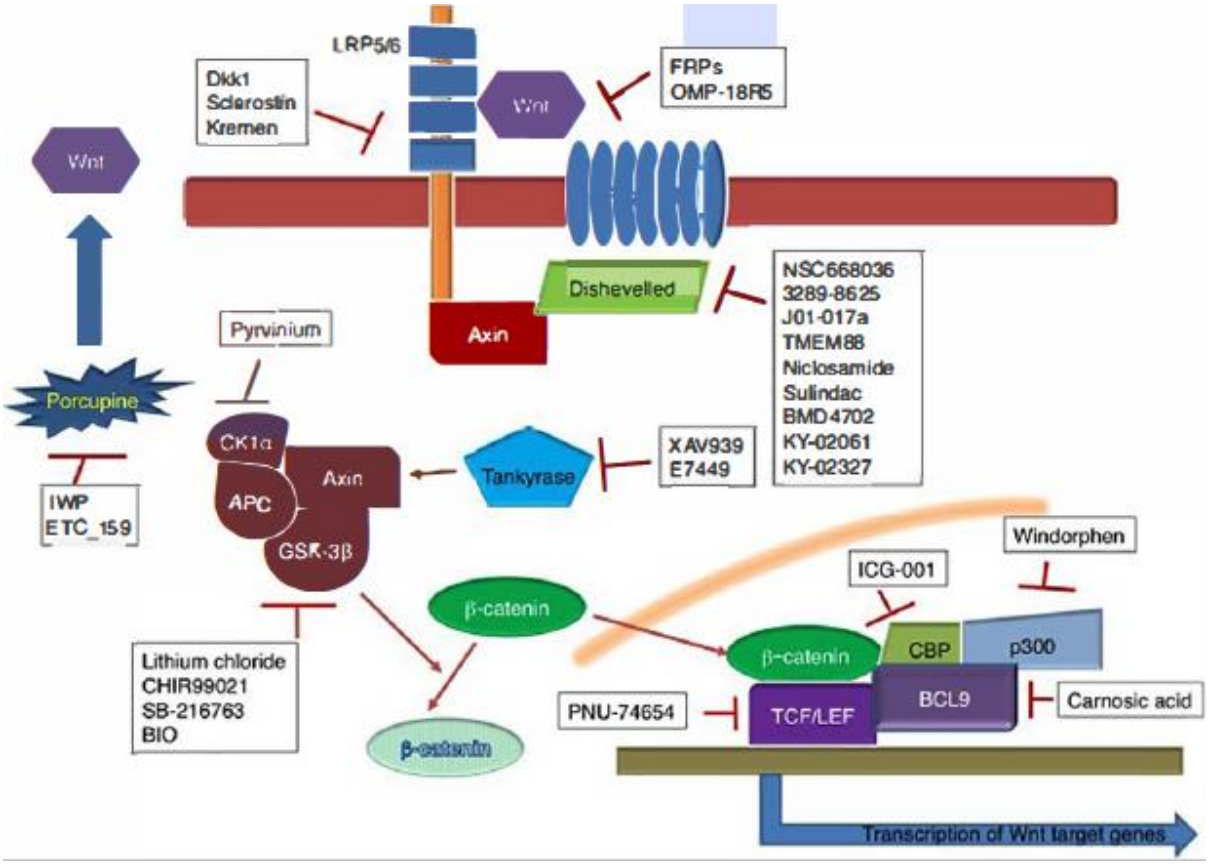

Figure 3-4 ***Schematic representation of site of action for ETC-159 and other canonical Wnt modulators.*** *Figure adapted, with minor modifications, from (Tran and Zheng 2017).*

Herein, I examined the effect of ETC-159 on β-catenin dependent transcriptional activation. ETC-159 at a concentration of 300 μM decreased Wnt3a driven canonical Wnt signalling slightly (non-significantly) **(Figure 4-5).** However, ETC-159 decreased canonical Wnt signalling driven by LiCl in a dose-dependent manner with IC_{50} of 15.97 μM **(Figure 4-5).**

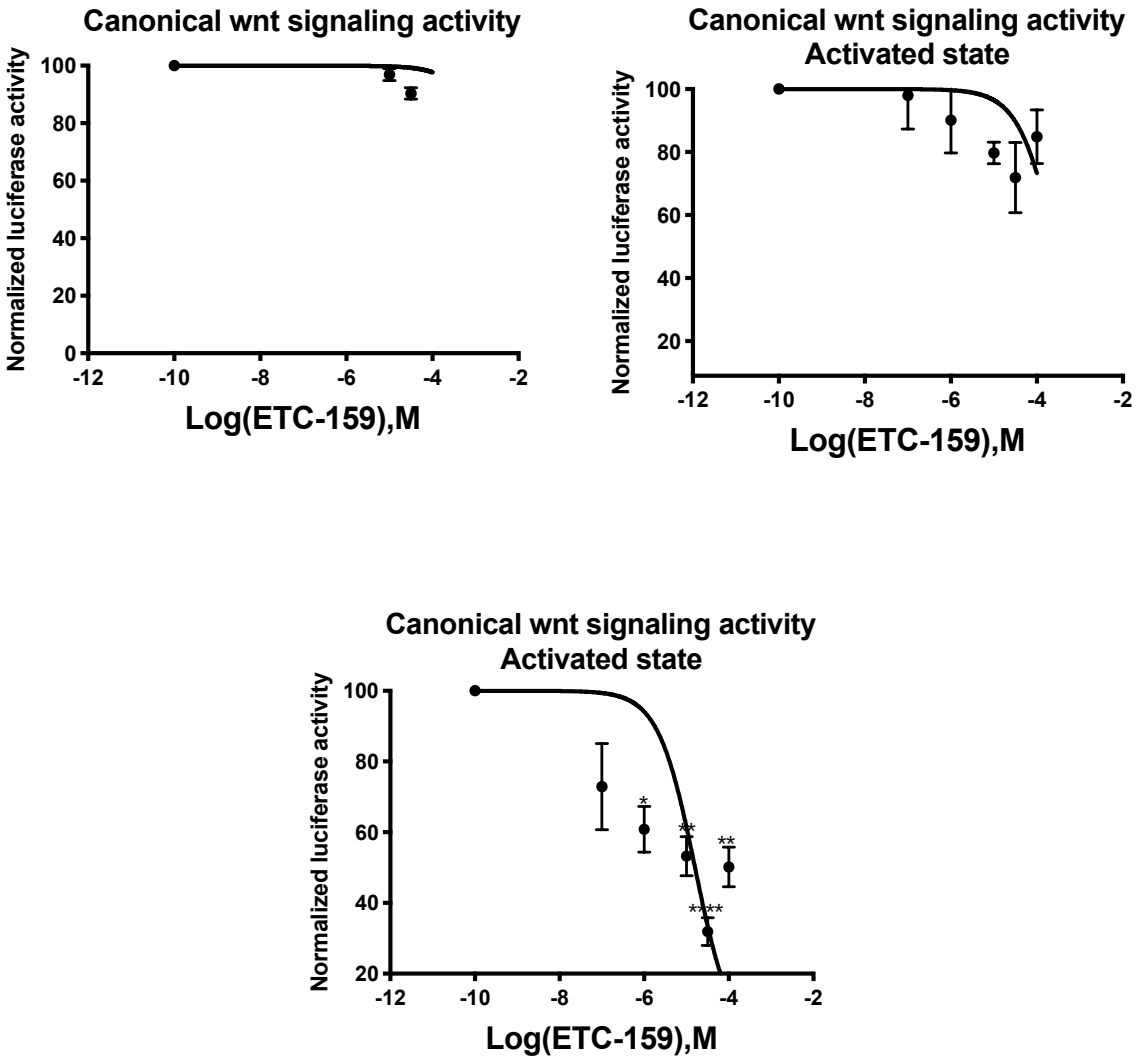

Figure 3-5 ***: Perturbation of canonical Wnt signalling using ETC-159****:TCF/LEF-Luciferase reporter activity was measured 5 hours after exposure to different concentrations of ETC-159 in SH-SY5Y cells. Quantification of the bioluminescence as a result of ETC-159 treatment compared to PBS using IVIS on the basal and Wnt3a driven activated state(n=4)(Top). Quantification of the bioluminescence as a result of ETC-159 treatment compared to PBS using IVIS LiCl driven activated state(n=4). Statistical significance was determined by one-way ANOVA followed by post hoc Tukey's test. *p < 0.05, ** p < 0.01, ****p < 0.0001.*

3.2.4 LRRK2 kinase and GTPase inhibitors and their effect on canonical Wnt signalling

Here, two LRRK2 kinase inhibitors (PF-06447475 and Mli-2) that have been previously characterized were chosen. Their pharmacodynamics profile (measured by the ability to decrease autophosphorylation of LRRK2 at Ser935) in addition to the pharmacokinetics characteristics are summarized in Table 3-1.

Chemical	In-vitro activity (nM)	Cellular activity (nM)	Crosses the BBB	Selectivity (Off Target kinases/Total tested)	Reference
PF-06447475	3	25	Yes	3/39	(Henderson et al. 2015)
Mli-2	0.8	1.4	Yes	5/308	(Fell et al. 2015)
FX-2149	10	100	Yes	NA	(Li et al. 2014)

Table 3-1: ***pharmacodynamics profile of LRRK2 kinase and GTPase inhibitors showing their IC_{50} against the kinase and GTPase , respectively.***

There are several rationales behind choosing PF-06447475 and Mli-2. First, they have a very low inhibitory concentration (IC_{50}), which can be defined as the amount of ligand needed to decrease phosphorylation of LRRK2 at Ser935 by 50%. Second, they have a favourable pharmacokinetics profile as they are orally bioavailable and can cross the BBB. Third, they are relatively selective as they have been tested against a wide variety of kinases(Taymans and Greggio 2016, Fell et al. 2015).

Herein, the effects of two LRRK2 kinase inhibitors on basal and activated canonical Wnt signalling were investigated. SH-SY5Y neuroblastoma cells exhibit a low level of basal canonical Wnt signalling, and activating it (with wnt3a 100ng/ml) would simply intensify the signal and might show any perturbation of the pathway more apparent(Madan et al. 2016).

Both PF-06447475 and Mli-2 inhibited the canonical Wnt signalling under basal and activating conditions in a concentration-dependent manner **(Figure 3-6,7**). The inhibitory concentrations that gave 50% inhibition of the signal (IC_{50}) are summarized in table 4.2 at the end of this section.

Another drug discovery effort toward targeting LRRK2 resulted in the development of small molecules that target the GTPase domain of LRRK2. Several drugs were discovered and among them is FX-2149, which has been documented to have a favourable profile in neurodegeneration disease models. At 10 nM concentration, FX-2149 was able to decrease LRRK2 GTP binding activity by 90%. Additionally, it was able to protect SH-SY5Y cells from toxicity mediated by mutant LRRK2(Li et al. 2015, Li et al. 2014)

Unlike LRRK2 kinase inhibitors, FX-2149 only inhibited canonical Wnt signalling in the activated state, whereas in the basal state, no perturbation of the signal is apparent **(Figure 3-8).**

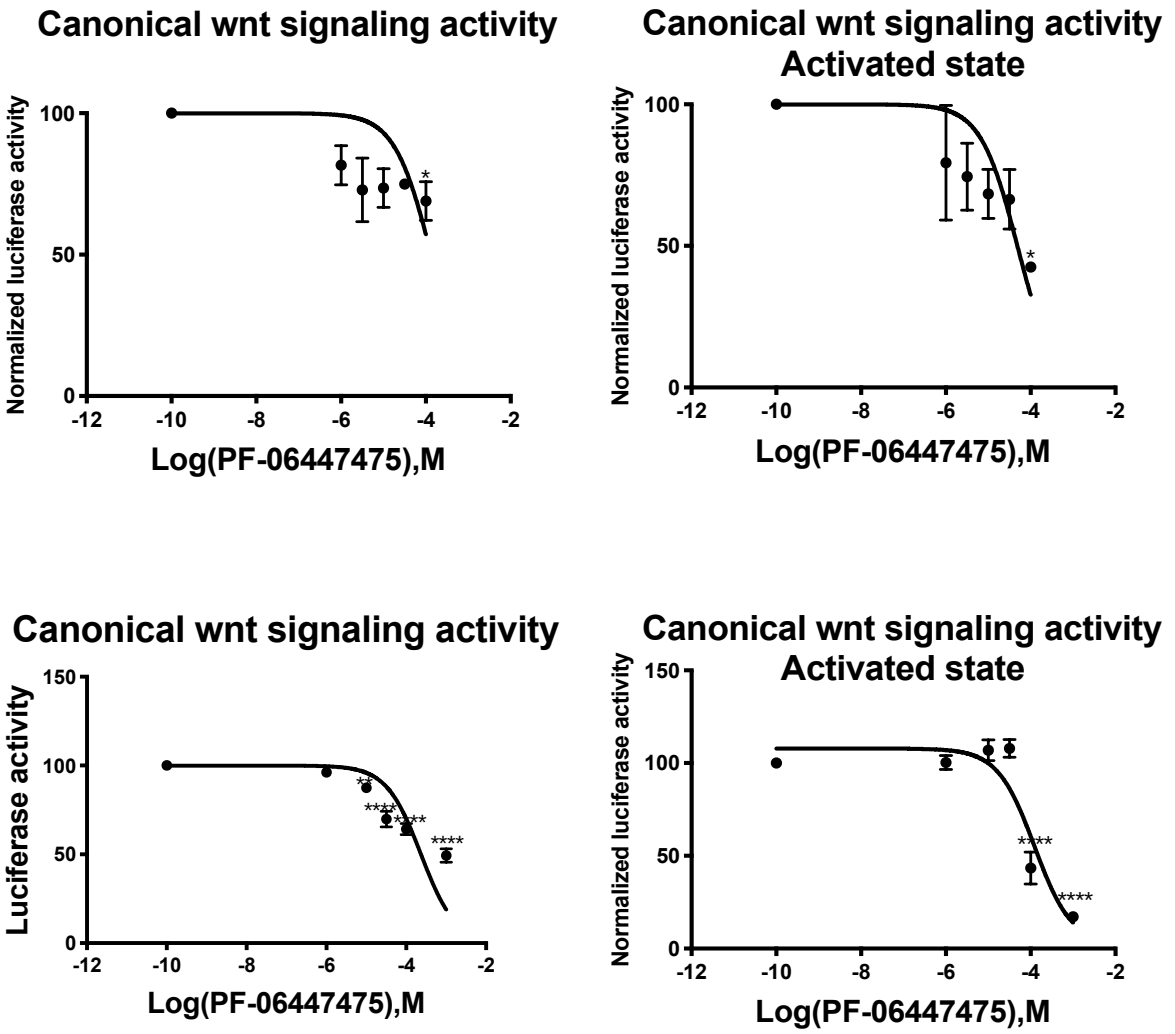

Figure 3-6 ***Inhibition of canonical Wnt signalling for PF-06447475:****TCF/LEF-Luciferase reporter activity was measured 5 hours after exposure to different concentrations of PF-06447475 in SH-SY5Y cells. Quantification of the bioluminescence as a result of PF-06447475 treatment compared to PBS using IVIS on the basal and activated state(n=4)(Top). Quantification of the bioluminescence as a result of PF-06447475 treatment compared to PBS using the luminometer on the basal and activated state(n=4)(bottom). Bars represent mean ± SEM (n=4). Statistical significance was determined by one-way ANOVA followed by post hoc Tukey's test. *p < 0.05, ** p < 0.01, ***p < 0.001, ****p < 0.0001.*

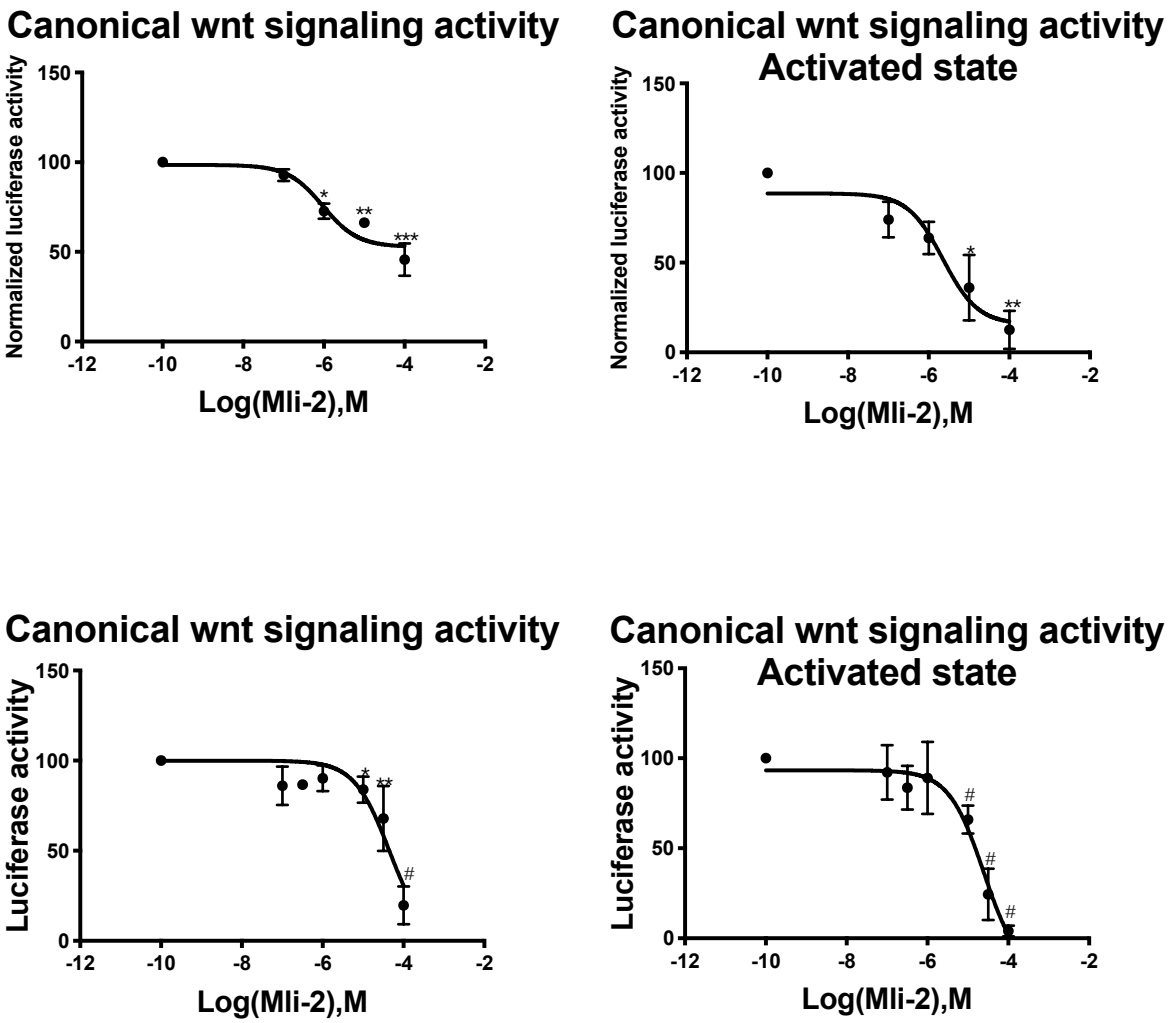

Figure 3-7 ***Inhibition of canonical Wnt signalling for Mli-2****.:TCF/LEF-Luciferase reporter activity was measured 5 hours after exposure to different concentrations of Mli-2 in SH-SY5Y cells. Quantification of the bioluminescence as a result of Mli-2 treatment compared to PBS using luminometer on the basal and activated state(n=4)(Top). Quantification of the bioluminescence as a result of Mli-2 treatment compared to PBS using the luminometer on the basal and activated state(n=4)(bottom). Statistical significance was determined by one-way ANOVA followed by post hoc Tukey's test. *p < 0.05, ** p < 0.01, ***p < 0.001, #p < 0.0001.*

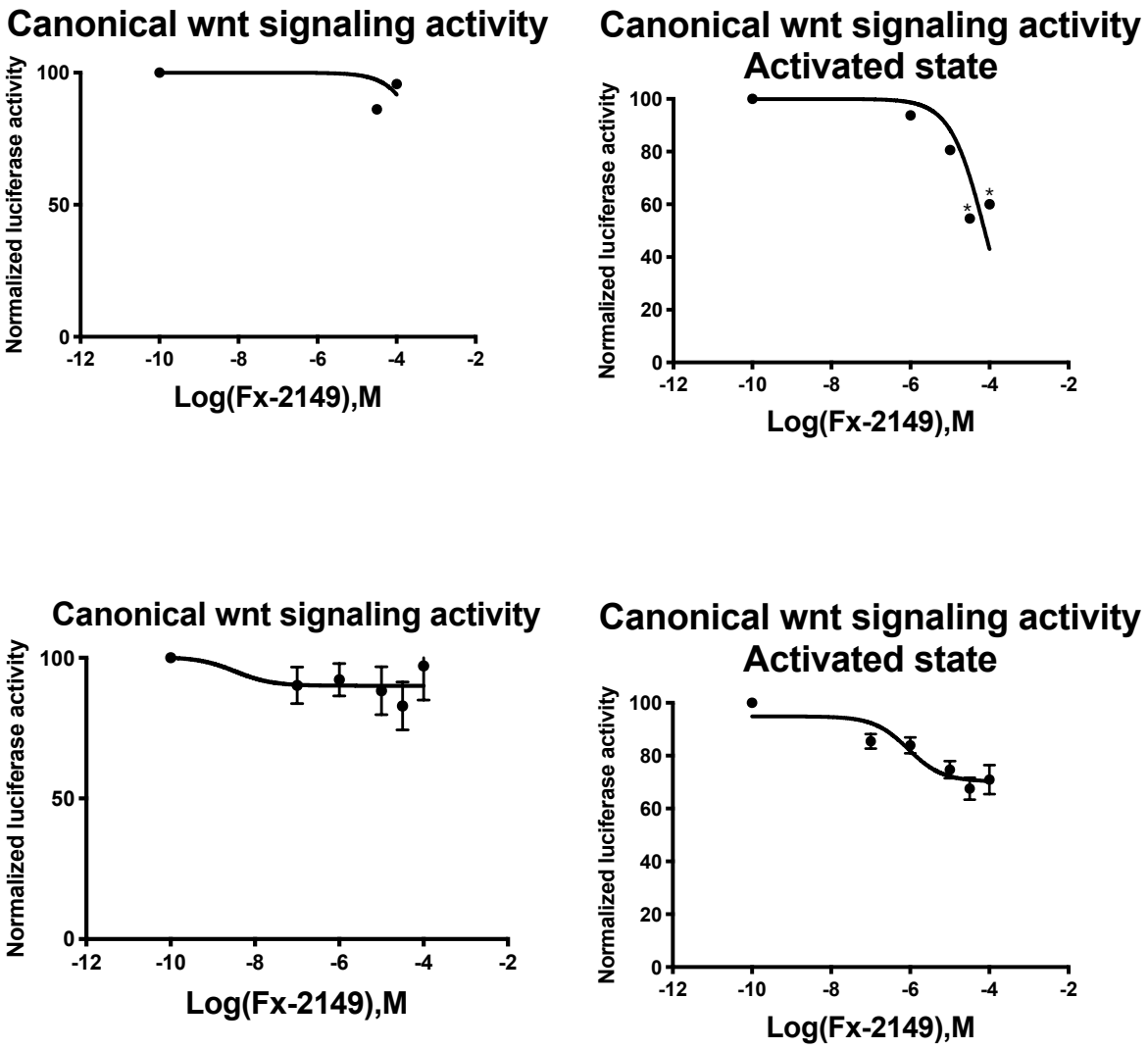

Figure 3-8 ***perturbation of canonical Wnt signalling for FX-2149****: TCF/LEF-Luciferase reporter activity was measured 5 hours after exposure to different concentrations of FX-2149 in SH-SY5Y cells. Quantification of the bioluminescence as a result of FX-2149 treatment compared to PBS using IVIS on the basal and activated state(n=4)(top). Quantification of the bioluminescence as a result of FX-2149treatment compared to PBS using the luminometer on the basal and activated state(n=4)(bottom). Statistical significance was determined by one-way ANOVA followed by post hoc Tukey's test. *p < 0.05.*

Chemical	Quantification method	IC_{50} In the Basal state	IC_{50} activated state
PF-06447475	IVIS	133.9 μM	48.7 μM
	luminometer	234.2 μM	123.2 μM
Mli-2	IVIS	0.9417 μM	2.239 μM
	luminomete	44.53 μM	24.8 μM
FX-2149	IVIS	No inhibition	75.65 μM
	luminometer	No inhibition	133.8 μM

*Table 3-2**: IC_{50} values for LRRK2 kinase and GTPase inhibitors***

3.2.5 Generating *LRRK2* CRISPR knockout construct

The CRISPR system was used in an attempt to generate *LRRK2* KO SH-SY5Y cells. The detailed method for generating the constructs can be found in section 2.11. I have used three pairs of gRNAs to generate three individual constructs, named(A-C) to be transfected at a later stage. The plasmid PX-459-V2(Addgene#62988), which encodes the Cas-9 protein, was used as cloning backbone **(Figure 2-8).** The plasmid also encodes a selection marker, which is puromycin-N-acetyltransferase. An illustration of Sanger sequencing chromatogram sections and a screenshot from the gRNA designing program benchling® from the three individual constructs are shown in **Figure 4-9**, which indicates successful cloning of individual gRNAs into the backbone of PX-459.

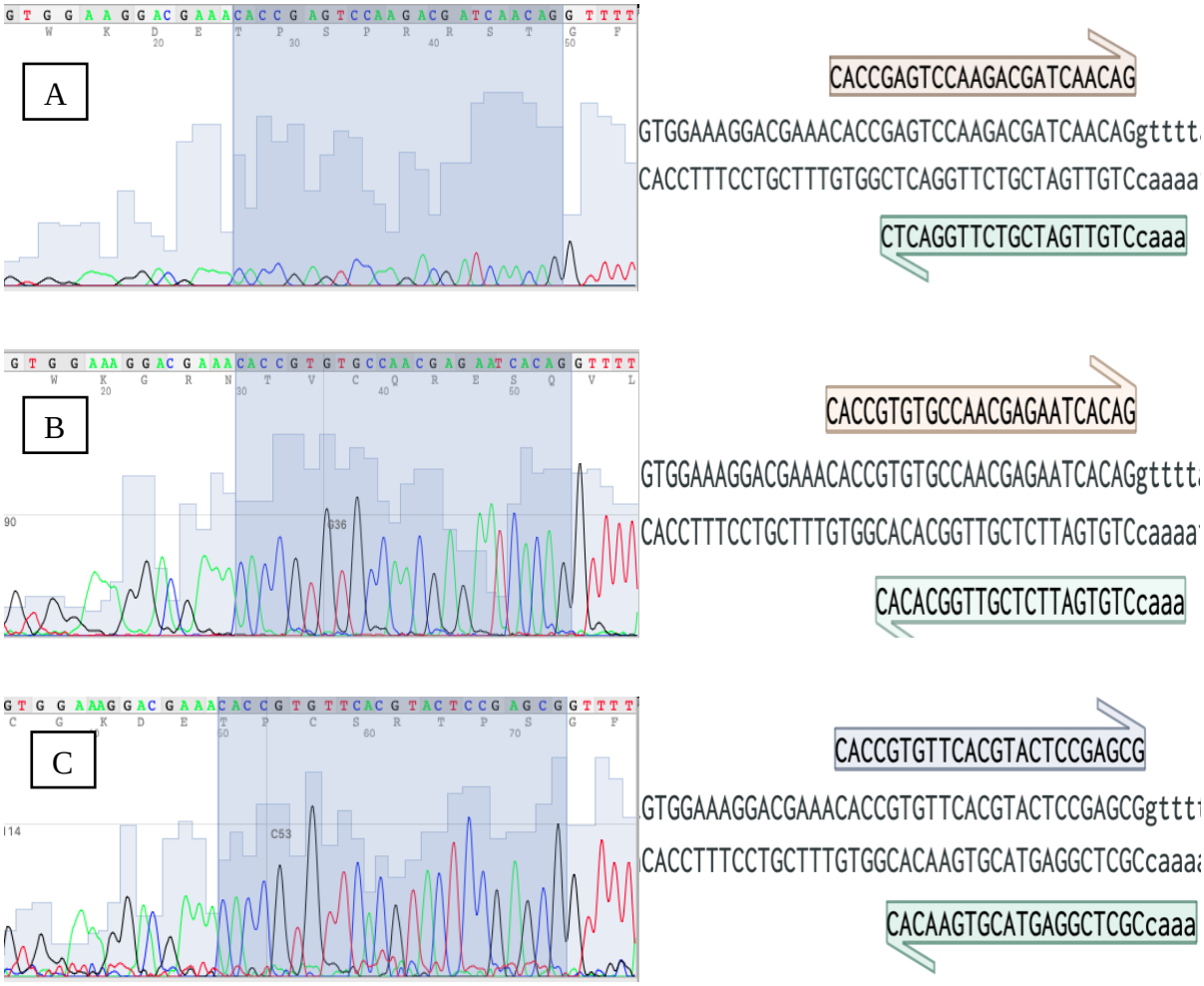

Figure 3-9: ***An illustration of sections of Sanger sequencing chromatogram from three Individual constructs (A-C) (left) along with screenshot from the gRNA designing program benchling®(right) confirming successful cloning.***

3.2.6 Puromycine concentration curve

Following the successful cloning and generating CRISPR constructs, the minimum concentration of the antibiotic puromycine that kills 90% of cells or more needs to be determine. This will help in the selection process. To this end, I have used the MTT assay, which measures the metabolic activity of the cells which generally infer cell viability. Two cell lines have been utilized: the SH-SY5Y and human embryonic kidney (HEK)-293 cells. The concentrations that were found to kill 90% or more in HEK 293 was 4 ug/ml whereas for the SH-SY5Y was 10 ug/ml(**Figure 3-10**).

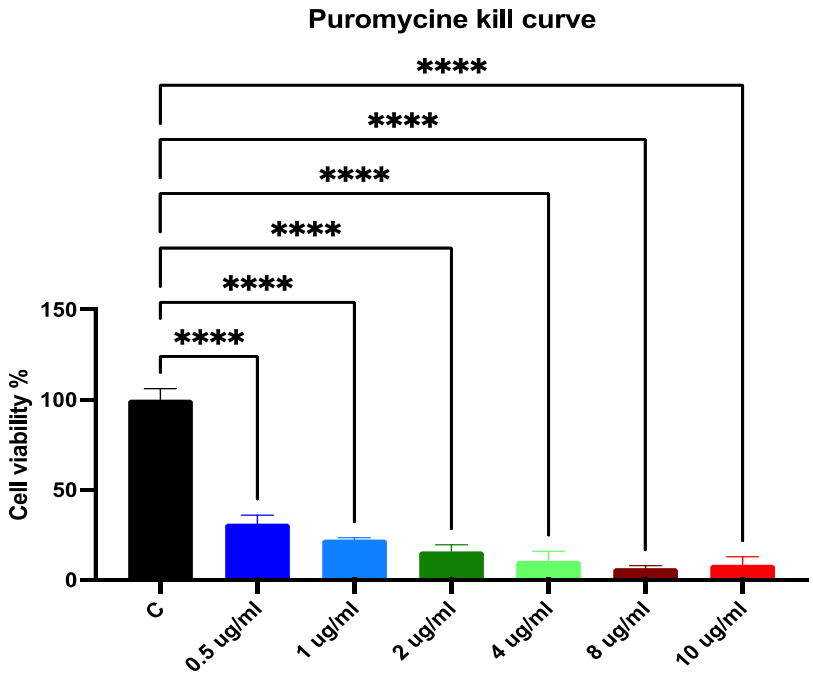

Figure 3-10 ***Puromycine kill curve in HEK-293 cells.*** *HEK 293 cells were seeded in a 24 well-plate and allowed to attach overnight. Different concentration of puromycine were added and incubated for 7 days. MTT assay was performed following the manufacturer instructions. The control untreated group was set 100%. Statistical significance was determined by one-way ANOVA followed by post hoc Tukey's test. All groups demonstrate statistical significance. ****p < 0.0001*

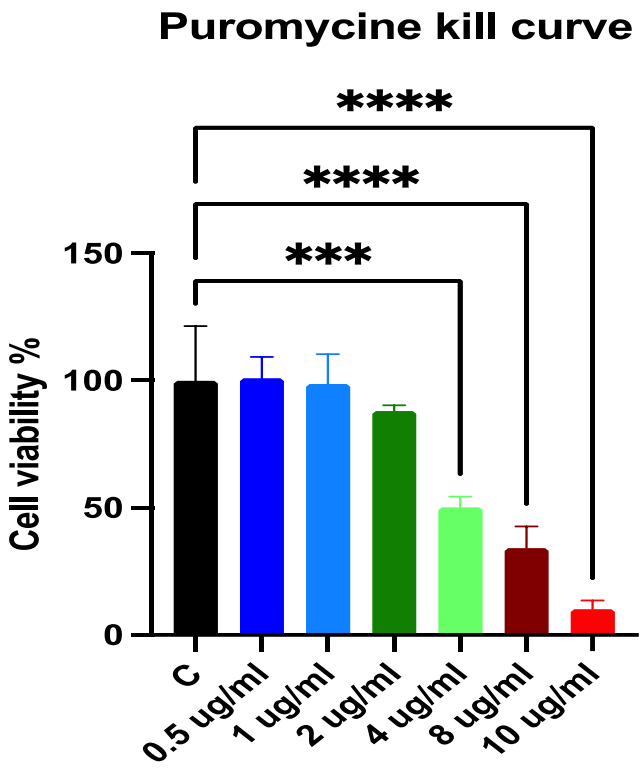

Figure 3-11 ***Puromycine kill curve in SH-SY5Y cells.*** *SH-SY5Y cells were seeded in a 24 well-plate and allowed to attach overnight. Different concentration of puromycine were added and incubated for 7 days. MTT assay was performed following the manufacturer instructions. The control untreated group was set 100%. Statistical significance was determined by one-way ANOVA followed by post hoc Tukey's test.***p < 0.001, ****p < 0.0001.*

3.3 Discussion

Previous reports support a role for LRRK2 in mediating canonical Wnt signalling. LRRK2 has been documented to interact with DVL1-3 and LRP6, which are considered main components of the canonical Wnt signalling pathway. Additionally, manipulation of *LRRK2* genetically results in perturbation of the transcriptional activity of β-catenin (Berwick et al. 2017). Furthermore, LRRK2 has also been associated with non-canonical Wnt signalling, namely the PCP pathway(Salasova et al. 2017). Since dysregulated Wnt signalling and *LRRK2* mutation are characteristic of PD, it would be interesting to examine the modulation of LRRK2 mediated canonical Wnt signalling in different *LRRK2* genotypes, including WT, G2019S and KO genotypes.

The results presented in this report substantiate the functional relationship between canonical Wnt signalling and LRRK2 protein. SH-SY5Y cells stably expressing the TCF/LEF-Luciferase reporter were used and tested with well-established controls(Granno et al. 2019). LiCl and Wnt3a, which are positive modulators for canonical Wnt signalling showed consistent activation (**Figure 4-1,3**). This is consistent with previous reports. ETC-159, a negative regulator for canonical Wnt signalling, was also used as a negative control, and it was tested in both basal and activated states, and it did decrease canonical Wnt signalling in a concentration-dependent manner in LiCl driven activation (**Figure 4-4**).

Previous studies documented the interaction between LRRK2 and canonical Wnt signalling pathway components, including DVL1-3, LRP6 and GSK3β (Berwick and Harvey 2012b). Furthermore, pathogenic mutations of *LRRK2* (R1441G, R1441C, Y1699C and G2019S) are associated with decreasing canonical Wnt signalling. Moreover, *LRRK2* knockout mice exhibited an elevation in the β-catenin mediated

transcriptional activation. Finally, Berwick and colleagues tested the effect of three non-selective LRRK2 kinase inhibitors (TAE684, LRRK2-in-1 and CZC25146) on canonical Wnt signalling with CZC25146 increasing canonical Wnt signalling while the other two decreasing it. However, when off-target effects are corrected, they all show consistent inhibition of canonical Wnt signalling(Berwick et al. 2017).

Herein, using selective LRRK2 kinase inhibitors (PF-06447475 and Mli-2), they decreased the β-catenin mediated transcriptional activity in a concentration-dependent manner under both basal and activated conditions (**Figure 3-6,7**), substantiating the previous experimental evidence of the involvement of LRRK2 in Wnt signalling. Interestingly, *LRRK2* deficient mice exhibited an increase in canonical Wnt signalling which indicate that LRRK2 acts as a repressor for canonical Wnt signalling (Berwick et al. 2017).

The kinase domain of LRRK2 represents an attractive target in the quest for developing PD therapy. However, the fact that LRRK2 kinase inhibition decreases canonical Wnt signalling, a pathway that is essential for adult neurogenesis and dysregulated in PD, should warrant a closer consideration. Rodents exposed to LRRK2 inhibitors already show an aberrant phenotype in the lungs and kidney(Fuji et al. 2015, Baptista et al. 2020).

The IC_{50} values obtained here are quite different from those reported in the literature; for instance, PF-06447475 was reported to have a cellular IC_{50} of 25 nM, while here, the value of IC_{50} is 133.9 µM under basal condition and 48.7 µM for the activated state. The difference in the values could be attributed to differences in the experimental conditions and the endpoint of the assay being used. The values

reported here are for the β-catenin mediated transcription, whereas the ones reported in the literature are for the decrease in the phosphorylation of LRRK2 at serine-935.

The majority of *LRRK2* mutations occurs either in the kinase or GTPase domains. Both domains have been documented and reported to contribute to PD pathogenesis in various model systems(Esteves et al. 2014). In addition to the development of LRRK2 kinase inhibitors, several GTPase inhibitors were developed and among them is FX-2149, which has good pharmacokinetics and pharmacodynamics characteristics. It has a dual enzymatic inhibition activity inhibiting the LRRK2 kinase and the GTPase activity. It has been tested in a PD model of inflammation, in which FX-2149 was able to decrease the LPS-induced LRRK2 upregulation and microglial activation(Thomas et al. 2016, Li et al. 2015, Li et al. 2014)

Interestingly, the degree of repression of canonical Wnt signalling is quite different in the case of FX-2149, which only inhibits β-catenin mediated transcription in the activated state compared to the other LRRK2 kinase inhibitors (PF-06447475 and Mli-2) (**Figure 3-8)**. The difference in the repression activity in the basal state could be explained by the fact that LRRK2 kinase inhibitors are potent in terms of the kinase inhibition. Indeed, FX-2149 was reported to have an IC_{90} of 100 nM for LRRK2 kinase , and at 10 nM, it decreased LRRK2 autophosphorylation at S935 by only 15%, whereas Mli-2 cellular IC_{50} was 1.4 nM. In addition, the selectivity profile of FX-2149 has not been characterized contrary to PF-06447475 and Mli-2, which both have been tested against a wide variety of kinases(Fell et al. 2015, Henderson et al. 2015, Li et al. 2015).

The question whether those observations are clinically relevant remained to be determined and speculated. Wnt signalling are vital for the developments of

dopaminergic neurons in the substantia nigra and dysregulated Wnt signalling has been documented in PD models(Joksimovic and Awatramani 2014, Purro, Galli and Salinas 2014). Furthermore, modulating and activating Wnt signalling had a neuroprotection effect in several neurodegenerative models. Thus, it has been suggested that modulating Wnt signalling could be a therapeutic strategy for treating neurodegenerative diseases(Berwick et al. 2017). However, The inhibition seen in Wnt signalling seen here is in a relatively high concentration whereas the data in the literature mostly were in the low nanomolar concentration range. Thus, it is very likely those observation might not be clinically relevant. Nevertheless, the fact that the GTPase inhibitor only inhibited canonical Wnt signalling on the activated state, this means it has a theoretical advantage. Wnt signalling is ubiquitously expressed throughout the body and inhibiting with LRRK2 kinase inhibitors could translate in off-targets effects.

3.3.1 Generating CRISPR *LRRK2* KO construct:

RNA-guided CRISPR-Cas9 nuclease system is a powerful bioengineering tool for genome editing, and it has been explored extensively in the last decade(Ran et al. 2013). Here, I have used the plasmid PX-459-V2, which encodes the necessary proteins for genome editing, including the CAS-9 protein. The sgRNAs were cloned into the PX-459-V2, and the sequence of each individual construct was verified (**Figure 3-9)**, indicating successful cloning. A number of considerations had to be taken when designing the gRNA for CRISPR constructs(Ran et al. 2013). First, the 20-nucleotide guide sequence has to be preceded by a 5' NGG or protospacer adjacent motif (PAM). CAS-9 protein's specificity that is derived from *S. pyogenes* is determined by the gRNA that has to be preceded by PAM. Second, minimize off-target effects. CAS-9 protein can indeed cleave off-target DNA targets. To this end, I have

selected the gRNAs which had the lowest predicted off-target score generated by gRNA design tool benchling®. After that, concentration response curve against puromycin were generated for SH-SY5Y and HEK 293.

Following generating the puromycin kill curve and transfecting the plasmids into the cells, puromycin was used as a selection marker. The cells didn't confer resistance against puromycin despite successful transfection, which was confirmed by transfecting a plasmid encoding GFP (Data not shown). Troubleshooting strategies have been utilized, including using a lower concentration of puromycin, sequencing the PX-459-V2 and confirming there was no mutation in the gene encoding the selection markers, puromycin-N-acetyltransferase (*Pac*) gene and using an easier cell to transfect (HEK-293), all unfortunately failed. At this point the project has been detoured toward exploring the inflammatory role of LRRK2 in immune cell.

Chapter 4 Changes in Wnt signalling activity following inflammatory stimulation in RAW 264 macrophages.

4.1 Introduction

While mutations in the *LRRK2* gene have been first linked to PD, it also has been linked to inflammatory disorders, including CD and leprosy. The exact pathomechanisms by which LRRK2 impact the aforementioned inflammatory pathologies is unknown. However, an accumulating body of literature suggest that *LRRK2* mutations and *LRRK2* KO impair immune responses in several immune cells, including the RAW 264 macrophages(Wallings, Herrick and Tansey 2020). Nevertheless, the data are inconsistent. This chapter will study the impact of *LRRK2* KO on LPS driven inflammation and associated changes in Wnt and other immune signalling pathways in RAW 264 macrophages. The involvement of the LRRK2 substrate Rab10 will be examined. Furthermore, Given Wnt signalling's role in mediating inflammatory responses, I tested the significance of Wntless (WLS) protein in mediating inflammatory response and studies associated changes in LRRK2-Rab10 signalling. WLS is a vital protein involved in the secretion and post-translation modification of Wnt ligands(Palevski et al. 2017, Dai et al. 2018).

The RAW 264 macrophages are immortalized cell lines that are derived from BALB/c mice and transformed using the Abelson leukaemia virus(Raschke et al. 1978). They possess many macrophage characteristics, such as the ability to release pro-inflammatory cytokines and NO upon TLR4 agonist stimulation. Furthermore, they have the capability to phagocyte foreign particles. Thus, RAW 264 macrophages have been used for more than four decades as a model for macrophages(Merly and Smith

2017). Generally, immortalized cell lines are easy to maintain, stable genetically and phenotypically and readily available commercially. They often produce experimentally reproducible and reliable data.

However, RAW 264 macrophages have been reported to exhibited changes in phenotype behaviour as the passage increases. Cytokines and NO release in response to LPS have been shown to change as the passage increase(Taciak et al. 2018). Therefore, throughout this thesis, experiments with RAW 264 macrophages were done between passages 1 and 12. Zinc finger nuclease gene-editing tool was used to make *LRRK2* KO RAW 264, which was available commercially(ATCC® SC-6004).

LPS is a component of gram-negative bacterial cell wall essential for the membrane's integrity. It initiates the inflammatory cascade by binding and activating TLR4 in microglia and macrophages, releasing pro-inflammatory cytokines and NO that mediate a variety of acute systematic effects ranging from fever, rash to septic shock. In the last 20 years, LPS has been used extensively in the literature to mimic the neuroinflammatory manifestation in PD. It has the ability to replicate some PD features, including activating the microglia and causing a dopaminergic neuronal loss in the nigrostriatal system(Castano et al. 1998, Liu and Bing 2011).

WLS protein, also called GPR177 in mammals, is a conserved transmembrane G protein critical for the post-translation modification of Wnt ligands(Dai et al. 2018). A couple of reports have pointed to role for WLS in immune cells and functions. For instance, heart macrophages-targeted deletion of Wls extract from mice secreted less IL-1a, profibrotic basic fibroblast growth factor (bFGF) and IL-13 compared to control macrophages(Palevski et al. 2017). Furthermore, WLS deletion in macrophages has

been shown to aggravates and increase liver injury and fibrosis in chronic liver disease models(Irvine et al. 2015).

Chapter objectives:

1) Determine the inflammatory response differences between *LRRK2* genotypes using a battery of immune assays.
2) Explore possible mechanistic insights explaining the differences between the *LRRK2* genotypes in response to inflammatory challenge.
3) Determine associated changes in Wnt and NFAT signalling
4) Determine the impact of Wnt modulator differences using biosensors for canonical Wnt and NFAT transcriptional activation.
5) Investigate the potential involvement of the recently identified LRRK2 substrate, Rab10, in mediating the inflammatory processes.
6) Study the impact of knocking-down Wntless proteins on the expression levels of Rab10, LRRK2, COX-2 and TLR-4.

4.2 Results

4.2.1 Luciferase Assay and Lentiviral Biosensor Validation

Initially, I conducted optimization and characterisation experiments. Those serve two purposes. First, chose an appropriate multiplicity of infection (MOI), which is defined as the number of viral particles to be added to a single cell. Second, Validate the lentiviruses to be used throughout this thesis with their respective positive control. SH-SY5Y neuroblastoma cells have been shown to have a high transduction efficiency and to response effectively to the positive controls for the biosensors. Thus, it has been used in paralleled with RAW 264 macrophages.

4.2.1.1 Transduction efficiency studies

The transduction efficiency studies were conducted to help guide in choosing an appropriate number of viral particles to be added to cells (MOI). To this end, a lentivirus encoding GFP (VSV.G.CMV.eGFP.WPRE) has been used to test the transduction efficiency. A range of MOIs were used (10,25, and 50), and fluorescent microscopy and flow cytometry were used to evaluate the number of transduced cells. The table below summarises the results reported in (**Figure 4-1,2**).

Cell line	MOI	Transduction efficiency
SHSY5Y	10	75.5 %.
SHSY5Y	25	91.1%
SHSY5Y	50	98%
RAW 264	10	35.8%
RAW 264	25	45.8%
RAW 264	50	88%

Table 4-1 ***Transduction efficiency in SHSY5Y and RAW 264 utilizing lentivirus encoding GFP***

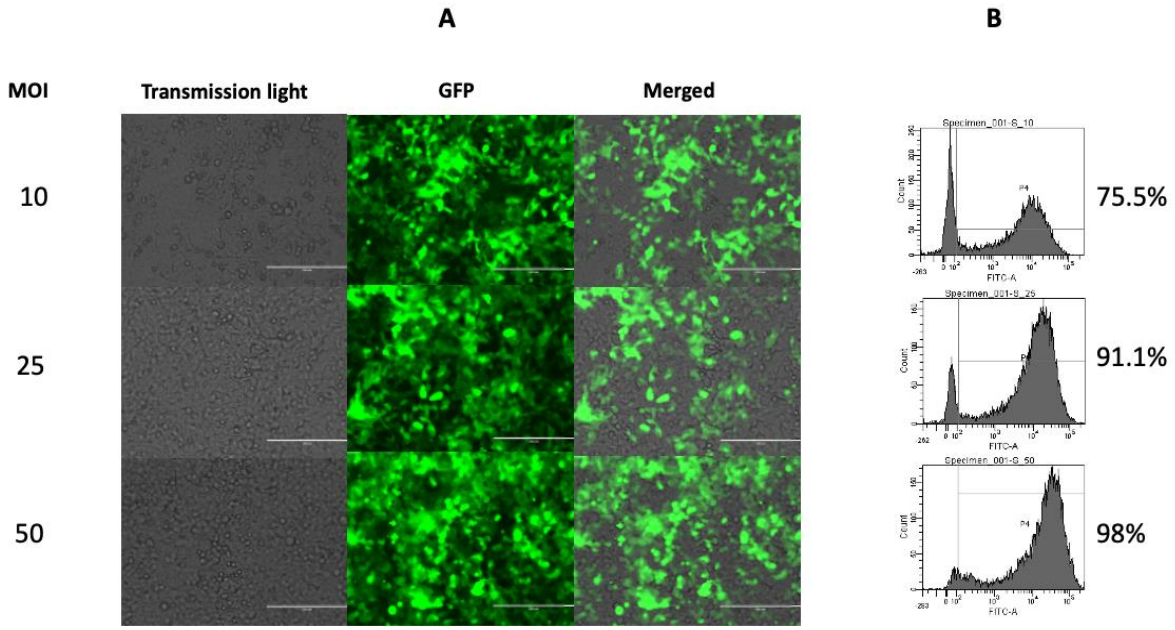

Figure 4-1 ***SH-SY5Y cells expressing Lentiviral GFP 48 hours post-transduction.*** *Lentivirus encoding GFP has been used to transduce SH-SY5Y cells at the indicated MOIs for 48 hours. Fluorescent microscopy image showing positive GFP cells(A). Quantification of GFP expression using flow cemetery showing transduction efficiency percentage for each MOI (B).*

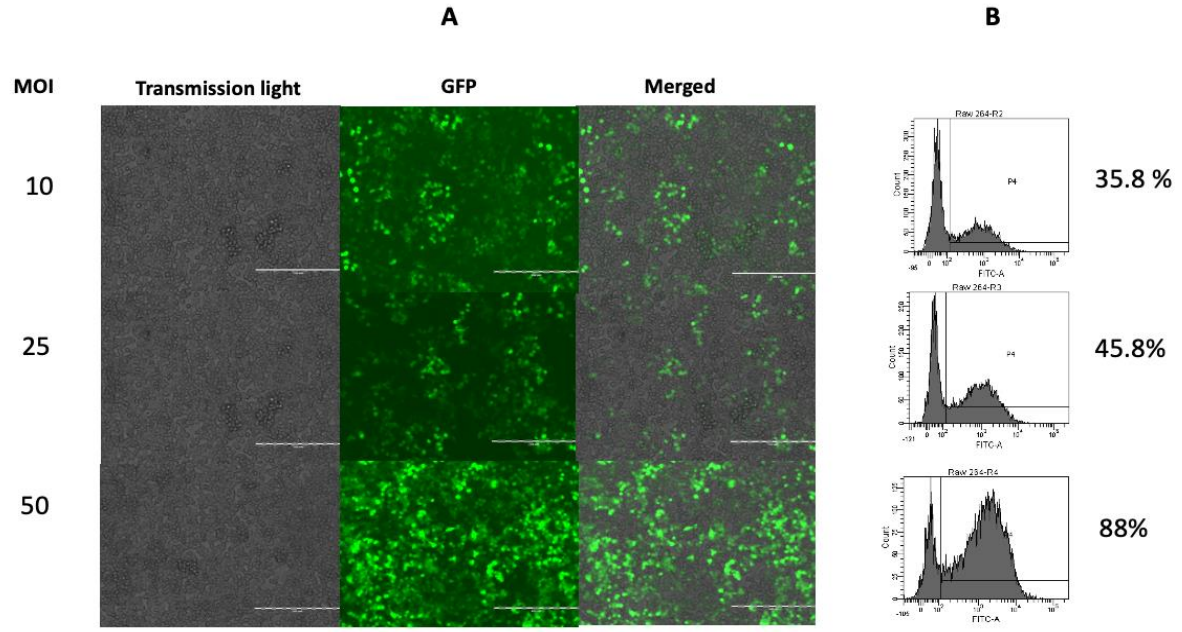

Figure 4-2 ***RAW 264 cells expressing Lentiviral GFP 48 hours post-transduction.*** *Lentivirus encoding GFP has been used to transduced Raw 264 cells at the indicated MOIs for 48 hours. Fluorescent microscopy image showing positive GFP cells(A). Quantification of GFP expression using flow cemetery showing transduction efficiency percentage for each MOI (B).*

4.2.1.2 Correlation between Luciferase expression and MOI

After determining the transduction efficiency, I sought to determine the luciferase bioluminescence signal expression in relation to the tested MOIs in RAW 264 macrophages. Having high transduction efficiency doesn't necessitate high luciferase expression.

Interestingly, the luciferase expression for the TCF/LEF was very low. The fold changes difference compared to the non-transduced cells were approximately 1.8-, 3- and 6-fold differences for MOIs 25, 50 and 100. On the other hand, the NFAT luciferase expression was substantially higher than that of the TCF/LEF. The fold differences were 7-, 36- and 81-fold differences for MOIs 25, 50 and 100 compared to the non-transduced cells **(Figure 4-3).**

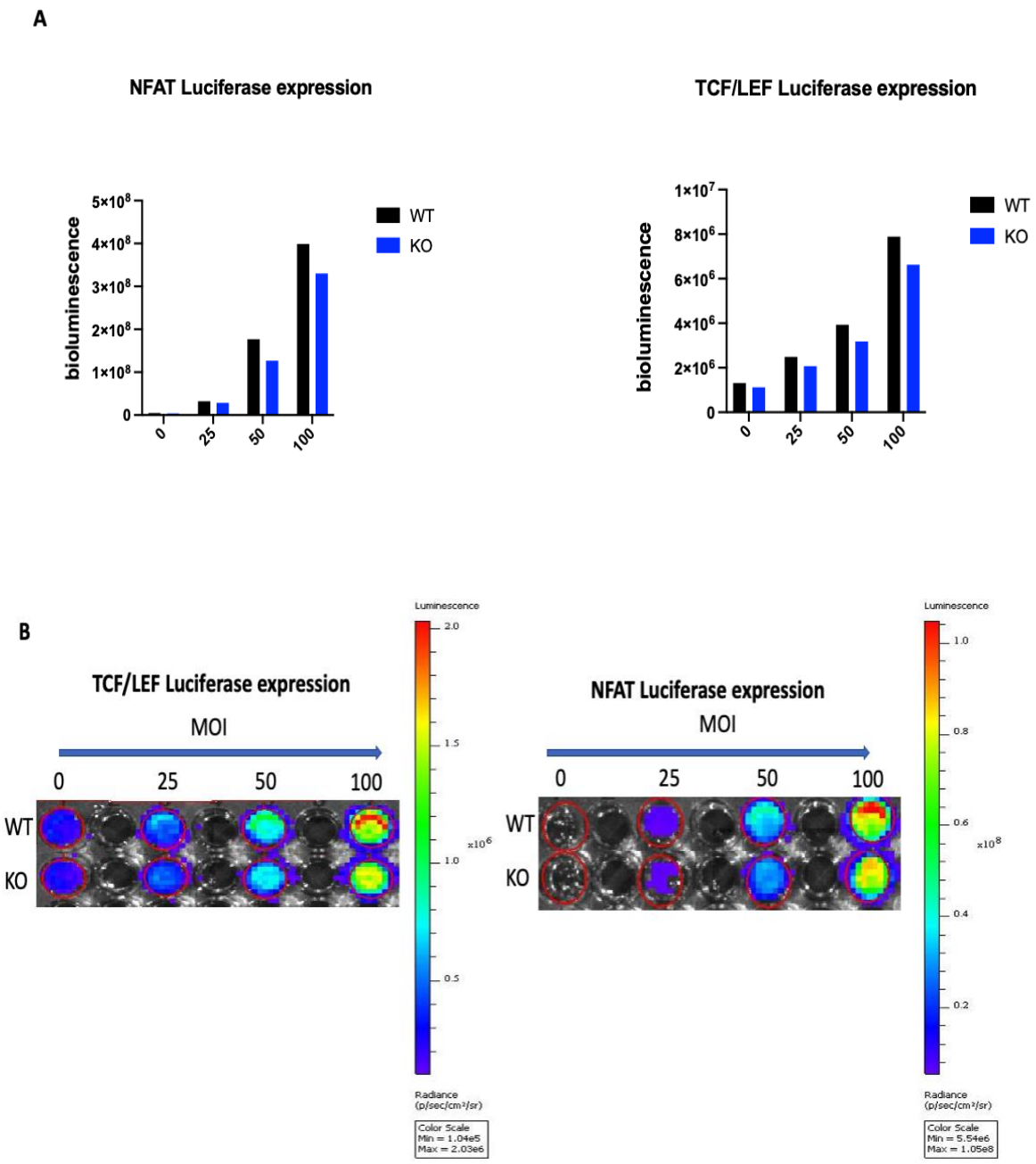

Figure 4-3 ***The luciferase bioluminescence signal expression in RAW 264 in response to TCF/LEF and NFAT lentiviruses.*** *RAW 264 cells were transduced with either TCF/LEF or NFAT lentiviruses for 48 hours, followed by measuring bioluminescence in culture media. Raw bioluminescence values from IVIS instrument(A). Bioluminescence image from the IVIS instrument. The parameter for taking the bioluminescence image is as follows: Duration=1 second, Binning =8, and the F-number =1.*

4.2.1.3 Characterization and validation of TCF/LEF and NFAT lentiviruses

Before conducting experiments in RAW 264 macrophages, which are known to be difficult to transduce (Wu and Lu 2010), TCF/LEF and NFAT lentiviruses were validated with cells that are known to be easy to transduce and for their rapid responsiveness to positive modulators for canonical Wnt and NFAT signalling.

4.2.1.3.1 Validation of TCF/LEF Lentivirus

The responsiveness of the TCF/LEF lentivirus to LiCl, a well-established positive control for canonical Wnt signalling, was tested in SH-SY5Y cells(Buckley et al. 2015). Treating the cells with 40 mM LiCl result in a 26-fold increase compared to the respective control**(Figure 4-4).**

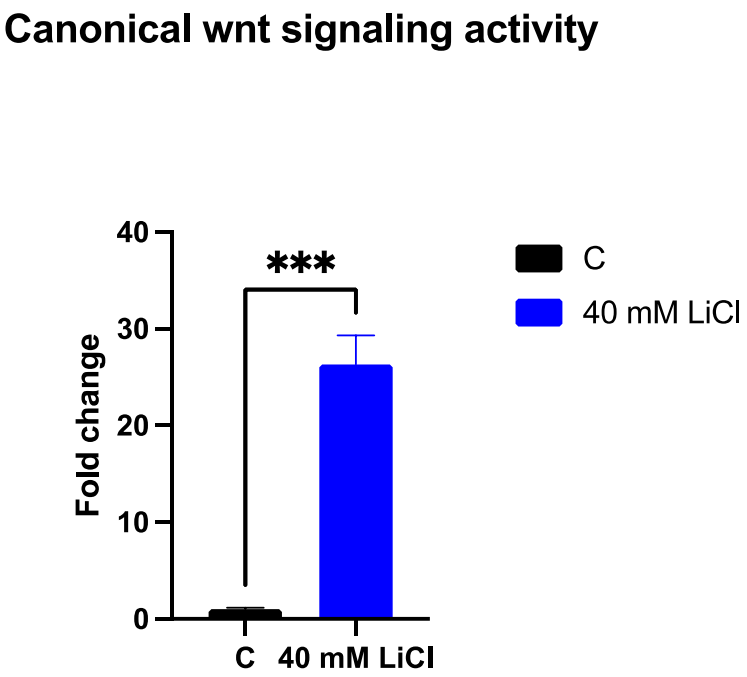

Figure 4-4 ***Validation of TCF/LEF lentivirus in SH-SY5Y stimulating with LiCl.*** *SH-SY5Y cells were transduced with TCF/LEF lentivirus for 24 hours. LiCl or control vehicle were added, and the cells were further incubated for additional 24 hours. Culture media containing secreted luciferase were assayed for bioluminescence. Statistical significance was determined by student's t-test. Values represent the mean ± S.E.M. of 3 independent experiments (with internal triplicates in each experiment). ***p < 0.001.*

4.2.1.3.2 Validation of NFAT Lentivirus

The responsiveness of the NFAT lentivirus to phorbol myristate acetate (PMA) and Ionomycin(Io), a well-established positive control for NFAT signalling, was tested in SH-SY5Y cells(Buckley et al. 2015). Treating the cells with 5,10, and 20 ng/ml PMA in combination with 0.5 uM Ionomycin resulted in 104-, 127- and 154-fold increase in NFAT signalling **(Figure 4-5).**

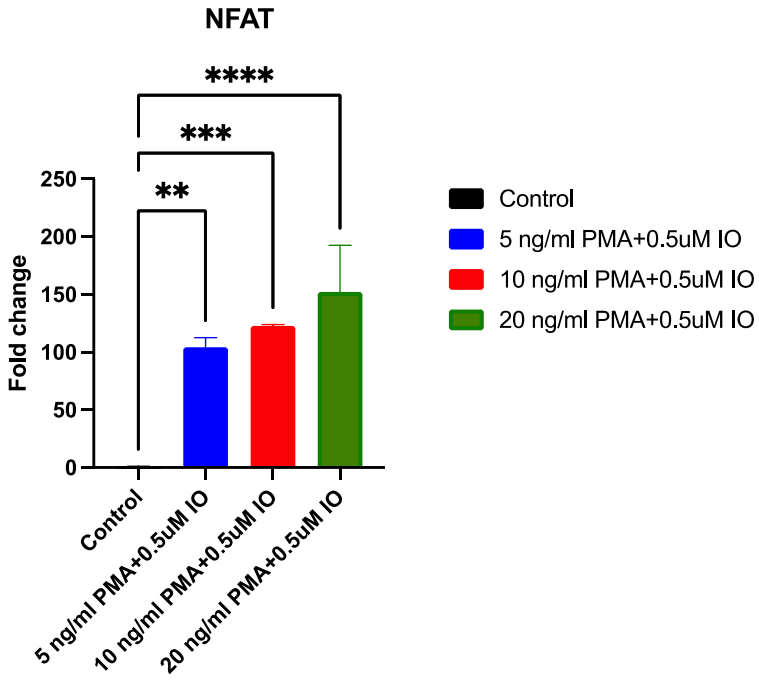

Figure 4-5 ***Validation of NFAT lentivirus in SH-SY5Y cells with PMA and Ionomycin.*** *SH-SY5Y cells were transduced with NFAT lentivirus for 24 hours. PMA and Ionomycin or control vehicle were added, and the cells were further incubated for an additional 24 hours. Culture media containing secreted luciferase were assayed for bioluminescence. Statistical significance was determined by student's t-test. Values represent the mean ± S.E.M. of 3 experiments (with internal triplicates in each experiment). ** p < 0.01, ***p < 0.001, ****p < 0.0001.*

4.2.2 Validation of *LRRK2* KO in RAW 264

Initially, I carried out KO validation experiments that serve dual purposes. First, confirm the specificity of the LRRK2 antibody and more importantly, the *LRRK2* KO cells don't express endogenous LRRK2 levels(Bordeaux et al. 2010). As expected, RAW 264 *LRRK2* KO cells don't express endogenous LRRK2 as shown in the figure below where WB reveals no band at the expected molecular weight of 286 kDa **(Figure 4-6).**

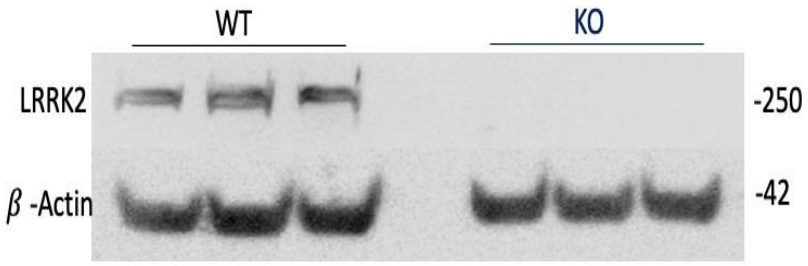

Figure 4-6: ***LRRK2 KO Validation in RAW 264 macrophages.***

4.2.3 LRRK2 expression in response to inflammatory challenge

LRRK2 upregulation in response to LPS has been debatable in the literature as most studies reported LRRK2 upregulation, whereas a handful of studies didn't see a difference(Lee et al. 2017, Moehle et al. 2012, Gillardon et al. 2012). In RAW 264, I observed a significant increase in LRRK2 expression in response to LPS **(Figure 4-7).** The total level of LRRK2 phosphorylated form (LRRK2-pS935) was increased in line with the total LRRK2 protein level. However, there was no difference in the phosphorylation pattern in response to LPS.

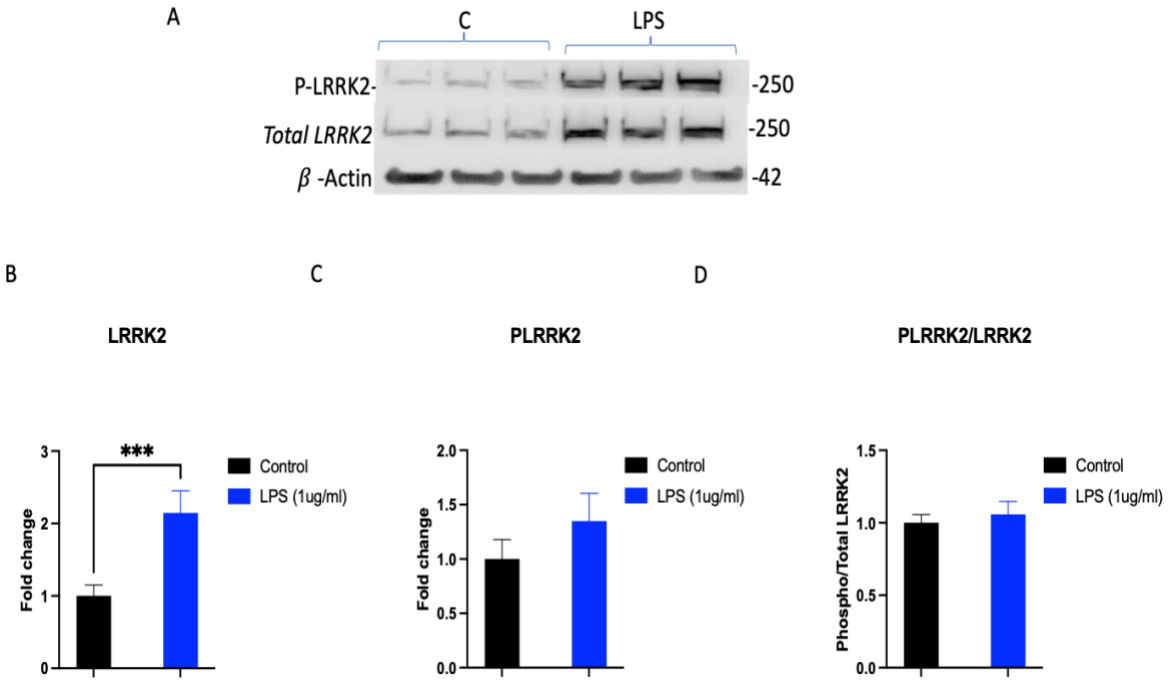

Figure 4-7 ***Analysis of LRRK2 protein level by western blot. (n=4).*** *Immunoblot image showing total LRRK2 and P-LRRK2 expression in the basal and challenged conditions in RAW 264 cells. The image represents one of four representative experiments(**A**). Densitometric analysis of the immunoblot image including total LRRK2, p-LRRK2 and the ratio of the phosphorylated form to the total protein level (**B, C and D**). The values were adjusted to the loading control β-actin. For quantification, all values have been normalised to WT control. Statistical significance was determined by student-t-test followed by post hoc Tukey's test. Values represent the mean ± S.E.M. of 4 independent experiments (with internal triplicates in each experiment). ***p < 0.001.*

4.2.4 Rab10 involvement in mediating LRRK2 immunological responses

Next, I sought to characterize the recently identified LRRK2 substrate, Rab10. Rab10 has been reported to be essential for TLR4 trafficking from the Golgi to the plasma membrane. Furthermore, knockdown of Rab10 leads to a reduction in LPS induced cytokines, substantiating a role for Rab10 in mediating immunological responses(Liu et al. 2020, Wang et al. 2010). Given the apparent effect of *LRRK2* KO on immunological responses shown here (**Figure 4-13**) and, in the literature, it is curious to look for Rab10 expression and its phosphorylation form in the LRRK2 KO cells. As

expected, genetic deletion of *LRRK2* result in significant decrease of the expression of p-RAB10 (0.59 fold ±0.12) **(Figure 5 8).** Interestingly, LPS challenged result in significant reduction of p-RAB10 in both genotypes without affecting total Rab10. The WT-LPS groups displayed (0.38 fold ±0.08) whereas the KO-LPS displayed (0.21 fold ±0.12) fold decrease.

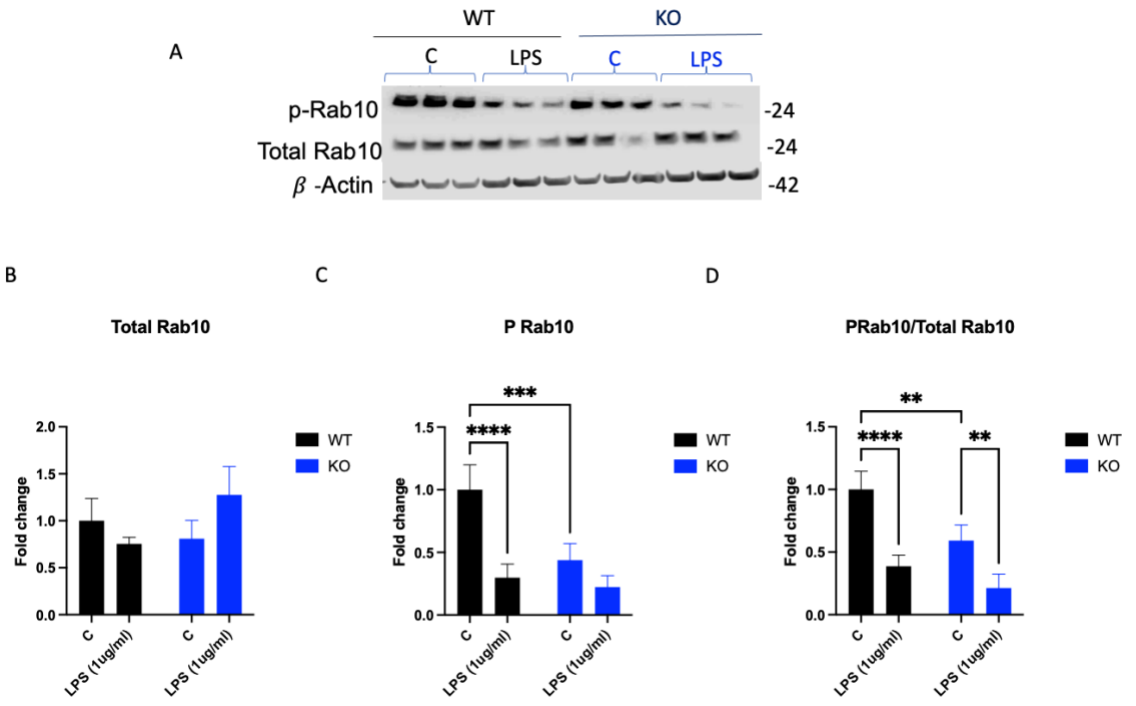

Figure 4-8 ***Analysis of Rab10 protein level by western blot. (n=4).*** *Immune-blot image showing total Rab10and p-Rab10 expression in the basal and challenged conditions in RAW 264 LRRK2 WT and LRRK2 KO cells. The image represents one of four representative experiments(**A**). Densitometric analysis of the immune-blot image including total Rab10 and p-Rab10 and the ratio of the p-Rab10 to the total Rab10 proteins level (**B, C and D**). The values were adjusted to the loading control β-actin. For quantification, all values have been normalised to WT control. Statistical significance was determined by two-way ANOVA followed by post hoc Tukey's test(n=3). Values represent the mean ± S.E.M. of 3 experiments ** p < 0.01,**** p < 0.0001.*

4.2.5 NO production

The production of NO release from the RAW 264 macrophages was assessed utilizing the Griess assay system(see2.6). As expected, treating the cells with LPS resulted in sharp increase in the production of NO in both genotypes. The concentration of NO in the basal level was almost undetectable (0.28±2.78 μM) for the *LRRK2* WT and (0.51±1.33 μM) for the *LRRK2* KO. The *LRRK2* KO-LPS treated group produced a non-significant, slightly higher NO than *LRRK2* WT control(35.00±9.33 uM vs 29.70±9.89 uM**(Figure 4-9).**

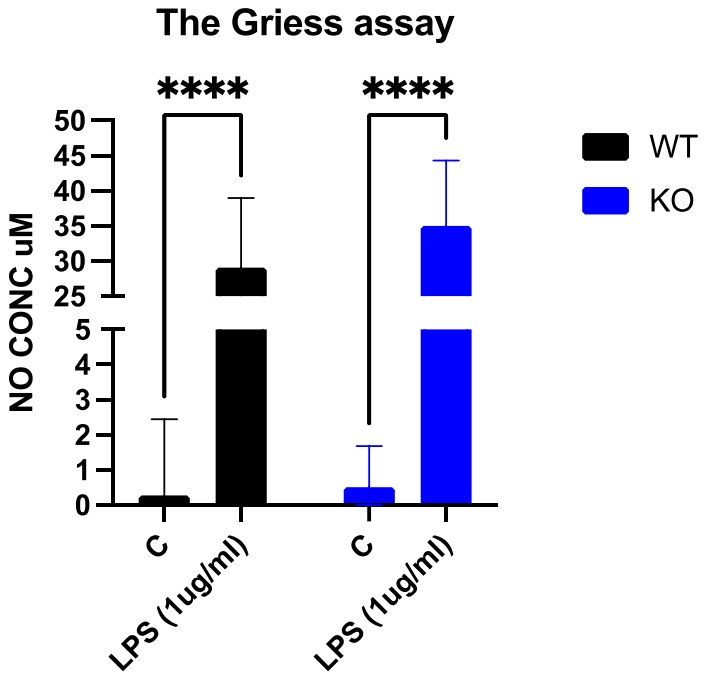

Figure 4-9 ***Effect of LRRK2 genotype on NO production in RAW264.7 cells in response to LPS****. NO production as indicated by the level of nitrite formed in the supernatant using Griess reagent. The absorbance at 540 nm was measured against culture media with Griess reagent as a blank and sodium nitrite as a standard. Statistical significance was determined by two-way ANOVA followed by post hoc Tukey's test(n=7). Values represent the mean ± S.E.M. of 7 independent experiments (with internal triplicates in each experiment) ****p < 0.0001.*

4.2.6 Phagocytotic activity in response to inflammatory challenge

The phagocytic activity of the RAW 264 macrophages was analysed by testing the cells' ability to internalise fluorescently labelled dead E-coli. The ability of the *LRRK2* KO cells to phagocyte was lower in both the basal and challenged state. However, the decrease in both was not statistically significant. The *LRRK2* WT-LPS displayed (190 ±47) % increase in the phagocyte activity, whereas the *LRRK2* KO-LPS showed (150±104). The decrease also extends to the basal level where the *LRRK2* KO-C group was (67±21) % lower than the control **(Figure 4-10).** The observed decrease was substantiated by fluorescent microscopy imaging and analysis.

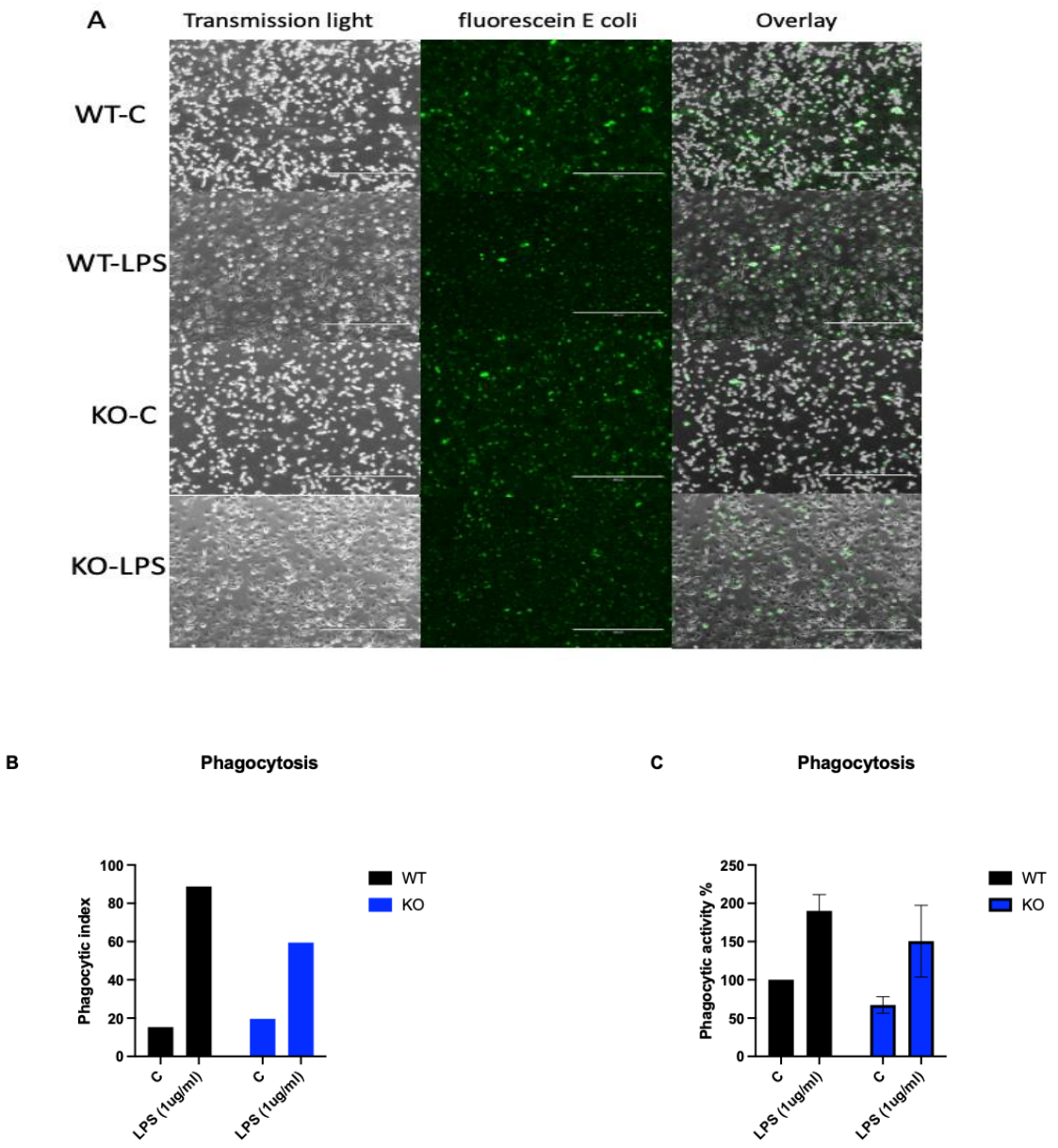

Figure 4-10 ***Phagocytic activity in RAW 264 macrophages WT and KO.*** *Raw 264 macrophages were treated with LPS or control media for 24 hr followed by labelling with fluorescein E coli for 2 hrs. Fluorescent microscopy image showing uptake of fluorescein label E coli across the different groups(**A**) Quantifications of the phagocytotic index in the fluorescent microscopy image by dividing the total number of green cells by the total number of cells(**B**). Phagocytic activity was determined by normalizing the green fluorescence intensity emitted by the WT group to 100%(**C**). Statistical significance was determined by two-way ANOVA followed by post hoc Tukey's test(n=3).*

4.2.7 Cathepsin D enzyme is not involved in mediating LRRK2 immunological responses

Given the involvement of LRRK2 in the lysosomal system and its close association with phagocytosis (Rocha et al. 2020) , I have asked if it is possible that a compromised lysosomal system could mediate the changes in immunological responses. To this end, I have measured the activity of Cathepsin D, which didn't differ across the genotypes, suggesting the difference in immunological responses were not mediated by impairment in the activity of Cathepsin D **(Figure 4-11).** Pepstatin A is a broad spectrum protease inhibitor that has been document to inhibit Cathepsin D and it was used as negative control(Yoshida et al. 2006).

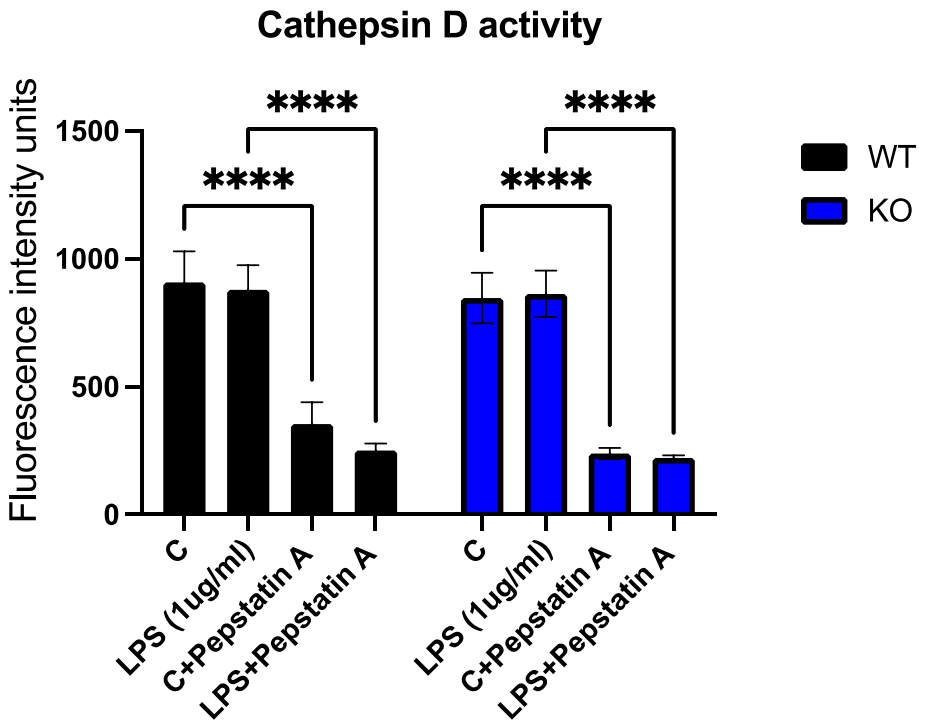

Figure 4-11 ***Cathepsin D activity in RAW 264 macrophages WT and KO.*** *Raw 264 macrophages were treated with LPS or control media for 24 hr. Cell were trypsinized processed for fluorometric assay for Cathepsin D activity(2.17). The Statistical significance was determined by two-way ANOVA followed by post hoc Tukey's test(n=3). Values represent the mean ± S.E.M. of 3 independent experiments (with internal triplicates in each experiment). ****p < 0.0001.*

4.2.8 Cytokines and chemokines analysis in response to inflammatory challenge

The observed LRRK2 upregulation and the decrease in p-Rab10 in response to LPS do suggest an inflammatory role for LRRK2. Thus, a more comprehensive method for cytokine and chemokine analysis has been utilized for further characterisation.

The proinflammatory cytokines release and expression from the macrophages in response to LPS challenge was evaluated utilising Mouse Cytokine Array Panel A (see 2.7), western blot, Griess assay and qPCR. In general, the response to LPS of the LRRK2 KO cells can be characterised by under-responsive compared to the WT **(Figure 4-13).**

4.2.8.1.1 Mouse Cytokine Array Panel A

Initially, the genetic deletion effect of *LRRK2* on LPS driven cytokines was tested. The level of cytokines release of MIP-1α, MIP-2, IL-16, IL-4, IFN-γ and TNF-α were lower in the *LRRK2* KO cells compared with *LRRK2* WT cells when stimulated with LPS (**Figure 4-14**). A subtle decrease in the *LRRK2* KO-LPS groups was also detected in BLC, C5/C5a, I-309, sICAM-1, IL-3, IL-5, IL-7, IL-17, KC, SDF-1, TIMP-1**(Figure 4-15).**

On the other hand, the release of G-CSF, IL-1α. IL-1ra, IL-6, IL-27, IP-10, I-TAC, M-CSF, JE, RANTES was higher in *LRRK2* KO cells **(Figure 4-16).**

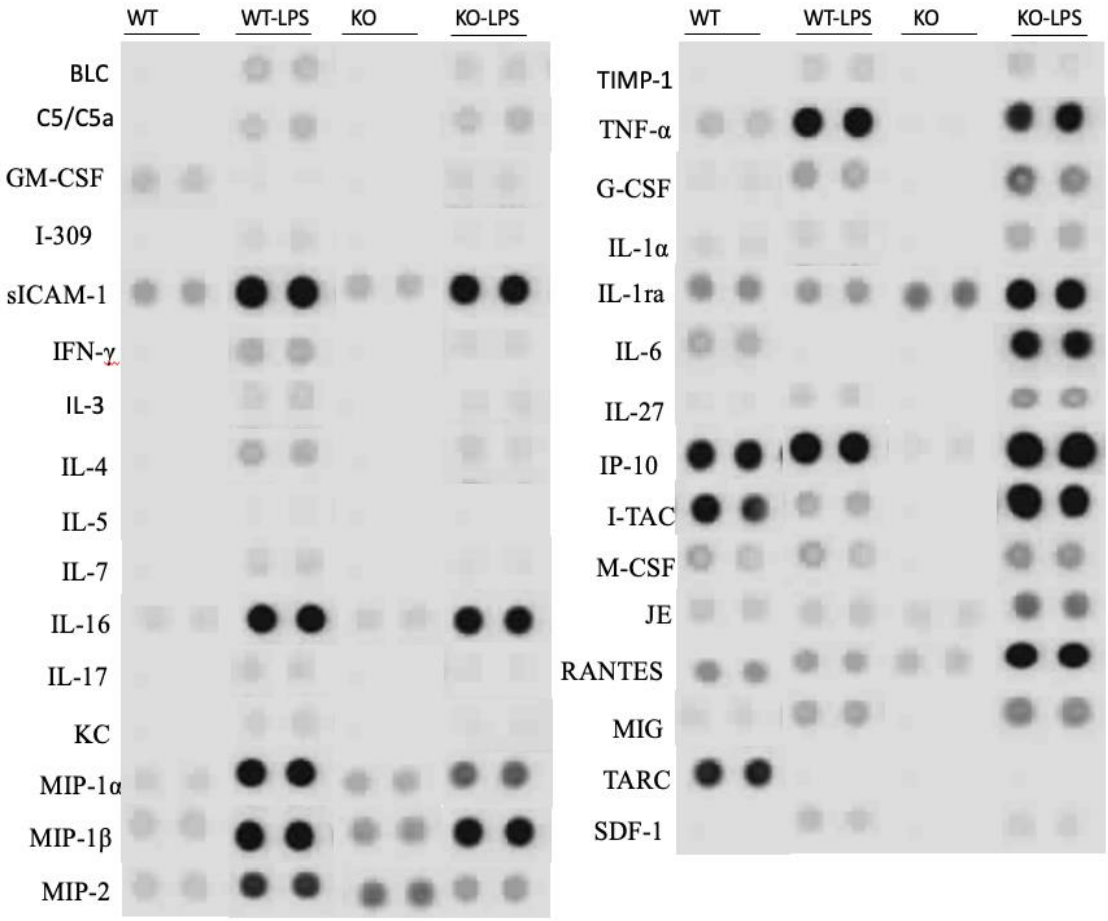

Figure 4-12. ***The production of cytokines and chemokines in murine macrophages in response to LPS treatment in LRRK2 WT and LRRK2 KO cells***. RAW 264 macrophages were seeded in 100 mm dish and treated with either LPS 1 ug/ml or control for 24 hours after which the 1 ml of cell culture supernatants were collected. To detect the production of cytokines and chemokines, the Mouse Cytokine Array Panel A was used. The images above are enlarged dots from developed membrane (*Figure 4-13*). Data represent one of three representative experiments.

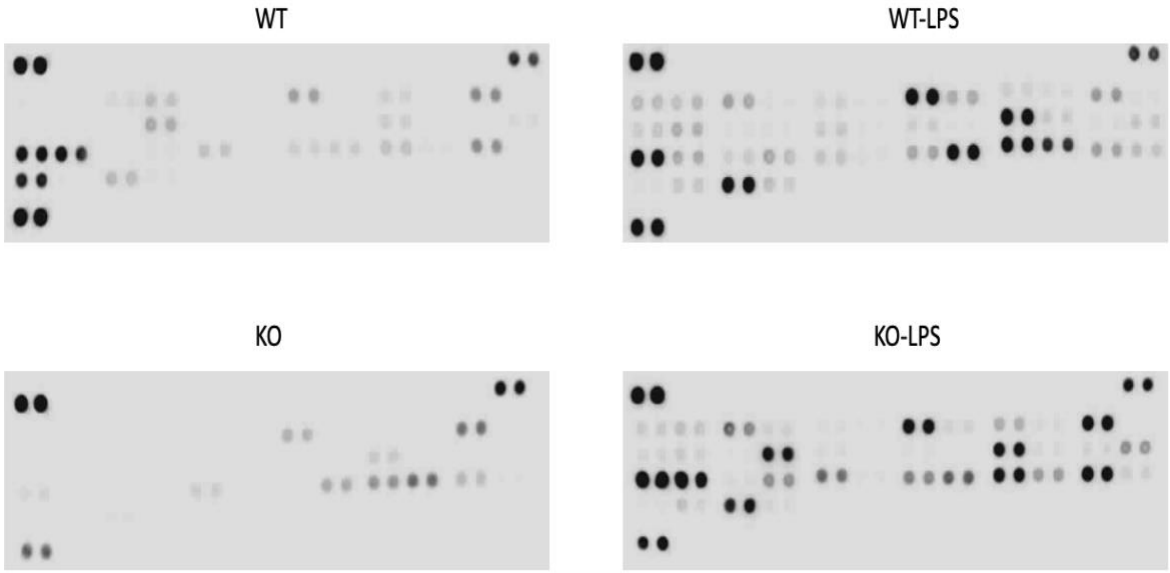

Figure 4-13 ***The production of cytokines and chemokines in murine macrophages in response to LPS treatment in LRRK2 WT and LRRK2 KO cells.*** *Immunoblot images of the whole membranes of the Mouse Cytokine Array Panel A. A Chemiluminescence agent was added to the membranes, followed by immediately placing the membranes in the GeneGnome® XRQ Chemiluminescence imager and 1 min exposure time. For coordination of the individual cytokine, please see 2.7.*

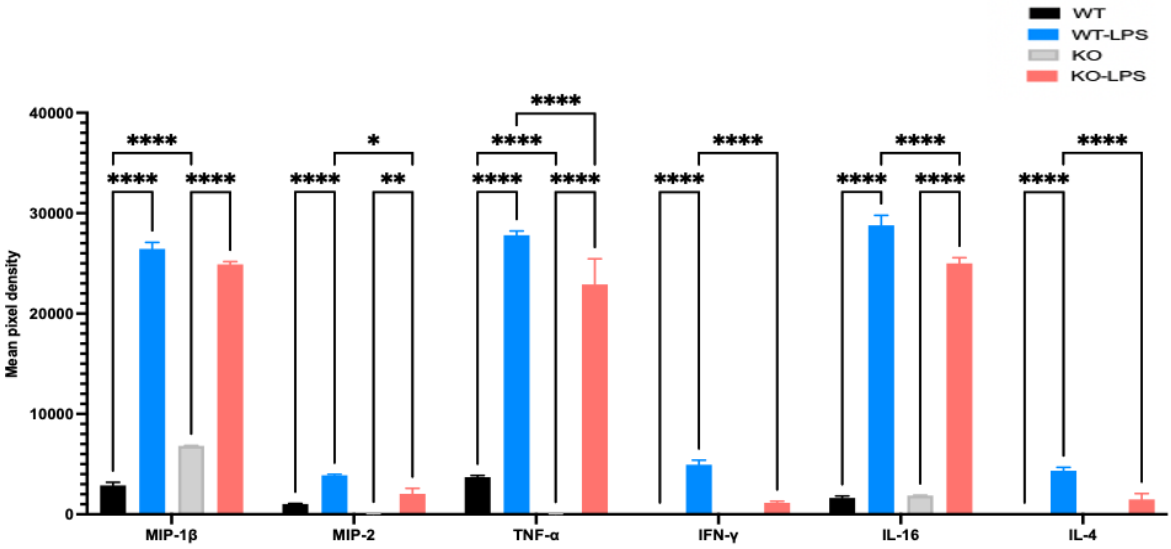

Figure 4-14 ***The densitometric analysis of cytokines and chemokines secretion that are under-responsive following LPS challenge in RAW 264 LRRK2 KO.*** *Values represent the mean ± S.E.M. of 2 independent experiments (with internal duplicate in each experiment). Statistical significance was determined by two-way ANOVA followed by post hoc Tukey's test(n=4). *p < 0.05, ** p < 0.01, ****p < 0.0001.*

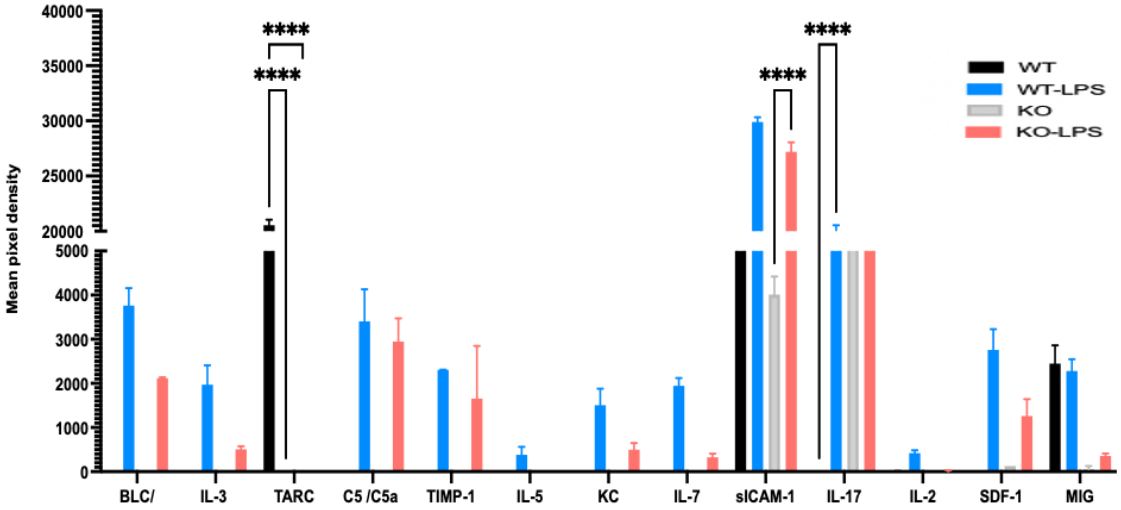

Figure 4-15 ***The densitometric analysis of cytokines and chemokines secretion that tend to be under-responsive following LPS challenge in RAW 264 LRRK2 KO.*** *Values represent the mean ± S.E.M.of 2 independent experiments (with internal duplicate in each experiment).Statistical significance was determined by two-way ANOVA followed by post hoc Tukey's test(n=4). p < 0.001.*

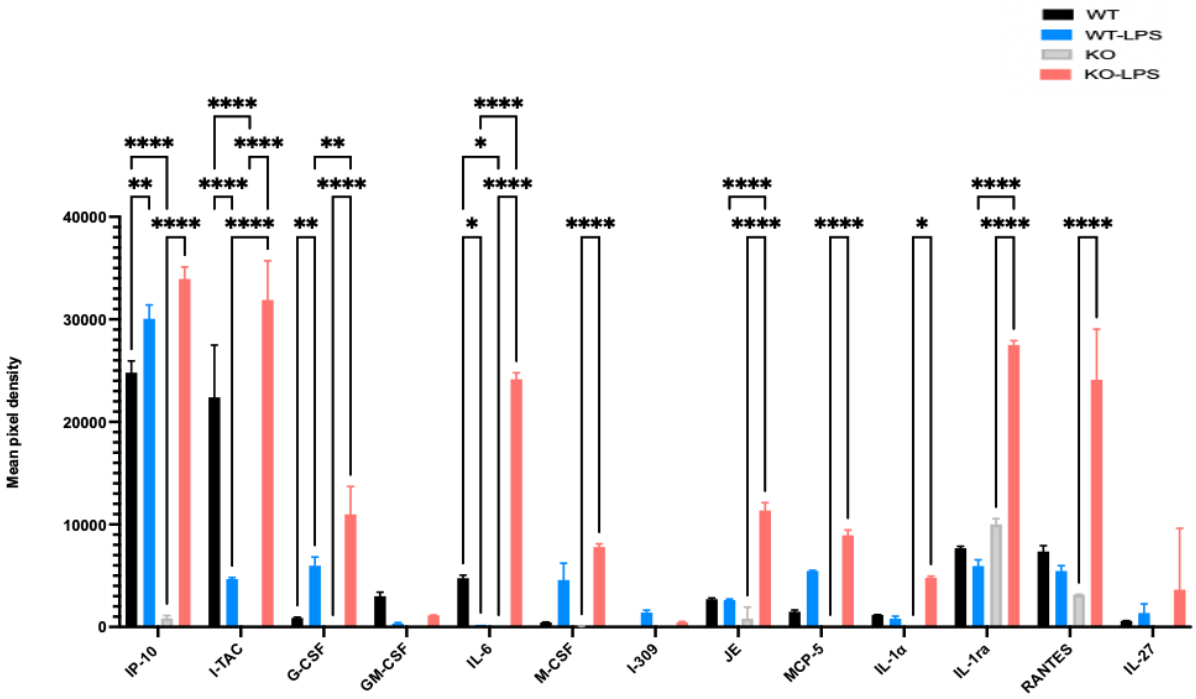

Figure 4-16 ***The densitometric analysis of cytokines and chemokines secretion that tend to be over-responsive following LPS challenge in RAW 264 LRRK2 KO.*** *Values represent the mean ± S.E.M. of 2 independent experiments (with internal duplicate in each experiment). Statistical significance was determined by two-way ANOVA followed by post hoc Tukey's test(n=4). *p < 0.05, ** p < 0.01, ***p < 0.001, ****p < 0.0001.*

After characterising the chemokines and cytokine release in response to LPS in both genotypes, I wanted to verify the results by employing different method to analyse selected cytokines : TNF-α and IFN-γ.

4.2.8.1.2 Analysis of TNF-α by qPCR analysis

The observed decreased secretion of TNF-α in *LRRK2* KO cells in response to LPS was further investigated by qPCR. The mRNA from RAW 264 macrophages WT and *LRRK2* KO cells were analysed for the expression of TNF-α in response to LPS and at the basal level. As expected, treating RAW 264 cells with LPS resulted in sharp

increase in TNF-α mRNA level in both genotypes by 29.71-fold and 11.25-fold, respectively. Interestingly and in agreement with cytokines and chemokines panel, TNF-α mRNA level in the *LRRK2* KO LPS treated cells displayed only 11.25-fold increase, though the difference was not statistically significant. The baselines response across the *LRRK2* WT and *LRRK2* KO cells were similar (1 vs 1.07) **(Figure 4-17).**

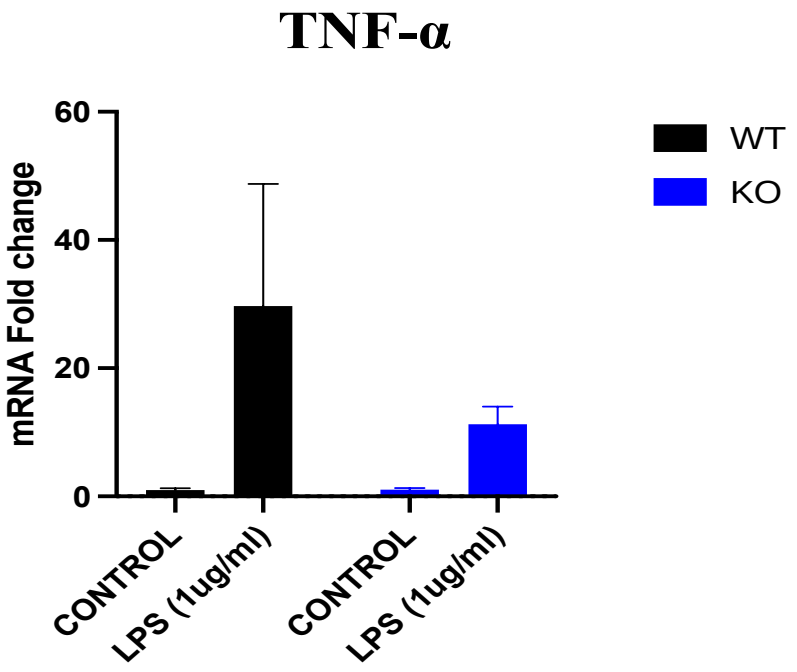

Figure 4-17 ***qPCR of TNF-α expression under β-actin housekeeping gene.*** *WT-normalised relative expression level of TNF-α was evaluated in RAW 264 macrophages LRRK2 WT and LRRK2 KO at the basal level and in response to LPS challenged. Statistical significance was determined by two-way ANOVA followed by post hoc Tukey's test(n=3). Values represent the mean ± S.E.M. of 3 independent experiments (with internal triplicates in each experiment).*

4.2.8.1.3 IFN-γ analysis by qPCR

The mRNA from RAW 264 macrophages *LRRK2* WT and *LRRK2* KO cells were analysed for the expression of IFN-γ in response to LPS and at the basal level. As expected, treating RAW 264 cells with LPS result in sharp increase in IFN-γ's mRNA

level in both genotypes by 4-fold and 13-fold, respectively. Interestingly, the basal mRNA levels in the *LRRK2* KO-C control groups displayed a 4-fold increase in comparison to WT-C **(Figure 4-18).**

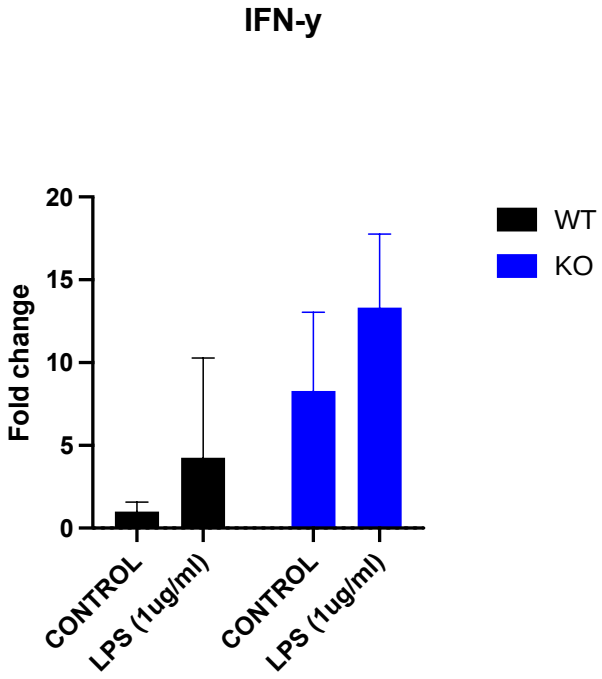

Figure 4-18 ***qPCR of IFN-γ expression under β-actin housekeeping gene (n=3).*** *WT-normalised relative expression level of IFN-γ was evaluated in RAW 264 macrophages LRRK2 WT and LRRK2 KO at the basal level and in response to LPS challenged. Statistical significance was determined by two-way ANOVA followed by post hoc Tukey's test. Values represent the mean ± S.E.M. of 3 independent experiments (with internal triplicates in each experiment).*

4.2.9 NFAT and NF-κB signalling in response to LPS and Wnt modulators and the impact of LRRK2 deletion

Given the well-established role of NFAT and NF-κB in mediating inflammatory processes and the reported association they have with LRRK2 in the literature(Lopez de Maturana et al. 2016, Liu et al. 2011), I have asked the question whether impairment in NFAT and NF-κB signalling could explain the dysregulated immune response seen in LRRK2 KO to LPS. Luciferase assay, western blot and qPCR were employed.

4.2.9.1 Luciferase assay measuring NFAT transcriptional activity

To measure changes in NFAT transcriptional activity in response to LPS and other modulators, Luciferase-mediated bioluminescence using lentiviruses were used. The lentiviruses encode the luciferase enzyme's secreted form, allowing direct and reliable measurements of either NFAT transcriptional activation or canonical Wnt signalling activity (Please see 4.2.10.1). The secreted luciferase is under the control of a promotor of natively expressed proteins of interest. TCF/LEF for the canonical Wnt signalling and NFAT for the non-canonical Wnt signalling and Ca^{+2} signalling.

The changes in NFAT transcriptional activation in response to LPS and /or Wnt modulators were tested. The *LRRK2* WT-C group raw bioluminescence values were normalized to one and the treatment groups were expressed as fold change.

4.2.9.1.1 LPS

Challenging the cells with LPS for 5 hours resulted in marked decrease (almost 50%) in NFAT transcriptional activation in both genotypes. There were no differences across the genotypes either in the basal or the challenged state.

Interestingly, a further time course analysis at 24 hours revealed that the LPS impact on NFAT transcriptional activation was diminished and basal and challenged conditions were about the same(**Figure 4-19).**

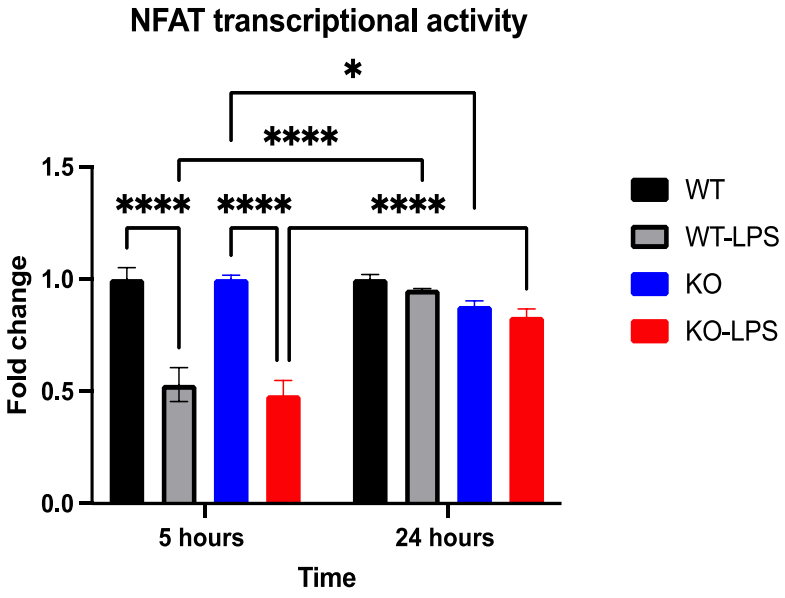

Figure 4-19 ***Modulation of NFAT transcriptional activation by LPS****. RAW 264 cells were transduced with NFAT lentivirus for 24 hours. LPS 1 ug/ml or control vehicle were added, and the cells were further incubated for additional 5 or 24 hours. Culture medium containing secreted luciferase were assayed for bioluminescence. Statistical significance was two-way ANOVA followed by post hoc Tukey's test(n=3). Values represent the mean ± S.E.M. of 3 experiments (with internal triplicates in each experiment). *p < 0.05, ****p < 0.0001.*

4.2.9.1.2 PMA/IO

Next, the activation of NFAT transcriptional activation in *LRRK2* WT and *LRRK2* KO in response to PMA (20 ng/ml) and IO (0.5 uM) were tested. PMA/IO treatment increased the NFAT transcriptional activation in both genotypes. There were no differences across the genotypes.

Similar to LPS, NFAT transcriptional activation after incubating the cells 24 hours with PMA/IO resulted in no differences in the basal and challenged conditions.

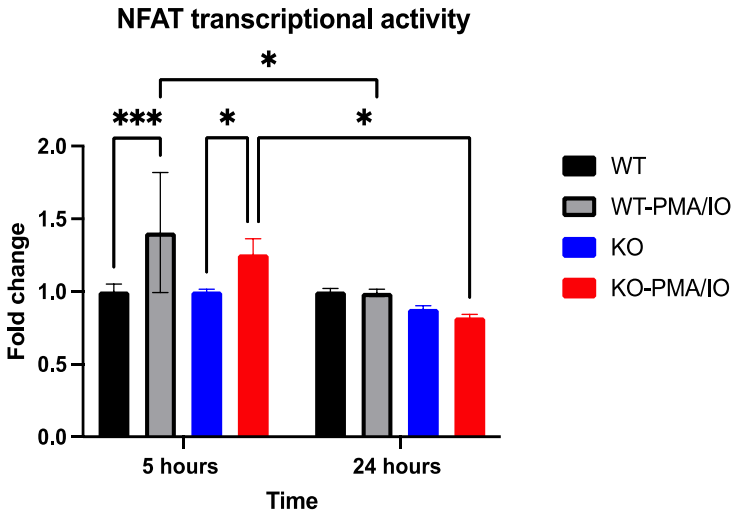

Figure 4-20 ***Modulation of NFAT transcriptional activation by PMA/IO****. RAW 264 cells were transduced with NFAT lentivirus for 24 hours. LPS 1 ug/ml or control vehicle were added, and the cells were further incubated for additional 5 or 24 hours. Culture media containing secreted luciferase were assayed for bioluminescence. Statistical significance was two-way ANOVA followed by post hoc Tukey's test(n=3). Values represent the mean ± S.E.M. of 3 experiments.). *p < 0.05, ** p < 0.01, ***p < 0.001, ****p < 0.0001.*

4.2.9.1.3 LiCL

While LiCl is traditionally known as an activator for canonical Wnt signalling, several studies have documented that LiCl can also increase non-canonical Wnt signalling(Whitley et al. 2020, Puri et al. 2004). To this end, I have tested the impact of LiCl on NFAT transcriptional activation.

Treating the cells with LiCl resulted in a significant increase in non-canonical Wnt signalling in both genotypes. Intriguingly, the increase in the *LRRK2* KO-LPS group was (1.38± 0.19) fold difference which was significantly lower compared to the *LRRK2* WT-LPS group (1.65 ±0.39). Further analysis at 24 hours time point reveals no differences across the different groups (**Figure 4-21)**.

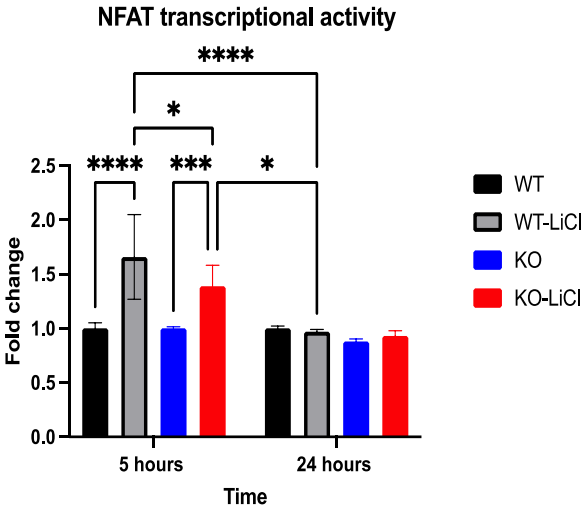

Figure 4-21 ***Modulation of NFAT transcriptional activation by LiCl 40 mM****. RAW 264 cells were transduced with NFAT lentivirus for 24 hours. LiCl 40 mM or control vehicle were added, and the cells were further incubated for additional 5 or 24 hours. Culture media containing secreted luciferase were assayed for bioluminescence. Statistical significance was two-way ANOVA followed by post hoc Tukey's test(n=3). Values represent the mean ± S.E.M. of 3 experiments). *p < 0.05, ** p < 0.01, ***p < 0.001, ****p < 0.0001.*

4.2.9.1.4 Wnt3a and Wnt5a

A considerable amount of literature has been published on the role that Wnt secreted proteins play in immune cells1.3.21.3.5). Wnt3a and Wnt5a, in particular, seemed to have a substantial role in microglia, whereas they upregulate pro-inflammatory cytokines on their own but decrease LPS driven cytokines(Halleskog and Schulte 2013). For this reason, it would be interesting to see if genetic deletion of *LRRK2* will impact Wnt3 or Wnt5a mediated Wnt signalling or NFAT transcriptional activity on the basal and challenged conditions.

Wnt3a:

Treating the cells with Wnt3a resulted in a decrease in NFAT transcriptional activity in both genotypes. However, the reduction in the *LRRK2* KO was significantly lower (0.68 fold ± 0.17) VS (0.91 fold ± 0.0.07) for the *LRRK2* WT-Wnt3a. When Wnt3a is

combined with LPS, the difference across the groups is mitigated, and the changes in NFAT transcriptional activity is non-significantly lower in the *LRRK2* KO groups. The *LRRK2* KO-Wnt3a group displayed (0.83 fold ±0.07), whereas the *LRRK2* KO-Wnt3a+LPS showed a (0.88 fold ± 0.01) fold decrease (**Figure 4-22**).

Wnt5A:

Treating the cells with Wnt5a did not result in a change in NFAT transcriptional activity in both genotypes. However, the *LRRK2* KO-Wnt5a group displayed a significant decrease (0.87 fold ±0.02) compared to the respective *LRRK2* WT-Wnt5a control group (0.97 fold ± 0.04). The same trend was observed in the challenged combined conditions whereby the *LRRK2* KO group displayed a lower NFAT transcriptional activity. The fold decrease in the *LRRK2* KO-Wnt5a+LPS group was (0.86 fold ±0.02) compared to (0.95 fold ±0.02) for the *LRRK2* WT- Wnt5a+LPS group**(Figure 4-22).**

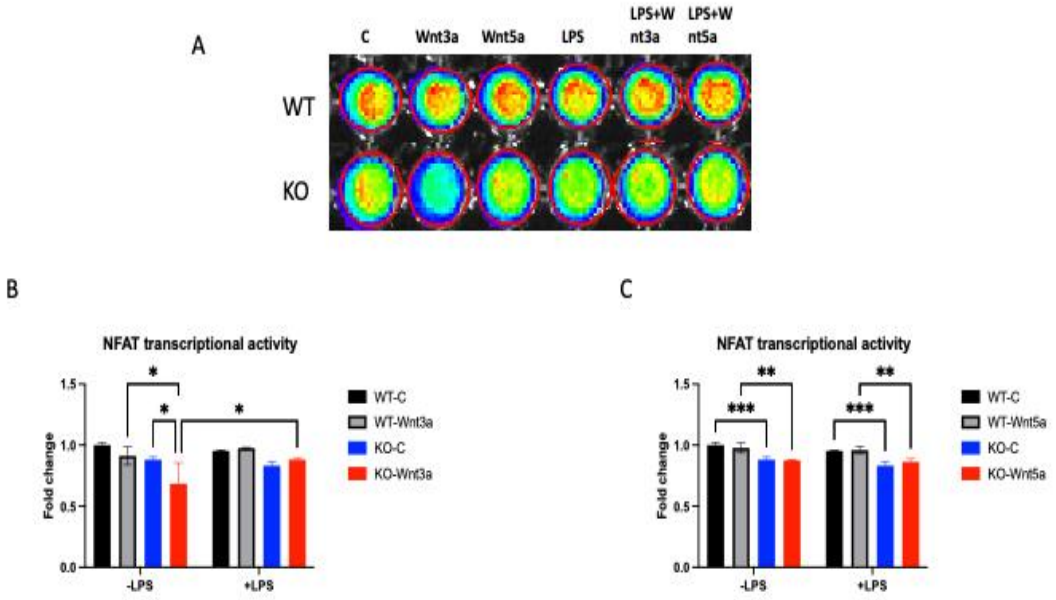

Figure 4-22 ***Modulation of NFAT transcriptional activation by Wnt modulators.*** *RAW 264 cells were transduced with NFAT lentivirus for 24 hours. The indicated treatments have been added and further incubated for 24 hours. Representative image showing bioluminescence as a result of different treatment in WT and KO (A). Culture media containing secreted luciferase were assayed for bioluminescence. Statistical significance was two-way ANOVA followed by post hoc Tukey's test(n=3). Values represent the mean ± S.E.M. of 3 experiments.). *p < 0.05, ** p < 0.01, ***p < 0.001, ****p < 0.0001.*

4.2.9.2 NF-κB

4.2.9.2.1 NF-κB analysis by western blot

The total protein expression levels of NF-κB was analysed in response to LPS and at the basal level. A decrease in total NF-κB protein levels was observed in both genotypes in response to LPS. The decrease in *LRRK2* KO-LPS group is more notable in comparison to *LRRK2* WT-LPS (0.4 fold ± 0.16, p=0.062 vs 0.66 fold ±0.07, p=0.36,**Figure 4-23**). There were no differences at the basal level.

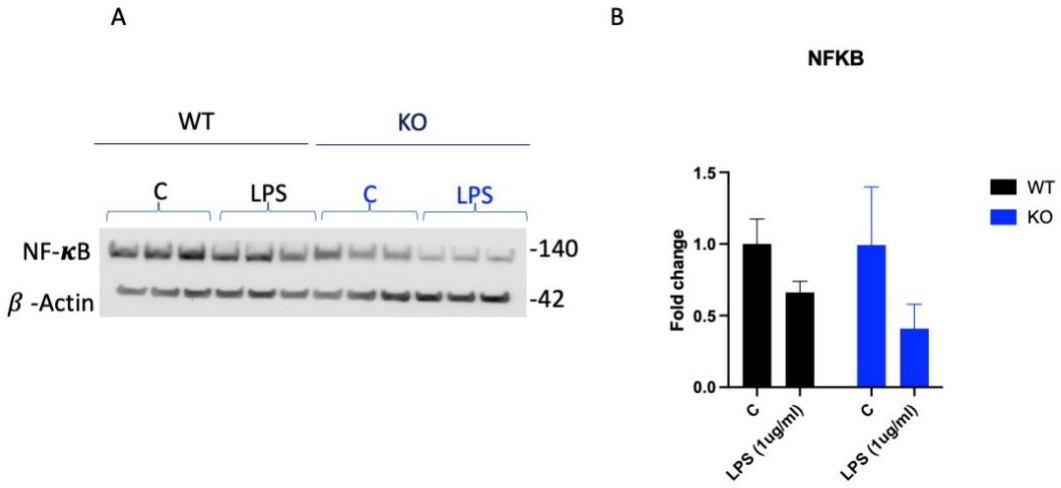

Figure 4-23 ***Expression analysis of NF-κB protein level(n=3).*** *Immune-blot image showing NF-**κ**B expression in the basal and challenged conditions in RAW 264 LRRK2 WT and LRRK2 KO cells. The image represents one of three representative experiments(**A**). Densitometric analysis of the immune-blot image(**B**). The values were adjusted to the loading control β-actin. For quantification, all values have been normalised to WT control. Statistical significance was determined by two-way ANOVA followed by post hoc Tukey's test. Values represent the mean ± S.E.M. of 3 independent experiments (with internal triplicates in each experiment).*

4.2.9.2.2 NF-κB analysis by qPCR

The mRNA from RAW 264 macrophages *LRRK2* WT and *LRRK2* KO cells were analysed for the expression of NF-κB in response to LPS and at the basal level. In line with western blot data, a decrease in mRNA level of NF-κB levels was observed in both genotypes in response to LPS. *LRRK2* WT-LPS group showed a significant decrease (0.16 fold ±0.09) fold decrease whereas the *LRRK2* KO-LPS groups displayed (0.18 fold ±0.09,p=0.15). In comparison to *LRRK2* WT-C group. A noticeable reduction at the basal in the *LRRK2* KO cells is observed (0.41 fold ±0.27) **(Figure 4-24).**

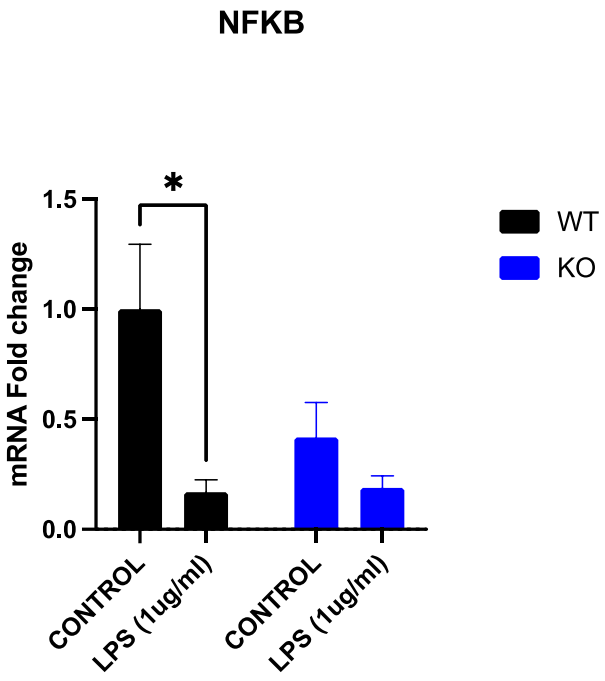

Figure 4-24 ***qPCR of NF-κB expression under β-actin housekeeping gene (n=3).*** *WT-normalised relative expression level of NF-κB was evaluated in RAW 264 macrophages WT and LRRK KO at the basal level and in response to LPS challenged. Statistical significance was determined by two-way ANOVA followed by post hoc Tukey's test. Values represent the mean ± S.E.M. of 3 independent experiments (with internal triplicates in each experiment). *p < 0.05.*

4.2.9.3 TLR-4 could be involved in mediating LRRK2 immunological responses

Next, I wanted to investigate possible explanation(s) for the differences in immune response across the *LRRK2* genotypes. LPS molecular pharmacological target is TLR-4, and it is critical for LPS induced immune responses. To this end, I hypothesized that the differences in immune responses could be attributed to the downregulation of TLR-4. Indeed, As shown in **Figure 5-25**, TLR-4 protein levels tend to be substantially lower in the *LRRK2* KO-LPS group compared to other groups, though the difference is not statistically significant. TLR-4 protein expression level for *LRRK2* KO-LPS group was (0.44 fold ±0.09) compared to (0.76 fold ±0.21) for *LRRK2* WT-LPS group.

Additionally, the basal level of *LRRK2* KO cells was (0.84 fold ±0.11) in comparison to *LRRK2* WT-C group.

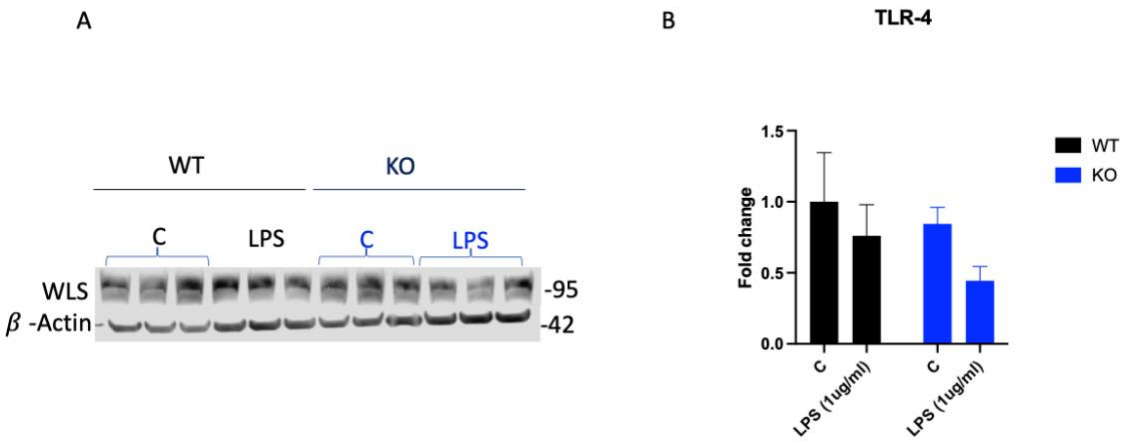

Figure 4-25 ***TLR-4 receptor expression in WT and LRRK2-KO RAW 264 macrophages in response to LPS****) Immune-blot image showing TLR-4 expression in the basal and challenged conditions in RAW 264 LRRK2 WT and LRRK2 KO cells. The image represents one of three representative experiments(**A**). Densitometric analysis of the immune-blot image(**B**). The values were adjusted to the loading control β-actin. For quantification, all values have been normalized to WT control. Statistical significance was determined by two-way ANOVA followed by post hoc Tukey's test(n=3). Values represent the mean ± S.E.M. of 3 independent experiments (with internal triplicates in each experiment).*

4.2.9.3.1 NFAT analysis by western blot

The total protein expression level of NFAT was analysed in response to LPS and at the basal level. A significant decrease was observed in both genotypes in the challenged state. The reduction in the *LRRK2* WT-LPS group was (0.53±0.17) fold decrease and for the *LRRK2* KO-LPS group was (0.44±0.13) fold decrease (**Figure 4-26).** No significant differences are observed across the *LRRK2* genotypes at the basal and challenged state.

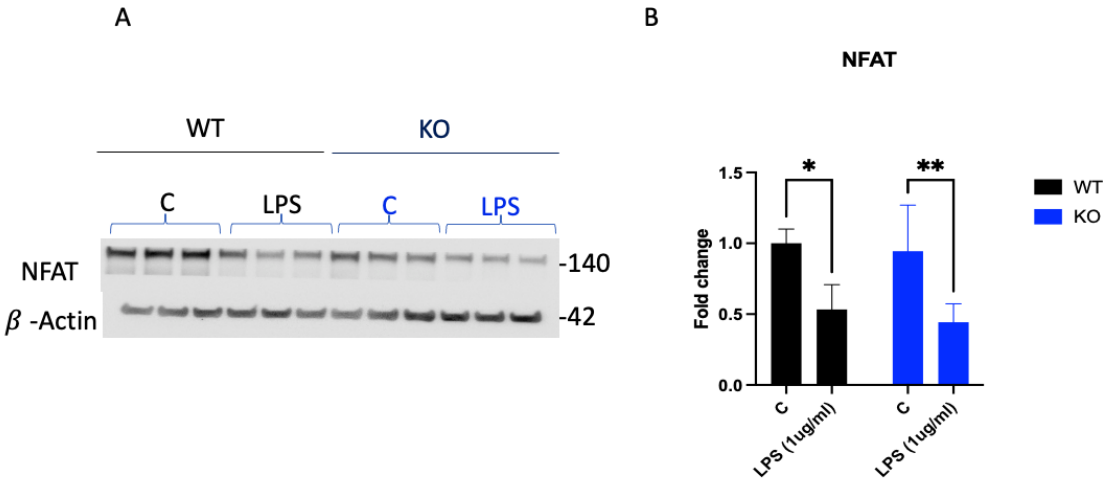

Figure 4-26 ***Expression analysis of NFAT protein level(n=5).*** *Immune-blot image showing NFAT expression in the basal and challenged conditions in RAW 264 LRRK2 WT and LRRK2 KO cells. The image represents one of five representative experiments(**A**). Densitometric analysis of the immune-blot image(**B**). The values were adjusted to the loading control β-actin. For quantification, all values have been normalised to WT control. Statistical significance was determined by two-way ANOVA followed by post hoc Tukey's test. Values represent the mean ± S.E.M. of 3 independent experiments (with internal triplicates in each experiment). *p < 0.05, ** p < 0.01.*

4.2.9.3.2 NFAT analysis by qPCR

The mRNA from RAW 264 macrophages *LRRK2* WT and *LRRK2* KO cells were analysed for the expression of NFAT in response to LPS and at the basal level. In agreement with the western blot data, LPS treatment decreased the total NFAT mRNA level in both genotypes. At the basal level, there was a slight non-significant decrease in the *LRRK2* KO cells (0.75 fold ±0.6). At the challenged state, the NFAT mRNA level was tend to be higher in the *LRRK2* KO cells compared with WT (0.46 fold ±0.35 vs 0.17 fold ±0.15)(**Figure 4-27)**. Though the difference was not significant.

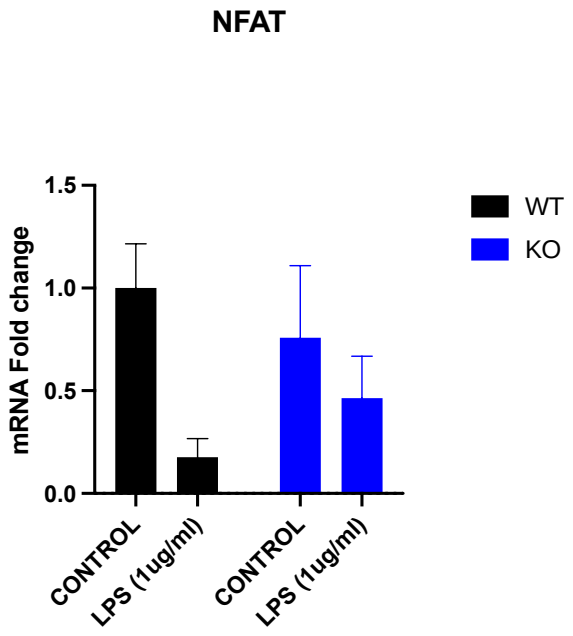

Figure 4-27 ***qPCR of NFAT expression under β-actin housekeeping gene*** *WT-normalised relative expression level of NFAT was evaluated in RAW 264 macrophages WT and LRRK KO at the basal level and in response to LPS challenged. Statistical significance was determined by two-way ANOVA followed by post hoc Tukey's test (n=3). Values represent the mean ± S.E.M. of 3 independent experiments (with internal triplicates in each experiment).*

4.2.10 Canonical Wnt signalling changes in RAW 264 *LRRK2* WT and *LRRK2* KO in response to Inflammatory challenge

Wnt signalling has been reported to mediate a variety of immune responses and also to be associated with LRRK2. Initially, Luciferase based assay were used to measure the changes in canonical Wnt signalling changes in response to LPS and/ or Wnt modulators. After that, components of canonical Wnt signalling and its target gens were examined utilizing western blot and qPCR.

4.2.10.1 Luciferase assay measuring *β-catenin* transcriptional activity

4.2.10.1.1 LPS

Challenging the RAW 264 macrophages with LPS resulted in a significant increase in the *β*-catenin transcriptional activation in both genotypes. The increase is consistent with the western blot data. While the *LRRK2* KO-LPS displayed a higher canonical Wnt signalling than *LRRK2* WT-LPS, the difference is not statistically significant. The increase in the *LRRK2* WT-LPS was (1.19± 0.06) whereas the increase in the *LRRK2* KO-LPS was (1.3 ±0.05)(**Figure 4-28).**

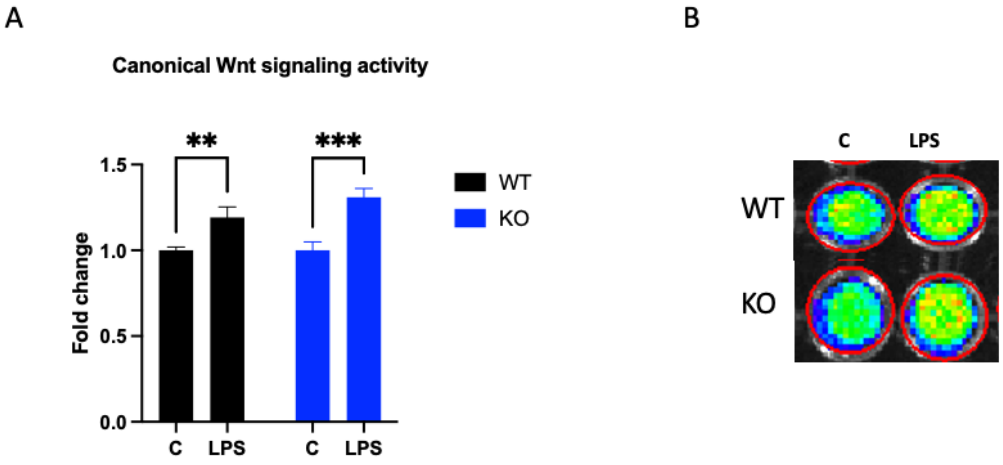

Figure 4-28 ***Modulation of TCF/LEF transcriptional activation by LPS.*** *RAW 264 cells were transduced with TCF/LEF lentivirus for 24 hours. LPS 1 ug/ml or control vehicle were added, and the cells were further incubated for additional 24 hours. Culture media containing secreted luciferase were assayed for bioluminescence. Statistical significance was determined using two-way ANOVA followed by post hoc Tukey's test. Representative image showing bioluminescence as a result of LPS treatment in WT and KO cells (n=3)(**B**). Values represent the mean ± S.E.M. of 3 experiments). *p < 0.05, ** p < 0.01, ***p < 0.001, ****p < 0.0001*

4.2.10.1.2 LiCl

Contrasting the SH-SY5Y cells, treating the RAW 264 macrophages didn't elicit any changes in β-catenin transcriptional activation in both genotypes(**Figure 4-29)**. As LiCl is a well-established activator of canonical Wnt signalling, the result was further investigated by choosing a different non-viral means to measure β-catenin transcriptional activation and using SH-SY5Y as a reference control; hence I was able to observe a substantial increase in β-catenin transcriptional activation by viral and non-viral means.

As shown in **Figure 5-30,** the unresponsiveness of the RAW 264 macrophages to LiCl was confirmed by non-viral means (TOP flash assay).

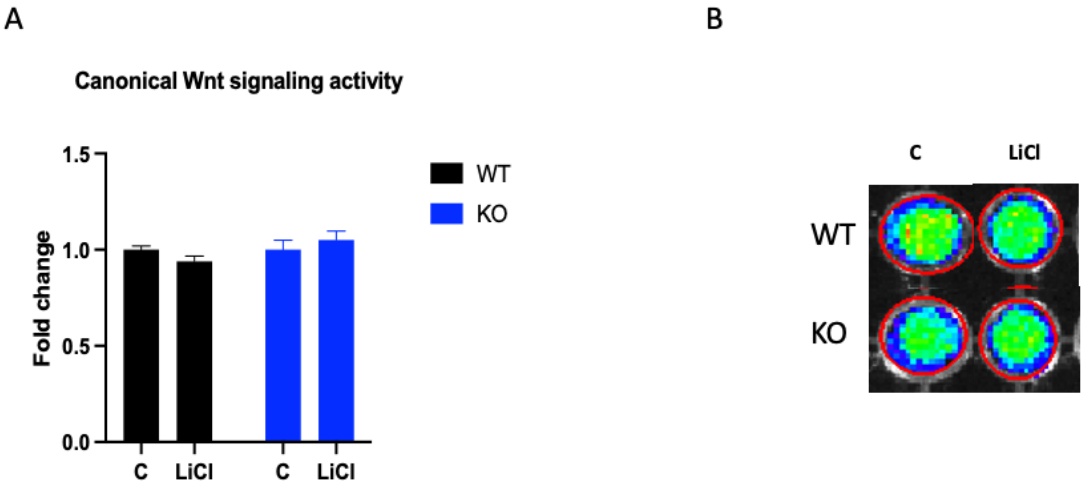

Figure 4-29 ***Modulation of TCF/LEF transcriptional activation by LiCl.*** *RAW 264 cells were transduced with TCF/LEF lentivirus for 24 hours. LiCl 40 mM or control vehicle were added, and the cells were further incubated for additional 24 hours. Culture media containing secreted luciferase were assayed for bioluminescence. Statistical significance was determined using two-way ANOVA followed by post hoc Tukey's test. Representative image showing bioluminescence as a result of LPS treatment in WT and KO cells (n=3)(**B**). Values represent the mean ± S.E.M. of 3 experiments*

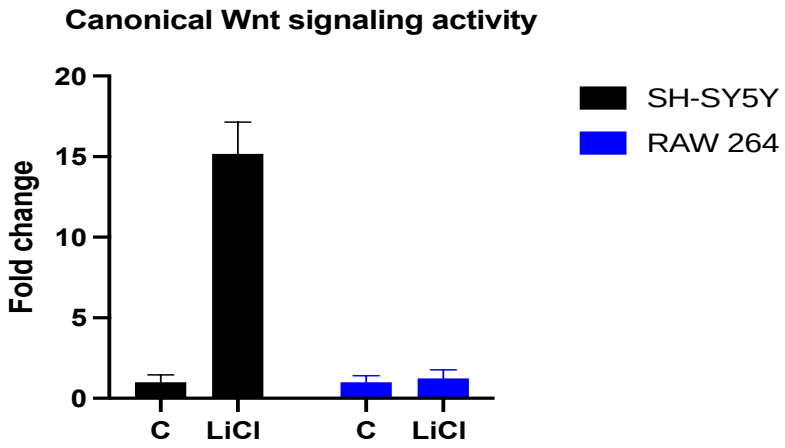

Figure 4-30 ***Response Comparison between RAW 264 and SH-SY5Y cells to LiCL.*** *RAW 264 and SH-SY5Y cells were transfected with a plasmid containing luciferase under the control of TCF/LEF response elements for 24 hours. LiCl 40 mM or control vehicle were added, and the cells were further incubated for additional 24 hours. Statistical significance was determined by student's t-test(n=3). Values represent the mean ± S.E.M. of independent experiments. *p < 0.05, ** p < 0.01, ***p < 0.001, ****p < 0.0001.*

4.2.10.1.3 Wnt3a and Wn5a modulation of canonical Wnt signalling

Wnt3a:

Treating the cells with Wnt3a did not change the TCF/LEF transcriptional activity in both genotypes at both the basal and challenged conditions. However, challenging the cells with LPS did increase the canonical Wnt signalling significantly across all treatment groups except the *LRRK2* WT-Wnt3a+LPS group, which was trending toward an increase as well (1.15±0.04, p#0.14). The increase in the *LRRK2* KO-Wnt3a+LPS group was (1.3±0.08) compared to (1.02±0.05) for the *LRRK2* KO-Wnt3a-LPS group **(Figure 4-31).**

Wnt5A:

Wnt5a treatment follows the trend as Wnt3a as treating the cells with Wnt5a didn't result in a change in the TCF/LEF transcriptional activity in both genotypes at both

the basal and challenged conditions. LPS did increase the canonical Wnt signalling significantly across all treatment groups**(Figure 4-31).**

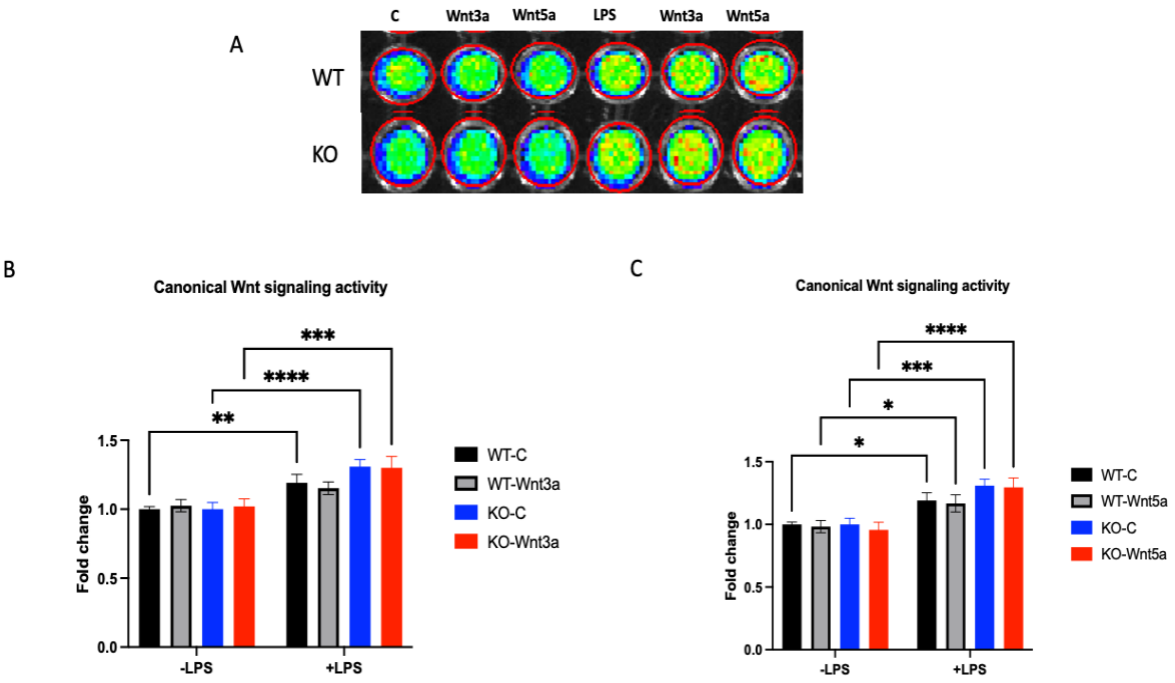

Figure 4-31 ***Modulation of TCF/LEF transcriptional activation by Wnt modulators.*** *RAW 264 cells were transduced with TCF/LEF lentivirus for 24 hours. The indicated treatments have been added and further incubated for 24 hours. Representative image showing bioluminescence as a result of different treatment in WT and KO (A). Culture media containing secreted luciferase were assayed for bioluminescence. Statistical significance was two-way ANOVA followed by post hoc Tukey's test(n=3). Values represent the mean ± S.E.M. of 3 experiments. *p < 0.05, ** p < 0.01, ***p < 0.001, ****p < 0.0001.*

4.2.10.2 β-catenin

4.2.10.2.1 β-catenin analysis by western blot

One of the most common ways to assess the activity of canonical Wnt signalling is detecting the dephosphorylated active form of the β-catenin and expressing it as a ratio to the total protein(MacDonald et al. 2009). To this end, cell lysates from RAW 264 macrophages were subjected to western blotting. In agreement with previous

reports(Gong et al. 2012), challenging the RAW 264 macrophages with LPS resulted in (1.5 fold ±0.09) and (1.78 fold ±0.29) fold increase for total and active β-catenin, respectively. *LRRK2* KO cells displayed a significant increase in Wnt signalling activity in the basal and challenged state. The basal fold increase was (1.69 fold ±0.06) and for the LPS treated cells (2.9 fold ±0.428) fold increase(**Figure 4-32**).

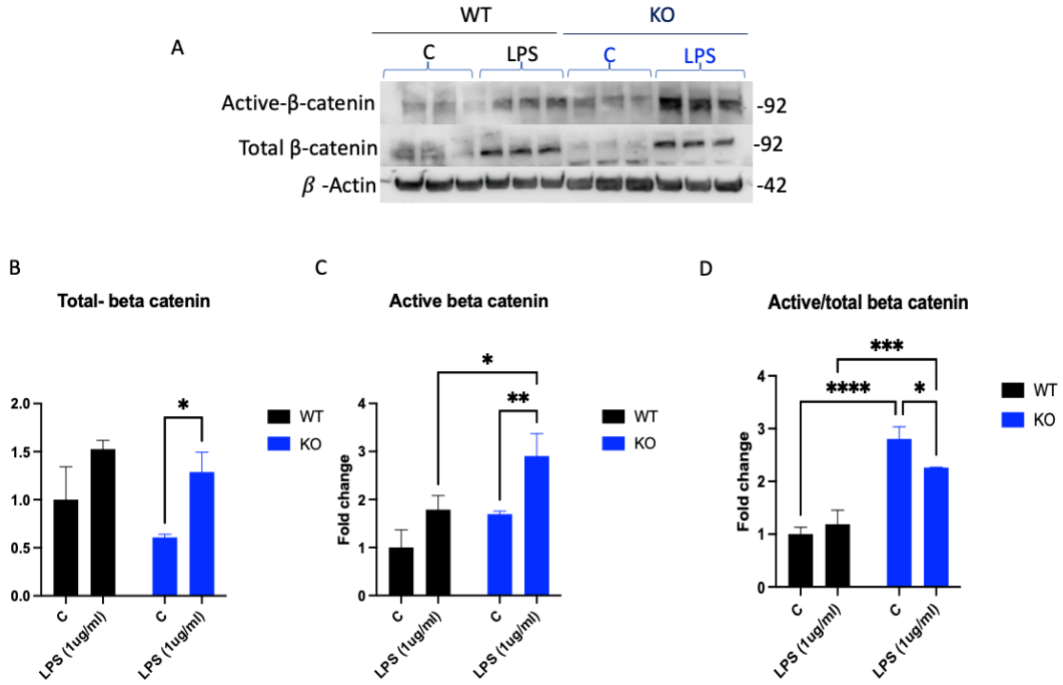

Figure 4-32 ***Analysis of β-catenin protein level by western blot.*** *Immune-blot image showing total β-catenin and active-β-catenin expression in the basal and challenged conditions in RAW 264 LRRK2 WT and LRRK2 KO cells. The image represents one of three representative experiments(**A**). Densitometric analysis of the immune-blot image including total β-catenin and active-β-catenin and the ratio of the active-β-catenin to the total protein level (**B, C and D**). The values were adjusted to the loading control β-actin. For quantification, all values have been normalised to WT control. Statistical significance was determined by two-way ANOVA followed by post hoc Tukey's test(n=3). Values represent the mean ± S.E.M. of 3 independent experiments (with internal triplicates in each experiment). *p < 0.05, ** p < 0.01, ***p < 0.001, ****p < 0.0001.*

4.2.10.2.2 β-catenin analysis by qPCR

The mRNA from RAW 264 macrophages *LRRK2* WT and *LRRK2* KO cells were analysed for the expression of β-catenin in response to LPS and at the basal level. There were no differences across the experimental groups in the mRNA level**(Figure 4-33).**

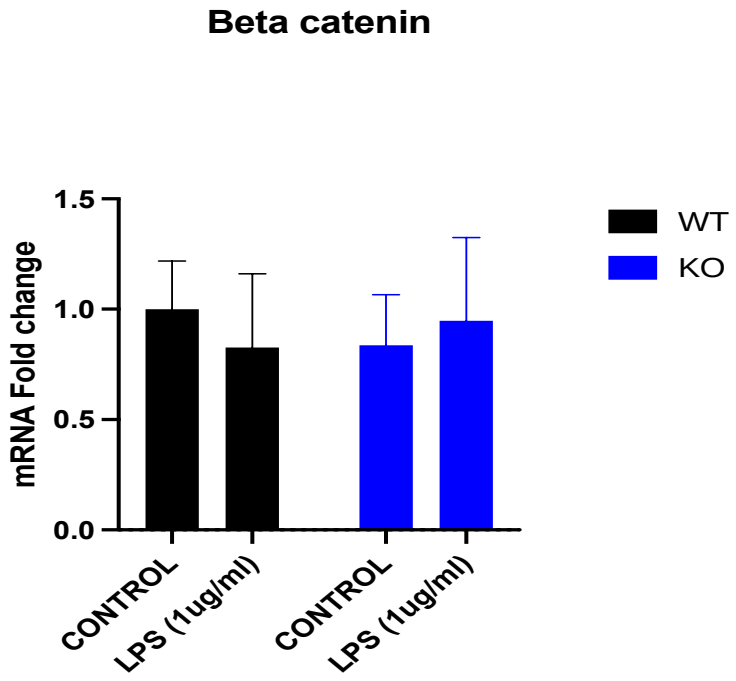

Figure 4-33 ***qPCR of β-catenin expression under β-actin housekeeping gene (n=3).*** *WT-normalised relative expression level of β-catenin was evaluated in RAW 264 macrophages WT and LRRK KO at the basal level and in response to LPS challenged. Statistical significance was determined by two-way ANOVA followed by post hoc Tukey's test. Values represent the mean ± S.E.M. of 3 independent experiments (with internal triplicates in each experiment).*

4.2.10.3 Wnt3a

4.2.10.3.1 Wnta3a analysis by qPCR

The mRNA from RAW 264 macrophages *LRRK2* WT and *LRRK2* KO cells were analysed for the expression of Wnt3a in response to LPS and at the basal level. mRNA

levels were elevated at both the basal and challenged state for all treatment groups. The *LRRK2* WT-LPS treatment group displayed a (3.02 fold ±4.7) fold increase. The *LRRK2* KO-C control group exhibited (9.22 fold ±09.55) whereas the *LRRK2* KO-LPS group showed (10.48 fold ±12.78)**(Figure 4-34).**

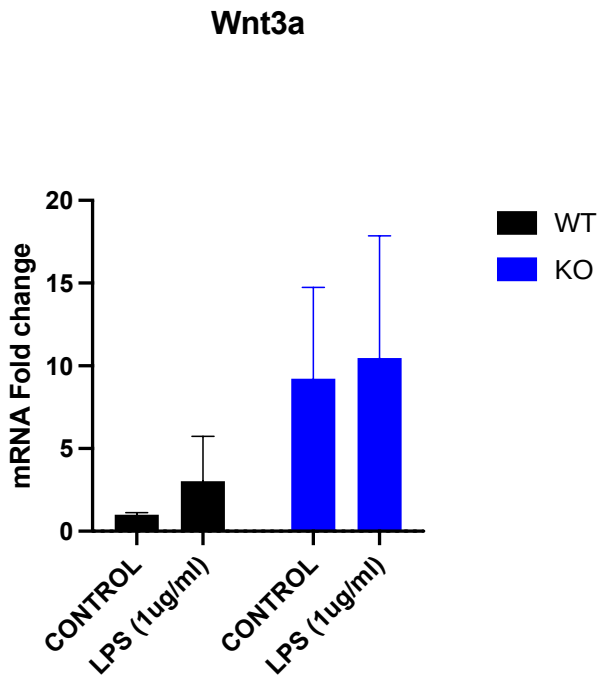

Figure 4-34 ***qPCR of Wnt3a expression under β-actin housekeeping gene.*** *WT-normalised relative expression level of Wnt3a was evaluated in RAW 264 macrophages WT and LRRK KO at the basal level and in response to LPS challenged. Statistical significance was determined by two-way ANOVA followed by post hoc Tukey's test(n=3). Values represent the mean ± S.E.M. of 3 independent experiments (with internal triplicates in each experiment).*

4.2.10.4 DKK-1

4.2.10.4.1 DKK-1 analysis by qPCR

The mRNA from RAW 264 macrophages *LRRK2* WT and *LRRK2* KO cells were analysed for the expression of DKK-1 in response to LPS and at the basal level. At the basal level, the *LRRK2* WT-LPS treated group had a lower mRNA level (0.5 fold ±0.29) in comparison to WT.

However, The *LRRK2* KO cells displayed elevated mRNA levels at both basal and challenged state. The basal levels of mRNA for the *LRRK2* KO cells were (2.67 fold ±1.39), whereas the *LRRK2* LPS group showed (2.27 fold ±1.45) fold increase**(Figure 4-35).**

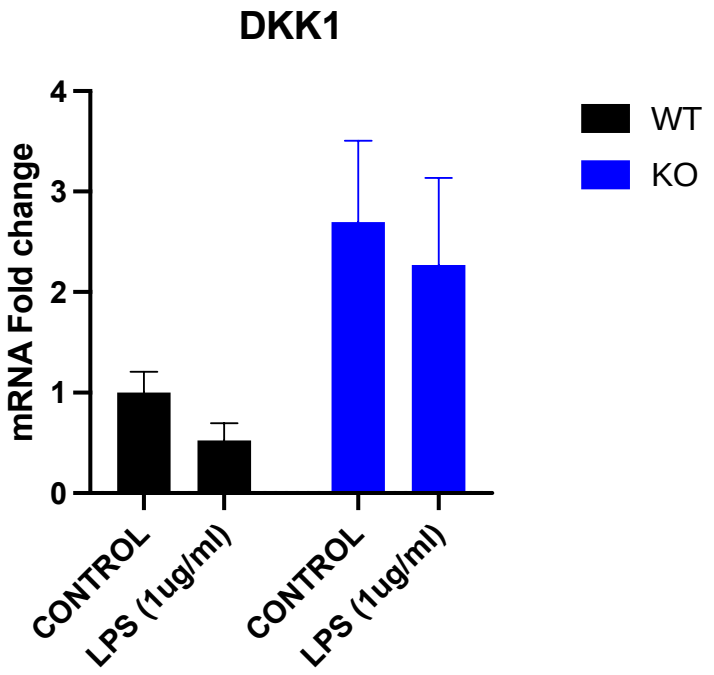

Figure 4-35 ***QPCR of DKK-1 expression under β-actin housekeeping gene. WT****-normalised relative expression level of DKK-1 was evaluated in RAW 264 macrophages WT and LRRK KO at the basal level and in response to LPS challenged. Statistical significance was determined by two-way ANOVA followed by post hoc Tukey's test(n=3). Values represent the mean ± S.E.M. of 3 independent experiments (with internal triplicates in each experiment).*

4.2.10.5 LRP-6

4.2.10.5.1 Analysis LRP6 by western blot

Treating RAW 264 macrophages resulted in a marked decrease in the expression of both total and the phosphorylated form LRP-6. This was observed in both genotypes. Interestingly, the expression level of LRP-6 and its phosphorylated form is lower in *LRRK2* KO cells in comparison to *LRRK2* WT in both the basal and challenged state.

The *LRRK2* KO cells displayed a (0.58±0.17) fold decrease for the total LRP-6 and (0.63±0.21) fold decrease for the p-LRP-6 at the basal level. On the challenged state, *LRRK2* KO cells total LRP-6 and p-LRP-6 displayed (0.22±0.155) and (0.31±0.17) fold decrease whereas *LRRK2* WT-LPS group showed (0.29±0.06) for the total LRP-6 and (0.37±0.12) for the p-LRP-6. The *LRRK2* KO cells displayed a slight non-significant increase in the p-LRP-6 (1.31±0.35**)(Figure 4-36).** p-LRP-6 is expressed as a ratio to total protein.

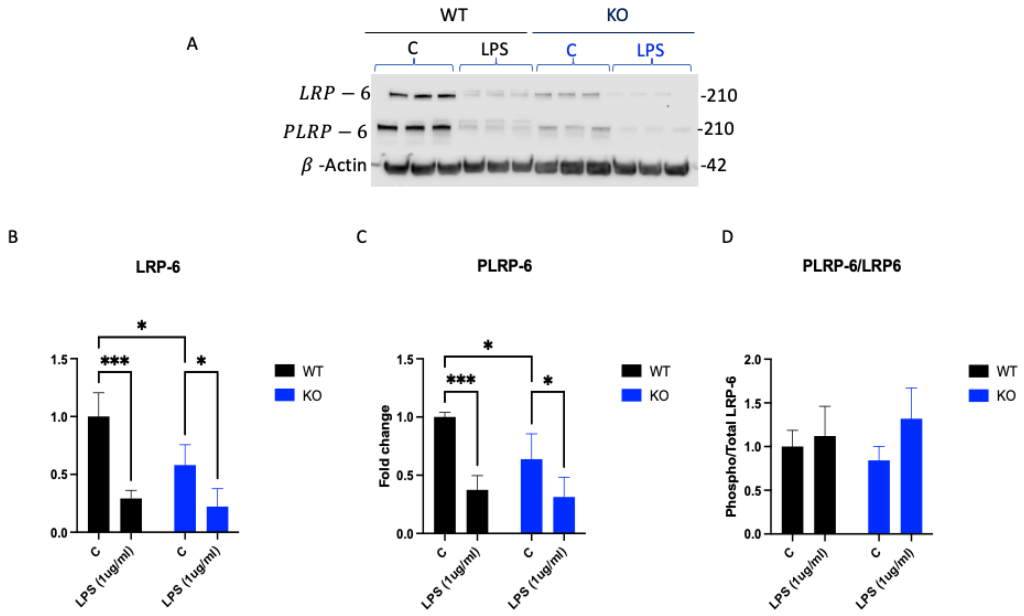

Figure 4-36 ***Analysis of LRP-6 protein level by western blot. (n=3).*** *Immune-blot image showing total LRP6 and P-LRP-6 expression in the basal and challenged conditions in RAW 264 LRRK2 WT and LRRK2 KO cells. The image represents one of three representative experiments(**A**). Densitometric analysis of the immune-blot image including total LRP6, P-LRP-6 and the ratio of the phosphorylated form to the total protein level (**B, C and D**). The values were adjusted to the loading β-actin. For quantification, all values have been normalised to WT control. Statistical significance was determined by two-way ANOVA followed by post hoc Tukey's test. Values represent the mean ± S.E.M. of 3 independent experiments (with internal triplicates in each experiment). *p < 0.05, ***p < 0.001.*

4.2.10.5.2 Analysis LRP6 by QPCR

The mRNA from RAW 264 macrophages *LRRK2* WT and *LRRK2* KO cells were analysed for the expression of LRP-6 in response to LPS and at the basal level. The *LRRK2* KO cells displayed a substantial higher mRNA level for the LRP-6 at both the basal and challenge conditions. The increase was (9.36 fold ±12.97) at the basal level and (9.82 fold ±15.02) with LPS treatment. In the *LRRK2* WT LPS group, there was (4.53fold ±6.65) fold increase**(Figure 4-37).**

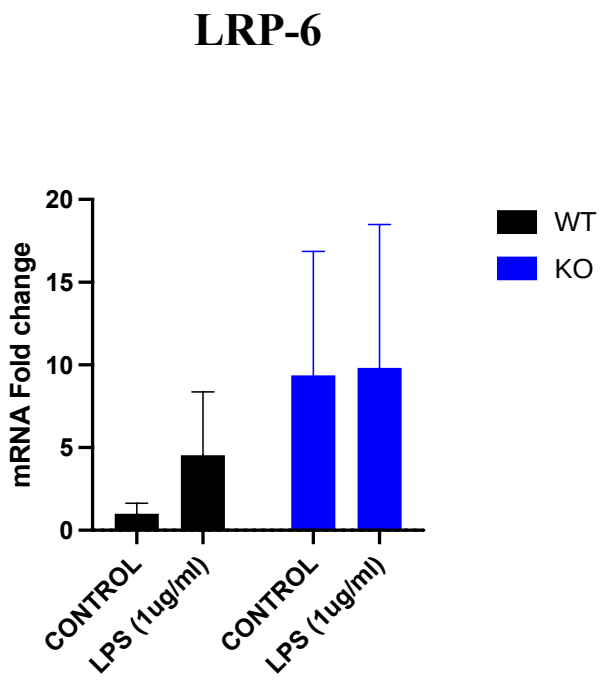

Figure 4-37 ***qPCR of LRP-6 expression under β-actin housekeeping gene (n=3).*** *WT-normalised relative expression level of LRP-6 was evaluated in RAW 264 macrophages WT and LRRK KO at the basal level and in response to LPS challenged. Statistical significance was determined by two-way ANOVA followed by post hoc Tukey's test. Values represent the mean ± S.E.M. of 3 independent experiments (with internal triplicates in each experiment).*

4.2.10.6 Axin-2

4.2.10.6.1 Axin-2 analysis by qPCR

The mRNA from RAW 264 macrophages *LRRK2* WT and *LRRK2* KO cells were analysed for the expression of Axin-2 in response to LPS and at the basal level. There were no differences in the mRNA levels in the LRRK2 WT cells at both basal and challenged state.

However, The *LRRK2* KO cells displayed elevated mRNA levels at both basal and challenged state. The basal levels of mRNA for the *LRRK2* KO cells were (4.26 fold ±3.39), whereas the LPS group displayed (6.64 fold ±7.46)**(Figure 4-38).**

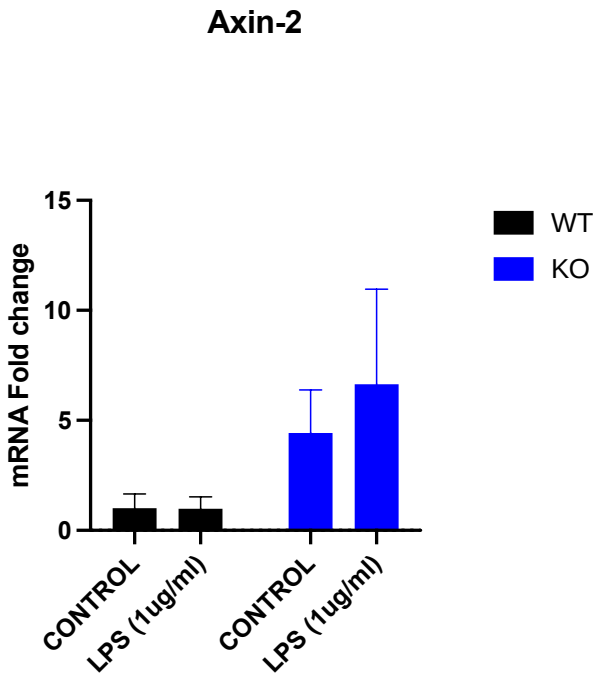

Figure 4-38 ***qPCR of Axin-2 expression under β-actin housekeeping gene.*** *WT-normalised relative expression level of Axin-2 was evaluated in RAW 264 macrophages WT and LRRK KO at the basal level and in response to LPS challenged. Statistical significance was determined by two-way ANOVA followed by post hoc Tukey's test. (n=3). Values represent the mean ± S.E.M. of 3 independent experiments (with internal triplicates in each experiment).*

4.2.10.7 Analysis of COX-2 by western blot

The protein expression level of the Wnt target gene, COX-2, was evaluated by western blot. As expected, LPS treatment resulted in a significant increase in COX-2 expression in both genotypes. The expression was significantly lower in the *LRRK2* KO than the *LRRK2* WT in the challenged conditions (2.94±0.27-fold vs 1.54±0.31-fold). **(Figure 4-39).**

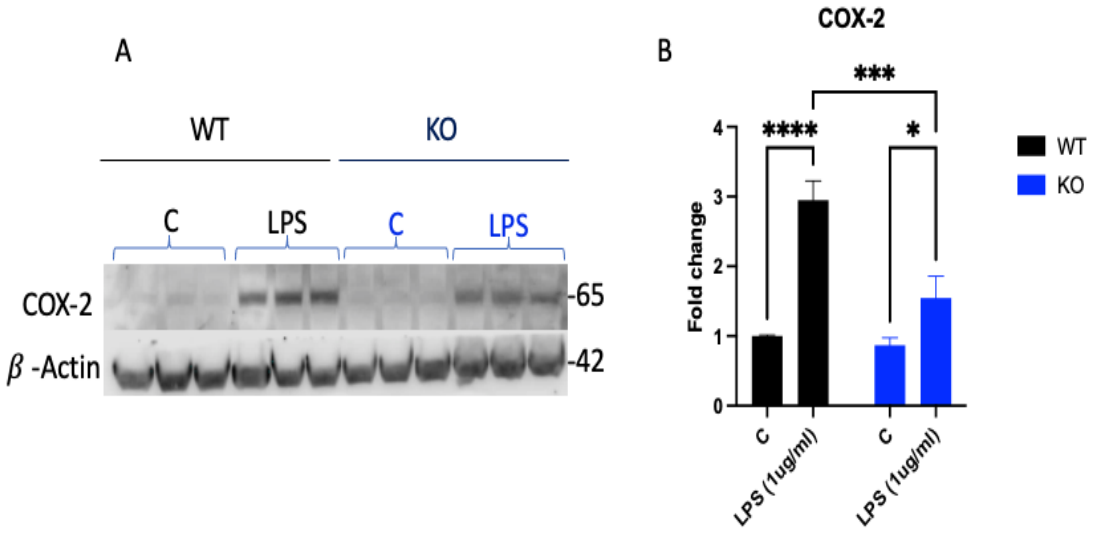

Figure 4-39 ***Expression analysis of COX-2 protein level(n=3).*** *Immunoblot image showing COX-2 expression in the basal and challenged conditions in RAW 264 LRRK2 WT and LRRK2 KO cells. The image represents one of three representative experiments(**A**). Densitometric analysis of the immune-blot image(**B**). The values were adjusted to the loading control β-actin. For quantification, all values have been normalised to WT control. Statistical significance was determined by two-way ANOVA followed by post hoc Tukey's test. Values represent the mean ± S.E.M. of 3 independent experiments (with internal triplicates in each experiment). *p < 0.05, ** p < 0.01, ***p < 0.001, ****p < 0.0001.*

4.2.10.8 Analysis of COX-2 by QPCR

To examine if the increase in COX-2 protein expression levels in the *LRRK2* KO cells is due to an increase in COX-2 transcription, the mRNA from RAW 264 macrophages *LRRK2* WT and *LRRK2* KO cells were analysed for the expression of COX-2 in

response to LPS and at the basal level. As expected, treating RAW 264 cells with LPS resulted in sharp increase in COX-2 mRNA level in both genotypes by 271-fold and 108-fold, respectively. Interestingly and in agreement with the western blot data, COX-2 mRNA level in the *LRRK2* KO LPS treated cells displayed only 108-fold increase compared to 271 fold increase in the *LRRK2* WT-LPS treated group, the difference was not statistically significant(p=0.07) **(Figure 4-40).**

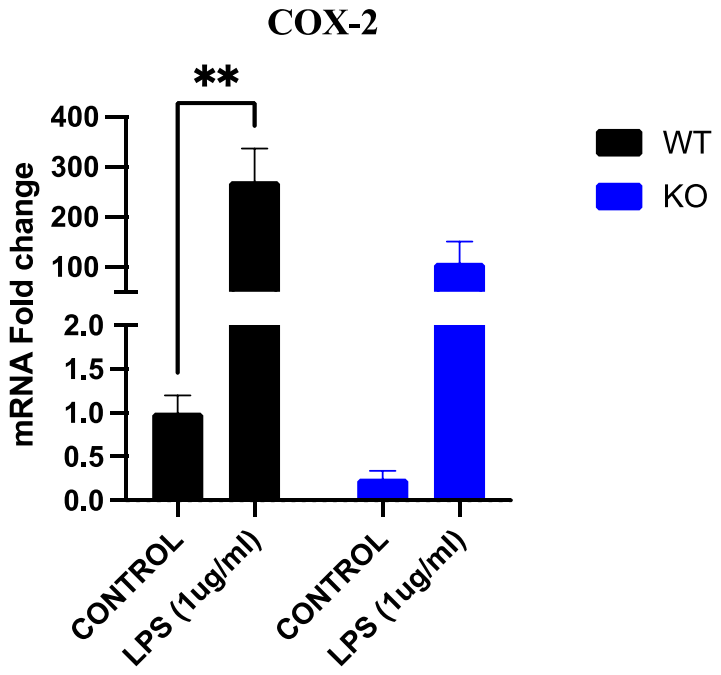

Figure 4-40 ***qPCR of COX-2 expression under β-actin housekeeping gene.*** *The WT-normalised relative expression level of COX-2 was evaluated in RAW 264 macrophages WT and LRRK KO at the basal level and in response to LPS challenged. Statistical significance was determined by two-way ANOVA followed by post hoc Tukey's test(n=3). Values represent the mean ± S.E.M. of 3 independent experiments (with internal triplicates in each experiment)** p < 0.01.*

4.2.10.9 Wntless

4.2.10.9.1 Wntless analysis by western blot

WLS is a vital conserved protein for the secretion of the Wnt ligands. (Banziger et al. 2006). The protein expression levels of WLS showed a steep significant increase in both genotypes upon LPS treatment. The *LRRK2* WT-LPS group showed a (4.67±2.27) fold increase, whereas the *LRRK2* KO-LPS showed an (8.21±4.5) fold increase. The *LRRK2* KO cells displayed a (1.625±0.41) fold increase on the basal level compared to *LRRK2* WT-C group. Comparing LPS treated groups, the *LRRK2* KO cells showed a significant increase in comparison to the *LRRK2* WT group (**Figure 4-41**).

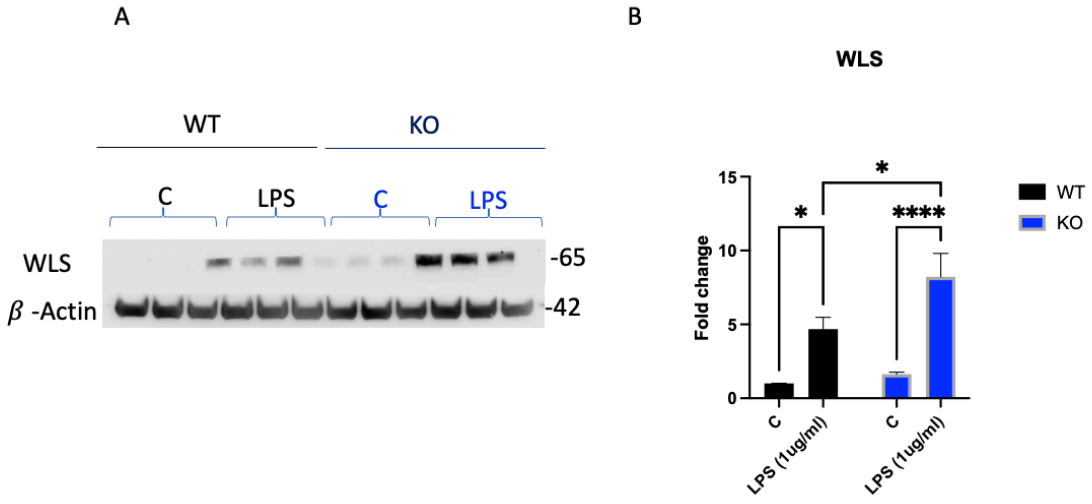

Figure 4-41 ***Expression analysis of WLS protein level.*** *Immune-blot image showing WLS expression in the basal and challenged conditions in RAW 264 LRRK2 WT and LRRK2 KO cells. The image represents one of eight representative experiments(**A**). Densitometric analysis of the immune-blot image(**B**). The values were adjusted to the loading control β-actin. For quantification, all values have been normalised to WT control. Statistical significance was determined by two-way ANOVA followed by post hoc Tukey's test(n=8). Values represent the mean ± S.E.M. of 8 independent experiments (with internal triplicates in each experiment). *p < 0.05, ****p < 0.0001.*

4.2.10.9.2 Wntless analysis by qPCR

The mRNA from RAW 264 macrophages *LRRK2* WT and *LRRK2* KO cells were analysed for the expression of WLS in response to LPS and at the basal level. In drastic difference to the western blot data, LPS treatment resulted in an opposite effect in both genotypes. *LRRK2* WT-LPS group showed a non-significant increase (1.26 fold ±0.66) fold increase compared to a slight decrease in the *LRRK2* KO-LPS groups (0.5 fold ±0.49). A slight non-significant reduction at the basal level in the *LRRK2* KO cells is observed (0.85 fold ±0.36). **(Figure 4-42).**

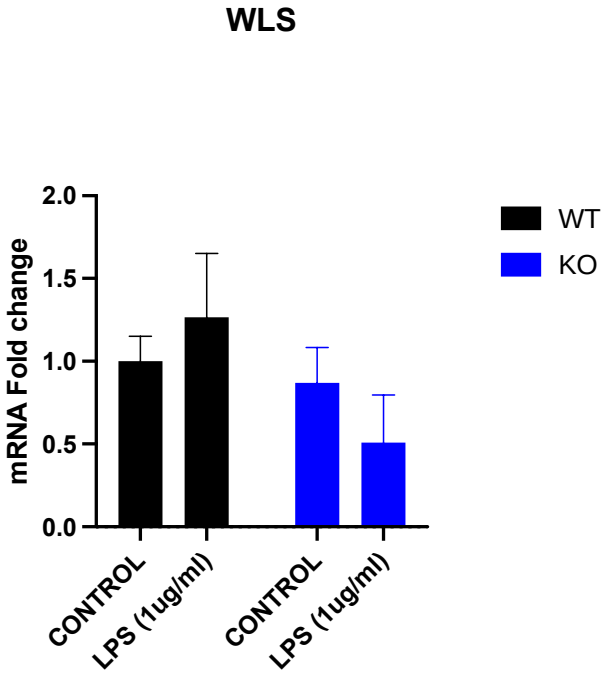

Figure 4-42 ***qPCR of WLS expression under β-actin housekeeping gene.*** *WT-normalised relative expression level of WLS was evaluated in RAW 264 macrophages WT and LRRK KO at the basal level and in response to LPS challenged. Statistical significance was determined by two-way ANOVA followed by post hoc Tukey's test(n=3). Values represent the mean ± S.E.M. of 3 independent experiments (with internal triplicates in each experiment).*

4.2.11 Wntless involvement in LPS mediated inflammation

Given the robust increase of WLS in response to LPS, particularly in the *LRRK2* KO cells, I wanted to test the impact of knocking-down WLS on Rab10, LRRK2, TLR-4 and COX-2 expression.

4.2.11.1 LRRK2

Silencing WLS resulted in a significant decrease in the expression of LRRK2. The reduction in the basal level was a more substantial (0.24 fold ±0.05) fold changed compared to siRNA-C-C. The decrease in the siRNA-WLS-LPS was (0.01 fold ±0.04) compared to (0.2 ±0.05) for the siRNA-C -LPS**(Figure 4-43).**

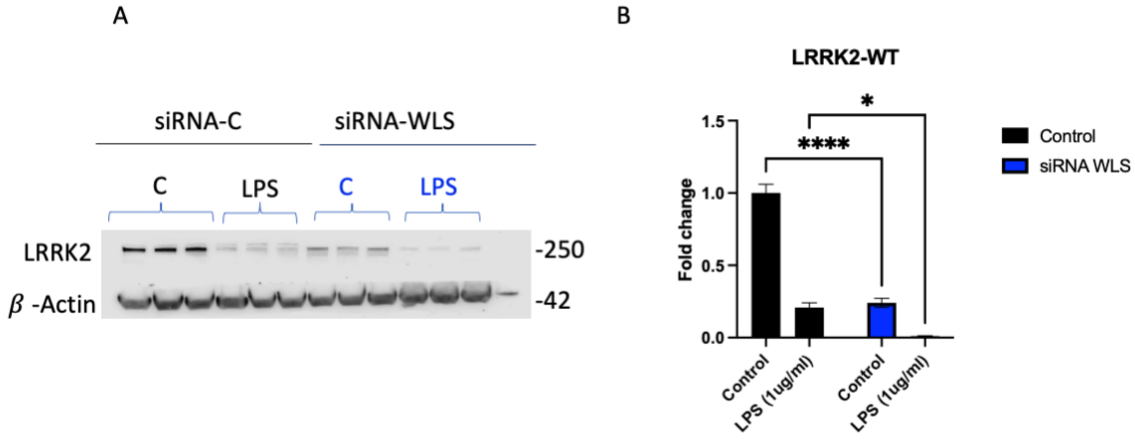

Figure 4-43 ***Effect of siRNA-WLS on LRRK2 protein level.*** *Immune-blot image showing LRRK2 expression in the basal and challenged conditions in RAW 264 treated with either siRNA-C or siRNA-WLS. (**A**). Densitometric analysis of the immune-blot image(**B**). The values were adjusted to the loading control β-actin. For quantification, all values have been normalised to siRNA-WT control. Statistical significance was determined by two-way ANOVA followed by post hoc Tukey's test(n=3). Values represent the mean ± S.E.M. of 3 experiments.*

4.2.11.2 COX-2

As mentioned in 4.2.10.7 , the RAW 264 *LRRK2* KO cells displayed lower COX-2 LPS induction compared to the respective *LRRK2* WT control. The WLS protein expression seemed consequential to LRRK2 expression (Figure 4-43). In addition, the canonical Wnt signalling pathway has been reported to be involved in the transcriptional activation of the COX-2 gene(Buchanan and DuBois 2006, Nunez et al. 2011). Moreover, prostaglandin E2, a metabolic bioproduct of COX-2, activates components of canonical Wnt signalling, implying a possible feedback mechanism and crosstalk(Buchanan and DuBois 2006). Thus, it would be interesting to see if silencing WLS will impact COX-2.

Interestingly, silencing WLS resulted in a significant downregulation of LPS-induced COX-2 proteins expression level compared to the LPS-induced COX-2 in the non-target siRNA groups. The siRNA WLS group displayed (5.6 fold ±0.61) fold change compared to (8.5 fold 1.33) for the siRNA-C group. At the basal level, the siRNA WLS group showed a non-significant increase over the siRNA-C group (1.8 fold ±0.25) fold change**(Figure 4-44).**

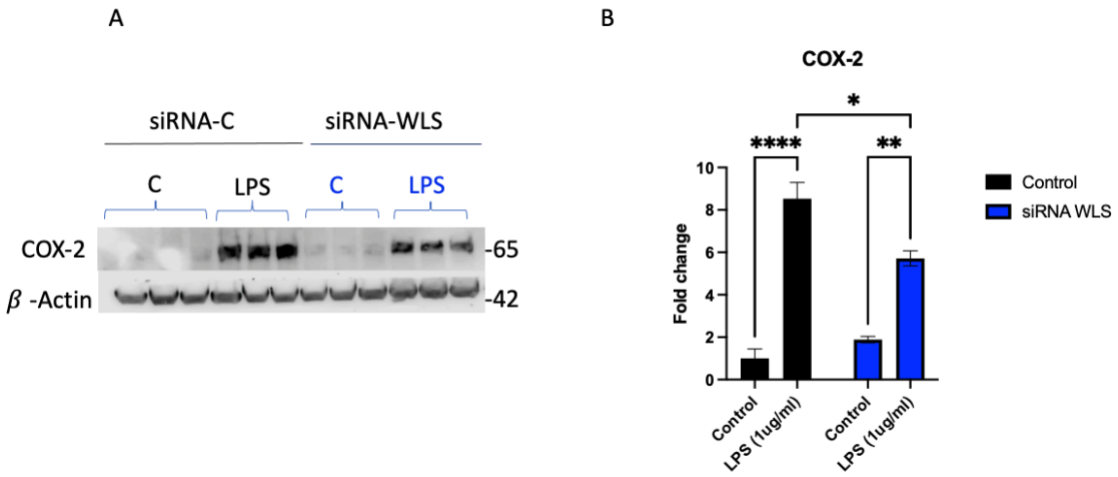

Figure 4-44 ***Effect of siRNA-WLS on COX-2 protein level.*** *Immune-blot image showing COX-2 expression in the basal and challenged conditions in RAW 264 treated with either siRNA-C or siRNA-WLS. (**A**). Densitometric analysis of the immune-blot image(**B**). The values were adjusted to the loading control β-actin. For quantification, all values have been normalised to siRNA-WT control. Statistical significance was determined by two-way ANOVA followed by post hoc Tukey's test(n=3). Values represent the mean ± S.E.M. of 3 experiments.*

4.2.11.3 TLR-4

LPS, a TLR-4 agonist, has been shown to activate and regulate canonical Wnt signalling. In addition, numerous reports indicate crosstalk and modulation function between TLR-4 and Wnt signalling(Casili et al. 2018, Yi et al. 2012). Therefore, it would be interesting to see the impact of silencing *WLS* on TLR-4 expression.

The results presented here indicate that WLS modulate the expression of TLR-4 when cells are stimulated with LPS. The siRNA WLS group displayed (0.41 fold ±0.0.18) fold change compared to (0.84 fold ±0.16) for the siRNA-C group. At the basal level, the siRNA WLS group showed a non-significant decrease over the siRNA-C group (0.68 fold ±0.03) fold change **(Figure 4-45).**

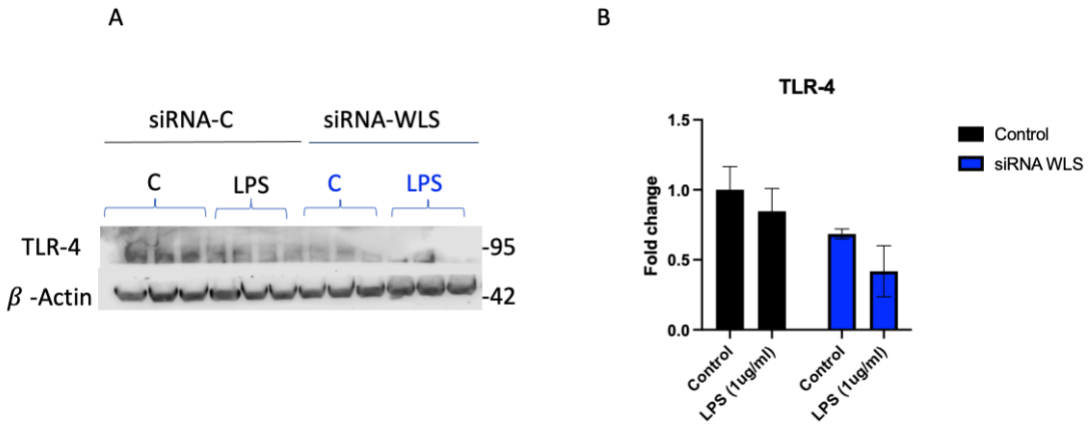

Figure 4-45 ***Effect of siRNA-WLS on TLR-4 protein level.*** *Immune-blot image showing TLR-4 expression in the basal and challenged conditions in RAW 264 treated with either siRNA-C or siRNA-WLS. The image represents one of three representative experiments(**A**). Densitometric analysis of the immune-blot image(**B**). The values were adjusted to the loading control β-actin. For quantification, all values have been normalised to siRNA-WT control. Statistical significance was determined by two-way ANOVA followed by post hoc Tukey's test(n=3). Values represent the mean ± S.E.M. of 3 experiments.*

4.2.11.4 Rab10

Rab-10, which is the *Caenorhabditis elegans* homologue of Rab10, has been reported to regulate and participate in WLS trafficking (Zhang et al. 2018). I wanted to look if silencing WLS will impact Rab10 expression and its phosphorylated form.

Silencing WLS resulted in a significant decrease in the expression of Rab10 in the basal conditions. The reduction was approximately 72 %, (0.38 fold±0.03) fold of the control. There was no change in the challenged conditions. Interestingly, the phosphorylated form of Rab10 showed a significant increase compared to the siRNA-WLS group compared to the siRNA-C at the basal conditions (3.9 fold ±0.64). In the challenged conditions, however, an opposite effect has been observed in the siRNA-

WLS group in which pRab10 was (0.36 fold ± 0.17) fold compared to (2.05 fold ±1.02) for the siRNA-C group**(Figure 4-46).**

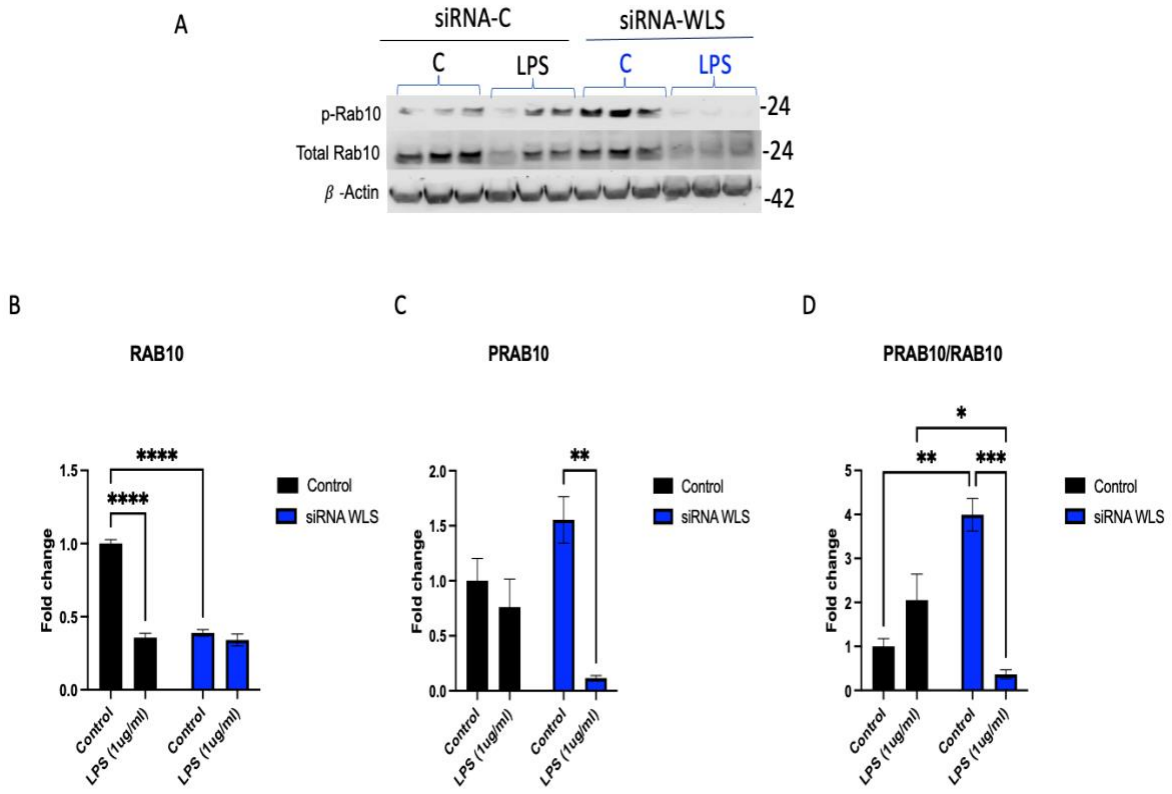

Figure 4-46 ***Effect of siRNA-WLS on Rab10 protein level.*** *Immune-blot image showing total Rab10and p-Rab10 expression in the basal and challenged conditions in RAW 264 treated with either siRNA-C or siRNA. (**A**). Densitometric analysis of the immune-blot image including total Rab10 and p-Rab10 and the ratio of the p-Rab10 to the total Rab10 proteins level (**B, C and D**). The values were adjusted to the loading control β-actin. For quantification, all values have been normalised to siRNA-WT control. Statistical significance was determined by two-way ANOVA followed by post hoc Tukey's test(n=3). Values represent the mean ± S.E.M. of 3 experiments.*

4.3 Summary and Discussion

Throughout this chapter, I examined the inflammatory response differences across the RAW 264 macrophages *LRRK2* WT and *LRRK2* KO cells. The *LRRK2* KO cells displayed a general under-responsive effect to LPS stimuli compared to *LRRK2* WT cells. The differences were associated with changes in key Wnt signalling components such as LRP-6 and WLS. In addition, the western blot data could attribute the inflammatory differences due to changes in Rab10 expression upon LPS stimulation across the *LRRK2* WT and *LRRK2* KO cells. Finally, silencing the WLS protein resulted in the downregulation of LRRK2 and RAB10, suggesting a mechanistic convergence pathway between WLS-LRRK2 and RAB10.

4.3.1 *LRRK2* KO resulted in immune response dysregulation

Initially, I investigated whether immune responses are differentially affected by *LRRK2* KO in RAW 264 macrophages. I have looked at the cytokines release and expression, phagocytosis and NO release. The Cytokines array panel screen allowed for the detection of 40 cytokines and chemokines simultaneously in culture media.

Interestingly, the *LRRK2* KO cells showed a substantial reduction in pro-inflammatory cytokine release and a decrease in the anti-inflammatory profile compared to *LRRK2* WT when challenged with LPS (**Table 5-2**). While primary microglia cells have been reported to have similar changes, mouse peripheral macrophages didn't exhibit any differences in the pro-inflammatory cytokine release upon LPS stimulation across *LRRK2* KO, G2019S and R1441G(Gillardon et al. 2012, Lee et al. 2017, Dzamko et al. 2012). A recent report by Kim and others reported a decrease in manganese induced TNF-α in RAW 264 *LRRK2* KO cells compared to *LRRK2* WT control, which is consistent with the data reported here, albeit with different stimuli(Kim et al.

2019).Moreover, the decrease in the TNF-α expression level observed in the cytokines panel was further investigated by looking at mRNA level, which was consistent with the panel **(Figure 4-17**).

Cytokine	Role	Impact of LRRK2 deletion
TNF-α	proinflammatory	decrease
MIP-2	proinflammatory	decrease
MIP-β	proinflammatory	decrease
IFN-γ	proinflammatory	decrease
IL-16	proinflammatory	decrease
IL-17,	proinflammatory	decrease
IL-4	proinflammatory	decrease
Cox-2	proinflammatory	decrease
JE	Chemotaxis/anti-tumour activity	increase
G-CSF	Chemotaxis	increase
I-TAC	Chemotaxis	increase
IP-10	Chemotaxis	increase
IL-1ra	Anti-inflammatory	increase
IL-6	Pleiotropic cytokines	increase

Table 4-2 ***Cytokines that were significantly changed as a result of LPS challenged showing the impact of LRRK2 deletion compared LPS challenged control group. The observed changes highlight the dampen immune associated with LRRK2 KO cells challenged with LPS.***

In addition to TNF-α, Cox-2 protein and mRNA levels are reduced in *LRRK2* KO cells stimulated with LPS in comparison to *LRRK2* WT-LPS group**(Figure 4-39,40).** Cox-2 is an enzyme responsible for the synthesis of mediators that play an important role in the inflammatory process and it is one of the canonical Wnt signalling target genes(Nunez et al. 2011). Cox-2, and it's by-product prostaglandin E2, have been suggested to play part in PD pathogenesis(Teismann 2012). Deletion of COX-2 or inhibiting it pharmacologically in mice had conferred neuroprotection in MPTP model of PD(Aubin et al. 1998, Feng et al. 2002).

In addition to TNF-α and Cox-2, other pro-inflammatory cytokines were found to be significantly increased in *LRRK2* WT compared to *LRRK2* KO upon LPS stimulation. Those include MIP-2, MIP-β,IFN-γ, IL-16, IL-17, IL-4**(Figure 4-14,15).** However, the mRNA level of IFN-γ did show the opposite **(Figure 4-18).** This could be explained by the fact that the cytokines panel measures the release of the cytokines whereas the qPCR measures the mRNA level. Interestingly, recent reports substantiate impairment in IFN-γ signalling in mediating LRRK2 inflammatory response(Weindel et al. 2020, Panagiotakopoulou et al. 2020). There were no differences in the release of NO measured in the Griess assay (**Figure 4-9**).

Interestingly, the cytokines that were increased in the *LRRK2* KO-LPS group were either chemotaxis and chemokines (JE, G-CSF, I-TAC and IP-10), anti-inflammatory cytokines (IL-1ra) or pleiotropic cytokine(IL-6)(Keeley, Mehrad and Strieter 2008, Nishimoto and Kishimoto 2004). This is a very interesting observation that might have implication in explaining LRRK2 role in inflammatory disorders and cancer. For instance, JE, is a chemokine involved in the recruiting the monocytes/macrophages to the cite of inflammation and has been reported to have anti-tumour activity(Rollins 1991). *LRRK2* WT-LPS group expressed significantly less JE compared *LRRK2* KO-LPS group, suggesting LRRK2 might act as repression for JE. Given *LRRK2* G2019S mutation has been associated with cancer(Chen et al. 2017) , it would be very curious to know if the *LRRK2* G2019S mutation would result in downregulation of JE.

Previous reports exploring the phagocytic activity in immune cells across the *LRRK2* genotypes revealed no effect as a result of *LRRK2* genetic manipulation. The results presented here are consistent with previous reports (**Figure 4-10**). Though *LRRK2* mutations had no effect on phagocytic activity, it had been reported to be recruited to the phagosome. Furthermore, genetic deletion of *LRRK2* impacted Rab8 and Rab10

presence in the phagosomes (Lee et al. 2020). In addition, LRRK2 has been linked to the enolysosomal system. To this end, I examined the differences in the lysosomal protease cathepsin-D activity across the *LRRK2* genotypes in the basal level and with LPS stimulation, which revealed no differences **(Figure 4-11).**

4.3.2 Wnt signalling changes associated with LRRK2 KO

The Wnt signalling changes associated with the differences in immune response across *LRRK2* genotypes are evident. In agreement with previous reports, western blot data revealed that LPS treatment in RAW 264 *LRRK2* WT cells result in changes in key Wnt signalling component including β-catenin, LRP-6 and WLS(Jang et al. 2017). Interestingly, the *LRRK2* KO-LPS group exhibited upregulation of active β-catenin and WLS compared to LRRK2-WT-LPS whereas total LRP-6 expression was significantly lower **(Figure 4-47).** There were no differences in the NFAT protein expressions.

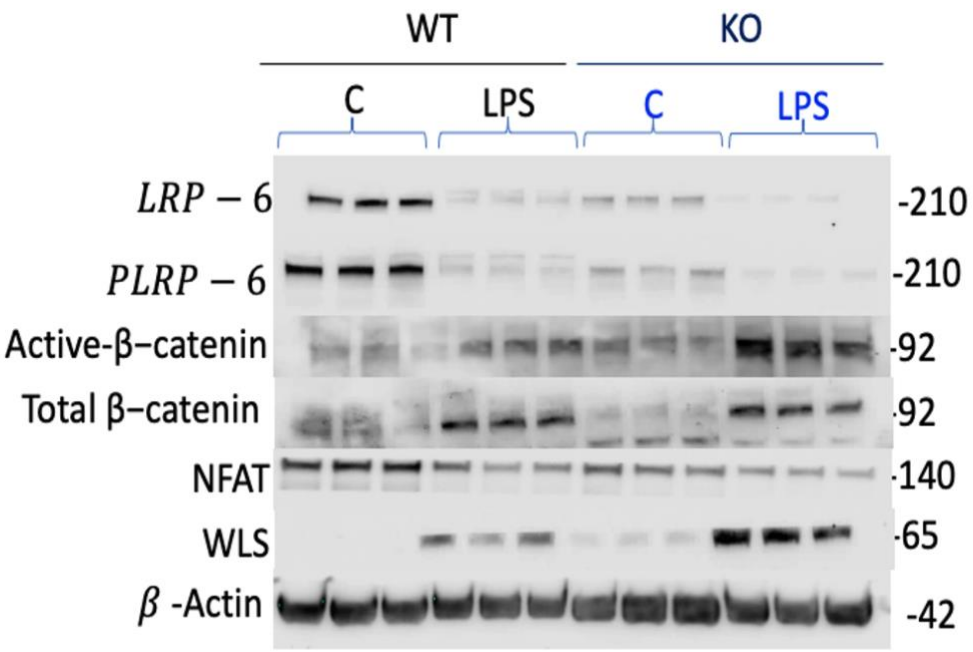

Figure 4-47 ***Summary Wnt and NFAT signalling changes in RAW 264 as result of LPS challenge showing upregulation of β-catenin and WLS proteins whereas LRP-6 was significantly decreased. There were no significant changes in NFAT expression.***

Examining the qPCR data for the *LRRK2* KO-LPS compared to *LRRK2* WT-LPS group yield many interesting observations. First, many components of canonical Wnt signalling were upregulated including Wnt3a, Axin-2 and LRP-6. This and together with immune blot of active β-catenin could indicate an activated canonical Wnt signalling. However, analysis of the mRNA level of β-catenin and the luciferase expression revealed no changes. Second, the canonical Wnt signalling antagonist DKK1 was upregulated. This could be explained as a compensatory mechanism to inhibit the over-active canonical Wnt signalling. The upregulation of DKK1 gene could also explain the significant decrease in the LRP-6 expression as it was shown previously DKK1 can bind to the LRP-6 with high affinity can cases the receptor to internalize causing it degradation(Semenov, Zhang and He 2008). The following table

summarise the changes observed in Wnt, NFAT and NF-κB signalling in the *LRRK2* KO-LPS group in relation to the *LRRK2* WT-LPS group.

Protein	Signalling	WB	qPCR
β-catenin	Canonical Wnt signalling	Increased	No change
Wnt3a	Canonical Wnt signalling	NA	increased
DKK1	Canonical Wnt signalling antagonist	NA	increased
LRP-6	Canonical Wnt signalling	decrease	Increase
Axin-2	Canonical Wnt signalling	NA	Increase
Cox-2	Canonical Wnt signalling target gene	decrease	decrease
NFAT	NFAT signalling	no change	Tend to increase
NF-κB	NF-κB signalling	no change	Tend to decrease

Table 4-3 ***Changes in the Wnt, NFAT and NF-κB signalling observed in the LRRK2 KO-LPS groups compared to LRRK2 WT-LPS group***

Taken together, those data corroborate previous reports published in our lab observing upregulated canonical Wnt signalling in LRRK2 KO cells. Moreover, it suggested that the differences in immune response could be explain in part by differences in canonical Wnt signalling.

4.3.3 LRRK2 upregulation and Rab10 phosphorylation are involved in mediating LPS inflammatory response

Next, I wanted to explore from a mechanistic perspective the reason in differences in the inflammatory responses across the *LRRK2* genotypes. I have looked into the expressions of the LRRK2 upon LPS stimulation, the expressions of LRRK2 substrate, Rab10 and finally I have looked at the expressions of TLR-4.

Examining the expression of LRRK2 upon LPS stimulation revealed a significant induction and upregulation (**Figure 4-7**). This is consistent with many studies documenting upregulation of LRRK2 upon inflammatory stimuli in-*vivo* and *in-*

vitro(Litteljohn et al. 2018, Kozina et al. 2018, Yan and Liu 2017, Cook et al. 2017).The precise mechanism by which LPS upregulate LRRK2 is unknown. However, NF-κB and IRF8 transcription factors are known to mediate TLR-4 signalling. Consequently, it is plausible that LRRK2 upregulation is mediated by NF-κB and/or IRF8(Medzhitov and Horng 2009). It is worth mentioning that other inflammatory stimuli including IFN-γ upregulate LRRK2 through Janus kinase (JAK)/signal transducers and activators of transcription (STAT)(Kuss, Adamopoulou and Kahle 2014).

The TLR-4 is the molecular target for LPS, and it is responsible to mediate its action. I asked the question whether different TLR-4 expression could be explaining the under-responsiveness in the *LRRK2* -KO-LPS group. The western blot data revealed no significant differences across the *LRRK2* genotypes either in the basal or challenged conditions **(Figure 4-25).**

Rab10 emerged as physiological substrate for LRRK2 whereby the kinase domain of LRRK2 would phosphorylate Rab10(Steger et al. 2016). In addition, Rab10 has been reported to be involved in mediating TLR-4 trafficking and play a critical role in LPS driven pro-inflammatory release(Wang et al. 2010). It would be very interesting to look into the expression of Rab10, and its phosphorylated form at the basal and challenged conditions in *LRRK2* KO RAW 264 macrophages. As predicted, *LRRK2* KO result in a significant decrease in the p-Rab10 at both basal and under inflammatory stimuli **(Figure 4-8).** It is very likely the decrease in p-RAB10 is due to *LRRK2* KO as a study by Dong and colleagues showed LRRK2 kinase inhibition result in a decrease in p-Rab10 when astrocytes were challenged with LPS (Dong et al. 2019). This does suggest that Rab10 is a mediator for LRRK2 inflammatory role.

Surprisingly, LPS treatment resulted in decrease in pRAB10. Nazish and colleagues has reported similar results in RAW 264 macrophages and iPSC-derived macrophages (Nazish et al. 2021). It was predicted that LPS will increase pRAB10 as consequence to LRRK2 upregulation. It is not clear how LPS mediate the decrease in the phosphorylation of Rab10. The decrease in pRab10 might infer a decrease in LRRK2 kinase activity. However, the *LRRK2* KO cells also displayed a decrease in pRAB10 in response to LPS, which indicate that the decrease in pRab10 might not be mediated by LRRK2 kinase activity.

4.3.4 WLS is critical in mediating LRRK2 inflammatory response

Wintless (WLS, also called GPR177) is chaperon G- protein essential for Wnt ligands regulation and secretion. It is a transmembrane protein expressed in the ER, Golgi, vesicles and plasma membrane(Das et al. 2012, Coombs et al. 2010). Wnt ligands and Wnt signalling play a vital role in the immune system1.3.5). The fact that LPS induced the expressions of WLS significantly higher in the *LRRK2* KO compared to *LRRK2* WT is very intriguing. Thus, I wanted to see how WLS mediates the inflammatory process and the impact on LRRK2 and Rab10 expressions. To this end, siRNA technology was used as a means to silence the *WLS* / *GPR177* gene.

Remarkably, knocking-down the WLS protein resulted in the downregulation of Rab-10 and LRRK2, suggesting the significance of the Wnt pathway for LRRK2-Rab10 signalling (**Figure 4-48**). Furthermore, the decrease in both LRRK2 and Rab10 was associated with a decrease in both Cox-2 and TLR-4 expression, highlighting a potential role of LRRK2-Rab10 in mediating inflammatory processes via canonical Wnt signalling. Previously and the throughout this thesis, LRRK2 has been shown to modulate canonical Wnt signalling(Nixon-Abell et al. 2016). The result presented here

substantiate the interplay and association between LRRK2 and Wnt signalling. It is not clear how silencing WLS results in downregulation and destabilization of LRRK2. However, the associated decrease in Rab10 and Cox-2 indicate the significance of WLS to LRRK2 biological function.

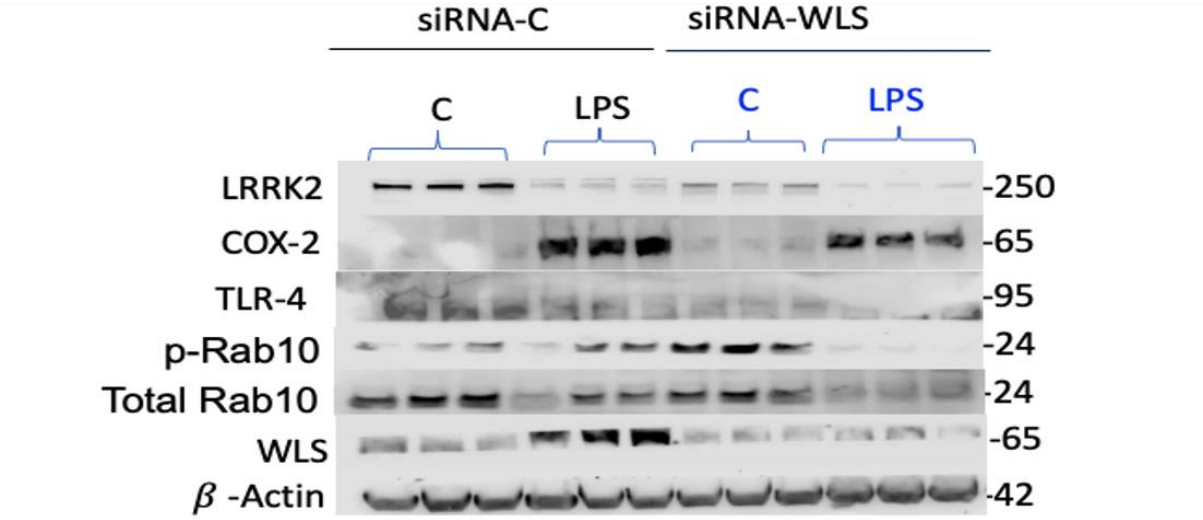

Figure 4-48 ***Summary of the impact of silencing WLS on LRRK2-Rab10 mediated inflammation***

4.3.5 Main finding and summary

Throughout this chapter, it is evident that *LRRK2* KO resulted in dysregulation in immune response evident by differences in the cytokines and chemokines release. The immune response tended to dampen evident by the downregulation of TNF-α and Cox-2. This was associated with changes in the protein expression and mRNA level of several Wnt signalling components. LRRK2 upregulation and the decrease in pRAB10 in response to LPS highlight the relevance of those proteins in mediating the inflammatory processes. Furthermore, downregulation of LRRK2 and Rab10 as a consequence of knocking-down of WLS substantiates the interplay between LRRK2 and Wnt signalling.

Chapter 5 Wnt signalling following inflammatory trigger in BMDM

5.1 Introduction

After characterizing the inflammatory responses to LPS and associated changes in Wnt signalling in the immortalized RAW 264 macrophages *LRRK2* WT and *LRRK2* KO cells, I wanted to explore and validate the findings in a more physiologically and pathological relevant system. BMDM primary cells generally give better physiologically representation compared to immortalized cell lines as BMDM differ in their phagocyte ability, cytokines and chemokines production and have different cellular response to pathogen. Moreover, they have the advantage of being genetically modified and isolated from transgenic mice that harbour relevant pathogenic mutations(Levenson et al. 2018, Trouplin et al. 2013). To this end, BMDM isolated from mice that harbour the most common mutation in PD (G2019S) were compared to WT and *LRRK2* KO mice.

BMDM are primary macrophages widely used in research setting to mimic *in-vivo* macrophages. They are derived from bone marrow stem cells after being differentiated in the presence of MCSF, which is a cytokine that facilitates the proliferation and commitment of myeloid progenitors' cells into macrophages and monocytes(Lee and Hu 2013). Typically, BMDM are isolated from the tibia and/or femur bones, but other bones can be utilized, and then differentiated in cultures in the presence of MCSF(Marim et al. 2010). Similar to the RAW 264 macrophages, BMDM have many macrophages' physiological characteristics. They can phagocyte foreign pathogens and respond to numerous stimuli, including TLR4 agonists such as LPS. Upon

stimulation with TLR agonists, they release pro- and anti-inflammatory cytokines, and they undergo polarization and upregulate nitric oxide synthase and subsequently release NO(Barrett et al. 2015).

The purity of BMDM can be determined by looking into macrophages specific markers such as CB11b and F4/80. Rapid response to LPS manifests in macrophages being polarized and the release of cytokines and NO confirm the presence of BMDM(Wang et al. 2013, Hume et al. 2002).

Several reports have been published highlighting the role LRRK2 plays in BMDM. Weindeland and colleagues have documented that unstimulated BMDM derived from *LRRK2* KO mice exhibited increased basal expression levels of interferon-stimulated genes (ISG), including Mx1, Ifit1, Irf7 and Rsad2. However, challenging the *LRRK2* KO BMDM with mycobacterium pathogen results in dampened response and lower expression of ISG compared to *LRRK2* WT and heterozygous control(Weindel et al. 2020). Another study has documented that BMDM derived from *LRRK2* KO mice were able to better control Mtb replication compared to WT, but their pro-inflammatory cytokines release (TNF-a and IL-6) are similar(Hartlova et al. 2018). In addition, BMDM extracted from *LRRK2* G2019S mice displayed a higher phagocytic activity, whereas the *LRRK2* KO had the opposite effect(Kim et al. 2018). As a result, those studies indicate that LRRK2 has a substantial role in mediating the inflammatory responses in BMDM, and that the manipulation of *LRRK2* genetically can alter those processes.

In this chapter, BMDM extracted from *LRRK2* WT, *LRRK2* KO and *LRRK2* KI mice were challenged with LPS and the expression of pro-inflammatory cytokines,

phagocytotic activity and NO release were investigated. The associated changes in Wnt signalling will be examined.

Chapter objectives:

1) Isolate and characterize the BMDM by looking into specific markers and confirm the isolation with NO release and polarization.
2) Challenge the BMDM with the TLR4 agonist LPS and examine differences in the mRNA expression levels of pro-inflammatory cytokines and NO release across the different *LRRK2* genotypes.
3) Determine the phagocytotic activity across the different *LRRK2* genotypes.
4) Determine the associated changes in Wnt signalling across *LRRK2* genotypes by looking into the mRNA levels of the Wnt signalling components.

5.2 Results

5.2.1 Characterization of BMDM

Initially, the purity had to be confirmed as the bone marrow initial culture is a collection of hematopoietic and mesenchymal stem cells. F4/80 is a common surface marker routinely used to determine the purity of BMDM(Wynn et al. 2013). As illustrated in **(Figure 5-1),** all the cells present in the culture expressed F4/80, and hence the culture consist of pure BMDM. Polarization and the release of NO in response to LPS further confirmed the presence of BMDM(**Figure 5-1,2**).

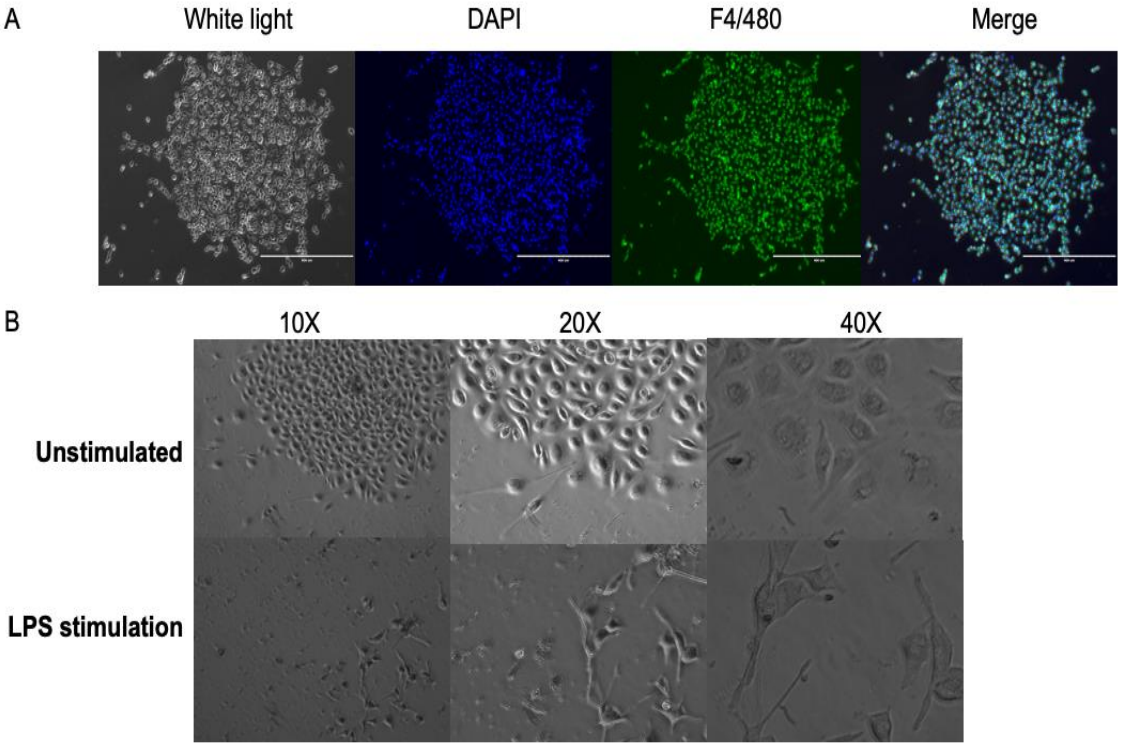

Figure 5-1 ***Purity and characterization of BMDM****. Fluorescent microscopy image depicting the expression of F4/80 on BMDM(**A**). Polarization of BMDM in response to LPS (**B**).*

5.2.2 Pro-inflammatory cytokines, Phagocytosis and NO release in response to LPS

5.2.2.1 NO production.

The Griess assay system(see2.6) was used to assess the production of NO release from the BMDM. As expected, treating the cells with LPS resulted in a sharp increase in NO in all genotypes. Importantly, the WT-LPS group displayed a substantial significant increase in release of NO compared to KO and the G2019S in the challenged conditions. The NO concentration in the culture media was (15.3 uM ±0.52) for the WT-LPS, whereas the KO-LPS and G2019S-LPS NO concentration were (3.2 uM ±0.43) and (2.96 uM ±0.26), respectively**(Figure 5-2).**

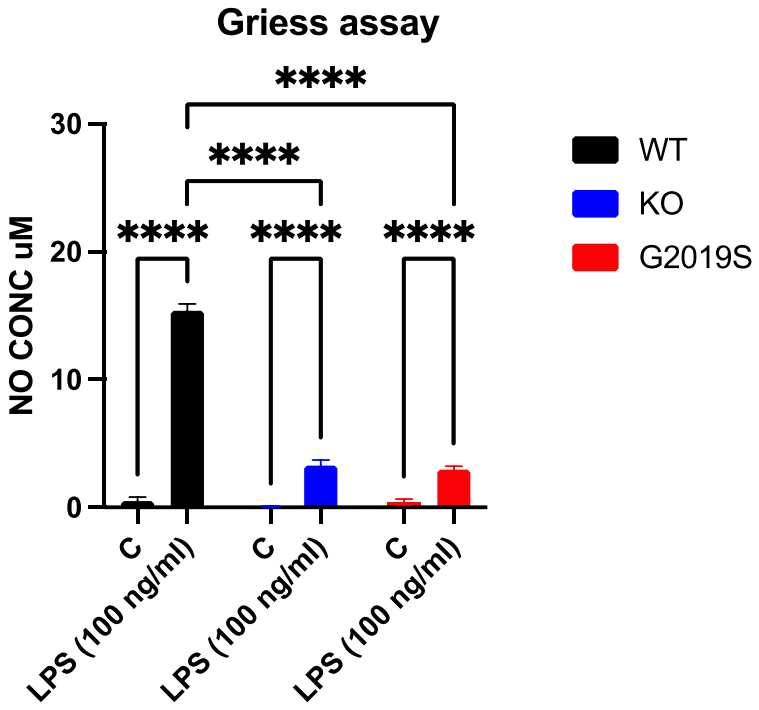

Figure 5-2 ***Effect of LRRK2 genotype on NO production in BMDM cells in response to LPS****. NO production as indicated by the level of nitrite formed in the supernatant using Griess reagent. The absorbance at 540 nm was measured against culture media with Griess reagent as a blank and sodium nitrite as a standard. Statistical significance was determined by two-way ANOVA followed by post hoc Tukey's test(n=3) Values represent the mean ± S.E.M. of 3 experiments.*

5.2.2.2 Phagocytotic activity in response to inflammatory challenge

The phagocytic activity of the BMDM macrophages was examined by determining the ability of the cells to internalize fluorescently labelled dead E-coli. The constitutive phagocytotic index was higher in the *LRRK2* KO BMDM (96.4%) compared to *LRRK2* WT (73.4%). Upon LPS stimulation, a contrasting effect is observed whereby the *LRRK2* WT-LPS group displayed (96.8%) whereas the KO-LPS was (80.6%). However, the differences were not significant **(Figure 5-3).**

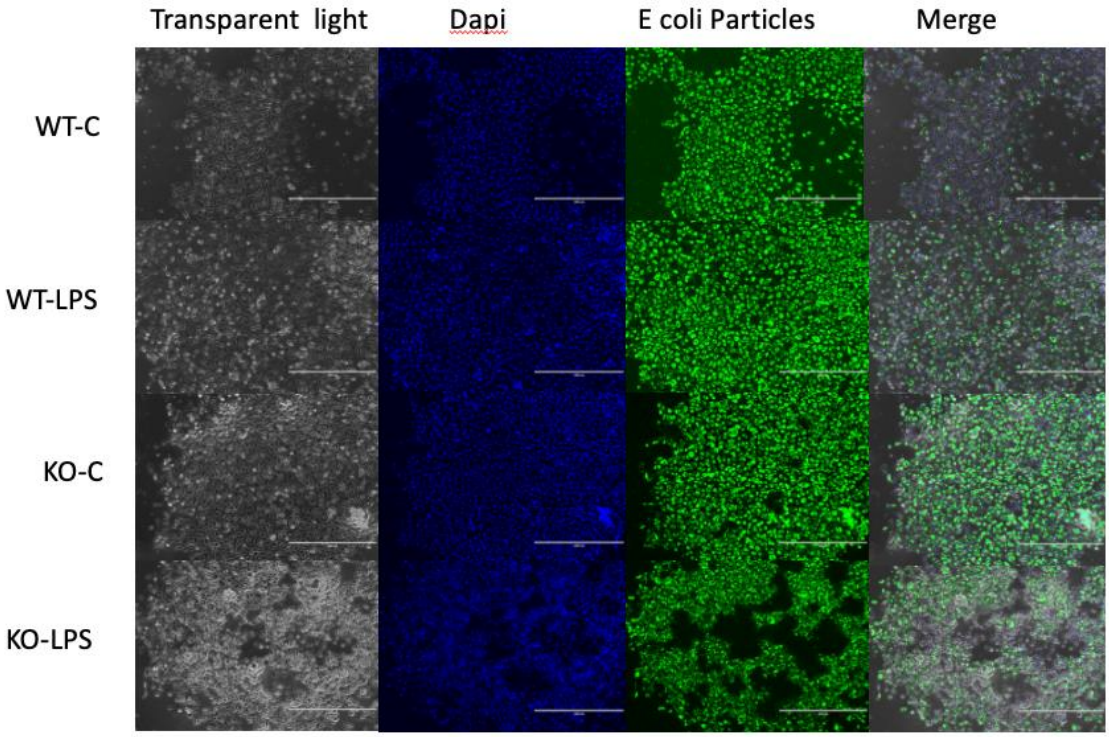

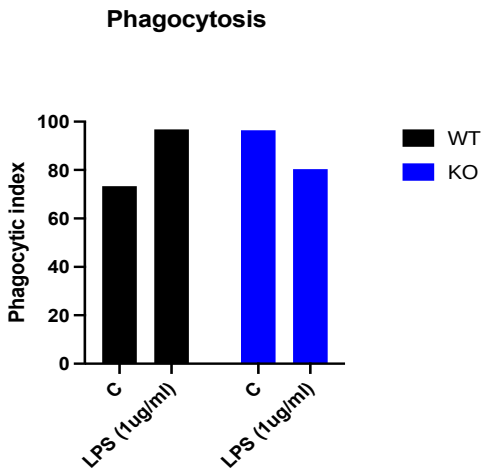

Figure 5-3 ***Phagocytic activity in BMDM LRRK2 WT and LRRK2 KO.*** *BMDM were treated with LPS or control media for 24 hr followed by labelling with fluorescein E coli for 2 hrs. Fluorescent microscopy image showing uptake of fluorescein label E coli across the different groups(**A**) Quantifications of the phagocytotic index in the fluorescent microscopy image by dividing the total number of green cells by the total number of cells(**B**).*

5.2.2.3 Pro-inflammatory cytokines

The release of pro-inflammatory cytokines from BMDM in response to the LPS challenge was assessed by qPCR. Overall, the BMDM from *LRRK2* KO and *LRRK2* KI mice displayed higher mRNA expression levels compared to control, though the differences were not significant (**Figure 5-4).** The WT-C control group was set to 1.

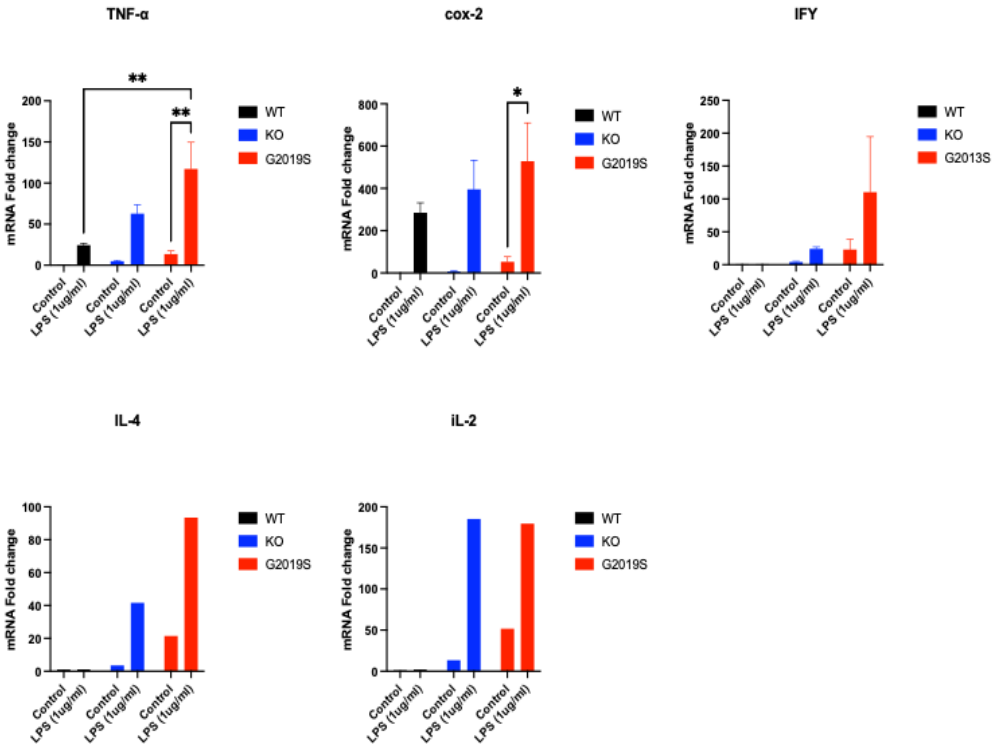

Figure 5-4 ***Cytokines mRNA expression.*** *WT-normalised relative mRNA expression levels of TNFα, Cox-2, IFN-γ, IL-4 and IL-2 cytokines were evaluated in BMDM at the basal level and in response to LPS challenged. Statistical significance was determined by two-way ANOVA followed by post hoc Tukey's test(n=3). Values represent the mean ± S.E.M. of 3 experiments.*

The following table summarises the fold changes and the standard deviation compared to the WT control group, which is normalized to 1.

Cytokines	WT-LPS	KO	KO-LPS	G2019S	G2019S-LPS
TNFα	24.64 ±3.82	4.85 ±1.7	62.69 ±18.82	13.82 ±6.65	117.17± 56.28
IFN-γ	0.93±0.17	4.05±1.66	24.01±4.97	23.03±26.87	110.32±146.15
Cox-2	285.2±81.91	7.83±4.78	385.47±239.43	53.28±41.39	528.7±315.00
IL-2	1.9	13.42	185.27	51.75	179.53
IL-4	1.09	3.54	41.5	21.46	93.49

Table 5-1 ***Fold changes in mRNA expression for TNFα, Cox-2, IFN-γ, IL-4 and IL-2 cytokines at the basal and challenged conditions.***

5.2.3 Canonical & non-canonical Wnt and NF-κB signalling changes in BMDM in response to Inflammatory challenge

The associated changes in Wnt signalling components at the basal level and in response to LPS was evaluated at the mRNA level. Overall, consistent with the results in the RAW 264 macrophages and previous reports published in our lab, the *LRRK2* KO cells displayed an augmented increase in the mRNA level for Wnt signalling components (**Figure 5-5**). The WT-C control group was set to 1.

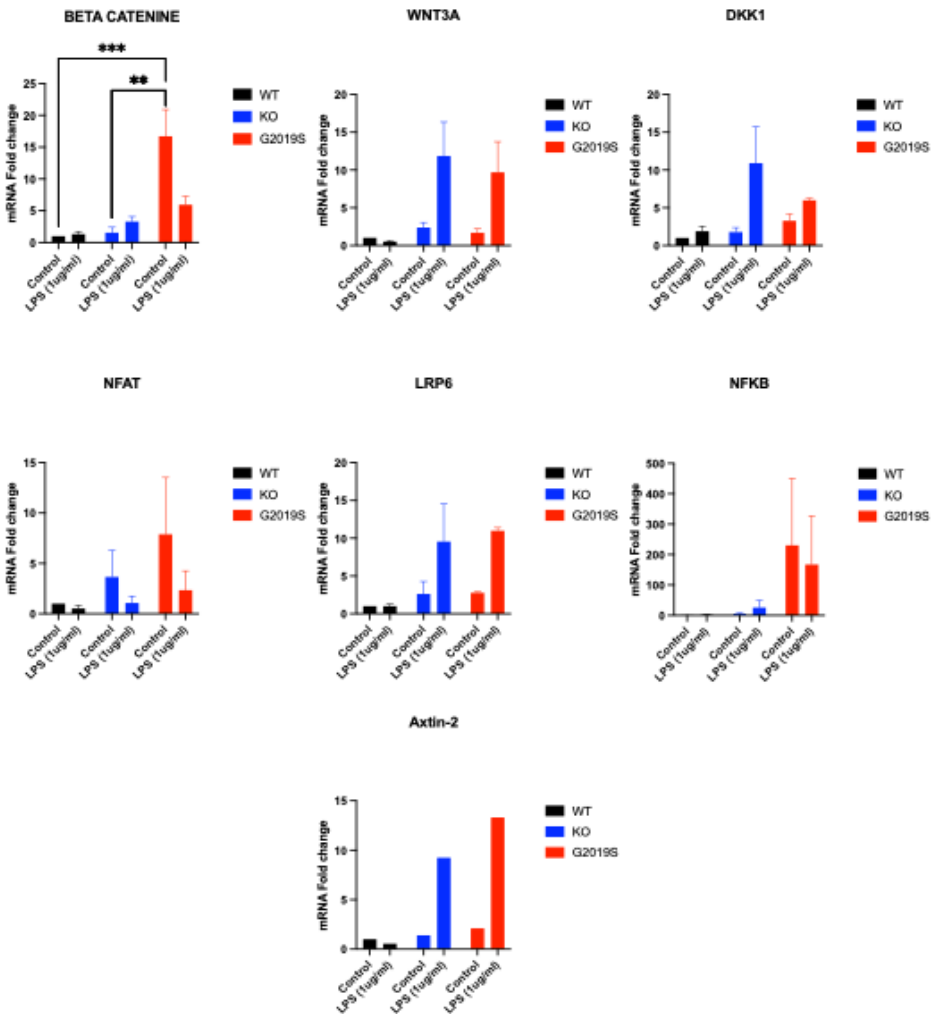

Figure 5-5 ***Wnt, NFAT and NF-κB signalling components mRNA expression under β-actin housekeeping gene.*** *WT-normalised relative mRNA expression levels of indicated Wnt and NF-κB signalling components was evaluated in BMDM at the basal level and in response to LPS challenged. Statistical significance was determined by two-way ANOVA followed by post hoc Tukey's test(n=3). Values represent the mean ± S.E.M. of 3 experiments.*

The following table summarises fold change in mRNA levels across the basal and challenged conditions.

Wnt signalling component	WT-LPS	KO	KO-LPS	G2019S	G2019S-LPS
β-catenin	1.31±0.69	1.55±1.43	3.29±1.32	16.7±7.28	5.92±2.3
Wnt3a	0.51±0.25	2.37±1.2	11.89±7.79	1.69±0.88	9.65±7.03
DDK-1	1.89±1.17	1.79±1	10.9±8.31	3.27±1.54	5.99±0.47
NFAT	0.5±0.53	3.65±4.56	1.07±1.185	7.88±9.77	2.34±3.3
LRP-6	1±047	2.62±2.87	9.55±8.63	2.76±0.27	10.98±0.77
Axin-2	0.56	1.4	9.2	2.1	13.31
NFκ B	2.35±0.26	4.7±5.36	25.51±41.04	230.2±380	167.44±277

Table 5-2 ***Fold changes in mRNA expression for Wnt signalling components at the basal and challenged conditions***

5.3 Discussion

As mentioned in the introduction, BMDM are advantageous in comparison to the RAW 264 macrophages as they are more physiologically relevant, and they can be separated transgenic mice harbouring pathogenic mutation relevant to PD(G2019S). Accordingly, I have separated BMDM from *LRRK2* WT, *LRRK2* KO and *LRRK2* G2019S mice. Initially, I have separated the bone marrow cells from the tibia and femur bones and differentiate them using M-CSF for 7 days. As shown in **Figure 5-1**, all the cells expressed the BMDM specific marker F4/80 and the polarization in response to LPS further confirm BMDM's purity.

5.3.1 Immune response differences

Next, I examined the release of NO in response to LPS utilizing the Griess assay. As expected, treating the BMDM result in a significant increase in NO production in all genotypes. Interestingly, the increase in the WT-LPS cell group was significantly higher compared to cells from *LRRK2* KO. This in agreement with a study by Kim and others showing LRRK2 knock-down in BV-2 transform microglia result in a decrease in NO release in response to LPS(Kim et al. 2012). However, data observed in the RAW 264 macrophages showed no differences. Paradoxically, the BMDM from *LRRK2* -G2019S mice also exhibited a significant decrease similar to *LRRK2* KO cells. This is in contrast to many studies suggesting that the *LRRK2* G2019S is a gain of function mutation driving neuroinflammation(Dzamko et al. 2016). Although most of those studies were done in over-expression models whereas the *LRRK2* -G2019S knock-in mice explored in this thesis is not an overexpression model.

Many reports have pointed to a possible role for LRRK2 in phagocytosis. LRRK2 has an established role in autophagy, a process that has a common convergence pathway

with phagocytosis(Ferguson and Green 2014). To this end, I have looked at the differences in the phagocytic activity across the *LRRK2* WT and *LRRK2* KO. Consistent with the results seen in RAW 264 macrophages, the *LRRK2* KO cells displayed less, albeit non-significant phagocytotic activity compared to *LRRK2* WT when challenge with LPS **(Figure 5-3).**

Analysing the mRNA levels of cytokines from the BMDM across the *LRRK2* genotypes revealed interesting observations. Pro-inflammatory cytokines mRNAs were upregulated in BMDM from both *LRRK2* KO and *LRRK2* G2019S mice. Those include TNF-α, Cox-2, IFN-γ, lL-4 and IL-2. The *LRRK2 G2019S* mutation has been reported to be gain of function mutation as serum from asymptomatic patients with *LRRK2* G2019S mutation displayed an increased in expressions pro-inflammatory cytokines(Dzamko et al. 2016). The result presented here are consistent with this observation. However, the *LRRK2* KO mutation has been associated with either a decrease or no change in the in pro-inflammatory cytokines. There are two reports demonstrated that *LRRK2* deletion had no effect on cytokine release in mice BMDM(Hakimi et al. 2011, Dzamko et al. 2012). There could be a couple of explanations, First, the incubation time with the inflammatory stimulus was different. Also, one of those reports looked at the cytokine release only without looking at mRNA level. Nevertheless, this warrants further investigation.

5.3.2 Wnt signalling changes

The Wnt signalling changes in response to LPS stimulation in *LRRK2* KO BMDM genotypes are in line with the data generated in RAW 264 macrophages. *LRRK2* deletion result in substantial, non-significant increase in key canonical Wnt signalling

components including Wnt3a, LRP-6 and Axin-2 **(Figure 5-5).** Interestingly, DDK-1 was also increased perhaps as feedback mechanism.

Paradoxically, the *LRRK2* G2019S mutation also resulted in augmentation of canonical Wnt signalling. While there are no data in the literature documenting the association between *LRRK2* G2019S mutation and canonical Wnt signalling in BMDM. Previous work in our lab demonstrated that *LRRK2* pathogenic mutations R144G, R144C and G2019S and the risk variant G2385R decreased canonical Wnt signalling in SH-SY5Y cells. (Nixon-Abell et al. 2016, Berwick et al. 2017).However , the system employed in those studies were luciferase system in immortalized non-immune cells. Nonetheless, it is an interesting observation need to be investigated and addressed.

5.3.3 Main finding and summary

The results presented in this chapter provide further evidence of the involvement of LRRK2 in mediating LPS inflammatory response. BMDM isolated from *LRRK2* G2019S mice displayed an augmented gene expression level of several inflammatory cytokines consistent with several previous reports in other systems. Paradoxically and contesting to the RAW 264 macrophages, BMDM *LRRK2* KO cells also displayed upregulation of inflammatory cytokines. The upregulation in Wnt signalling observed in *LRRK2* KO are in line with the previous data reported in the RAW 264 macrophages and the literature whereas the changes observed in the BMDM *LRRK2* G2019S were in contrast to data generated in our lab. It is plausible that LRRK2 role in inflammatory response bee mediated partially through Wnt signalling.

Chapter 6 Wnt signalling in activated T lymphocytes

6.1 Introduction

After investigating the role of LRRK2 mediated inflammatory processes in innate immune cells, I sought to explore its role in the adaptive immunity, specifically the T cells. While many reports have investigated LRRK2 in the context of innate immunity looking at microglia and macrophages(Moehle et al. 2012, Marker et al. 2012), it has also been reported to play a role in the adaptive immunity(Gardet et al. 2010, Wallings et al. 2020). LRRK2 expression was found to be upregulated in T and B cells from patients diagnosed with PD carrying the *LRRK2* G2019S mutation compared to a healthy matched controls. Additionally, LRRK2 expressions was upregulated in activated T cells(Cook et al. 2017).Consequently, T cells have chosen as a representative of the adaptive immunity.

T cells are a type of lymphocyte originating from hematopoietic stem cells in the bone marrow and mature and differentiate in the thymus (T cells). They are consequential for the adaptive immune response and carry many essential functions such as directly killing host-infected cells and activating other immune cells (B cells) to differentiate and produce antibodies. The spleen in rodents, including mice, is considered an excellent source of T cells. There are about 100 million splenocytes in the spleen; 25-30 % are T cells. Generally, the T cells can be isolated from the splenocytes either by fluorescence-activated cell sorting (FACS) or Magnetic cell sorting. The latter has two main advantages(Lim, Berger and Su 2016). First, it is less invasive technically than FACS, which often needs a highly skilled dedicated personal. Second, the T cells can be untouched (unstimulated or native T cells) by utilizing negative selection whereby

non-target cells are labelled and depleted, leaving the T cells intact (negative selection).

Initially, the expression of LRRK2 in T cells had been questionable as Thévenet reported that T cells express very low levels of LRRK2 at the mRNA and protein level compared to other PBMC cells(Thevenet et al. 2011). Many scientists cited Thévenet's paper as evidence that T cells don't express LRRK2 though immuno-blot images clearly showed that CD3+ cells (T cells) expressed LRRK2(Cook et al. 2017, Thevenet et al. 2011). Nevertheless, follow up studies by Hakimi and others documented the expression of LRRK2 in several human PBMC immune cells, including the T cells(Hakimi et al. 2011, Cook et al. 2017).

Furthermore, the expression of LRRK2 in T cells appears to be augmented in PD patients compared to matched healthy control, which is consistent with data in other immune cells presented here and elsewhere. Moreover, stimulated T cells from PD patients secrete more TNF-α compared to controls, suggesting that LRRK2 could have a role in mediating T cells immune responses(Cook et al. 2017).

Chapter objectives:

1) Isolate and characterize the T cells by looking into the expression of specific markers (CD+3).
2) Detect LRRK2 expression in T cells isolated from the spleen.
3) Mimic the in-vivo T cells activation by using CD+3/CD+28 antibodies, and examine differences in the mRNA expression levels of pro-inflammatory cytokines and NO release across the different genotypes.

4) Determine the associated changes in Wnt signalling across the genotypes by looking into the mRNA levels of the Wnt signalling components at the basal and activated.

6.2 Results

6.2.1 Isolation and characterization of T lymphocytes

After the T cells have been isolated from the spleen using magnetic cell sorting, the cells' purity had to be determined. To this end, markers specific for T cells and non-T cells were used, CD+3 is a surface marker expressed specifically on T cells, whereas CD+45 is a surface marker expressed ubiquitously on all other lymphocytes including T cells.

Figure 6-1 showed that magnetic cell sorting resulted in a culture that is 98.5% pure CD+3 T cells, whereas splenocytes had only 35% CD+3 T cells. This confirms successful isolation of pure native untouched T cells.

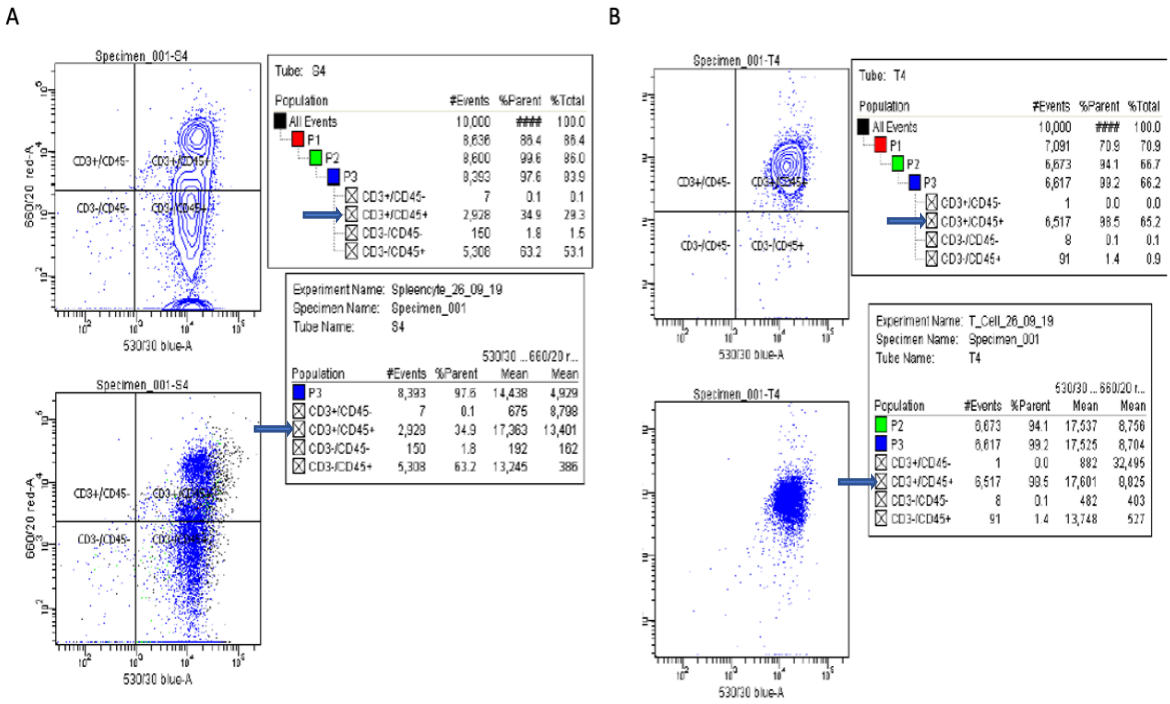

Figure 6-1 ***Purity analysis of T cells by flow cytometry.*** *T cells were purified by magnetic cell sorting, and their purity was determined by flow cytometry. Splenocytes and T cells were stained with either control(no antibody), CD+3, CD+45 and both CD+3 and CD+45. Data-plot depicting splenocytes stained with CD+3 and CD+45 showing only 35% T cells (**A**). Data-plot representing T cells after being separated and stained with CD+3 and CD+45 showing 98.5% T cells purity(B).*

6.2.2 LRRK2 expression in T lymphocytes

As mentioned previously, LRRK2 expression in the T cells was a subject of controversy. Thus, I sought to investigate if T cells isolated from the spleen express LRRK2 or not. Utilizing the LRRK2 antibody MJF2 from *Abcam*®, LRRK2 was detectable in both the WT and the G2019S T cells separated from the spleen(**Figure 6-2).**

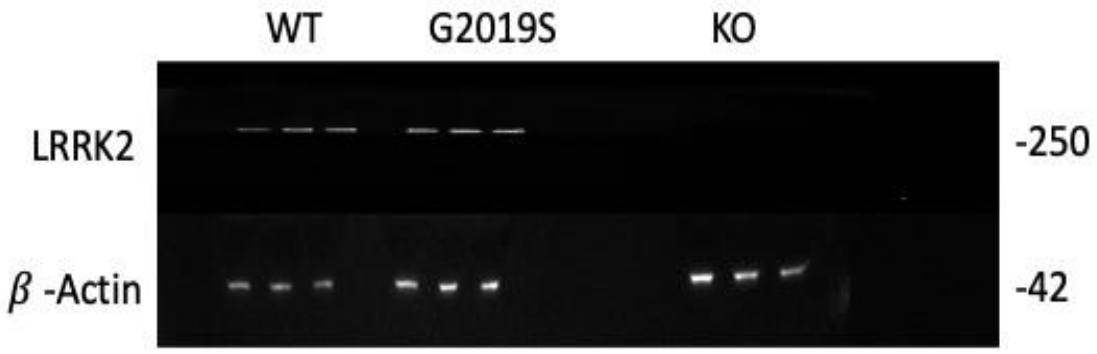

Figure 6-2 ***LRRK2 expression in T cells.*** *Immunoblot image depicting LRRK2 expression in WT and G2019S T cells freshly isolated from the spleen.*

6.2.3 Pro-and anti-inflammatory cytokines release in T cells at the basal and activated state

The release of Pro-inflammatory cytokines releases from T cells at the basal level and in response to exposure to CD+3/CD+28 mimicking *in-vivo* activation was assessed by qPCR.

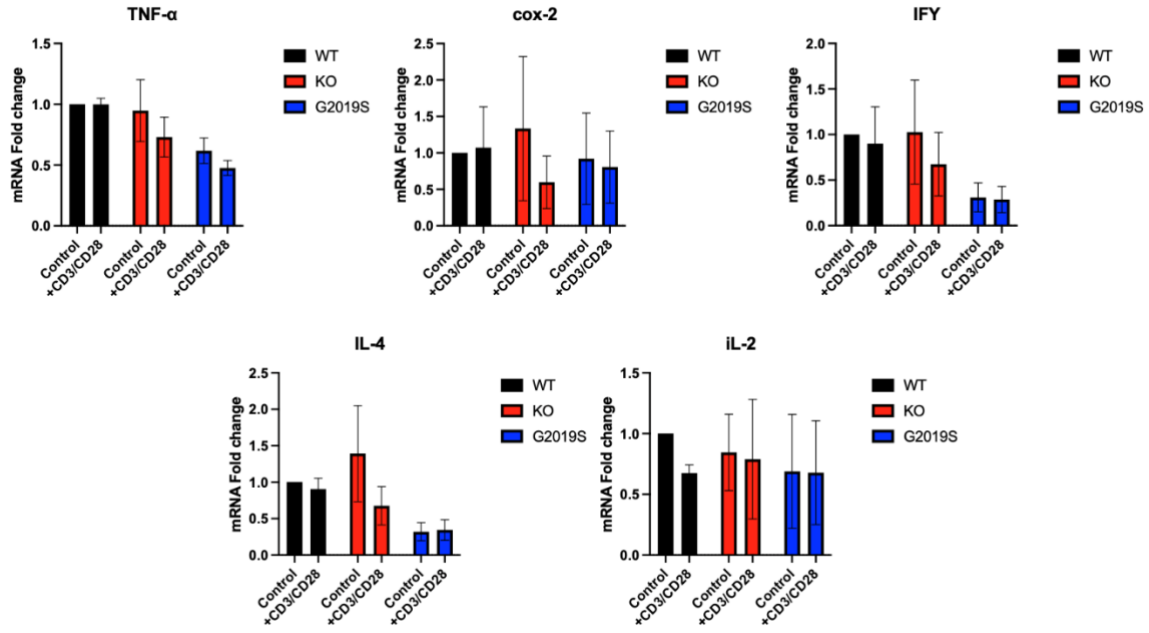

Figure 6-3 ***Cytokine's mRNA expression under β-actin housekeeping gene in T cells*** *WT-normalised relative mRNA expression levels of TNFα, Cox-2, IFN-γ, IL-4 and IL-2 cytokines were evaluated in T cells at the basal level and in the activated state. Statistical significance was determined by two-way ANOVA followed by post hoc Tukey's test(n=3). Values represent the mean ± S.E.M. of 3 experiments.*

The following table summarises the fold changes and the standard deviation compared to the WT control group, which is normalized to 1.

Cytokines	WT-LPS	KO	KO-LPS	G2019S	G2019S-LPS
TNFα	0.99±0.08	0.94±0.44	0.73±0.28	0.61±0.18	0.47±0.10
IFN-γ	0.90±0.70	1.02±0.98	0.67±0.60	0.3±0.27	0.28±0.25
Cox-2	1.07±0.96	1.33±1.7	0.59±0.062	0.91±1.085	0.80±0.85
IL-2	0.67±0.11	0.85±0.54	0.78±0.85	0.69±0.81	0.67±0.73
IL-4	0.90±0.25	1.39±1.14	0.67±0.45	0.32±0.21	0.34±0.24

Table 6-1 ***Fold changes in mRNA expression for TNFα, Cox-2, IFN-γ, IL-4 and IL-2 cytokines at the basal and challenged conditions.***

6.2.4 Canonical Wnt, NFAT and NF-κB signalling in T cells at the basal and activated state

The associated changes in Wnt signalling components at the basal level and in the activation state was evaluated at the mRNA level. Overall, and contrasting to the results in the RAW 264 macrophages and with previous reports published in our lab, the *LRRK2* WT cells displayed an augmented increase in the mRNA level for Wnt signalling components.

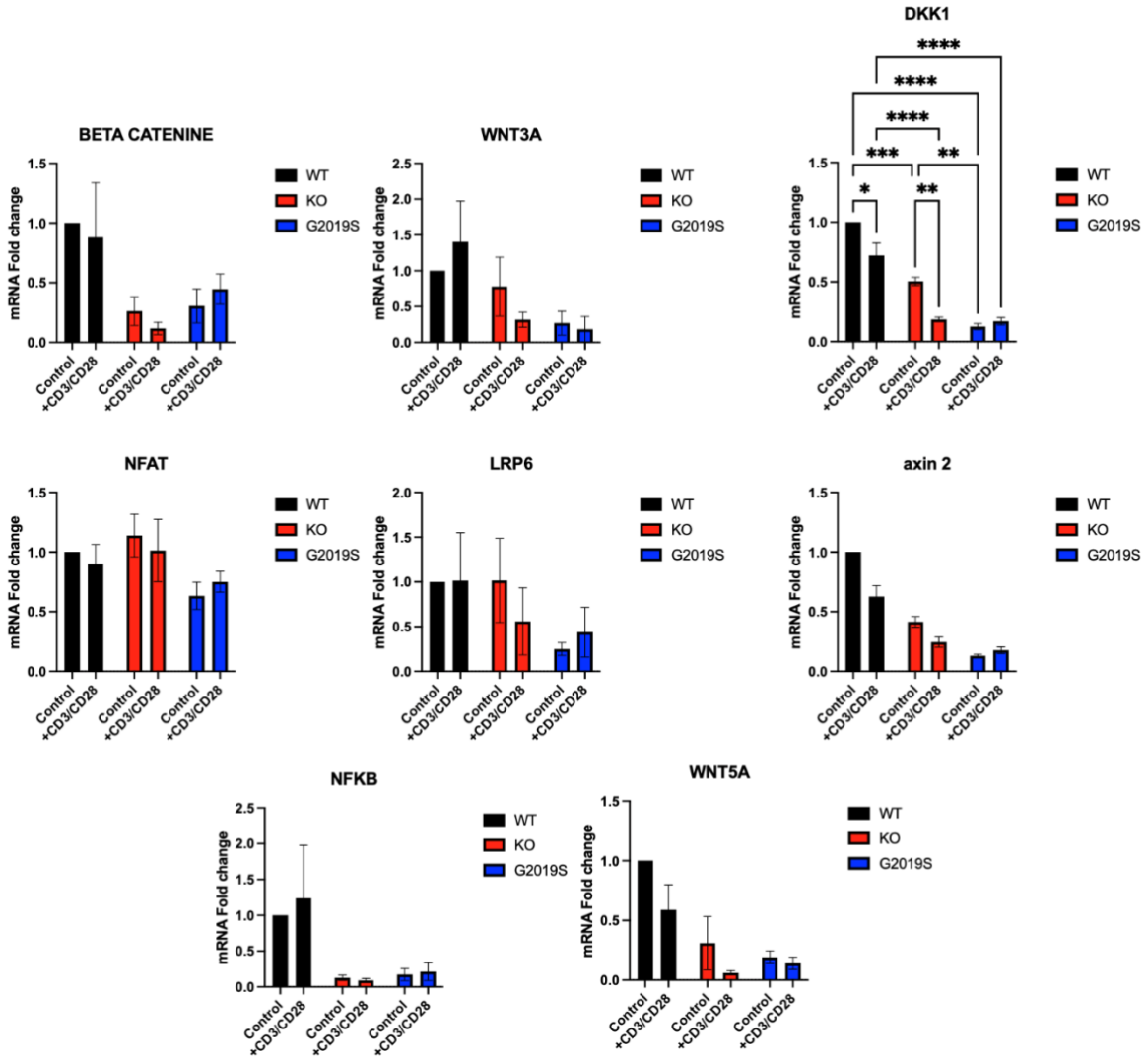

Figure 6-4 ***Wnt, NFAT and NF-κB signalling components mRNA expression levels under β-actin housekeeping gene in T cells.*** *WT-normalised relative mRNA expression levels of indicated Wnt and NF-κB signalling components was evaluated in T cells at the basal level and in the activation state. Statistical significance was determined by two-way ANOVA followed by post hoc Tukey's test(n=3). Values represent the mean ± S.E.M. of 3 experiments.*

The following table summarises fold change in mRNA levels across the basal and challenged conditions. The WT-C control group was set to 1.

Wnt signalling component	WT-LPS	KO	KO-LPS	G2019S	G2019S-LPS
β-Catenin	0.88±0.79	0.26±0.2	0.11±0.09	0.3±0.24	0.44±0.21
Wnt3a	1.4±0.98	0.77±0.71	0.31±0.18	0.26±0.28	0.18±0.3
DDK-1	0.72±0.18	0.5±0.05	0.18±0.03	0.12±0.04	0.17±0.05
NFAT	0.9±0.28	1.13±0.31	1.01±0.45	0.65±0.19	0.75±0.14
LRP-6	1.01±0.92	1.01±0.81	0.55±0.65	0.24±0.12	0.43±0.48
Axin-2	0.62±0.16	0.41±0.07	0.24±0.07	0.13±0.02	0.17±0.04
NFκ B	1.23±1.27	0.12±0.06	0.09±0.04	0.17±0.14	0.21±0.21
Wnt5a	0.58 ±0.36	0.3±0.38	0.06±0.03	0.19±0.09	0.14±0.09

Table 6-2 ***Fold changes in mRNA expression levels for Wnt signalling components at the basal and challenged conditions in T cells(n=3).***

6.2.5 Lentivirus transduction efficiency studies

Similar to the transduction's efficiency study conducted in section 4.2.1.1, lentivirus encoding GFP was used to determine the appropriate MOI for the T cells. Mouse T cells are known to be difficult to transduce, especially with lentivirus derived from HIV(Baumann et al. 2004, Gilham et al. 2010) . To this end, I used cyclosporine H to test if it would enhance the transduction's efficiency. Cyclosporine H (CsH) is a non-immunosuppressant derivative of cyclosporine, and it has been used to improve the transduction efficiency in several cell lines, including T cells(Petrillo et al. 2018, Peel and Scribner 2013). The rationale is CsH can enhance viral entry by preventing VSV glycoprotein-mediated vector entry through the inhibition of interferon-induced

transmembrane protein 3 (IFITM3), a protein known to broad antiviral activity and known to be expressed by T cells(Petrillo et al. 2018).

Overall, the finding shown in **Figure 6-5** confirmed low transductions efficiency in mouse T cells. At the highest MOIs, the transductions efficiency was less than 5%.

In addition, using CsH didn't enhance the transductions efficiency but rather decrease in all tested MOIs. I have decided to choose MOI 100 as it has been shown that even with transductions efficiency as low as 2%, mouse T cells can still be transduced with lentivirus for certain applications.

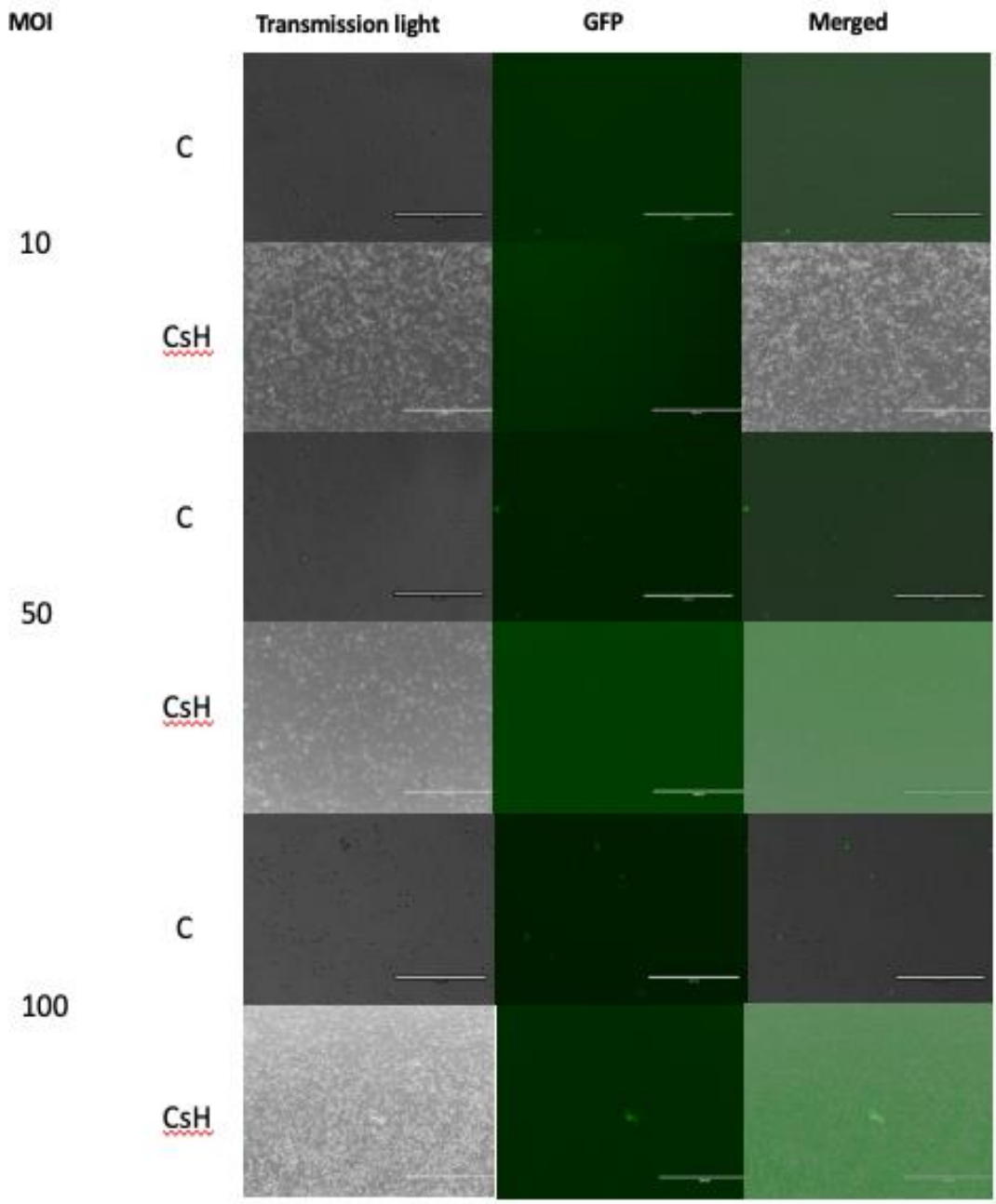

Figure 6-5 ***T cells expressing Lentiviral GFP 48 hours post-transduction.*** *Lentivirus encoding GFP has been used to transduced T cells at the indicated MOIs for 24 hours with or without Cyclosporine H (CsH). Fluorescent microscopy image showing positive GFP cells.*

6.2.6 Luciferase assays measuring NFAT transcriptional changes in T cells at the basal and activated state

The changes in NFAT transcriptional activation in response to Wnt modulators in T cells at the basal and the activation state with the CD28/CD3 antibodies was evaluated. Each control group at both states raw bioluminescence value was normalized to one, and the treatment groups were expressed as fold change.

6.2.6.1 Changes at the basal state

Initially, the constitutive activity of NFAT transcriptional activity was compared between the *LRRK2* WT and *LRRK2* KO cells at the basal and the stimulated level. The luciferase activity was significantly lower in *LRRK2* KO T cells compared to *LRRK2* WT-C. The fold decrease in the *LRRK2* KO-C group was (0.86 fold ±0.07). There were no differences between the genotypes at the activation state**(Figure 6-6).**

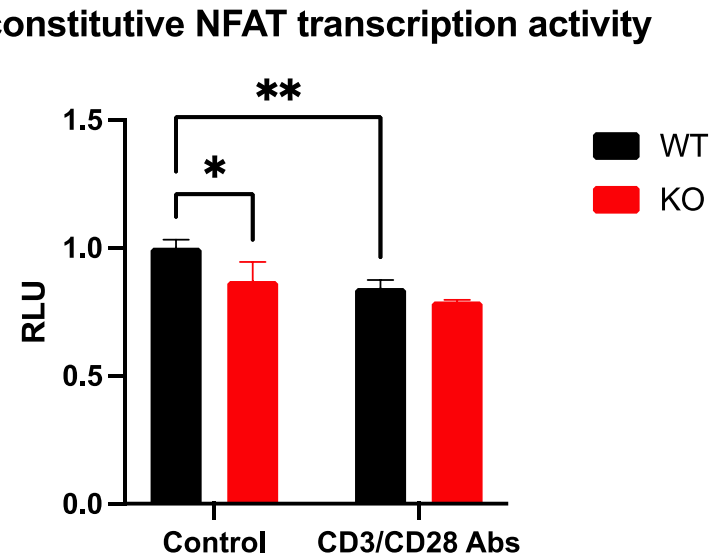

Figure 6-6 ***NFAT transcriptional change at the basal level****. T cells were transduced with NFAT lentivirus for 24 hours. Culture medium containing secreted luciferase were assayed for bioluminescence. Statistical significance was determined utilizing two-way ANOVA followed by post hoc Tukey's test(n=3). Values represent the mean ± S.E.M. of 3 experiment.*

6.2.6.2 LPS

Treating the T cells with LPS resulted in a significant decrease in NFAT signalling in the *LRRK2* WT groups at both the basal and the activated stage. The reduction in the basal level was (0.71±0.11) fold decrease, while the decline was (0.68±0.09) fold decrease in the activated state. Interestingly, The *LRRK2* KO cells didn't follow the pattern as LPS challenge didn't change the NFAT transcriptional activation**(Figure 6-7).**

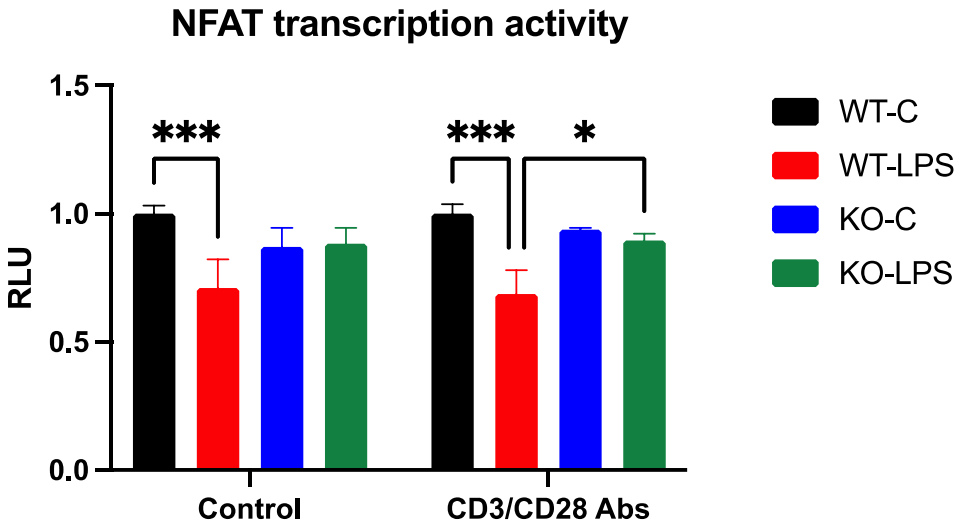

Figure 6-7 ***Modulation of NFAT transcriptional activation by LPS.*** *T cells were transduced with NFAT lentivirus for 24 hours. The indicated treatments have been added and further incubated for 24 hours. Culture medium containing secreted luciferase were assayed for bioluminescence. Statistical significance was determined utilizing two-way ANOVA followed by post hoc Tukey's test(n=3). Values represent the mean ± S.E.M. of 3 experiments.*

6.2.6.3 Wnt3a and LPS

At the basal level, treating the T cells with Wnt3a decreased NFAT transcriptional activation in both genotypes. The decrease in the *LRRK2* WT-Wnt3a group was (0.87 ±0.07), whereas the *LRRK2* KO-Wnt3a displayed a (0.79 ±0.04) fold decrease. Interestingly, treating the cells with the combination of Wnt3a and LPS resulted in diminishing the effect of Wnt3a alone, in which the *LRRK2* WT cells displayed (0.93± 0.02) fold change whereas the *LRRK2* KO cells showed (0.92 ±0.03) fold change.

At the activation state, Wnt3a treatment decreased the Nfat transcriptional activation only in the *LRRK2* WT group. There were no differences in the other groups**(Figure 6-8).**

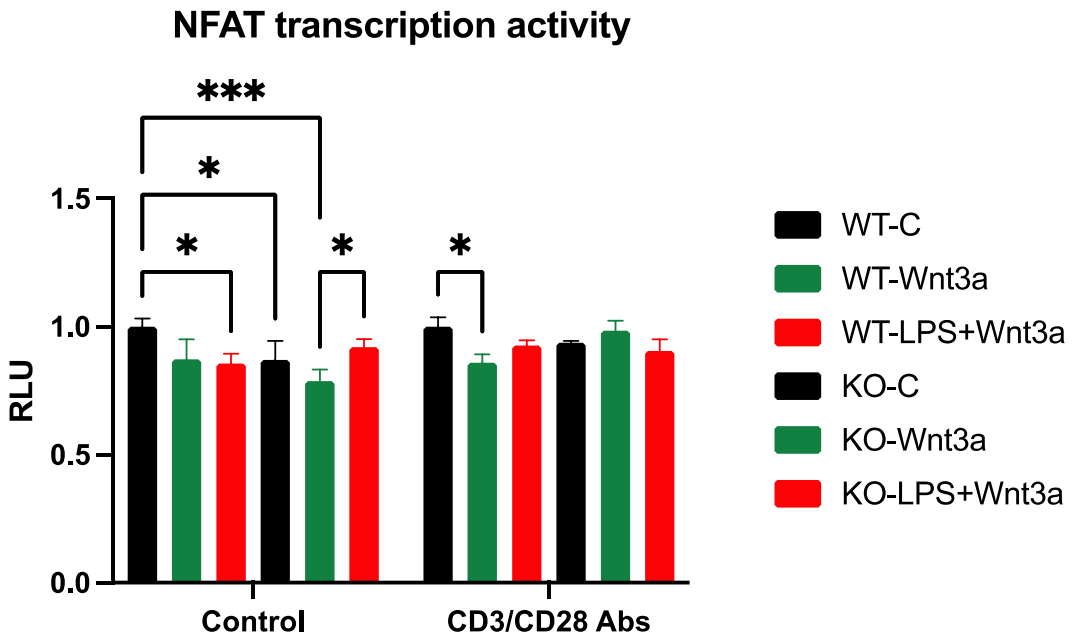

Figure 6-8 ***Modulation of NFAT transcriptional activation by Wnt3a.*** *T cells were transduced with NFAT lentivirus for 24 hours. The indicated treatments have been added and further incubated for 24 hours. Culture medium containing secreted luciferase were assayed for bioluminescence. Statistical significance was determined utilizing two-way ANOVA followed by post hoc Tukey's test(n=3). Values represent the mean ± S.E.M. of 3 experiment.*

6.2.6.4 Wnt5a and LPS

Treating the cells with Wnt5a resulted in decreased NFAT transcriptional activation In both genotypes at the basal level. The decrease in the *LRRK2* WT-Wnt5a group was (0.79 ±0.01) fold, whereas the *LRRK2* KO- Wnt5a group displayed (0.86±0.06) fold decrease. Dual treatments of Wnt5a and LPS resulted in restoring the reduction induced by Wnt5a alone. The combination of Wnt5a and LPS resulted in (0.85 ±0.05) fold change in the WT, whereas the *LRRK2* KO cells displayed (0.94 ±0.02) fold change.

At the activation state,the same trend is observed. Wnt5a treatment resulted in a non-significant decrease for both genotypes in which dual treatment with LPS diminish the reduction effect of Wnt5a**(Figure 6-9).**

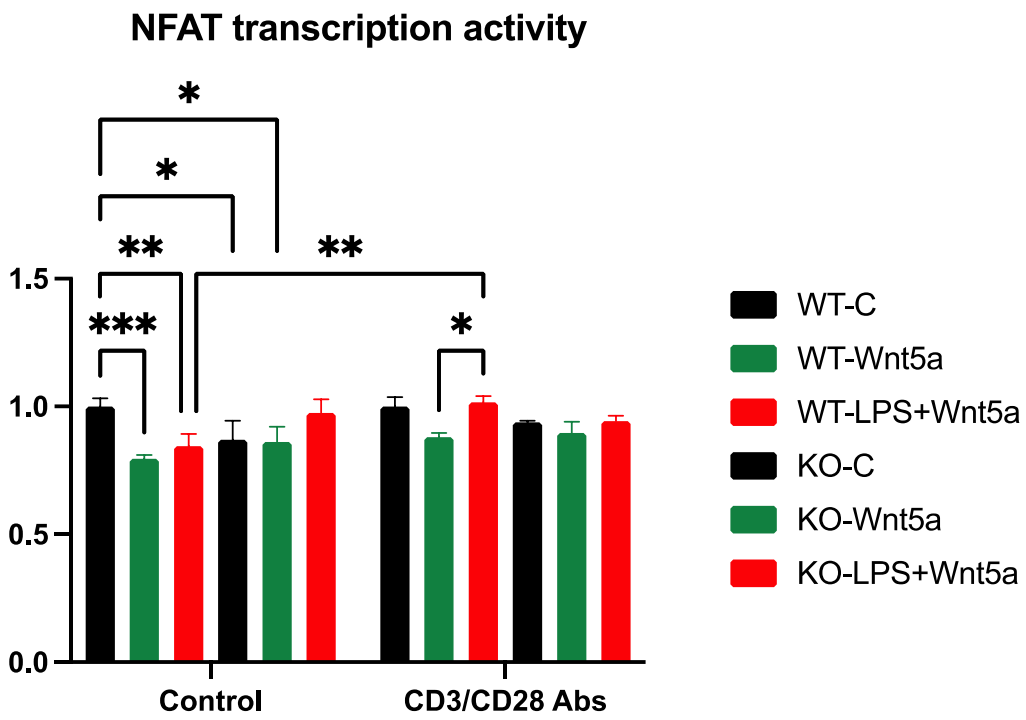

Figure 6-9 ***Modulation of NFAT transcriptional activation by Wnt5a.*** *T cells were transduced with NFAT lentivirus for 24 hours. The indicated treatments have been added and further incubated for 24 hours. Culture medium containing secreted luciferase were assayed for bioluminescence. Statistical significance was determined utilizing two-way ANOVA followed by post hoc Tukey's test (n=3). Values represent the mean ± S.E.M. of 3 experiments.*

6.2.6.5 PMA/IO

Next, I wanted to test the impact of PMA/IO, which is known to activate T cells and NFAT signalling. Unexpectedly, treating the T cells with PMA/IO didn't change NFAT transcriptional activation. Furthermore, there were no differences across the different genotypes**(Figure 6-10).**

.

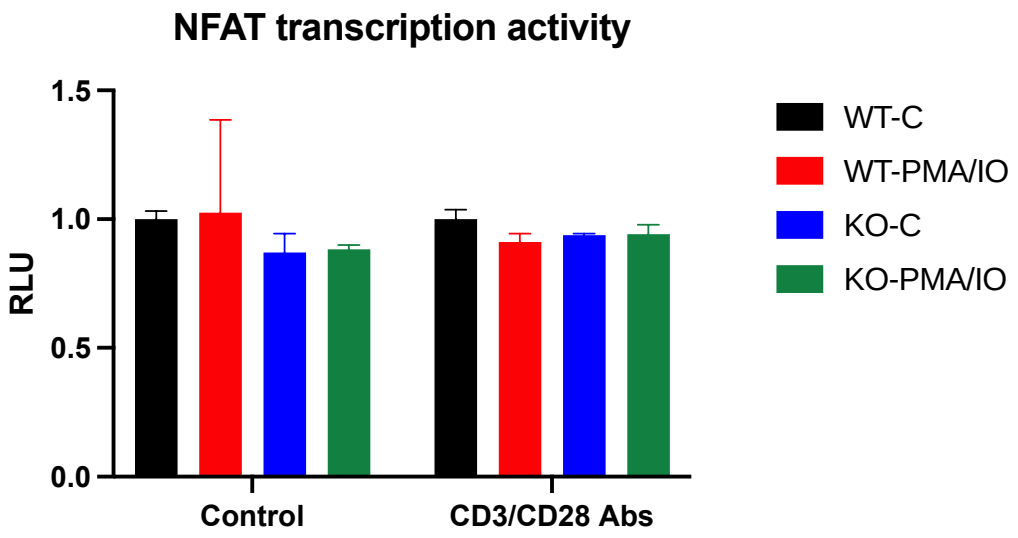

Figure 6-10 ***Modulation of NFAT transcriptional activation by PMA/IO.*** *T cells were transduced with NFAT lentivirus for 24 hours. The indicated treatments have been added and further incubated for 24 hours. Culture medium containing secreted luciferase were assayed for bioluminescence. Statistical significance was determined utilizing two-way ANOVA followed by post hoc Tukey's test(n=3). Values represent the mean ± S.E.M. of 3 experiments*

6.2.6.6 LiCl

Treating the cells with GSK3β inhibitor LiCl didn't result in changes at the basal level for both genotypes. Interestingly, when the cells are stimulated, LiCl decreased the NFAT transcriptional activation in the *LRRK2* WT groups only (0.56±0.36), whereas NFAT transcriptional activation didn't change in the *LRRK2* KO T cells**(Figure 6-11).**

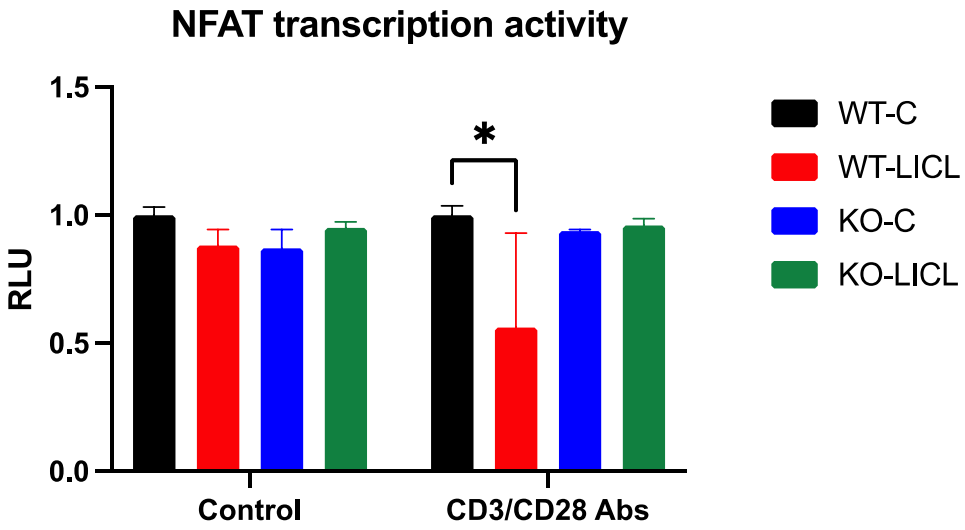

Figure 6-11 ***Modulation of NFAT transcriptional activation by LiCl.*** *T cells were transduced with NFAT lentivirus for 24 hours. The indicated treatments have been added and further incubated for 24 hours. Culture medium containing secreted luciferase were assayed for bioluminescence. Statistical significance was determined utilizing two-way ANOVA followed by post hoc Tukey's test(n=3). Values represent the mean ± S.E.M. of 3 experiments*

6.3 Discussion

Following characterizing and exploring LRRK2 inflammatory role in cells that represents the innate immunity (chapters 4 and 5), T cells has been chosen as an example of adaptive immunity. Initially, there were conflicting reports about LRRK2 expression in T cells. Thus, I have started this chapter with the isolation and characterisation of T cells, followed by looking at the LRRK2 expressions. In agreement with the study by Hakimi and Cook(Hakimi et al. 2011, Cook et al. 2017), I confirmed the presence of LRRK2 in the T lymphocytes isolated from mice (**Figure 6-2**).

Next, the mRNA levels of pro-inflammatory were investigated in native (untouched) and activated T cells. To mimic the T cells *in-vivo* activation, anti-CD3/CD28 coated beads have been utilised to activate T cells *in-vitro* setting.

Interestingly, mRNA expressions level for the pro-inflammatory cytokines in T cells follow a very different pattern seen in the RAW 264 and BMDM macrophages. The activation of the T cells did not elicit an up-regulation of cytokines' mRNA levels. The *LRRK2* G2019S T cells did display a tend to decrease in the IL-4 and IFN-γ. The *LRRK2* KO T cells exhibited a slight decrease in the IL-4, Cox-2 and IFN-γ when activated. Those data are in contrast to previous report whereby activated T cells showed an increase in pro-inflammatory cytokines(Cook et al. 2017). Differences in the activation protocol or T cell isolation processes could be a contributing factor for the conflicting data reported here.

Similar to the mRNA level of the pro-inflammatory cytokines, Wnt signalling changes across the *LRRK2* genotypes follow a different pattern to RAW 264 and BMDM macrophages. Both the *LRRK2* KO and *LRRK2* G2019S mutation showed a reduction

in key components of Wnt signalling, including LRP-6, Axin-2, Wnt3a, Wnt5a and β-catenin. The decrease in canonical Wnt signalling associated with *LRRK2* G2019S mutation has been reported previously(Berwick et al. 2017). However, the decrease observed in the *LRRK2* KO T cells is in contrast with data presented in chapter 5 and chapter 6, which merit further exploration. A recent study by Panagiotakopoulou and others reported a decrease in NFAT transcriptional activity in neurons differentiated from iPSC carrying *LRRK2*-G2019S mutation compared to control, an observation consistent the data presented here(Panagiotakopoulou et al. 2020).

Finally, NFAT plays a critical role in mediating inflammatory processes in T cells. Since LRRK2 has been reported to repress NFAT transcriptional activation(Liu et al. 2011), it would be interesting to study the changes in NFAT transcriptional activation in response to Wnt signalling modulators across the LRRK2 genotypes. Mouse T cells typically are very challenging to transduce with lentiviruses derived from HIV, which I have confirmed. I have tried and utilised CsH as it has been reported to enhance the transduction in mouse T cells(Petrillo et al. 2018). Still, the transduction efficiency is extremely low, even with MOI as high as 100. Nevertheless, I proceeded with the transduction. The raw luminance value measured in the IVIS as a result of transducing NFAT lentivirus was $5.26E^{07}$ Photos/sec indicating sufficient luciferase expression.

Examining the changes in NFAT transcriptional activation as a result of Wnt modulators revealed interesting observations. First, at the basal level, the constitutive NFAT transcriptional activation is significantly less in *LRRK2* KO T cells. This decrease became more substantial when the cells are challenged with LPS at the activated state (**Figure 6-6,7).**

Previous reports demonstrated that combining LPS+Wnt3a or LPS+Wnt5a decrease LPS induces inflammation(Halleskog and Schulte 2013). Combining the Wnt3a or Wnt5a with LPS revealed impairment in the regulation of NFAT transcriptional activation in the *LRRK2* KO T cells **(Figure 6-9,10).** This can imply a complex interplay between NFAT signalling and LRRK2 that becomes apparent in inflammatory conditions.

6.3.1 Main finding and summary

Several studies in the literature pointed to possible pleiotropic effects for *LRRK2*. The results presented in this chapter substitute this observation. Examining *LRRK2* genic deletion or pathogenic mutation on the mRNA level of pro-inflammatory cytokines revealed that LRRK2 inflammatory regulatory role in T cells is quite different than BMDM and RAW 264 macrophages. Furthermore, looking at the impact of *LRRK2* genetic manipulation on Wnt signalling changes revealed different pattern observed in innate immune cells.

Chapter 7 Discussion

Since the discovery that mutation in the *LRRK2* gene is linked to familial PD in 2004, most studies have focused on the role of LRRK2 in the context of neuronal function in PD models. However, accumulating evidence from GWAS have associated *LRRK2* with CD and leprosy, suggesting LRRK2 could have a substantial role in mediating inflammatory processes. Thus, many reports have been published investigating LRRK2 physiological and pathological function in immune responses. The results of those experiments created a debate about the exact inflammatory role for LRRK2 and the impact of its deletion or harbouring the pathogenic mutations associated with PD. Previous work in our lab have pointed to the involvement of LRRK2 in canonical Wnt signalling. Given the involvement of Wnt signalling in immune functions, it is possible that Wnt signalling pathways could be involved in mediate LRRK2 inflammatory role.

7.1 Overview and summary of key findings

The overall aim of this thesis was to determine if there are inflammatory response differences across the *LRRK2* genotypes and examine associated changes in Wnt, NFAT and NFκB signalling in different subsets of immune cells. To this end, I have used a LPS inflammatory model in RAW 264 immortalized macrophages, mice BMDM and T cells. This study highlights that *LRRK2* genetic deletion in RAW 264 macrophages resulted in a compromised immune response accompanying changes in Wnt signalling. Moreover, it suggests mechanistic insights involving Rab10, TLR-4 and WLS as possible mediators for LRRK2 inflammatory role. This study extends to include primary cells, including BMDM and T cells from mice harbouring the PD pathogenic *LRRK2* mutation G2019S and *LRRK2* KO mice. Primary cells yielded conflicting data in different cell types with those obtained in the RAW 264

macrophages, suggesting and confirming previous reports pointing to pleiotropic effects for *LRRK2*(Fava et al. 2019, Zhang et al. 2020, Lewis 2019).

Chapter 3 results substantiated the association between LRRK2 and canonical Wnt signalling previously documented in our lab. Treating SH-SY5Y neuroblastoma cells with two structurally distinct LRRK2 kinase inhibitors and GTPase inhibitor resulted in the reduction of the signal (**Figure 3-6,7,8**). This does suggest that the kinase activity is not the only factor mediating the inhibition. However, the perturbation of the signal was observed in the 10-100 uM concentration range. Thus, it is very likely that those observations are not clinical relevant as those drugs are reported to have low IC_{50} against their pharmacodynamic target(Fuji et al. 2015, Fell et al. 2015, Li et al. 2015, Henderson et al. 2015).

In Chapter 4, I investigated the consequences of *LRRK2* deletion in a LPS inflammatory model in RAW 264 macrophages. Examining the pro-inflammatory cytokines by proteomic analysis, qPCR and western blot revealed an "under-responsive" effect to LPS as a result for *LRRK2* deletion. For instance, TNF-α and Cox-2 were confirmed to be down-regulated by qPCR, western blot, and cytokines array assay **(Figure 4-17,39-40).** This is consistent with recent reports whereby RAW 264 *LRRK2* KO release less TNF-α compared to *LRRK2* WT control in a manganese-induced inflammatory model(Kim et al. 2019). However, it is worth mentioning that LPS-driven cytokines in peripheral mouse macrophages didn't display attenuated release of pro-inflammatory cytokines in LRRK2 PD models(Lee et al. 2017, Hakimi et al. 2011).

Remarkably, all cytokines that were increased in the *LRRK2* KO cells are either chemotaxis, chemokines, anti-inflammatory cytokines, or cytokines with pleiotropic effects **(Table 4-2).** This suggests that LRRK2 acts as an inflammatory mediator.

Examining Wnt signalling changes across LRRK2 genotypes in response to LPS revealed very interesting observations. First, *LRRK2* KO cells expression levels of key canonical Wnt signalling components, including β-catenin and LRP-6, are significantly changed. Second and more notably, WLS protein, which has a vital role in post-translational modification and secretion of Wnt proteins, was significantly induced in LRRK2 KO cells in response to LPS compared to LRRK2 WT**(Figure 4-41),** suggesting Wnt signalling dysregulation is exacerbated in inflammatory conditions when *LRRK2* is deleted.

However, how LRRK2 mediate inflammation is matter of conjecture. Previously, LRRK2 has been documented to interact with 14-3-3 protein through the phosphorylation of S935 and S910 in the ANK-LRR interdomain region within LRRK2(Dzamko et al. 2010). 14-3-3 proteins are ubiquitously expressed regulatory proteins that binds to more than 200 proteins by interacting with phosphorylated serine/threonine residues, forming protein complexes mediating many cellular and signalling processes including inflammation(Munier, Ottmann and Perry 2021). Interestingly, overexpression of 14-3-3 protein in HEK 293 cells resulted in exacerbation of LPS effects on NFκB signalling measured by luciferase assay(Schuster et al. 2011). Thus, it is plausible that LRRK2 might also mediate its inflammatory processes through the signalling hub, 14-3-3. However, this merits further experimental evidence. A suggested signalling mechanism by which LRRK2 might mediate inflammatory responses through NF-κB and canonical Wnt signalling is illustrated(**Figure 7-1**). Furthermore, LPS treatment resulted in significant decrease

in pRAB10 in both genotypes with *LRRK2* KO displaying more intense reduction. Wang and others documented that knockdown of Rab10 results in reduction of LPS driven cytokines with reduction in NFκB signalling in RAW 264 macrophages and overexpression had the opposite effect(Wang et al. 2010). It is not clear how LPS treatment results in a decrease in pRAB10. However, the decrease in pRAB10 in *LRRK2* KO cells could be a contributing factor for the diminished immune response observed in RAW 264 LRRK2 KO cells.

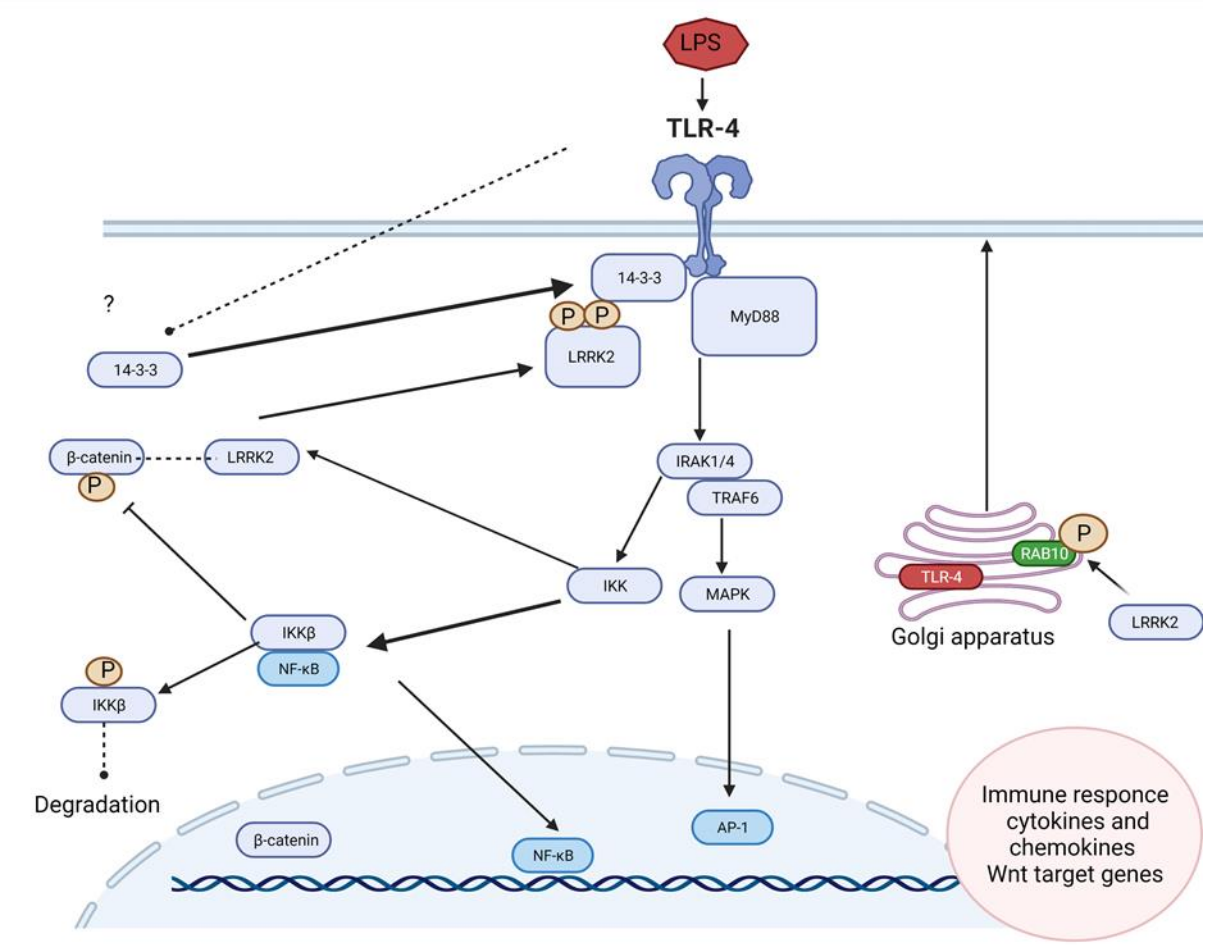

Figure 7-1 ***Suggested crosstalk signalling mechanism for canonical Wnt signalling and NFκB through LRRK2.*** *Activation of TLR-4 by LPS causes confirmational change in the receptor which lead to activation of myD88 and recruitment of adaptor proteins including the 14.3.3 proteins. LPS also causes increase in the phosphorylation of LRRK2 mediating physical interaction with 14.3.3. myD88 signalling results in the activation of IKK and MAPK kinases causing the NFκB and AP-1 transcription factors to translocate into the nucleus and bind to their respective response elements ultimately causing transcription of target genes. Activation of IKK result in dephosphorylation of β-catenin and causing it to translocate to the nucleus and activate canonical Wnt signalling target genes (Sui et al. 2018). Rab10 participates in TLR4 trafficking whereas LRRK2 phosphorylates RAB10.*

Next, I looked into mechanisms of LRRK2 mediated inflammatory responses. First, I investigated LRRK2 expression, which was upregulated in response to LPS(**Figure 4-7).** It has been documented in several reports that inflammatory stimuli (LPS or IFN-

γ) upregulate LRRK2 expression in several subsets of immune cells including human PBMCs, T cells and B cells (Gardet et al. 2010, Gillardon et al. 2012, Kuss et al. 2014). However, other reports have documented no change in LRRK2 expression following LPS treatment (Nazish et al. 2021, Dzamko and Halliday 2012, Russo et al. 2015). Nevertheless, I have observed the upregulation in both total LRRK2 and its phosphorylated form utilizing two antibodies, indicating a clear significant increase in LRRK2 expression.

Then, I examined the LRRK2 kinase substrate, Rab10. LPS treatment resulted in a significant decrease in p-RAB10 levels in both genotypes. Remarkably, *LRRK2* KO cells treated with LPS displayed a significant decrease in pRab10 compared to the *LRRK2* WT-LPS control group**(Figure 4-8)**. This does strongly implicate LRRK2-Rab10 in mediating inflammatory processes. This is in agreement with a report published recently(Nazish et al. 2021). However, while it was expected that LRRK2 deletion will result in lower expression of pRAB10, it is very interesting to observe a decrease in pRAB10 as a result of LPS treatment despite an increase in LRRK2 expression. This observation is not easily explained and warrants further investigation.

Given the significant induction of WLS in *LRRK2* KO cells in response to LPS, I sought to determine its significance in LRRK2-Rab10 mediated inflammatory response. Remarkably, knockdown of *WLS* resulted in downregulation of both LRRK2 and Rab10 that is associated with the reduction of expression of Cox-2 and TLR-4 (**Figure 4-48**). A report by Jang and colleagues suggested that canonical Wnt signalling played a substantial role in LPS induced inflammatory response in BEAS-2B human bronchial epithelial cells. Furthermore, downregulation of Wnt3a and Wnt5a using siRNAs resulted in a decrease in LPS driven cytokines(Jang et al. 2017). This is consistent

with the observation noted here as silencing WLS resulted in a reduction of Cox-2 and TLR-4.

Following examining the role of LRRK2 in mediating LPS inflammatory responses in transformed cell lines, I moved to immune primary cell lines which are more physiologically and pathologically relevant system. I have chosen BMDM as representative of the innate immune system and the T cells as representative of the adaptive immune system.

In BMDM, the *LRRK2 G2019S* mutation resulted in the upregulation of the mRNA expression level of the LPS driven pro-inflammatory cytokines TNF-α, Cox-2, IFN-γ, IL-4 and IL-2**(Figure 5-4).** This is in agreement with a report by Dzamko and others documenting an increase in the pro-inflammatory cytokines in serum from patients with PD carrying the *LRRK2* G2019S mutation(Dzamko et al. 2016). However, the mRNA expression levels of the pro-inflammatory cytokines were also elevated in the *LRRK2* KO BMDM. This is in contrast to the results obtained in the RAW 264 macrophages and the literature(Hartlova et al. 2018). Wnt signalling changes were confirmed, including the upregulation of key Wnt signalling components, including Wnt3a, LRP-6 and Axin-2 in *LRRK2* KO BMDM **(Figure 5-5).**

In T cells, previous reports were ambivalent about the presence of LRRK2 in T cells(Cook et al. 2017). Here, I report that T cells separated from the mice spleen using the specific marker CD+3 do indeed express LRRK2(**Figure** 6-2**).** Following *ex-vivo* activation with CD+3/CD+28, mRNA analysis of pro-inflammatory cytokines did not reveal upregulation compared to non-stimulated cells. Furthermore, there were subtle non-significant differences across *LRRK2* genotypes. Examining Wnt signalling changes in T cells in the basal and activated state revealed a contrasting observation

of what have been reported for the RAW 264 and BMDM. A reduction in key components of Wnt signalling, including LRP-6, Axin-2, Wnt3a, Wnt5a and β-catenin in both *LRRK2* KO and *LRRK2* G2019S T cells (**Figure 6-4).** This does suggest that both LRRK2 and Wnt signalling could have different biological actions in different subsets of immune cells.

In summary, this thesis substantiates previous work in our lab linking LRRK2 to Wnt signalling. In addition, it showed that LRRK2 genetic deletions resulted in changes in LPS driven cytokines in which Wnt signalling played important roles. Moreover, results from a LPS inflammatory model across LRRK2 genotypes in BMDM and T cells revealed that LRRK2 and Wnt signalling could have pleiotropic effects. Overall, this study highlights the significance of LRRK2 inflammatory role in immune setting, with Wnt signalling playing a consequential part.

7.2 Future Work

There is no doubt there is increasing recognition for LRRK2 role in mediating inflammatory processes. This thesis reaffirms and expands upon current knowledge by providing experimental evidence documenting impairment in immune response as a result of *LRRK2* genetic manipulation. This was associated with changes in key components in Wnt signalling and pRAB10 expression. There are intriguing opportunities to expand upon this thesis and build upon potential projects. I provide a couple of examples below with a brief explanation.

7.2.1 LRRK2 role in cancer

The association between *LRRK2* variants and cancer is growing as many studies have observed and published LRRK2 role in cancer setting. In cytokines data generated in chapter 5, I have observed upregulation of MCP-1 cytokine as a result of LPS challenge in *LRRK2* KO RAW 264 macrophages. MCP-1(referred as CCL2 in humans), has been observed to be critical in tumour environment where it has been suggested to both tumoricidal and carcinogenic, depending on the microenvironment. The increase in MCP-1 release in the *LRRK2* KO suggest that LRRK2 might has a suppression activity on the release of MCP-1. Thus, it would be very interesting to study the impact of *LRRK2* genetic manipulation in an *in-vitro* cancer model. Migration or invasion assays could be an excellent start.

7.2.2 Cross talk between TLR-4, Wnt and LRRK2 signalling

Another interesting observation from my data and literature is the possible crosstalk between TLR-4 and Wnt signalling and the involvement of LRRK2. The experimental evidence pointing to such a crosstalk are: First, 14.3.3 protein, Rab10 and Wnt signalling has been suggested to be involved in mediating TLR-4 signalling(Wang et al. 2010, Munier et al. 2021, Ma and Hottiger 2016). Second, Rab10 and 14.3.3 interact physically with LRRK2(Manschwetus et al. 2020). Third, genetic or pharmacological manipulation of either of Rab10, 14.3.3, LRRK2 and Wnt signalling result in perturbation in the release of cytokines and chemokines(Liu et al. 2015, Wang et al. 2010). Fourth, an association between canonical Wnt signalling and NFκB is already documented(Ma and Hottiger 2016). As result, it would be enlightening to design a study to test the hypothesis that LRRK2 could be at the convergence hub between TLR-4 and Wnt signalling in macrophages

Chapter 8 References

1. Agalliu, I., M. San Luciano, A. Mirelman, N. Giladi, B. Waro, J. Aasly, R. Inzelberg, S. Hassin-Baer, E. Friedman, J. Ruiz-Martinez, J. F. Marti-Masso, A. Orr-Urtreger, S. Bressman & R. Saunders-Pullman (2015) Higher frequency of certain cancers in LRRK2 G2019S mutation carriers with Parkinson disease: a pooled analysis. *JAMA Neurol,* 72**,** 58-65.
2. Alam, M. & W. J. Schmidt (2002) Rotenone destroys dopaminergic neurons and induces parkinsonian symptoms in rats. *Behav Brain Res,* 136**,** 317-24.
3. Albanese, F., S. Novello & M. Morari (2019) Autophagy and LRRK2 in the Aging Brain. *Front Neurosci,* 13**,** 1352.
4. Alkhuja, S. (2013) Parkinson disease: research update and clinical management. *South Med J,* 106**,** 334.
5. Allegra, R., S. Tunesi, R. Cilia, G. Pezzoli & S. Goldwurm (2014) LRRK2-G2019S mutation is not associated with an increased cancer risk: a kin-cohort study. *Mov Disord,* 29**,** 1325-6.
6. Alvarez-Erviti, L., M. C. Rodriguez-Oroz, J. M. Cooper, C. Caballero, I. Ferrer, J. A. Obeso & A. H. Schapira (2010) Chaperone-mediated autophagy markers in Parkinson disease brains. *Arch Neurol,* 67**,** 1464-72.
7. Atashrazm, F., D. Hammond, G. Perera, M. F. Bolliger, E. Matar, G. M. Halliday, B. Schule, S. J. G. Lewis, R. J. Nichols & N. Dzamko (2019) LRRK2-mediated Rab10 phosphorylation in immune cells from Parkinson's disease patients. *Mov Disord,* 34**,** 406-415.
8. Aubin, N., O. Curet, A. Deffois & C. Carter (1998) Aspirin and salicylate protect against MPTP-induced dopamine depletion in mice. *J Neurochem,* 71**,** 1635-42.
9. Bajaj, A., J. A. Driver & E. S. Schernhammer (2010) Parkinson's disease and cancer risk: a systematic review and meta-analysis. *Cancer Causes Control,* 21**,** 697-707.
10. Ball, N., W. P. Teo, S. Chandra & J. Chapman (2019) Parkinson's Disease and the Environment. *Front Neurol,* 10**,** 218.
11. Bandres-Ciga, S., M. Diez-Fairen, J. J. Kim & A. B. Singleton (2020) Genetics of Parkinson's disease: An introspection of its journey towards precision medicine. *Neurobiol Dis,* 137**,** 104782.

12. Banziger, C., D. Soldini, C. Schutt, P. Zipperlen, G. Hausmann & K. Basler (2006) Wntless, a conserved membrane protein dedicated to the secretion of Wnt proteins from signaling cells. *Cell,* 125**,** 509-22.
13. Baptista, M. A. S., K. Merchant, T. Barrett, S. Bhargava, D. K. Bryce, J. M. Ellis, A. A. Estrada, M. J. Fell, B. K. Fiske, R. N. Fuji, P. Galatsis, A. G. Henry, S. Hill, W. Hirst, C. Houle, M. E. Kennedy, X. Liu, M. L. Maddess, C. Markgraf, H. Mei, W. A. Meier, E. Needle, S. Ploch, C. Royer, K. Rudolph, A. K. Sharma, A. Stepan, S. Steyn, C. Trost, Z. Yin, H. Yu, X. Wang & T. B. Sherer (2020) LRRK2 inhibitors induce reversible changes in nonhuman primate lungs without measurable pulmonary deficits. *Sci Transl Med,* 12.
14. Barrett, J. P., D. A. Costello, J. O'Sullivan, T. R. Cowley & M. A. Lynch (2015) Bone marrow-derived macrophages from aged rats are more responsive to inflammatory stimuli. *J Neuroinflammation,* 12**,** 67.
15. Baumann, J. G., D. Unutmaz, M. D. Miller, S. K. Breun, S. M. Grill, J. Mirro, D. R. Littman, A. Rein & V. N. KewalRamani (2004) Murine T cells potently restrict human immunodeficiency virus infection. *J Virol,* 78**,** 12537-47.
16. Berwick, D. C. & K. Harvey (2012a) The importance of Wnt signalling for neurodegeneration in Parkinson's disease. *Biochem Soc Trans,* 40**,** 1123-8.
17. --- (2012b) LRRK2 functions as a Wnt signaling scaffold, bridging cytosolic proteins and membrane-localized LRP6. *Hum Mol Genet,* 21**,** 4966-79.
18. Berwick, D. C., G. R. Heaton, S. Azeggagh & K. Harvey (2019) LRRK2 Biology from structure to dysfunction: research progresses, but the themes remain the same. *Mol Neurodegener,* 14**,** 49.
19. Berwick, D. C., B. Javaheri, A. Wetzel, M. Hopkinson, J. Nixon-Abell, S. Granno, A. A. Pitsillides & K. Harvey (2017) Pathogenic LRRK2 variants are gain-of-function mutations that enhance LRRK2-mediated repression of beta-catenin signaling. *Mol Neurodegener,* 12**,** 9.
20. Blumenthal, A., S. Ehlers, J. Lauber, J. Buer, C. Lange, T. Goldmann, H. Heine, E. Brandt & N. Reiling (2006) The Wingless homolog WNT5A and its receptor Frizzled-5 regulate inflammatory responses of human mononuclear cells induced by microbial stimulation. *Blood,* 108**,** 965-73.
21. Bordeaux, J., A. Welsh, S. Agarwal, E. Killiam, M. Baquero, J. Hanna, V. Anagnostou & D. Rimm (2010) Antibody validation. *Biotechniques,* 48**,** 197-209.

22. Bravo-San Pedro, J. M., M. Niso-Santano, R. Gomez-Sanchez, E. Pizarro-Estrella, A. Aiastui-Pujana, A. Gorostidi, V. Climent, R. Lopez de Maturana, R. Sanchez-Pernaute, A. Lopez de Munain, J. M. Fuentes & R. A. Gonzalez-Polo (2013) The LRRK2 G2019S mutant exacerbates basal autophagy through activation of the MEK/ERK pathway. *Cell Mol Life Sci,* 70**,** 121-36.
23. Buchanan, F. G. & R. N. DuBois (2006) Connecting COX-2 and Wnt in cancer. *Cancer Cell,* 9**,** 6-8.
24. Buckley, S. M., J. M. Delhove, D. P. Perocheau, R. Karda, A. A. Rahim, S. J. Howe, N. J. Ward, M. A. Birrell, M. G. Belvisi, P. Arbuthnot, M. R. Johnson, S. N. Waddington & T. R. McKay (2015) In vivo bioimaging with tissue-specific transcription factor activated luciferase reporters. *Sci Rep,* 5**,** 11842.
25. Cai, Y. Q., S. R. Chen & H. L. Pan (2013) Upregulation of nuclear factor of activated T-cells by nerve injury contributes to development of neuropathic pain. *J Pharmacol Exp Ther,* 345**,** 161-8.
26. Cantuti-Castelvetri, I., C. Keller-McGandy, B. Bouzou, G. Asteris, T. W. Clark, M. P. Frosch & D. G. Standaert (2007) Effects of gender on nigral gene expression and parkinson disease. *Neurobiol Dis,* 26**,** 606-14.
27. Casili, G., M. Caffo, M. Campolo, V. Barresi, G. Caruso, S. M. Cardali, M. Lanza, R. Mallamace, A. Filippone, A. Conti, A. Germano, S. Cuzzocrea & E. Esposito (2018) TLR-4/Wnt modulation as new therapeutic strategy in the treatment of glioblastomas. *Oncotarget,* 9**,** 37564-37580.
28. Castano, A., A. J. Herrera, J. Cano & A. Machado (1998) Lipopolysaccharide intranigral injection induces inflammatory reaction and damage in nigrostriatal dopaminergic system. *J Neurochem,* 70**,** 1584-92.
29. Chen, C. Y., Y. H. Weng, K. Y. Chien, K. J. Lin, T. H. Yeh, Y. P. Cheng, C. S. Lu & H. L. Wang (2012) (G2019S) LRRK2 activates MKK4-JNK pathway and causes degeneration of SN dopaminergic neurons in a transgenic mouse model of PD. *Cell Death Differ,* 19**,** 1623-33.
30. Chen, L., J. Hou, X. Zeng, Q. Guo, M. Deng, J. A. Kloeber, X. Tu, F. Zhao, Z. Wu, J. Huang, K. Luo, W. Kim & Z. Lou (2021) LRRK2 inhibition potentiates PARP inhibitor cytotoxicity through inhibiting homologous recombination-mediated DNA double strand break repair. *Clin Transl Med,* 11**,** e341.

31. Chen, Z., Z. Cao, W. Zhang, M. Gu, Z. D. Zhou, B. Li, J. Li, E. K. Tan & L. Zeng (2017) LRRK2 interacts with ATM and regulates Mdm2-p53 cell proliferation axis in response to genotoxic stress. *Hum Mol Genet,* 26**,** 4494-4505.
32. Cheung, M., Y. Kadariya, E. Sementino, M. J. Hall, I. Cozzi, V. Ascoli, J. A. Ohar & J. R. Testa (2021) Novel LRRK2 mutations and other rare, non-BAP1-related candidate tumor predisposition gene variants in high-risk cancer families with mesothelioma and other tumors. *Hum Mol Genet*.
33. Chin-Chan, M., J. Navarro-Yepes & B. Quintanilla-Vega (2015) Environmental pollutants as risk factors for neurodegenerative disorders: Alzheimer and Parkinson diseases. *Front Cell Neurosci,* 9**,** 124.
34. Chu, Y., H. Dodiya, P. Aebischer, C. W. Olanow & J. H. Kordower (2009) Alterations in lysosomal and proteasomal markers in Parkinson's disease: relationship to alpha-synuclein inclusions. *Neurobiol Dis,* 35**,** 385-98.
35. Civiero, L., M. D. Cirnaru, A. Beilina, U. Rodella, I. Russo, E. Belluzzi, E. Lobbestael, L. Reyniers, G. Hondhamuni, P. A. Lewis, C. Van den Haute, V. Baekelandt, R. Bandopadhyay, L. Bubacco, G. Piccoli, M. R. Cookson, J. M. Taymans & E. Greggio (2015) Leucine-rich repeat kinase 2 interacts with p21-activated kinase 6 to control neurite complexity in mammalian brain. *J Neurochem,* 135**,** 1242-56.
36. Cook, D. A., G. T. Kannarkat, A. F. Cintron, L. M. Butkovich, K. B. Fraser, J. Chang, N. Grigoryan, S. A. Factor, A. B. West, J. M. Boss & M. G. Tansey (2017) LRRK2 levels in immune cells are increased in Parkinson's disease. *NPJ Parkinsons Dis,* 3**,** 11.
37. Coombs, G. S., J. Yu, C. A. Canning, C. A. Veltri, T. M. Covey, J. K. Cheong, V. Utomo, N. Banerjee, Z. H. Zhang, R. C. Jadulco, G. P. Concepcion, T. S. Bugni, M. K. Harper, I. Mihalek, C. M. Jones, C. M. Ireland & D. M. Virshup (2010) WLS-dependent secretion of WNT3A requires Ser209 acylation and vacuolar acidification. *J Cell Sci,* 123**,** 3357-67.
38. Cosin-Roger, J., D. Ortiz-Masia, S. Calatayud, C. Hernandez, J. V. Esplugues & M. D. Barrachina (2016) The activation of Wnt signaling by a STAT6-dependent macrophage phenotype promotes mucosal repair in murine IBD. *Mucosal Immunol,* 9**,** 986-98.
39. Cuenca, L., A. L. Gil-Martinez, L. Cano-Fernandez, C. Sanchez-Rodrigo, C. Estrada, E. Fernandez-Villalba & M. T. Herrero (2019) Parkinson's disease: a short story of 200 years. *Histol Histopathol,* 34**,** 573-591.

40. Dai, Z. M., Y. Xiong, W. He, Y. Fang, Y. Q. Qian & X. J. Zhu (2018) Wntless, a conserved Wnt-transport protein, is involved in the innate immune response of Macrobrachium rosenbergii. *Fish Shellfish Immunol,* 80**,** 437-442.
41. Das, S., S. Yu, R. Sakamori, E. Stypulkowski & N. Gao (2012) Wntless in Wnt secretion: molecular, cellular and genetic aspects. *Front Biol (Beijing),* 7**,** 587-593.
42. Davis, B. K. (2013) Isolation, culture, and functional evaluation of bone marrow-derived macrophages. *Methods Mol Biol,* 1031**,** 27-35.
43. Deng, H., P. Wang & J. Jankovic (2018) The genetics of Parkinson disease. *Ageing Res Rev,* 42**,** 72-85.
44. Dickson, D. & R. O. Weller. 2011. *Neurodegeneration: the molecular pathology of dementia and movement disorders*. John Wiley & Sons.
45. Dikic, I. & Z. Elazar (2018) Mechanism and medical implications of mammalian autophagy. *Nat Rev Mol Cell Biol,* 19**,** 349-364.
46. Dzamko, N., M. Deak, F. Hentati, A. D. Reith, A. R. Prescott, D. R. Alessi & R. J. Nichols (2010) Inhibition of LRRK2 kinase activity leads to dephosphorylation of Ser(910)/Ser(935), disruption of 14-3-3 binding and altered cytoplasmic localization. *Biochem J,* 430**,** 405-13.
47. Dzamko, N. & G. M. Halliday (2012) An emerging role for LRRK2 in the immune system. *Biochem Soc Trans,* 40**,** 1134-9.
48. Dzamko, N., F. Inesta-Vaquera, J. Zhang, C. Xie, H. Cai, S. Arthur, L. Tan, H. Choi, N. Gray, P. Cohen, P. Pedrioli, K. Clark & D. R. Alessi (2012) The IkappaB kinase family phosphorylates the Parkinson's disease kinase LRRK2 at Ser935 and Ser910 during Toll-like receptor signaling. *PLoS One,* 7**,** e39132.
49. Dzamko, N., D. B. Rowe & G. M. Halliday (2016) Increased peripheral inflammation in asymptomatic leucine-rich repeat kinase 2 mutation carriers. *Mov Disord,* 31**,** 889-97.
50. Eguchi, T., T. Kuwahara, M. Sakurai, T. Komori, T. Fujimoto, G. Ito, S. I. Yoshimura, A. Harada, M. Fukuda, M. Koike & T. Iwatsubo (2018) LRRK2 and its substrate Rab GTPases are sequentially targeted onto stressed lysosomes and maintain their homeostasis. *Proc Natl Acad Sci U S A,* 115**,** E9115-E9124.
51. El-Sahli, S., Y. Xie, L. Wang & S. Liu (2019) Wnt Signaling in Cancer Metabolism and Immunity. *Cancers (Basel),* 11.

52. England, C. G., E. B. Ehlerding & W. Cai (2016) NanoLuc: A Small Luciferase Is Brightening Up the Field of Bioluminescence. *Bioconjug Chem,* 27**,** 1175-1187.
53. Esteves, A. R., R. H. Swerdlow & S. M. Cardoso (2014) LRRK2, a puzzling protein: insights into Parkinson's disease pathogenesis. *Exp Neurol,* 261**,** 206-16.
54. Exner, N., A. K. Lutz, C. Haass & K. F. Winklhofer (2012) Mitochondrial dysfunction in Parkinson's disease: molecular mechanisms and pathophysiological consequences. *EMBO J,* 31**,** 3038-62.
55. Fava, V. M., J. Manry, A. Cobat, M. Orlova, N. Van Thuc, N. N. Ba, V. H. Thai, L. Abel, A. Alcais, E. Schurr & T. Canadian Lrrk2 in Inflammation (2016) A Missense LRRK2 Variant Is a Risk Factor for Excessive Inflammatory Responses in Leprosy. *PLoS Negl Trop Dis,* 10**,** e0004412.
56. Fava, V. M., Y. Z. Xu, G. Lettre, N. Van Thuc, M. Orlova, V. H. Thai, S. Tao, N. Croteau, M. A. Eldeeb, E. J. MacDougall, G. Cambri, R. Lahiri, L. Adams, E. A. Fon, J. F. Trempe, A. Cobat, A. Alcais, L. Abel & E. Schurr (2019) Pleiotropic effects for Parkin and LRRK2 in leprosy type-1 reactions and Parkinson's disease. *Proc Natl Acad Sci U S A,* 116**,** 15616-15624.
57. Fell, M. J., C. Mirescu, K. Basu, B. Cheewatrakoolpong, D. E. DeMong, J. M. Ellis, L. A. Hyde, Y. Lin, C. G. Markgraf, H. Mei, M. Miller, F. M. Poulet, J. D. Scott, M. D. Smith, Z. Yin, X. Zhou, E. M. Parker, M. E. Kennedy & J. A. Morrow (2015) MLi-2, a Potent, Selective, and Centrally Active Compound for Exploring the Therapeutic Potential and Safety of LRRK2 Kinase Inhibition. *J Pharmacol Exp Ther,* 355**,** 397-409.
58. Feng, Z. H., T. G. Wang, D. D. Li, P. Fung, B. C. Wilson, B. Liu, S. F. Ali, R. Langenbach & J. S. Hong (2002) Cyclooxygenase-2-deficient mice are resistant to 1-methyl-4-phenyl1, 2, 3, 6-tetrahydropyridine-induced damage of dopaminergic neurons in the substantia nigra. *Neurosci Lett,* 329**,** 354-8.
59. Ferguson, T. A. & D. R. Green (2014) Autophagy and phagocytosis converge for better vision. *Autophagy,* 10**,** 165-7.
60. Fuji, R. N., M. Flagella, M. Baca, M. A. Baptista, J. Brodbeck, B. K. Chan, B. K. Fiske, L. Honigberg, A. M. Jubb, P. Katavolos, D. W. Lee, S. C. Lewin-Koh, T. Lin, X. Liu, S. Liu, J. P. Lyssikatos, J. O'Mahony, M. Reichelt, M. Roose-Girma, Z. Sheng, T. Sherer, A. Smith, M. Solon, Z. K. Sweeney, J. Tarrant, A. Urkowitz, S. Warming, M. Yaylaoglu, S. Zhang,

H. Zhu, A. A. Estrada & R. J. Watts (2015) Effect of selective LRRK2 kinase inhibition on nonhuman primate lung. *Sci Transl Med,* 7**,** 273ra15.

61. Funayama, M., K. Hasegawa, H. Kowa, M. Saito, S. Tsuji & F. Obata (2002) A new locus for Parkinson's disease (PARK8) maps to chromosome 12p11.2-q13.1. *Ann Neurol,* 51**,** 296-301.
62. Gandhi, P. N., S. G. Chen & A. L. Wilson-Delfosse (2009) Leucine-rich repeat kinase 2 (LRRK2): a key player in the pathogenesis of Parkinson's disease. *J Neurosci Res,* 87**,** 1283-95.
63. Gardet, A., Y. Benita, C. Li, B. E. Sands, I. Ballester, C. Stevens, J. R. Korzenik, J. D. Rioux, M. J. Daly, R. J. Xavier & D. K. Podolsky (2010) LRRK2 is involved in the IFN-gamma response and host response to pathogens. *J Immunol,* 185**,** 5577-85.
64. Gasser, T. (2009) Molecular pathogenesis of Parkinson disease: insights from genetic studies. *Expert Rev Mol Med,* 11**,** e22.
65. Gatica-Andrades, M., D. Vagenas, J. Kling, T. T. K. Nguyen, H. Benham, R. Thomas, H. Korner, B. Venkatesh, J. Cohen & A. Blumenthal (2017) WNT ligands contribute to the immune response during septic shock and amplify endotoxemia-driven inflammation in mice. *Blood Adv,* 1**,** 1274-1286.
66. Gilham, D. E., A. L. M. Lie, N. Taylor & R. E. Hawkins (2010) Cytokine stimulation and the choice of promoter are critical factors for the efficient transduction of mouse T cells with HIV-1 vectors. *J Gene Med,* 12**,** 129-36.
67. Gillardon, F., R. Schmid & H. Draheim (2012) Parkinson's disease-linked leucine-rich repeat kinase 2(R1441G) mutation increases proinflammatory cytokine release from activated primary microglial cells and resultant neurotoxicity. *Neuroscience,* 208**,** 41-8.
68. Goetz, C. G. (2011) The history of Parkinson's disease: early clinical descriptions and neurological therapies. *Cold Spring Harb Perspect Med,* 1**,** a008862.
69. Gomez-Suaga, P., P. Rivero-Rios, E. Fdez, M. Blanca Ramirez, I. Ferrer, A. Aiastui, A. Lopez De Munain & S. Hilfiker (2014) LRRK2 delays degradative receptor trafficking by impeding late endosomal budding through decreasing Rab7 activity. *Hum Mol Genet,* 23**,** 6779-96.

70. Gong, K., F. Zhou, H. Huang, Y. Gong & L. Zhang (2012) Suppression of GSK3beta by ERK mediates lipopolysaccharide induced cell migration in macrophage through beta-catenin signaling. *Protein Cell,* 3**,** 762-8.
71. Gorell, J. M., C. C. Johnson, B. A. Rybicki, E. L. Peterson & R. J. Richardson (1998) The risk of Parkinson's disease with exposure to pesticides, farming, well water, and rural living. *Neurology,* 50**,** 1346-50.
72. Granno, S., J. Nixon-Abell, D. C. Berwick, J. Tosh, G. Heaton, S. Almudimeegh, Z. Nagda, J. C. Rain, M. Zanda, V. Plagnol, V. L. J. Tybulewicz, K. Cleverley, F. K. Wiseman, E. M. C. Fisher & K. Harvey (2019) Downregulated Wnt/beta-catenin signalling in the Down syndrome hippocampus. *Sci Rep,* 9**,** 7322.
73. Greggio, E., S. Jain, A. Kingsbury, R. Bandopadhyay, P. Lewis, A. Kaganovich, M. P. van der Brug, A. Beilina, J. Blackinton, K. J. Thomas, R. Ahmad, D. W. Miller, S. Kesavapany, A. Singleton, A. Lees, R. J. Harvey, K. Harvey & M. R. Cookson (2006) Kinase activity is required for the toxic effects of mutant LRRK2/dardarin. *Neurobiol Dis,* 23**,** 329-41.
74. Greggio, E., I. Zambrano, A. Kaganovich, A. Beilina, J. M. Taymans, V. Daniels, P. Lewis, S. Jain, J. Ding, A. Syed, K. J. Thomas, V. Baekelandt & M. R. Cookson (2008) The Parkinson disease-associated leucine-rich repeat kinase 2 (LRRK2) is a dimer that undergoes intramolecular autophosphorylation. *J Biol Chem,* 283**,** 16906-14.
75. Hakimi, M., T. Selvanantham, E. Swinton, R. F. Padmore, Y. Tong, G. Kabbach, K. Venderova, S. E. Girardin, D. E. Bulman, C. R. Scherzer, M. J. LaVoie, D. Gris, D. S. Park, J. B. Angel, J. Shen, D. J. Philpott & M. G. Schlossmacher (2011) Parkinson's disease-linked LRRK2 is expressed in circulating and tissue immune cells and upregulated following recognition of microbial structures. *J Neural Transm (Vienna),* 118**,** 795-808.
76. Halleskog, C. & G. Schulte (2013) WNT-3A and WNT-5A counteract lipopolysaccharide-induced pro-inflammatory changes in mouse primary microglia. *J Neurochem,* 125**,** 803-8.
77. Hartlova, A., S. Herbst, J. Peltier, A. Rodgers, O. Bilkei-Gorzo, A. Fearns, B. D. Dill, H. Lee, R. Flynn, S. A. Cowley, P. Davies, P. A. Lewis, I. G. Ganley, J. Martinez, D. R. Alessi, A. D. Reith, M. Trost & M. G. Gutierrez (2018) LRRK2 is a negative regulator of Mycobacterium tuberculosis phagosome maturation in macrophages. *EMBO J,* 37.
78. Harvey, K. & T. F. Outeiro (2019) The role of LRRK2 in cell signalling. *Biochem Soc Trans,* 47**,** 197-207.

79. Haseeb, M., R. H. Pirzada, Q. U. Ain & S. Choi (2019) Wnt Signaling in the Regulation of Immune Cell and Cancer Therapeutics. *Cells,* 8.
80. He, S., Y. Lu, X. Liu, X. Huang, E. T. Keller, C. N. Qian & J. Zhang (2015) Wnt3a: functions and implications in cancer. *Chin J Cancer,* 34**,** 554-62.
81. Heinz, S., A. Freyberger, B. Lawrenz, L. Schladt, G. Schmuck & H. Ellinger-Ziegelbauer (2017) Mechanistic Investigations of the Mitochondrial Complex I Inhibitor Rotenone in the Context of Pharmacological and Safety Evaluation. *Sci Rep,* 7**,** 45465.
82. Henderson, J. L., B. L. Kormos, M. M. Hayward, K. J. Coffman, J. Jasti, R. G. Kurumbail, T. T. Wager, P. R. Verhoest, G. S. Noell, Y. Chen, E. Needle, Z. Berger, S. J. Steyn, C. Houle, W. D. Hirst & P. Galatsis (2015) Discovery and preclinical profiling of 3-[4-(morpholin-4-yl)-7H-pyrrolo[2,3-d]pyrimidin-5-yl]benzonitrile (PF-06447475), a highly potent, selective, brain penetrant, and in vivo active LRRK2 kinase inhibitor. *J Med Chem,* 58**,** 419-32.
83. Henry, A. G., S. Aghamohammadzadeh, H. Samaroo, Y. Chen, K. Mou, E. Needle & W. D. Hirst (2015) Pathogenic LRRK2 mutations, through increased kinase activity, produce enlarged lysosomes with reduced degradative capacity and increase ATP13A2 expression. *Hum Mol Genet,* 24**,** 6013-28.
84. Ho, P. W., C. T. Leung, H. Liu, S. Y. Pang, C. S. Lam, J. Xian, L. Li, M. H. Kung, D. B. Ramsden & S. L. Ho (2020) Age-dependent accumulation of oligomeric SNCA/alpha-synuclein from impaired degradation in mutant LRRK2 knockin mouse model of Parkinson disease: role for therapeutic activation of chaperone-mediated autophagy (CMA). *Autophagy,* 16**,** 347-370.
85. Hui, K. Y., H. Fernandez-Hernandez, J. Hu, A. Schaffner, N. Pankratz, N. Y. Hsu, L. S. Chuang, S. Carmi, N. Villaverde, X. Li, M. Rivas, A. P. Levine, X. Bao, P. R. Labrias, T. Haritunians, D. Ruane, K. Gettler, E. Chen, D. Li, E. R. Schiff, N. Pontikos, N. Barzilai, S. R. Brant, S. Bressman, A. S. Cheifetz, L. N. Clark, M. J. Daly, R. J. Desnick, R. H. Duerr, S. Katz, T. Lencz, R. H. Myers, H. Ostrer, L. Ozelius, H. Payami, Y. Peter, J. D. Rioux, A. W. Segal, W. K. Scott, M. S. Silverberg, J. M. Vance, I. Ubarretxena-Belandia, T. Foroud, G. Atzmon, I. Pe'er, Y. Ioannou, D. P. B. McGovern, Z. Yue, E. E. Schadt, J. H. Cho & I. Peter (2018) Functional variants in the LRRK2 gene confer shared effects on risk for Crohn's disease and Parkinson's disease. *Sci Transl Med,* 10.

86. Hume, D. A., I. L. Ross, S. R. Himes, R. T. Sasmono, C. A. Wells & T. Ravasi (2002) The mononuclear phagocyte system revisited. *J Leukoc Biol,* 72**,** 621-7.
87. Irvine, K. M., A. D. Clouston, V. L. Gadd, G. C. Miller, W. Y. Wong, M. Melino, M. R. Maradana, K. MacDonald, R. A. Lang, M. J. Sweet, A. Blumenthal & E. E. Powell (2015) Deletion of Wntless in myeloid cells exacerbates liver fibrosis and the ductular reaction in chronic liver injury. *Fibrogenesis Tissue Repair,* 8**,** 19.
88. Ito, G., T. Okai, G. Fujino, K. Takeda, H. Ichijo, T. Katada & T. Iwatsubo (2007) GTP binding is essential to the protein kinase activity of LRRK2, a causative gene product for familial Parkinson's disease. *Biochemistry,* 46**,** 1380-8.
89. Jang, J., Y. Jung, Y. Kim, E. H. Jho & Y. Yoon (2017) LPS-induced inflammatory response is suppressed by Wnt inhibitors, Dickkopf-1 and LGK974. *Sci Rep,* 7**,** 41612.
90. Jin, W., Z. Lei, S. Xu, Z. Fachen, Z. Yixiang, Z. Shilei, G. Tao, S. Zhe, L. Fengzhou, W. H. Su & G. Chundong (2021) Genetic Mutation Analysis in Small Cell Lung Cancer by a Novel NGS-Based Targeted Resequencing Gene Panel and Relation with Clinical Features. *Biomed Res Int,* 2021**,** 3609028.
91. Joksimovic, M. & R. Awatramani (2014) Wnt/beta-catenin signaling in midbrain dopaminergic neuron specification and neurogenesis. *J Mol Cell Biol,* 6**,** 27-33.
92. Jordan, J., M. C. Blasco, M. G. Juste & J. M. Perez Gonzalez (1988) [Insulin receptors in intrauterine growth retardation]. *An Esp Pediatr,* 28**,** 417-21.
93. Kaksonen, M. & A. Roux (2018) Mechanisms of clathrin-mediated endocytosis. *Nat Rev Mol Cell Biol,* 19**,** 313-326.
94. Kawakami, F., N. Shimada, E. Ohta, G. Kagiya, R. Kawashima, T. Maekawa, H. Maruyama & T. Ichikawa (2014) Leucine-rich repeat kinase 2 regulates tau phosphorylation through direct activation of glycogen synthase kinase-3beta. *FEBS J,* 281**,** 3-13.
95. Keeley, E. C., B. Mehrad & R. M. Strieter (2008) Chemokines as mediators of neovascularization. *Arterioscler Thromb Vasc Biol,* 28**,** 1928-36.
96. Kim, B., M. S. Yang, D. Choi, J. H. Kim, H. S. Kim, W. Seol, S. Choi, I. Jou, E. Y. Kim & E. H. Joe (2012) Impaired inflammatory responses in murine Lrrk2-knockdown brain microglia. *PLoS One,* 7**,** e34693.

97. Kim, J., E. Pajarillo, A. Rizor, D. S. Son, J. Lee, M. Aschner & E. Lee (2019) LRRK2 kinase plays a critical role in manganese-induced inflammation and apoptosis in microglia. *PLoS One,* 14**,** e0210248.

98. Kim, K. S., P. C. Marcogliese, J. Yang, S. M. Callaghan, V. Resende, E. Abdel-Messih, C. Marras, N. P. Visanji, J. Huang, M. G. Schlossmacher, L. Trinkle-Mulcahy, R. S. Slack, A. E. Lang, T. Canadian Lrrk2 in Inflammation & D. S. Park (2018) Regulation of myeloid cell phagocytosis by LRRK2 via WAVE2 complex stabilization is altered in Parkinson's disease. *Proc Natl Acad Sci U S A,* 115**,** E5164-E5173.

99. Kovalevich, J. & D. Langford (2013) Considerations for the use of SH-SY5Y neuroblastoma cells in neurobiology. *Methods Mol Biol,* 1078**,** 9-21.

100. Kozina, E., S. Sadasivan, Y. Jiao, Y. Dou, Z. Ma, H. Tan, K. Kodali, T. Shaw, J. Peng & R. J. Smeyne (2018) Mutant LRRK2 mediates peripheral and central immune responses leading to neurodegeneration in vivo. *Brain,* 141**,** 1753-1769.

101. Kuss, M., E. Adamopoulou & P. J. Kahle (2014) Interferon-gamma induces leucine-rich repeat kinase LRRK2 via extracellular signal-regulated kinase ERK5 in macrophages. *J Neurochem,* 129**,** 980-7.

102. Kvam, E. & J. Moan (1990) A comparison of three photosensitizers with respect to efficiency of cell inactivation, fluorescence quantum yield and DNA strand breaks. *Photochem Photobiol,* 52**,** 769-73.

103. L'Episcopo, F., C. Tirolo, N. Testa, S. Caniglia, M. C. Morale, M. F. Serapide, S. Pluchino & B. Marchetti (2014) Wnt/beta-catenin signaling is required to rescue midbrain dopaminergic progenitors and promote neurorepair in ageing mouse model of Parkinson's disease. *Stem Cells,* 32**,** 2147-63.

104. Lamonaca, G. & M. Volta (2020) Alpha-Synuclein and LRRK2 in Synaptic Autophagy: Linking Early Dysfunction to Late-Stage Pathology in Parkinson's Disease. *Cells,* 9.

105. Langston, J. W., P. Ballard, J. W. Tetrud & I. Irwin (1983) Chronic Parkinsonism in humans due to a product of meperidine-analog synthesis. *Science,* 219**,** 979-80.

106. Lee, B. D., J. H. Shin, J. VanKampen, L. Petrucelli, A. B. West, H. S. Ko, Y. I. Lee, K. A. Maguire-Zeiss, W. J. Bowers, H. J. Federoff, V. L. Dawson & T. M. Dawson (2010) Inhibitors of leucine-rich repeat kinase-2 protect against models of Parkinson's disease. *Nat Med,* 16**,** 998-1000.

107. Lee, C. M. & J. Hu (2013) Cell density during differentiation can alter the phenotype of bone marrow-derived macrophages. *Cell Biosci,* 3**,** 30.

108. Lee, H., R. Flynn, I. Sharma, E. Haberman, P. J. Carling, F. J. Nicholls, M. Stegmann, J. Vowles, W. Haenseler, R. Wade-Martins, W. S. James & S. A. Cowley (2020) LRRK2 Is Recruited to Phagosomes and Co-recruits RAB8 and RAB10 in Human Pluripotent Stem Cell-Derived Macrophages. *Stem Cell Reports,* 14**,** 940-955.

109. Lee, H., W. S. James & S. A. Cowley (2017) LRRK2 in peripheral and central nervous system innate immunity: its link to Parkinson's disease. *Biochem Soc Trans,* 45**,** 131-139.

110. Levenson, E. A., C. Martens, K. Kanakabandi, C. V. Turner, K. Virtaneva, M. Paneru, S. Ricklefs, S. V. Sosnovtsev, J. A. Johnson, S. F. Porcella & K. Y. Green (2018) Comparative Transcriptomic Response of Primary and Immortalized Macrophages to Murine Norovirus Infection. *J Immunol,* 200**,** 4157-4169.

111. Lewis, P. A. (2009) The function of ROCO proteins in health and disease. *Biol Cell,* 101**,** 183-91.

112. --- (2019) Leucine rich repeat kinase 2: a paradigm for pleiotropy. *J Physiol,* 597**,** 3511-3521.

113. Li, T., X. He, J. M. Thomas, D. Yang, S. Zhong, F. Xue & W. W. Smith (2015) A novel GTP-binding inhibitor, FX2149, attenuates LRRK2 toxicity in Parkinson's disease models. *PLoS One,* 10**,** e0122461.

114. Li, T., D. Yang, S. Zhong, J. M. Thomas, F. Xue, J. Liu, L. Kong, P. Voulalas, H. E. Hassan, J. S. Park, A. D. MacKerell, Jr. & W. W. Smith (2014) Novel LRRK2 GTP-binding inhibitors reduced degeneration in Parkinson's disease cell and mouse models. *Hum Mol Genet,* 23**,** 6212-22.

115. Lim, J. F., H. Berger & I. H. Su (2016) Isolation and Activation of Murine Lymphocytes. *J Vis Exp*.

116. Lin, C. H., P. I. Tsai, R. M. Wu & C. T. Chien (2010a) LRRK2 G2019S mutation induces dendrite degeneration through mislocalization and phosphorylation of tau by recruiting autoactivated GSK3ss. *J Neurosci,* 30**,** 13138-49.

117. Lin, S. L., B. Li, S. Rao, E. J. Yeo, T. E. Hudson, B. T. Nowlin, H. Pei, L. Chen, J. J. Zheng, T. J. Carroll, J. W. Pollard, A. P. McMahon, R. A. Lang & J. S. Duffield (2010b)

Macrophage Wnt7b is critical for kidney repair and regeneration. *Proc Natl Acad Sci U S A,* 107**,** 4194-9.

118. Lin, W. W., S. A. Nish, B. Yen, Y. H. Chen, W. C. Adams, R. Kratchmarov, N. J. Rothman, A. Bhandoola, H. H. Xue & S. L. Reiner (2016) CD8(+) T Lymphocyte Self-Renewal during Effector Cell Determination. *Cell Rep,* 17**,** 1773-1782.

119. Lin, X., L. Parisiadou, X. L. Gu, L. Wang, H. Shim, L. Sun, C. Xie, C. X. Long, W. J. Yang, J. Ding, Z. Z. Chen, P. E. Gallant, J. H. Tao-Cheng, G. Rudow, J. C. Troncoso, Z. Liu, Z. Li & H. Cai (2009) Leucine-rich repeat kinase 2 regulates the progression of neuropathology induced by Parkinson's-disease-related mutant alpha-synuclein. *Neuron,* 64**,** 807-27.

120. Litteljohn, D., C. Rudyk, Z. Dwyer, K. Farmer, T. Fortin, S. Hayley & T. Canadian Lrrk2 in Inflammation (2018) The impact of murine LRRK2 G2019S transgene overexpression on acute responses to inflammatory challenge. *Brain Behav Immun,* 67**,** 246-256.

121. Liu, C. C., C. W. Tsai, F. Deak, J. Rogers, M. Penuliar, Y. M. Sung, J. N. Maher, Y. Fu, X. Li, H. Xu, S. Estus, H. S. Hoe, J. D. Fryer, T. Kanekiyo & G. Bu (2014) Deficiency in LRP6-mediated Wnt signaling contributes to synaptic abnormalities and amyloid pathology in Alzheimer's disease. *Neuron,* 84**,** 63-77.

122. Liu, L., Y. Lin, L. Liu, Y. Bian, L. Zhang, X. Gao & Q. Li (2015) 14-3-3gamma Regulates Lipopolysaccharide-Induced Inflammatory Responses and Lactation in Dairy Cow Mammary Epithelial Cells by Inhibiting NF-kappaB and MAPKs and Up-Regulating mTOR Signaling. *Int J Mol Sci,* 16**,** 16622-41.

123. Liu, M. & G. Bing (2011) Lipopolysaccharide animal models for Parkinson's disease. *Parkinsons Dis,* 2011**,** 327089.

124. Liu, Z., J. Lee, S. Krummey, W. Lu, H. Cai & M. J. Lenardo (2011) The kinase LRRK2 is a regulator of the transcription factor NFAT that modulates the severity of inflammatory bowel disease. *Nat Immunol,* 12**,** 1063-70.

125. Liu, Z., E. Xu, H. T. Zhao, T. Cole & A. B. West (2020) LRRK2 and Rab10 coordinate macropinocytosis to mediate immunological responses in phagocytes. *EMBO J***,** e104862.

126. Lopez de Maturana, R., V. Lang, A. Zubiarrain, A. Sousa, N. Vazquez, A. Gorostidi, J. Aguila, A. Lopez de Munain, M. Rodriguez & R. Sanchez-Pernaute (2016)

Mutations in LRRK2 impair NF-kappaB pathway in iPSC-derived neurons. *J Neuroinflammation,* 13**,** 295.

127. Luo, J., L. Sun, X. Lin, G. Liu, J. Yu, L. Parisiadou, C. Xie, J. Ding & H. Cai (2014) A calcineurin- and NFAT-dependent pathway is involved in alpha-synuclein-induced degeneration of midbrain dopaminergic neurons. *Hum Mol Genet,* 23**,** 6567-74.

128. Ma, B. & M. O. Hottiger (2016) Crosstalk between Wnt/beta-Catenin and NF-kappaB Signaling Pathway during Inflammation. *Front Immunol,* 7**,** 378.

129. MacDonald, B. T., K. Tamai & X. He (2009) Wnt/beta-catenin signaling: components, mechanisms, and diseases. *Dev Cell,* 17**,** 9-26.

130. Madan, B., Z. Ke, N. Harmston, S. Y. Ho, A. O. Frois, J. Alam, D. A. Jeyaraj, V. Pendharkar, K. Ghosh, I. H. Virshup, V. Manoharan, E. H. Ong, K. Sangthongpitag, J. Hill, E. Petretto, T. H. Keller, M. A. Lee, A. Matter & D. M. Virshup (2016) Wnt addiction of genetically defined cancers reversed by PORCN inhibition. *Oncogene,* 35**,** 2197-207.

131. Manolio, T. A. (2010) Genomewide association studies and assessment of the risk of disease. *N Engl J Med,* 363**,** 166-76.

132. Manschwetus, J. T., M. Wallbott, A. Fachinger, C. Obergruber, S. Pautz, D. Bertinetti, S. H. Schmidt & F. W. Herberg (2020) Binding of the Human 14-3-3 Isoforms to Distinct Sites in the Leucine-Rich Repeat Kinase 2. *Front Neurosci,* 14**,** 302.

133. Manzoni, C. & P. A. Lewis (2017) LRRK2 and Autophagy. *Adv Neurobiol,* 14**,** 89-105.

134. Marim, F. M., T. N. Silveira, D. S. Lima, Jr. & D. S. Zamboni (2010) A method for generation of bone marrow-derived macrophages from cryopreserved mouse bone marrow cells. *PLoS One,* 5**,** e15263.

135. Marker, D. F., J. M. Puccini, T. E. Mockus, J. Barbieri, S. M. Lu & H. A. Gelbard (2012) LRRK2 kinase inhibition prevents pathological microglial phagocytosis in response to HIV-1 Tat protein. *J Neuroinflammation,* 9**,** 261.

136. Medzhitov, R. & T. Horng (2009) Transcriptional control of the inflammatory response. *Nat Rev Immunol,* 9**,** 692-703.

137. Merly, L. & S. L. Smith (2017) Murine RAW 264.7 cell line as an immune target: are we missing something? *Immunopharmacol Immunotoxicol,* 39**,** 55-58.

138. Moehle, M. S., P. J. Webber, T. Tse, N. Sukar, D. G. Standaert, T. M. DeSilva, R. M. Cowell & A. B. West (2012) LRRK2 inhibition attenuates microglial inflammatory responses. *J Neurosci,* 32**,** 1602-11.

139. Mukherjee, T. & K. N. Balaji (2019) The WNT Framework in Shaping Immune Cell Responses During Bacterial Infections. *Front Immunol,* 10**,** 1985.

140. Munier, C. C., C. Ottmann & M. W. D. Perry (2021) 14-3-3 modulation of the inflammatory response. *Pharmacol Res,* 163**,** 105236.

141. Nalls, M. A., C. Blauwendraat, C. L. Vallerga, K. Heilbron, S. Bandres-Ciga, D. Chang, M. Tan, D. A. Kia, A. J. Noyce, A. Xue, J. Bras, E. Young, R. von Coelln, J. Simon-Sanchez, C. Schulte, M. Sharma, L. Krohn, L. Pihlstrom, A. Siitonen, H. Iwaki, H. Leonard, F. Faghri, J. R. Gibbs, D. G. Hernandez, S. W. Scholz, J. A. Botia, M. Martinez, J. C. Corvol, S. Lesage, J. Jankovic, L. M. Shulman, M. Sutherland, P. Tienari, K. Majamaa, M. Toft, O. A. Andreassen, T. Bangale, A. Brice, J. Yang, Z. Gan-Or, T. Gasser, P. Heutink, J. M. Shulman, N. W. Wood, D. A. Hinds, J. A. Hardy, H. R. Morris, J. Gratten, P. M. Visscher, R. R. Graham, A. B. Singleton, T. andMe Research, C. System Genomics of Parkinson's Disease & C. International Parkinson's Disease Genomics (2019) Identification of novel risk loci, causal insights, and heritable risk for Parkinson's disease: a meta-analysis of genome-wide association studies. *Lancet Neurol,* 18**,** 1091-1102.

142. Nazish, I., C. Arber, T. M. Piers, T. T. Warner, J. A. Hardy, P. A. Lewis, J. M. Pocock & R. Bandopadhyay (2021) Abrogation of LRRK2 dependent Rab10 phosphorylation with TLR4 activation and alterations in evoked cytokine release in immune cells. *Neurochem Int,* 147**,** 105070.

143. Nishimoto, N. & T. Kishimoto (2004) Inhibition of IL-6 for the treatment of inflammatory diseases. *Curr Opin Pharmacol,* 4**,** 386-91.

144. Nixon-Abell, J., D. C. Berwick, S. Granno, V. A. Spain, C. Blackstone & K. Harvey (2016) Protective LRRK2 R1398H Variant Enhances GTPase and Wnt Signaling Activity. *Front Mol Neurosci,* 9**,** 18.

145. Nubler-Jung, K. (1987) Insect epidermis: disturbance of supracellular tissue polarity does not prevent the expression of cell polarity. *Roux Arch Dev Biol,* 196**,** 286-289.

146. Nunez, F., S. Bravo, F. Cruzat, M. Montecino & G. V. De Ferrari (2011) Wnt/beta-catenin signaling enhances cyclooxygenase-2 (COX2) transcriptional activity in gastric cancer cells. *PLoS One,* 6**,** e18562.

147. Ohta, E., F. Kawakami, M. Kubo & F. Obata (2011) LRRK2 directly phosphorylates Akt1 as a possible physiological substrate: impairment of the kinase activity by Parkinson's disease-associated mutations. *FEBS Lett,* 585**,** 2165-70.

148. Orenstein, S. J., S. H. Kuo, I. Tasset, E. Arias, H. Koga, I. Fernandez-Carasa, E. Cortes, L. S. Honig, W. Dauer, A. Consiglio, A. Raya, D. Sulzer & A. M. Cuervo (2013) Interplay of LRRK2 with chaperone-mediated autophagy. *Nat Neurosci,* 16**,** 394-406.

149. Paisan-Ruiz, C., S. Jain, E. W. Evans, W. P. Gilks, J. Simon, M. van der Brug, A. Lopez de Munain, S. Aparicio, A. M. Gil, N. Khan, J. Johnson, J. R. Martinez, D. Nicholl, I. Marti Carrera, A. S. Pena, R. de Silva, A. Lees, J. F. Marti-Masso, J. Perez-Tur, N. W. Wood & A. B. Singleton (2004) Cloning of the gene containing mutations that cause PARK8-linked Parkinson's disease. *Neuron,* 44**,** 595-600.

150. Palevski, D., L. P. Levin-Kotler, D. Kain, N. Naftali-Shani, N. Landa, T. Ben-Mordechai, T. Konfino, R. Holbova, N. Molotski, R. Rosin-Arbesfeld, R. A. Lang & J. Leor (2017) Loss of Macrophage Wnt Secretion Improves Remodeling and Function After Myocardial Infarction in Mice. *J Am Heart Assoc,* 6.

151. Panagiotakopoulou, V., D. Ivanyuk, S. De Cicco, W. Haq, A. Arsic, C. Yu, D. Messelodi, M. Oldrati, D. C. Schondorf, M. J. Perez, R. P. Cassatella, M. Jakobi, N. Schneiderhan-Marra, T. Gasser, I. Nikic-Spiegel & M. Deleidi (2020) Interferon-gamma signaling synergizes with LRRK2 in neurons and microglia derived from human induced pluripotent stem cells. *Nat Commun,* 11**,** 5163.

152. Park, S., S. Han, I. Choi, B. Kim, S. P. Park, E. H. Joe & Y. H. Suh (2016) Interplay between Leucine-Rich Repeat Kinase 2 (LRRK2) and p62/SQSTM-1 in Selective Autophagy. *PLoS One,* 11**,** e0163029.

153. Parrilla Castellar, E. R., J. K. Plichta, R. Davis, C. Gonzalez-Hunt & L. H. Sanders (2020) Somatic Mutations in LRRK2 Identify a Subset of Invasive Mammary Carcinomas Associated with High Mutation Burden. *Am J Pathol,* 190**,** 2478-2482.

154. Peel, M. & A. Scribner (2013) Cyclophilin inhibitors as antiviral agents. *Bioorg Med Chem Lett,* 23**,** 4485-92.

155. Pereira, C., D. J. Schaer, E. B. Bachli, M. O. Kurrer & G. Schoedon (2008) Wnt5A/CaMKII signaling contributes to the inflammatory response of macrophages and is a target for the antiinflammatory action of activated protein C and interleukin-10. *Arterioscler Thromb Vasc Biol,* 28**,** 504-10.

156. Petrillo, C., L. G. Thorne, G. Unali, G. Schiroli, A. M. S. Giordano, F. Piras, I. Cuccovillo, S. J. Petit, F. Ahsan, M. Noursadeghi, S. Clare, P. Genovese, B. Gentner, L. Naldini, G. J. Towers & A. Kajaste-Rudnitski (2018) Cyclosporine H Overcomes Innate Immune Restrictions to Improve Lentiviral Transduction and Gene Editing In Human Hematopoietic Stem Cells. *Cell Stem Cell,* 23**,** 820-832 e9.

157. Plowey, E. D., S. J. Cherra, 3rd, Y. J. Liu & C. T. Chu (2008) Role of autophagy in G2019S-LRRK2-associated neurite shortening in differentiated SH-SY5Y cells. *J Neurochem,* 105**,** 1048-56.

158. Poewe, W., K. Seppi, C. M. Tanner, G. M. Halliday, P. Brundin, J. Volkmann, A. E. Schrag & A. E. Lang (2017) Parkinson disease. *Nat Rev Dis Primers,* 3**,** 17013.

159. Polymeropoulos, M. H., C. Lavedan, E. Leroy, S. E. Ide, A. Dehejia, A. Dutra, B. Pike, H. Root, J. Rubenstein, R. Boyer, E. S. Stenroos, S. Chandrasekharappa, A. Athanassiadou, T. Papapetropoulos, W. G. Johnson, A. M. Lazzarini, R. C. Duvoisin, G. Di Iorio, L. I. Golbe & R. L. Nussbaum (1997) Mutation in the alpha-synuclein gene identified in families with Parkinson's disease. *Science,* 276**,** 2045-7.

160. Price, A., C. Manzoni, M. R. Cookson & P. A. Lewis (2018) The LRRK2 signalling system. *Cell Tissue Res*.

161. Przedborski, S., V. Jackson-Lewis, R. Djaldetti, G. Liberatore, M. Vila, S. Vukosavic & G. Almer (2000) The parkinsonian toxin MPTP: action and mechanism. *Restor Neurol Neurosci,* 16**,** 135-142.

162. Puri, S., B. S. Magenheimer, R. L. Maser, E. M. Ryan, C. A. Zien, D. D. Walker, D. P. Wallace, S. J. Hempson & J. P. Calvet (2004) Polycystin-1 activates the calcineurin/NFAT (nuclear factor of activated T-cells) signaling pathway. *J Biol Chem,* 279**,** 55455-64.

163. Purlyte, E., H. S. Dhekne, A. R. Sarhan, R. Gomez, P. Lis, M. Wightman, T. N. Martinez, F. Tonelli, S. R. Pfeffer & D. R. Alessi (2018) Rab29 activation of the Parkinson's disease-associated LRRK2 kinase. *EMBO J,* 37**,** 1-18.

164. Purro, S. A., S. Galli & P. C. Salinas (2014) Dysfunction of Wnt signaling and synaptic disassembly in neurodegenerative diseases. *J Mol Cell Biol,* 6**,** 75-80.

165. Pyo, J. O., S. M. Yoo, H. H. Ahn, J. Nah, S. H. Hong, T. I. Kam, S. Jung & Y. K. Jung (2013) Overexpression of Atg5 in mice activates autophagy and extends lifespan. *Nat Commun,* 4**,** 2300.

166. Quadrato, G., M. Benevento, S. Alber, C. Jacob, E. M. Floriddia, T. Nguyen, M. Y. Elnaggar, C. M. Pedroarena, J. D. Molkentin & S. Di Giovanni (2012) Nuclear factor of activated T cells (NFATc4) is required for BDNF-dependent survival of adult-born neurons and spatial memory formation in the hippocampus. *Proc Natl Acad Sci U S A,* 109**,** E1499-508.

167. Ran, F. A., P. D. Hsu, J. Wright, V. Agarwala, D. A. Scott & F. Zhang (2013) Genome engineering using the CRISPR-Cas9 system. *Nat Protoc,* 8**,** 2281-2308.

168. Raschke, W. C., S. Baird, P. Ralph & I. Nakoinz (1978) Functional macrophage cell lines transformed by Abelson leukemia virus. *Cell,* 15**,** 261-7.

169. Rawal, N., O. Corti, P. Sacchetti, H. Ardilla-Osorio, B. Sehat, A. Brice & E. Arenas (2009) Parkin protects dopaminergic neurons from excessive Wnt/beta-catenin signaling. *Biochem Biophys Res Commun,* 388**,** 473-8.

170. Rivero-Rios, P., M. Romo-Lozano, J. Madero-Perez, A. P. Thomas, A. Biosa, E. Greggio & S. Hilfiker (2019) The G2019S variant of leucine-rich repeat kinase 2 (LRRK2) alters endolysosomal trafficking by impairing the function of the GTPase RAB8A. *J Biol Chem,* 294**,** 4738-4758.

171. Rocha, E. M., B. R. De Miranda, S. Castro, R. Drolet, N. G. Hatcher, L. Yao, S. M. Smith, M. T. Keeney, R. Di Maio, J. Kofler, T. G. Hastings & J. T. Greenamyre (2020) LRRK2 inhibition prevents endolysosomal deficits seen in human Parkinson's disease. *Neurobiol Dis,* 134**,** 104626.

172. Rollins, B. J. (1991) JE/MCP-1: an early-response gene encodes a monocyte-specific cytokine. *Cancer Cells,* 3**,** 517-24.

173. Rui, Q., H. Ni, D. Li, R. Gao & G. Chen (2018) The Role of LRRK2 in Neurodegeneration of Parkinson Disease. *Curr Neuropharmacol*.

174. Ruiz-Martinez, J., P. de la Riva, M. C. Rodriguez-Oroz, E. Mondragon Rezola, A. Bergareche, A. Gorostidi, B. Gago, A. Estanga, N. Larranaga, C. Sarasqueta, A. Lopez de

Munain & J. F. Marti Masso (2014) Prevalence of cancer in Parkinson's disease related to R1441G and G2019S mutations in LRRK2. *Mov Disord,* 29**,** 750-5.

175. Russo, I., G. Berti, N. Plotegher, G. Bernardo, R. Filograna, L. Bubacco & E. Greggio (2015) Leucine-rich repeat kinase 2 positively regulates inflammation and down-regulates NF-kappaB p50 signaling in cultured microglia cells. *J Neuroinflammation,* 12**,** 230.

176. Russo, I., G. Di Benedetto, A. Kaganovich, J. Ding, D. Mercatelli, M. Morari, M. R. Cookson, L. Bubacco & E. Greggio (2018) Leucine-rich repeat kinase 2 controls protein kinase A activation state through phosphodiesterase 4. *J Neuroinflammation,* 15**,** 297.

177. Saha, S., P. E. Ash, V. Gowda, L. Liu, O. Shirihai & B. Wolozin (2015) Mutations in LRRK2 potentiate age-related impairment of autophagic flux. *Mol Neurodegener,* 10**,** 26.

178. Salasova, A., C. Yokota, D. Potesil, Z. Zdrahal, V. Bryja & E. Arenas (2017) A proteomic analysis of LRRK2 binding partners reveals interactions with multiple signaling components of the WNT/PCP pathway. *Mol Neurodegener,* 12**,** 54.

179. Sancho, R. M., B. M. Law & K. Harvey (2009) Mutations in the LRRK2 Roc-COR tandem domain link Parkinson's disease to Wnt signalling pathways. *Hum Mol Genet,* 18**,** 3955-68.

180. Saunders-Pullman, R., M. J. Barrett, K. M. Stanley, M. S. Luciano, V. Shanker, L. Severt, A. Hunt, D. Raymond, L. J. Ozelius & S. B. Bressman (2010) LRRK2 G2019S mutations are associated with an increased cancer risk in Parkinson disease. *Mov Disord,* 25**,** 2536-41.

181. Schaale, K., J. Neumann, D. Schneider, S. Ehlers & N. Reiling (2011) Wnt signaling in macrophages: augmenting and inhibiting mycobacteria-induced inflammatory responses. *Eur J Cell Biol,* 90**,** 553-9.

182. Schapansky, J., S. Khasnavis, M. P. DeAndrade, J. D. Nardozzi, S. R. Falkson, J. D. Boyd, J. B. Sanderson, T. Bartels, H. L. Melrose & M. J. LaVoie (2018) Familial knockin mutation of LRRK2 causes lysosomal dysfunction and accumulation of endogenous insoluble alpha-synuclein in neurons. *Neurobiol Dis,* 111**,** 26-35.

183. Schuster, T. B., V. Costina, P. Findeisen, M. Neumaier & P. Ahmad-Nejad (2011) Identification and functional characterization of 14-3-3 in TLR2 signaling. *J Proteome Res,* 10**,** 4661-70.

184. Semenov, M. V., X. Zhang & X. He (2008) DKK1 antagonizes Wnt signaling without promotion of LRP6 internalization and degradation. *J Biol Chem,* 283**,** 21427-32.

185. Seol, W., D. Nam & I. Son (2019) Rab GTPases as Physiological Substrates of LRRK2 Kinase. *Exp Neurobiol,* 28**,** 134-145.

186. Sheng, Z., S. Zhang, D. Bustos, T. Kleinheinz, C. E. Le Pichon, S. L. Dominguez, H. O. Solanoy, J. Drummond, X. Zhang, X. Ding, F. Cai, Q. Song, X. Li, Z. Yue, M. P. van der Brug, D. J. Burdick, J. Gunzner-Toste, H. Chen, X. Liu, A. A. Estrada, Z. K. Sweeney, K. Scearce-Levie, J. G. Moffat, D. S. Kirkpatrick & H. Zhu (2012) Ser1292 autophosphorylation is an indicator of LRRK2 kinase activity and contributes to the cellular effects of PD mutations. *Sci Transl Med,* 4**,** 164ra161.

187. Shin, N., H. Jeong, J. Kwon, H. Y. Heo, J. J. Kwon, H. J. Yun, C. H. Kim, B. S. Han, Y. Tong, J. Shen, T. Hatano, N. Hattori, K. S. Kim, S. Chang & W. Seol (2008) LRRK2 regulates synaptic vesicle endocytosis. *Exp Cell Res,* 314**,** 2055-65.

188. Simon-Sanchez, J., C. Schulte, J. M. Bras, M. Sharma, J. R. Gibbs, D. Berg, C. Paisan-Ruiz, P. Lichtner, S. W. Scholz, D. G. Hernandez, R. Kruger, M. Federoff, C. Klein, A. Goate, J. Perlmutter, M. Bonin, M. A. Nalls, T. Illig, C. Gieger, H. Houlden, M. Steffens, M. S. Okun, B. A. Racette, M. R. Cookson, K. D. Foote, H. H. Fernandez, B. J. Traynor, S. Schreiber, S. Arepalli, R. Zonozi, K. Gwinn, M. van der Brug, G. Lopez, S. J. Chanock, A. Schatzkin, Y. Park, A. Hollenbeck, J. Gao, X. Huang, N. W. Wood, D. Lorenz, G. Deuschl, H. Chen, O. Riess, J. A. Hardy, A. B. Singleton & T. Gasser (2009) Genome-wide association study reveals genetic risk underlying Parkinson's disease. *Nat Genet,* 41**,** 1308-12.

189. Soukup, S. F., S. Kuenen, R. Vanhauwaert, J. Manetsberger, S. Hernandez-Diaz, J. Swerts, N. Schoovaerts, S. Vilain, N. V. Gounko, K. Vints, A. Geens, B. De Strooper & P. Verstreken (2016) A LRRK2-Dependent EndophilinA Phosphoswitch Is Critical for Macroautophagy at Presynaptic Terminals. *Neuron,* 92**,** 829-844.

190. Staal, F. J. & H. C. Clevers (2003) Wnt signaling in the thymus. *Curr Opin Immunol,* 15**,** 204-8.

191. Staal, F. J., T. C. Luis & M. M. Tiemessen (2008) WNT signalling in the immune system: WNT is spreading its wings. *Nat Rev Immunol,* 8**,** 581-93.

192. Staal, F. J., J. Meeldijk, P. Moerer, P. Jay, B. C. van de Weerdt, S. Vainio, G. P. Nolan & H. Clevers (2001) Wnt signaling is required for thymocyte development and activates Tcf-1 mediated transcription. *Eur J Immunol,* 31**,** 285-93.

193. Steger, M., F. Diez, H. S. Dhekne, P. Lis, R. S. Nirujogi, O. Karayel, F. Tonelli, T. N. Martinez, E. Lorentzen, S. R. Pfeffer, D. R. Alessi & M. Mann (2017) Systematic proteomic analysis of LRRK2-mediated Rab GTPase phosphorylation establishes a connection to ciliogenesis. *Elife,* 6.

194. Steger, M., F. Tonelli, G. Ito, P. Davies, M. Trost, M. Vetter, S. Wachter, E. Lorentzen, G. Duddy, S. Wilson, M. A. Baptista, B. K. Fiske, M. J. Fell, J. A. Morrow, A. D. Reith, D. R. Alessi & M. Mann (2016) Phosphoproteomics reveals that Parkinson's disease kinase LRRK2 regulates a subset of Rab GTPases. *Elife,* 5.

195. Sui, Y., Z. Liu, S. H. Park, S. E. Thatcher, B. Zhu, J. P. Fernandez, H. Molina, P. A. Kern & C. Zhou (2018) IKKbeta is a beta-catenin kinase that regulates mesenchymal stem cell differentiation. *JCI Insight,* 3.

196. Taciak, B., M. Bialasek, A. Braniewska, Z. Sas, P. Sawicka, L. Kiraga, T. Rygiel & M. Krol (2018) Evaluation of phenotypic and functional stability of RAW 264.7 cell line through serial passages. *PLoS One,* 13**,** e0198943.

197. Tanner, C. M. (2013) A second honeymoon for Parkinson's disease? *N Engl J Med,* 368**,** 675-6.

198. Taylor, M. & D. R. Alessi (2020) Advances in elucidating the function of leucine-rich repeat protein kinase-2 in normal cells and Parkinson's disease. *Curr Opin Cell Biol,* 63**,** 102-113.

199. Taylor, S., M. Wakem, G. Dijkman, M. Alsarraj & M. Nguyen (2010) A practical approach to RT-qPCR-Publishing data that conform to the MIQE guidelines. *Methods,* 50**,** S1-5.

200. Taymans, J. M. & E. Greggio (2016) LRRK2 Kinase Inhibition as a Therapeutic Strategy for Parkinson's Disease, Where Do We Stand? *Curr Neuropharmacol,* 14**,** 214-25.

201. Teismann, P. (2012) COX-2 in the neurodegenerative process of Parkinson's disease. *Biofactors,* 38**,** 395-7.

202. Thevenet, J., R. Pescini Gobert, R. Hooft van Huijsduijnen, C. Wiessner & Y. J. Sagot (2011) Regulation of LRRK2 expression points to a functional role in human monocyte maturation. *PLoS One,* 6**,** e21519.

203. Thomas, J. M., T. Li, W. Yang, F. Xue, P. S. Fishman & W. W. Smith (2016) 68 and FX2149 Attenuate Mutant LRRK2-R1441C-Induced Neural Transport Impairment. *Front Aging Neurosci,* 8**,** 337.

204. Torres, J., S. Mehandru, J. F. Colombel & L. Peyrin-Biroulet (2017) Crohn's disease. *Lancet,* 389**,** 1741-1755.

205. Tran, F. H. & J. J. Zheng (2017) Modulating the wnt signaling pathway with small molecules. *Protein Sci,* 26**,** 650-661.

206. Trouplin, V., N. Boucherit, L. Gorvel, F. Conti, G. Mottola & E. Ghigo (2013) Bone marrow-derived macrophage production. *J Vis Exp***,** e50966.

207. van Amerongen, R. & R. Nusse (2009) Towards an integrated view of Wnt signaling in development. *Development,* 136**,** 3205-14.

208. van Meerloo, J., G. J. Kaspers & J. Cloos (2011) Cell sensitivity assays: the MTT assay. *Methods Mol Biol,* 731**,** 237-45.

209. Vannella, K. M. & T. A. Wynn (2017) Mechanisms of Organ Injury and Repair by Macrophages. *Annu Rev Physiol,* 79**,** 593-617.

210. Verbeek, S., D. Izon, F. Hofhuis, E. Robanus-Maandag, H. te Riele, M. van de Wetering, M. Oosterwegel, A. Wilson, H. R. MacDonald & H. Clevers (1995) An HMG-box-containing T-cell factor required for thymocyte differentiation. *Nature,* 374**,** 70-4.

211. Vihma, H., M. Luhakooder, P. Pruunsild & T. Timmusk (2016) Regulation of different human NFAT isoforms by neuronal activity. *J Neurochem,* 137**,** 394-408.

212. Wallings, R. L., M. K. Herrick & M. G. Tansey (2020) LRRK2 at the Interface Between Peripheral and Central Immune Function in Parkinson's. *Front Neurosci,* 14**,** 443.

213. Wallings, R. L. & M. G. Tansey (2019) LRRK2 regulation of immune-pathways and inflammatory disease. *Biochem Soc Trans,* 47**,** 1581-1595.

214. Wandinger-Ness, A. & M. Zerial (2014) Rab proteins and the compartmentalization of the endosomal system. *Cold Spring Harb Perspect Biol,* 6**,** a022616.

215. Wandu, W. S., C. Tan, O. Ogbeifun, B. P. Vistica, G. Shi, S. J. Hinshaw, C. Xie, X. Chen, D. M. Klinman, H. Cai & I. Gery (2015) Leucine-Rich Repeat Kinase 2 (Lrrk2) Deficiency Diminishes the Development of Experimental Autoimmune Uveitis (EAU) and the Adaptive Immune Response. *PLoS One,* 10**,** e0128906.

216. Wang, C., X. Yu, Q. Cao, Y. Wang, G. Zheng, T. K. Tan, H. Zhao, Y. Zhao, Y. Wang & D. Harris (2013) Characterization of murine macrophages from bone marrow, spleen and peritoneum. *BMC Immunol,* 14**,** 6.

217. Wang, D., J. Lou, C. Ouyang, W. Chen, Y. Liu, X. Liu, X. Cao, J. Wang & L. Lu (2010) Ras-related protein Rab10 facilitates TLR4 signaling by promoting replenishment of TLR4 onto the plasma membrane. *Proc Natl Acad Sci U S A,* 107**,** 13806-11.

218. Wang, D., L. Xu, L. Lv, L. Y. Su, Y. Fan, D. F. Zhang, R. Bi, D. Yu, W. Zhang, X. A. Li, Y. Y. Li & Y. G. Yao (2015a) Association of the LRRK2 genetic polymorphisms with leprosy in Han Chinese from Southwest China. *Genes Immun,* 16**,** 112-9.

219. Wang, W., S. A. Nag & R. Zhang (2015b) Targeting the NFkappaB signaling pathways for breast cancer prevention and therapy. *Curr Med Chem,* 22**,** 264-89.

220. Wang, Y. (2009) Wnt/Planar cell polarity signaling: a new paradigm for cancer therapy. *Mol Cancer Ther,* 8**,** 2103-9.

221. Weerkamp, F., M. R. Baert, B. A. Naber, E. E. Koster, E. F. de Haas, K. R. Atkuri, J. J. van Dongen, L. A. Herzenberg & F. J. Staal (2006) Wnt signaling in the thymus is regulated by differential expression of intracellular signaling molecules. *Proc Natl Acad Sci U S A,* 103**,** 3322-6.

222. Weinberger, T. & C. Schulz (2015) Myocardial infarction: a critical role of macrophages in cardiac remodeling. *Front Physiol,* 6**,** 107.

223. Weindel, C. G., S. L. Bell, K. J. Vail, K. O. West, K. L. Patrick & R. O. Watson (2020) LRRK2 maintains mitochondrial homeostasis and regulates innate immune responses to Mycobacterium tuberculosis. *Elife,* 9.

224. West, A. B. (2017) Achieving neuroprotection with LRRK2 kinase inhibitors in Parkinson disease. *Exp Neurol,* 298**,** 236-245.

225. West, A. B., D. J. Moore, S. Biskup, A. Bugayenko, W. W. Smith, C. A. Ross, V. L. Dawson & T. M. Dawson (2005) Parkinson's disease-associated mutations in leucine-rich repeat kinase 2 augment kinase activity. *Proc Natl Acad Sci U S A,* 102**,** 16842-7.

226. Whitley, K. C., S. I. Hamstra, R. W. Baranowski, C. J. F. Watson, R. E. K. MacPherson, A. J. MacNeil, B. D. Roy, R. Vandenboom & V. A. Fajardo (2020) GSK3 inhibition with low dose lithium supplementation augments murine muscle fatigue resistance and specific force production. *Physiol Rep,* 8**,** e14517.

227. Williamson, D. S., G. P. Smith, P. Acheson-Dossang, S. T. Bedford, V. Chell, I. J. Chen, J. C. A. Daechsel, Z. Daniels, L. David, P. Dokurno, M. Hentzer, M. C. Herzig, R. E. Hubbard, J. D. Moore, J. B. Murray, S. Newland, S. C. Ray, T. Shaw, A. E. Surgenor, L. Terry, K. Thirstrup, Y. Wang & K. V. Christensen (2017) Design of Leucine-Rich Repeat Kinase 2 (LRRK2) Inhibitors Using a Crystallographic Surrogate Derived from Checkpoint Kinase 1 (CHK1). *J Med Chem,* 60**,** 8945-8962.

228. Wu, C. & Y. Lu (2010) High-titre retroviral vector system for efficient gene delivery into human and mouse cells of haematopoietic and lymphocytic lineages. *J Gen Virol,* 91**,** 1909-1918.

229. Wynn, T. A., A. Chawla & J. W. Pollard (2013) Macrophage biology in development, homeostasis and disease. *Nature,* 496**,** 445-55.

230. Xicoy, H., B. Wieringa & G. J. Martens (2017) The SH-SY5Y cell line in Parkinson's disease research: a systematic review. *Mol Neurodegener,* 12**,** 10.

231. Yan, R. & Z. Liu (2017) LRRK2 enhances Nod1/2-mediated inflammatory cytokine production by promoting Rip2 phosphorylation. *Protein Cell,* 8**,** 55-66.

232. Yang, Q., J. Jeremiah Bell & A. Bhandoola (2010) T-cell lineage determination. *Immunol Rev,* 238**,** 12-22.

233. Yi, H., A. K. Patel, C. P. Sodhi, D. J. Hackam & A. S. Hackam (2012) Novel role for the innate immune receptor Toll-like receptor 4 (TLR4) in the regulation of the Wnt signaling pathway and photoreceptor apoptosis. *PLoS One,* 7**,** e36560.

234. Yoshida, H., K. Okamoto, T. Iwamoto, E. Sakai, K. Kanaoka, J. P. Hu, M. Shibata, H. Hotokezaka, K. Nishishita, A. Mizuno & Y. Kato (2006) Pepstatin A, an aspartic proteinase inhibitor, suppresses RANKL-induced osteoclast differentiation. *J Biochem,* 139**,** 583-90.

235. Yu, J., L. Chen, B. Cui, G. F. Widhopf, 2nd, Z. Shen, R. Wu, L. Zhang, S. Zhang, S. P. Briggs & T. J. Kipps (2016) Wnt5a induces ROR1/ROR2 heterooligomerization to enhance leukemia chemotaxis and proliferation. *J Clin Invest,* 126**,** 585-98.

236. Yue, M., K. M. Hinkle, P. Davies, E. Trushina, F. C. Fiesel, T. A. Christenson, A. S. Schroeder, L. Zhang, E. Bowles, B. Behrouz, S. J. Lincoln, J. E. Beevers, A. J. Milnerwood, A. Kurti, P. J. McLean, J. D. Fryer, W. Springer, D. W. Dickson, M. J. Farrer & H. L. Melrose (2015) Progressive dopaminergic alterations and mitochondrial abnormalities in LRRK2 G2019S knock-in mice. *Neurobiol Dis,* 78**,** 172-95.

237. Yun, H. J., H. Kim, I. Ga, H. Oh, D. H. Ho, J. Kim, H. Seo, I. Son & W. Seol (2015) An early endosome regulator, Rab5b, is an LRRK2 kinase substrate. *J Biochem,* 157**,** 485-95.

238. Yun, H. J., J. Park, D. H. Ho, H. Kim, C. H. Kim, H. Oh, I. Ga, H. Seo, S. Chang, I. Son & W. Seol (2013) LRRK2 phosphorylates Snapin and inhibits interaction of Snapin with SNAP-25. *Exp Mol Med,* 45**,** e36.

239. Zhang, D. F., D. Wang, Y. Y. Li & Y. G. Yao (2020) Is there an antagonistic pleiotropic effect of a LRRK2 mutation on leprosy and Parkinson's disease? *Proc Natl Acad Sci U S A,* 117**,** 10122-10123.

240. Zhang, J., J. Liu, A. Norris, B. D. Grant & X. Wang (2018) A novel requirement for ubiquitin-conjugating enzyme UBC-13 in retrograde recycling of MIG-14/Wntless and Wnt signaling. *Mol Biol Cell,* 29**,** 2098-2112.

241. Zhang, L., X. Yang, S. Yang & J. Zhang (2011) The Wnt /beta-catenin signaling pathway in the adult neurogenesis. *Eur J Neurosci,* 33**,** 1-8.

242. Zhang, P., J. Katz & S. M. Michalek (2009) Glycogen synthase kinase-3beta (GSK3beta) inhibition suppresses the inflammatory response to Francisella infection and protects against tularemia in mice. *Mol Immunol,* 46**,** 677-87.

243. Zimprich, A., S. Biskup, P. Leitner, P. Lichtner, M. Farrer, S. Lincoln, J. Kachergus, M. Hulihan, R. J. Uitti, D. B. Calne, A. J. Stoessl, R. F. Pfeiffer, N. Patenge, I. C. Carbajal, P. Vieregge, F. Asmus, B. Muller-Myhsok, D. W. Dickson, T. Meitinger, T. M. Strom, Z. K. Wszolek & T. Gasser (2004) Mutations in LRRK2 cause autosomal-dominant parkinsonism with pleomorphic pathology. *Neuron,* 44**,** 601-7.